A combined ingress-egress model for the Kianna unconformity-related uranium deposit, Shea Creek Project, Athabasca Basin, Canada

by

Caitlin A.R. Sheahan

A Thesis

Submitted to the Faculty of Graduate Studies of

The University of Manitoba

In Partial Fulfillment of the Requirements

for the Degree of

MASTER OF SCIENCE

Department of Geological Sciences

University of Manitoba

Winnipeg

Abstract

The Kianna deposit is an unconformity-related uranium deposit in the western Athabasca Basin of northern Saskatchewan, hosting uraninite in three distinct zones: 1) perched above the unconformity, hosted in sandstone; 2) at the unconformity, hosted in sandstone and basement rocks; and 3) below the unconformity in two separate pods, hosted by basement paragneiss. *In situ* secondary ion mass spectrometry (SIMS) was used to obtain radiogenic and stable isotope data to update the genetic model for the Kianna deposit. Primary basement-hosted ingress-style uraninite, associated with hematite and muscovite, has a minimum U-Pb age of ~1500 Ma. Recrystallization of basement uraninite occurred ~1100 Ma with the precipitation of coarse-grained illite. Late basement uraninite precipitated with fine-grained illite ~850 Ma. A separate, deeper basement pod formed ~1280 Ma. Egress-style uraninite at the unconformity, and perched uraninite in the sandstone, inter-grown with alumino-phosphate sulfate (APS) minerals and chalcopyrite, formed ~750 Ma. Later unconformity and perched uraninite precipitated with hematite, pyrite, and chalcopyrite ~500 Ma. Sulfides coeval with unconformity and perched uraninite have $\delta^{34}S$ values from -1.9 to 8.1‰ and 15.1 to 25.4‰, indicating two sources of sulfur: 1) sulfides in the metamorphosed basement and 2) APS minerals in the sandstone. Average $\delta^{18}O$ and δD mineral values for muscovite are 0.7 ± 4.3‰ and -33 ± 12‰, respectively, suggesting that muscovite formed from a marine brine. Average $\delta^{18}O$ and δD mineral values for coarse-grained illite are 0.4 ± 4.1‰ and -79 ± 16‰, respectively, indicating formation from hydrothermal fluids, whereas fine-grained illite $\delta^{18}O$ and δD mineral values are 6.5 ± 1.6‰ and -144 ± 21‰, respectively, suggesting formation from meteoric fluids.

Acknowledgements

I would like to sincerely thank everyone involved in the preparation of this thesis. Firstly, I extend my utmost gratitude to my advisor, Dr. Mostafa Fayek, whose dedication, motivation, and support enabled me to complete this thesis. Thank you for your guidance, advice, and commitment to your students. Thank you to Dave Quirt (AREVA Resources Canada Inc.) for all of your stimulating discussions and thoughtful questions, and for organizing sample collection and our very enjoyable field work at Shea Creek. Charlie Jefferson (Geological Survey of Canada) and Alfredo Camacho were always available for questions and this thesis greatly benefited from your comments and suggestions. SIMS analyses were carried out under the direction of Ryan Sharpe, to whom I am very thankful; you were always available for questions and ideas – for the entirety of my thesis work. EPMA work was carried out under the direction of Ravi Sidhu, who I always enjoyed working with.

This project was funded by the Natural Sciences and Engineering Research Council of Canada (NSERC), Natural Resources Canada (NRCan), AREVA Resources Canada Inc., the Canadian Foundation for Innovation (CFI) and the Manitoba Graduate Scholarship (MGS).

Finally, I extend my appreciation to my wonderful friends and family, a special thank you to Dr. T.K. Kyser for your encouragement and mentorship – for which I am exceedingly grateful. Thank you to Brandi Shabaga for your instruction in the lab, editing of figures, and fun adventures from Denver to Saskatoon to Fredericton. Lastly, my husband Andrew, thank you for supporting me through these years in Winnipeg, for your continual love and comedic relief, and for always standing by me.

Dedication

This thesis is dedicated to my loving, supportive, and brilliant parents, Drs. Jack and Laurie Rush, who have always been and continue to be the most inspirational people in my life.

Table of Contents

Abstract……..ii
Acknowledgements……...iii
Dedication……..iv
Table of Contents……....v
List of Tables……....vii
List of Figures……..viii
List of Copyrighted Material for which Permission was Obtained……ix

Chapter 1: Introduction……..1

Chapter 2: Geological Setting……4
2.1 Regional Geology……4
2.2 Local Geology……..6
2.3 Deposit Geology……...8

Chapter 3: Sampling and Methodology……13
3.1 Optical Microscopy and Scanning Electron Microscope (SEM)……13
3.2 Electron Probe Microanalysis (EPMA)……...13
3.3 Secondary Ion Mass Spectrometry (SIMS)……....14
3.3.1 Stable Isotopes……..14
3.3.2 Radiogenic Isotopes……..17

Chapter 4: Results……..19
4.1 Petrography and Mineral Paragenesis……..19
4.1.1 Basement……...21
4.1.2 Unconformity……26
4.1.3 Perched……..28
4.2 Stable Isotope Geochemistry……....30
4.2.1 Silicates, Clay Minerals, and Oxides……30
4.2.2 Sulfides……..34
4.3 Geochronology……36

Chapter 5: Discussion……38
5.1 Characterization of the Mineralizing Fluids……38
5.2 Geochronology and Tectonics……..47
5.3 Genetic Model……..51
5.3.1 Athabasca Basin Previous Studies……51
5.3.2 Structure Models……...52
5.3.3 Kianna Deposit Model……..54

Chapter 6: Conclusions and Recommendations……59
6.1 Conclusions……59
6.2 Recommendations for Future Work……60

References……62
Appendices……70
Appendix A: Thin Section Descriptions……...71

Appendix B: Electron Probe Microanalysis (EPMA) Standards and Data……...92
Table B1: EPMA Standards……..93
Table B2: Chemical compositions of uraninite……94
Table B3: Chemical compositions of silicates, clay minerals, and hematite……....122
Table B4: Chemical compositions of sulfides……..132
Table B5: Chemical compositions and calculated Si and K atoms per formula unit (apfu) for muscovite, coarse-grained illite, and fine-grained illite……..138
Table B6: SiO_2 + CaO compositions of uraninite and calculated chemical-Pb ages……..142
Table B7: Calculated temperature of formation of coarse-grained illite using Battaglia's (2004) equation……154

Appendix C: Secondary Ion Mass Spectrometry (SIMS) Standards and Data…...155
Table C1: Hydrogen isotope compositions of muscovite, coarse-grained illite and fine-grained illite……...156
Table C2: Oxygen isotope compositions of muscovite, coarse-grained illite and fine-grained illite……...159
Table C3: Oxygen isotope compositons of uraninite……...161
Table C4: Sulfur isotope compositions of chalcopyrite and pyrite……..163
Table C5: U-Pb data from Kianna deposit uraninite……166
Table C6: Corrected U-Pb data used to calculate Pb-Pb ages and plot U-Pb Concordia diagrams……182

List of Tables

Table 1: Measured $\delta^{18}O$ mineral values and calculated fluid values for the fluid in equilibrium with muscovite, coarse-grained illite, and fine-grained illite……30
Table 2: Measured δD mineral values and calculated fluid values for the fluid in equilibrium with muscovite, coarse-grained illite, and fine-grained illite……32
Table 3: Measured $\delta^{18}O$ values for uraninite in each mineralized zone……34
Table 4: Measured $\delta^{34}S$ values for chalcopyrite and pyrite associated with basement, unconformity and perched uraninite……..35

List of Figures

Figure 1: Simplified location map for the Shea Creek area, Athabasca Basin……2
Figure 2: Plan-view map of the Saskatoon Lake Conductor (SLC)……9
Figure 3: Schematic SW-NE cross-section of the Kianna deposit mineralized zones……...12
Figure 4: Mineral paragenesis for basement (A), unconformity (B), and perched mineralized pods (C)…….20
Figure 5: Photomicrographs and backscatter electron images of minerals of interest in the Kianna deposit basement rocks……...…….23
Figure 6: Si and K atoms per formula unit (apfu) for muscovite and illite……...…25
Figure 7: Photomicrographs and backscatter electron images of minerals of interest in the Kianna deposit unconformity and perched mineralized zones……..27
Figure 8: Plot of SiO_2 + CaO chemical composition versus calculated chemical-Pb age of uraninite in each mineralized zone……29
Figure 9: U-Pb Concordia diagrams for six stages of uraninite……37
Figure 10: Measured $\delta^{18}O$ and δD mineral values for coarse-grained illite and fine-grained illite……...40
Figure 11: $\delta^{18}O$ and δD discrimination diagram for the fluids in equilibrium with muscovite, coarse-grained illite, and fine-grained illite……..42
Figure 12: Paleolatitude reconstructions of Laurentia for ca. 1500 Ma (A) and for ca. 1100 Ma (B)…….44
Figure 13: $\delta^{34}S$ values for common reservoirs and sources of sulfur as well as SIMS data for Kianna deposit sulfides……46
Figure 14: Schematic representation of a fault before (A) and during (B) an earthquake……....54
Figure 15: Schematic representation of six stages of uranium mineralization from the Kianna deposit……...57

List of Copyrighted Material for which Permission was Obtained

Figure 1: Simplified location map for the Shea Creek area, Athabasca Basin (Laverett et al., 2006)…….2
Figure 2: Plan-view map of the Saskatoon Lake Conductor (SLC) (AREVA Resources Canada Inc., 2012)…….9
Figure 6: Si and K atoms per formula unit (apfu) for muscovite and illite (Quirt, 2010)…….....25
Figure 10: Measured $\delta^{18}O$ and δD mineral values for coarse-grained illite and fine-grained Illite (Kotzer and Kyser, 1995)……..40
Figure 11: $\delta^{18}O$ and δD discrimination diagram for the fluids in equilibrium with muscovite, coarse-grained illite, and fine-grained illite (Kotzer and Kyser, 1995)…….42
Figure 12: Paleolatitude reconstructions of Laurentia for ca. 1500 Ma (A) and ca. 1100 Ma (B) (Pesonen et al., 2003)…….44
Figure 13: $\delta^{34}S$ values for common reservoirs and sources of sulfur and SIMS data for Kianna deposit sulfides (Seal et al., 2000)……46
Figure 14: Schematic representation of a fault before (A) and during (B) an earthquake (Craw, 2013)…….54

Chapter 1: Introduction

The Athabasca Basin in northern Saskatchewan, Canada, is host to world-class high-grade unconformity-related uranium deposits. Most of the well-known and best-studied deposits occur in the eastern portion of the basin (e.g., McArthur River, Cigar Lake). Previous studies on these deposits have included deposit geological studies, host-rock alteration mineralogy, ore petrology, geochronology, and stable isotope geochemistry to develop genetic models and suggest potential sources of uranium (Hoeve and Quirt, 1984; Wallis et al., 1985; Kotzer and Kyser, 1995; Jefferson et al., 2007a,b; among others).

Three end-member styles of mineralization have been observed in deposits of the eastern Athabasca Basin: 1) uraninite at the unconformity and partially hosted by the metamorphosed basement, such as the McArthur River, Midwest, and Deilmann (Key Lake) deposits; 2) uraninite above the unconformity in pods perched in the overlying sandstone, such as Cigar Lake and McClean Lake; and 3) uraninite hosted primarily in the basement, such as Eagle Point and Sue C (Jefferson et al., 2007b). However, no deposit has been previously described to host uraninite in all three locations. Therefore, based on these deposit morphologies and bulk mineralogical and geochemical analytical techniques (Hoeve and Quirt, 1984; Kotzer and Kyser, 1995; Fayek et al., 1997; Alexandre et al., 2005; Alexandre et al., 2009a; Cloutier et al., 2009; among others), and more recently detailed *in situ* micro-analytical studies (Fayek et al., 2000; Fayek et al., 2002a; Fayek et al., 2002b; Alexandre et al., 2009b; Fayek et al., 2010; Mercadier et al., 2011), several genetic models (e.g., ingress, egress; Hoeve and Quirt, 1984; Quirt, 1989; Jefferson et al., 2007a) have been suggested for Athabasca Basin uranium deposits.

The Kianna deposit on the Shea Creek Project is an unconformity-related deposit in the lesser-studied western Athabasca Basin (Fig. 1). It is the first deposit described to host all three styles of uraninite: 1) perched, 2) at the unconformity and in shallow basement rocks, and 3) deep basement-hosted (Quirt et al., 2012). The Kianna deposit therefore provides a unique opportunity to study one deposit that hosts all three styles of uraninite previously observed throughout the basin, and link these styles of uraninite into one metallogenic model.

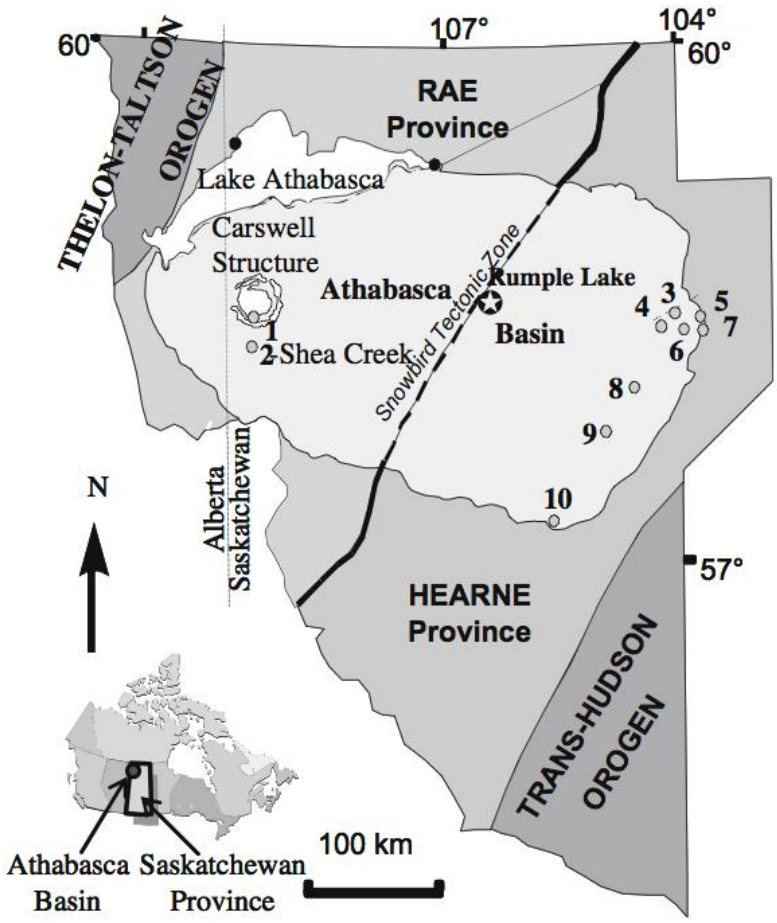

Figure 1: Simplified map of the Athabasca Basin, northern Saskatchewan, Canada and the locations of major unconformity-related uranium deposits: 1) Cluff Lake, 2) Shea Creek, 3) Dawn Lake, 4) Midwest, 5) Collins Bay, 6) McClean Lake and Sue, 7) Rabbit Lake, 8) Cigar Lake, 9) McArthur River, and 10) Key Lake (Laverret et al., 2006).

Recent advancements in micro-analytical techniques can provide information from zoned minerals, which can be used to refine previous genetic models that are based on bulk analytical data. Therefore, the objectives of this thesis are to (1) develop a mineral paragenetic hypothesis for the Kianna Deposit, (2) use this mineral paragenesis to guide *in situ* stable ($\delta^{18}O$, δD, and $\delta^{34}S$) and radiogenic (U-Pb) isotopic micro-analyses by SIMS of silicate and clay minerals, sulfides, and uraninite, (3) use these data to develop a metallogenic model for the Kianna deposit, and (4) compare the Kianna deposit model to previously published models for unconformity-related uranium deposits from the eastern Athabasca Basin.

Chapter 2: Geological Setting

2.1 Regional Geology

The expansive, intracratonic Athabasca Basin is primarily located in northern Saskatchewan and extends into northern Alberta, covering over 100,000 km^2 (Laverret et al., 2010). The Athabasca unconformity-related uranium deposits occur at the base of the Athabasca Group sandstone, flat-lying, fluvial redbed strata that unconformably overlie metamorphosed basement rocks. The Athabasca Group strata were deposited during post-Hudsonian (ca. 1750 Ma) tectonic activity and fault reactivation along Hudsonian northeast-trending zones. The present maximum thickness of the Athabasca Group sandstone is 1500 m in four major depositional sequences separated by basin-wide unconformities. These transgressive sedimentary units were dominantly deposited in braided stream systems and commonly show cross-bedding (Ramaekers et al., 2007).

Over 90% of the basin's known uranium resources are located in a limited region near the eastern margin of the basin. The majority of deposits and prospects in the eastern basin are located where the Athabasca Group unconformably overlies the Wollaston-Mudjatik Transition Zone. The western Wollaston Domain consists of metasedimentary rocks of the upper amphibolite to lower granulite facies, whereas the eastern Mudjatik Domain is comprised of dominantly orthogneiss of the upper amphibolite facies. The Wollaston-Mudjatik Transition Zone contains mainly pelitic and psammopelitic paragneiss, with lesser quartzite and arkosic paragneiss that structurally overlie Archean orthogneiss and are intruded by pegmatite (Annesley et al., 2005). Many significant deposits in the eastern basin are also associated with structures related to the deformed and metamorphosed unconformable contact between Archean granitoid gneiss and the

late Paleoproterozoic basal graphitic pelitic gneiss of the Wollaston Supergroup (Sibbald et al., 1990; Jefferson et al., 2007a,b).

In the western portion of the Athabasca Basin, significant, but fewer, deposits have been discovered. Deposits and prospects in the Cluff Lake area were exposed by the central uplift of the Carswell meteorite impact structure. Like the deposits in the eastern basin, these sandstone-hosted and basement-hosted deposits (e.g., the western Athabasca Shea Creek, Maybelle River, Patterson Lake South) are associated with graphitic basement lithologies close to the basal unconformity of the Athabasca Group, as well as graphitic shear zones and supracrustal belts in the underlying basement (Carroll et al., 2006; Jefferson et al., 2007b; Quirt et al., 2012; Fission Uranium Corp., 2014).

Due to their close association with structures related to mineralization in both the eastern and western Athabasca Basin, and their recognizable geophysical signature, the graphitic basement units hosting these structures are important exploration targets. In the eastern basin, the graphitic units are low in the sedimentary stratigraphy of the Wollaston Domain. The protolith to the graphitic pelitic gneiss was unconformably deposited on Archean granitoid gneiss and forms the basal interface of the overlying Wollaston Supergroup. These graphitic lithologies were structurally weak zones against rheologically more competent material and were therefore a foci for deformation during regional ductile deformation and later brittle faulting. The graphite content of these lithologies allow their detection by electromagnetic geophysical surveys as conductors. Similar graphitic pelitic gneiss lithologies are present in supracrustal belts in the Taltson Magmatic Zone, such as in the Shea Creek area in western Saskatchewan (Jefferson et al., 2007b).

2.2 Local Geology

The Shea Creek unconformity-related uranium deposits, Anne, Colette, 58B, and Kianna, lie in northwestern Saskatchewan, approximately 300 km west of the high-grade uranium deposits in the eastern basin, 15 km south of the decommissioned Cluff Lake mine, and 30 km east of the Saskatchewan-Alberta border (Fig. 1). The Shea Creek area is underlain by metamorphosed Archean to Paleoproterozoic basement rocks of the Lloyd Domain, Rae Province. The Lloyd Domain is divided into "east" and "west" parts along the Clearwater magnetic high (Clearwater Domain). The high-grade metamorphic Lloyd Domain is composed of granulite facies pelitic to psammitic gneiss, metaquartzite, amphibolite, and ultramafic rocks (Card et al., 2007). Retrograde metamorphism to amphibolite and greenschist facies is commonly present. The Clearwater Domain, characterized by a regional positive magnetic trend, bisects the entire Lloyd Domain in a north-northeast direction. Clearwater Domain rocks consist of granitic gneiss, potassium-feldspar porphyritic gneiss, and equigranular granite. The strong magnetic signature is attributed to magnetite within the granitic gneiss (Card, 2002).

Unconformably overlying the crystalline basement are the late Paleoproterozoic to Mesoproterozoic (~1760-1500 Ma) clastic strata of the Athabasca Group. The strata are dominantly composed of flat-lying quartzose fluvial beds, with minor conglomerate and siltstone, comprising four major sequences. The oldest sequence, Sequence 1, consists of the coarse-grained conglomerate and pebbly quartz arenite of the Fair Point Formation. Sequence 2 in the western basin begins with the sandy Smart Formation, which is overlain by the Manitou Falls Formation. The Manitou Falls Formation is comprised of the conglomeratic Bird, sandy Collins and clay-intraclast-rich Dunlop members in the

east and center, the sandy Warnes Member in the southeast, and the pebbly sandy Raibl Member to the northeast. Sequence 3 includes the Lazenby Lake Formation (conglomeritic Hodge, sandy-muddy Clampitt, pebbly Shiels, and sandy Larter members), followed by the Wolverine Point Formation (mudstone-rich Brule and sandy Claussen members). The final sequence, Sequence 4, is comprised of the Locker Lake, Otherside, Douglas, and Carswell Formations, in ascending order. The Locker Lake Formation is comprised of the pebbly Snare, conglomeritic Brudell, and pebbly Marsin members, while the Otherside Formation consists of the pebbly Archibald and sandy Birkbeck members. Quartz arenite and carbonaceous mudstone comprise the Douglas Formation, while the Carswell Formation is comprised of stromatolite and oolite with minor basal siliciclastic interbeds (Ramaekers et al., 2007).

Athabasca Group rocks are generally undeformed, but sandstone matrix minerals (e.g., clay minerals) indicate that the Athabasca Group rocks have undergone high-grade diagenesis, with temperatures around 150-200°C. The preserved Athabasca Group formed the lower portion of a sequence whose thickness was much greater than the present ~1500 m. Fluid inclusion studies of the Manitou Falls Formation indicate that the sequence was deeply buried, to a maximum of 5 km during peak diagenesis (Hoeve and Quirt, 1984).

Mackenzie dyke swarm diabase dykes intruded both the Athabasca Group and underlying basement (Quirt, 1993; Hulbert et al., 1993). They are dominantly oriented northwest and range from a few meters to over one hundred meters in width. An east-west trending diabase dyke outcrops north of the Shea Creek area and, based on its Rb-Sr age of 1236 ± 38 Ma (Armstrong et al., 1988), likely belongs to the 1267 Ma

(Lecheminant and Heaman, 1989) Mackenzie dyke swarm. Devonian and Cretaceous strata overlie Athabasca Group sandstones along the southwest basin margin (Ramaekers, 1990); they are not included in the Shea Creek stratigraphy. Finally, the Athabasca region is covered with glacial drift, outwash, and lacustrine sands that form an undulating, lake-covered plain, with low relief. With Quaternary deposits covering the sandstone, in some places up to 90 m, there is generally very poor outcrop exposure (Quirt et al., 2012).

2.3 Deposit Geology

The deposits at Shea Creek lie along the NW-trending Saskatoon Lake Conductor (SLC) (Fig. 2), an EM conductor related to a reverse fault rooted in graphitic pelitic gneiss in the metamorphic basement. This fault is referred to as the "R3" fault (Carroll et al., 2006). The Kianna basement rocks are comprised of Lloyd Domain aluminous paragneiss and felsic gneisses, likely orthogneiss, as well as minor fine-grained mafic gneiss. The aluminous gneisses are subdivided into two units: a garnetite and an overlying pelitic (aluminous) gneiss sequence. The aluminous gneiss consists mainly of quartz + feldspar + biotite, with graphite. The unit is commonly associated with graphite-rich and/or pyrite-rich faults or graphitic shear zones. Quartz dissolution and Fe-Mg chlorite and kaolinite alteration commonly occur where these structural zones cut the aluminous gneiss (Quirt et al., 2012).

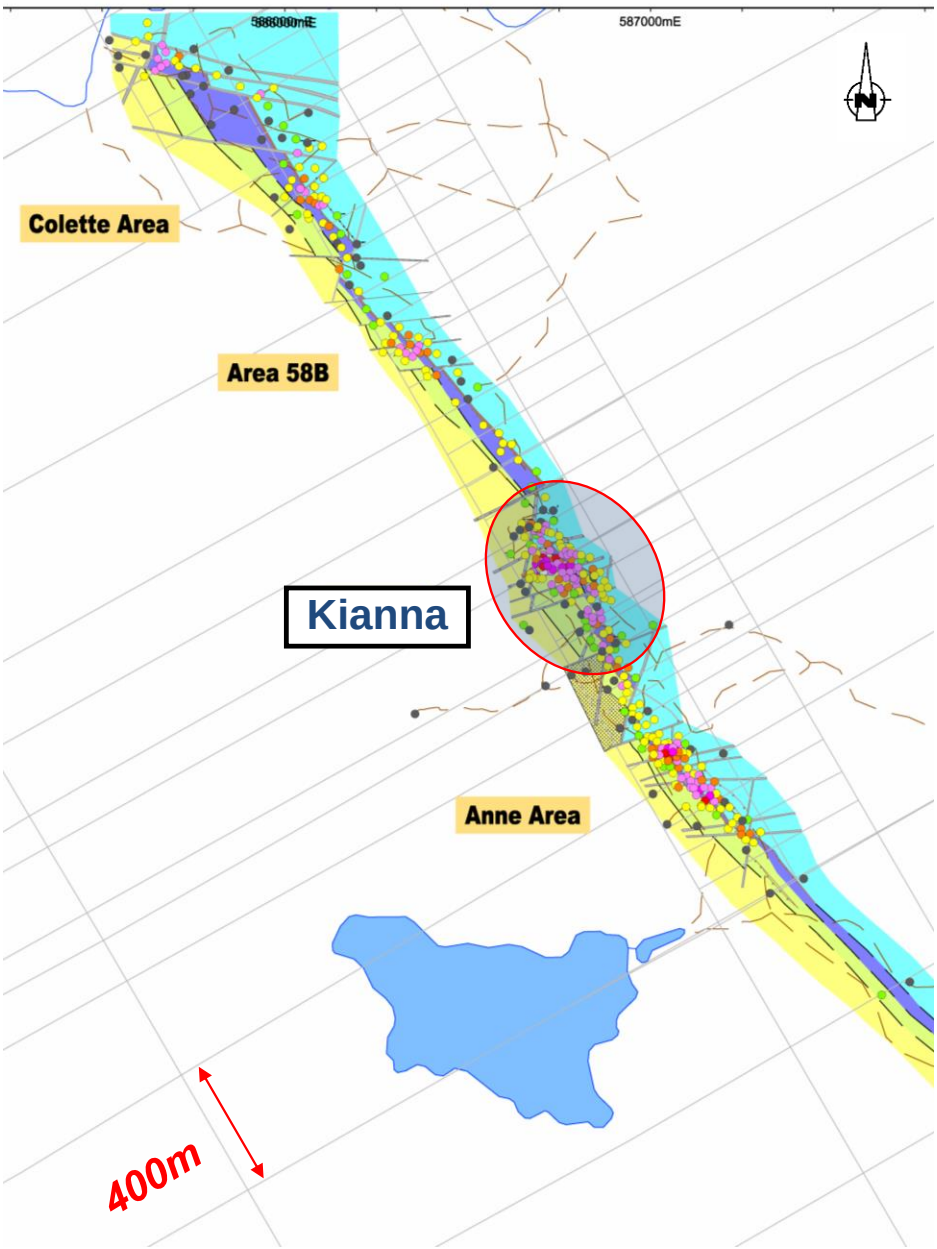

Figure 2: Plan map of the NW-trending Saskatoon Lake Conductor (SLC), a series of conductive graphite-rich faults associated with the four deposits at the Shea Creek Project (AREVA Resources Canada Inc., 2012)

The mafic gneiss is in sharp contact with the metapelite, occupying the upper part of the aluminous sequence only in the vicinity of the Kianna and 58B deposits, where it is chloritized with a glassy, soapstone appearance. The felsic gneiss underlies the aluminous and mafic gneisses, with fresh felsic gneiss consisting of quartz + feldspar ± garnet ±

biotite. However, alteration in much of the mineralized areas renders the original host rock unrecognizable (Carroll et al., 2006).

The host-rock alteration at the Shea Creek deposits is similar to that of the unconformity-type deposits in the eastern Athabasca Basin. The hydrothermal alteration at the Kianna deposit includes chloritization, hematization, illitization, kaolinization, silicification, and desilicification (Carroll et al., 2006; Quirt et al., 2012).

Chlorite alteration (i.e. sudoite and Mg-Fe chlorite) is associated with mineralized sandstone breccias and basement-hosted uraninite. Hydrothermal hematite is coeval with uraninite, occurring within a meter of mineralized pods, and is pervasive along well-developed redox fronts. Diagenetic hematite is disseminated throughout the sandstone and in the paleoweathered basement. Loss of diagenetic hematite due to reduction (i.e. bleaching) is common in the overlying sandstone above the deposits. Kaolinization widely occurs in the basement gneiss, replacing the entire rock mass as soft white clay. Hydrothermal kaolinized zones locally extend for tens of meters and frequently carry disseminated uraninite (Quirt et al., 2012).

The Kianna deposit hosts three distinct styles of mineralization:

1) Perched uraninite: massive to heavily disseminated, located within the sandstone up to tens of meters above the unconformity. The sandstone is often moderately to strongly chloritized and/or illitized.
2) Unconformity-hosted uraninite: massive to breccia-hosted, located just above, below, or at the unconformity in sandstone or shallow basement rocks. The host rock is generally illitized, chloritized, hematized, brecciated, and desilicified.

3) Basement-hosted uraninite: massive and vein-related, below the unconformity in the metamorphosed basement. Illite, sudoite, chlorite, kaolinite, and hematite alterations are common. There are two distinct basement-hosted pods of uraninite. The main pod is 50-175 m below the unconformity and will be referred to as "basement" uraninite. The other pod is deeper (230-240 m below the unconformity) and located to the east of the basement uraninite, and will be hereafter referred to as "lower basement" uraninite.

These styles of uranium mineralization have previously been described throughout the Athabasca Basin (Hoeve and Quirt, 1984; Wallis et al., 1985; Sibbald et al., 1990; Quirt, 2003), but the Kianna deposit is the first deposit described to host all three. The Kianna deposit uraninite pods and associated alteration are hosted in/around a transverse fault (Quirt et al., 2012). Movement of a jog in the fault caused a cavity to form, becoming a conduit for fluid-flow. Figure 3 shows a schematic SW-NE cross-section across the Kianna deposit with the approximate locations of original host rocks, structures, and uraninite pods projected together onto one cross-sectional plane.

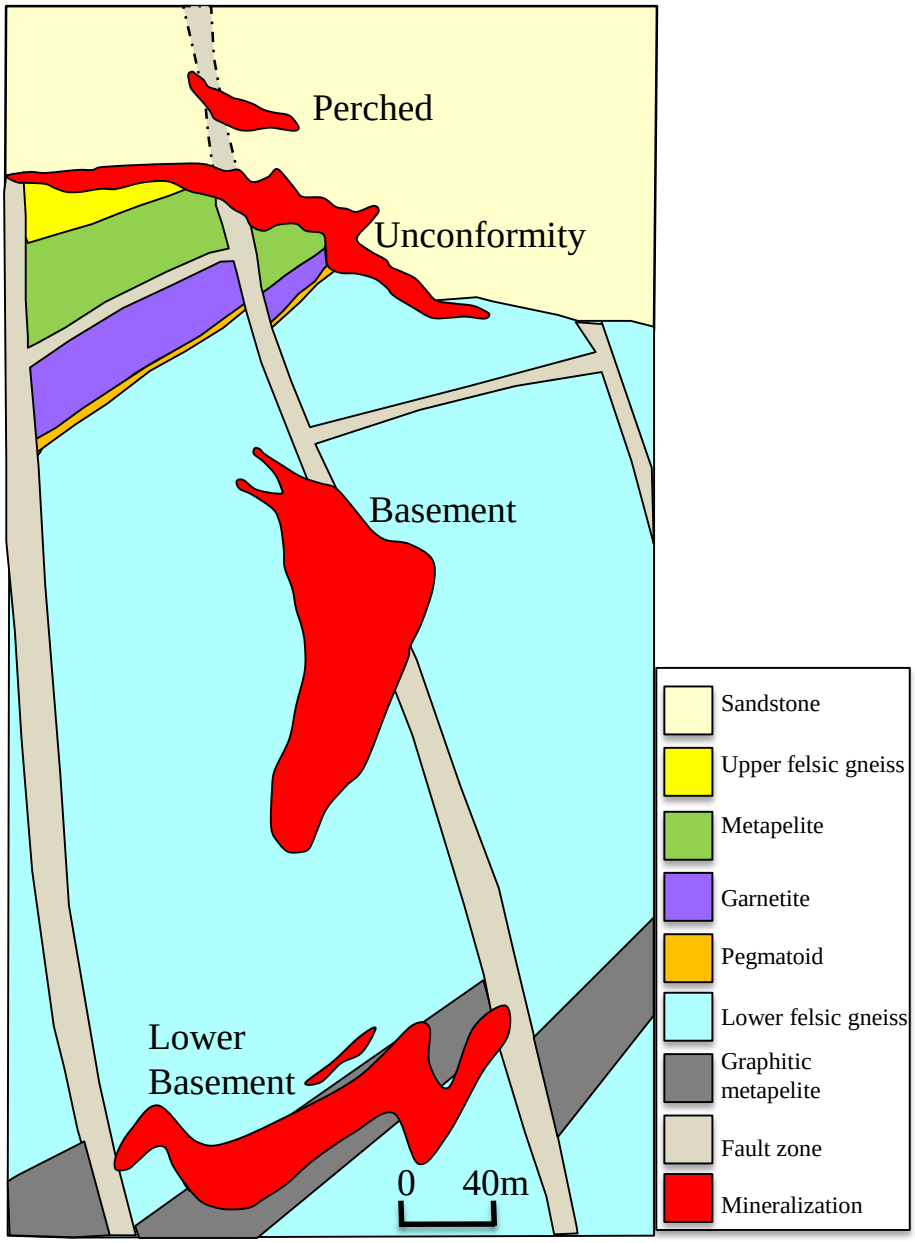

Figure 3: SW-NE cross-section of the Kianna deposit with approximate locations of uraninite pods, associated structures and original host rocks

Chapter 3: Sampling and Methodology

Forty-five uranium mineralized drill core samples were taken from 18 drill holes that intersected the Kianna deposit. Samples ranged from high-grade, massive uraninite to heavily-altered host rock containing minor uraninite and were selected from all three mineralized pods. Polished thin sections were prepared from these samples for analysis; thin section descriptions are included in Appendix A.

3.1 Optical Microscopy and Scanning Electron Microscope (SEM)

In order to develop a mineral paragenesis, the polished thin sections were examined for mineralogy and textures using a Nikon Eclipse 50i POL polarizing microscope, then carbon-coated and similarly examined at a smaller scale using a Cambridge Stereoscan 120 scanning electron microscope (SEM). The SEM was equipped with a back-scattered electron (BSE) detector and an energy dispersive x-ray spectroscopy (EDS) detector with digital-imaging capabilities. The BSE images were used to select areas of interest for subsequent electron probe microanalysis (EPMA).

3.2 Electron Probe Microanalysis (EPMA)

Thin sections were then characterized using a Cameca SX100 Universal EPMA. This instrument was equipped with a Princeton Gamma-Tech (PGT) EDS detector as well as five wavelength-dispersive spectroscopy (WDS) detectors. Quantitative microchemical analyses of various Kianna deposit minerals (e.g., uraninite, sulfides, silicates) were made with a 1-μm beam, an acceleration voltage of 15 keV, and 20 nA current. For analyses of muscovite and illite, a 5-μm beam was used. The following elements were quantified: Na, Si, U, Ca, Fe, Pb, Al, Th, S, K, F, Mg, Cl, P, Ti, V, Ni, Cu, As, Se, Zr, Sr, Ba, Co, Zn,

and rare earth elements (REEs). The standards used for quantifying these elements are outlined in Appendix B, Table B1. Detection limits were less than 1000 ppm for all elements except for U, Pb, Th, F, and REES. These elements had detection limits (in ppm) of ~3000, ~1200, ~1100, ~1000, and 1100-3000, respectively.

Chemical-lead (Pb) ages of uraninite grains were calculated using EPMA chemical compositions and the Cameron-Schiman (1978) equation:

$$t = Pb * 7550 / (U + 0.36Th) \quad (1)$$

where Pb, U, and Th are in wt% and t is given in years.

Chemical compositions obtained by EPMA for all minerals are included in Appendix B. Uraninite compositions, including calculated chemical-Pb ages, are presented in Table B2. EPMA data for silicates, clay minerals, and hematite is included in Table B3, and sulfide EPMA data is included in Table B4.

3.3 Secondary Ion Mass Spectrometry (SIMS)

In situ secondary ion mass spectrometry (SIMS) analyses were carried out on uraninite, muscovite, illite, pyrite, and chalcopyrite using a CAMECA 7f ion microprobe. Ions were detected with a Balzers SEV 1217 electron multiplier coupled with an ion-counting system using an overall deadtime of 28 ns.

3.3.1 Stable Isotopes

Sulfur isotopic analyses of chalcopyrite and pyrite were obtained using a ~10 nA primary beam of Cs^+, accelerated at 10 kV. The beam was focused to a 30 x 40 μm spot using a 100 μm aperture in the primary column, entrance slit of 220 μm, and mass resolving power of 347. A 250-volt sample voltage offset with electrostatic analyzer in

the secondary column set to -10 kV was used to eliminate molecular ion interferences. A typical analysis lasted ~7 minutes, comprising 50 cycles. The chalcopyrite internal standard, Trout Lake chalcopyrite from Flin Flon, Manitoba, has a true $\delta^{34}S$ value of 0.3‰ and spot to spot reproducibility of better than 0.5‰. The pyrite internal standard, Balmat pyrite from the Adirondack Mountains, New York, has a true $\delta^{34}S$ value of 15.1‰ and spot to spot reproducibility of better than 0.5‰.

SIMS hydrogen isotopic analysis of illite and muscovite were obtained using a ~25 nA primary beam of O^-, accelerated at 12.5 kV. The beam was focused to a 10 x 15 μm spot using a 750 μm aperture in the primary column. A 50-volt sample voltage offset with electrostatic analyzer in the secondary column set to +10 kV and a mass resolving power of 800 were used to eliminate molecular ion interferences. A typical analysis lasted ~13 minutes, with 90 cycles. The mica internal standard is MP-Mica from Pied des Mont, Quebec. It has a true δD value of -65‰ and spot to spot reproducibility of less than 1.0‰.

The oxygen-isotope compositions of illite, muscovite, and uraninite were measured using a ~2 nA primary beam of Cs^+. The beam was accelerated at 10 kV and focused to a 15 x 20 μm spot using a 100 μm aperture in the primary column. Similar to sulfur isotopic analysis, a 250-volt sample voltage offset with electrostatic analyzer in the secondary column set to -10 kV were used to eliminate molecular ion interferences. The entrance slits were set to 318 μm with a mass resolving power of 347. A typical analysis included 70 cycles and lasted ~10 minutes. The true $\delta^{18}O$ of the MP-Mica internal standard is 10.4‰ with spot to spot reproducibility of less than 0.9‰. The uraninite

internal standard is synthetic UO_2; it has a true $\delta^{18}O$ value of 8.1‰ and spot to spot reproducibility of less than 0.6‰.

During analyses by SIMS, a mass-dependent bias is introduced. This bias is known as instrumental mass fractionation (IMF) and will typically favor the light isotope. A number of processes contribute to IMF, the most influential of which are related to sample chemistry. For example, the relative ion-yields of two elements and their isotopes, such as U and Pb, may vary as a function of chemical composition, producing incorrect measurements of elemental and isotopic ratios. Therefore, isotopic analysis by SIMS requires calibration using a mineral standard that has similar chemical composition to the mineral of interest. The standard and minerals of interest were analyzed during the same analytical session. The value of the standard was used to correct for IMF using equation 2:

$$\alpha_{SIMS} = R_{SIMS}/R_{STD} \qquad (2)$$

where R_{SIMS} is the isotopic ratio (e.g., $^{18}O/^{16}O$, D/H, $^{206}Pb/^{238}U$) of the standard measured by SIMS and R_{STD} is the "true" value of the standard. The normalizing coefficient (α) was applied to the measured ratios from the minerals to obtain "true" isotopic ratios:

$$R_{TRUE} = \alpha * R_{SMPL} \qquad (3)$$

where R_{SMPL} is the measured isotopic ratio of the mineral of interest.

All stable isotope data are presented in the δ notation relative to the appropriate standard. Both hydrogen and oxygen are reported relative to Vienna Standard Mean Ocean Water (V-SMOW) in units of per mil (‰) and are calculated using equation 4:

$$\delta D \text{ or } \delta^{18}O\ (‰) = (R_{TRUE}/R_{V\text{-}SMOW} - 1) * 10^3 \qquad (4)$$

where R_{TRUE} is the ratio of the abundance of the heavy to the light isotope of the sample, which has been normalized to obtain "true" isotopic ratios (equation 3) and $R_{V\text{-}SMOW}$ is the ratio of the abundance of the heavy to the light isotope of the standard.

3.3.2 Radiogenic Isotopes

The analytical protocol for U-Pb isotopic measurements in uranium minerals using the CAMECA 7f is similar to that used by Fayek et al. (2002b). SIMS U-Pb isotopic analyses of uraninite were obtained using a ~5 nA primary ion beam of O^-, accelerated at 12.5 kV. The beam was focused to a 15 x 30 μm spot using a 750 μm aperture in the primary column. The sample accelerating voltage was +7.95 kV, with electrostatic analyzer in the secondary column set to accept +8.00 kV. This 50-volt offset suppressed hydride isobaric interferences. The entrance and exit slits were narrowed to obtain flat-top peaks, with the entrance slits set to 36.9 μm and a mass resolving power of 1300. The following species were detected sequentially by switching the magnetic field: ^{204}Pb, ^{206}Pb, ^{207}Pb, ^{208}Pb, ^{235}U, and ^{238}U. A typical analysis lasted ~8 minutes, comprising 40 cycles of analysis. Negligible common lead (^{204}Pb) was detected.

In uraninite, the fractionation of U/Pb isotope ratios vary as a function of Pb content, as Pb in the UO_2 structure affects the ionization of U during analysis by SIMS. Since the chemistry of the minerals of interest may vary among zones or between samples, a mass-bias model that accounts for variation in IMF with the mineral's chemical composition is necessary and can be developed using a suite of standards with varying chemical composition (i.e. calibration curve; Fayek et al., 2002b). Standards with varying weight percent (wt%) PbO were used to cover a large range of uraninite composition. Standard A has 20.7 wt% PbO, standard B has 12.7 wt% PbO, and standard C has 4.7 wt% PbO.

Standards were previously analyzed by thermal ionization mass spectrometry (TIMS) to obtain U-Pb ratios considered to be "true". Three standards and the minerals of interest were analyzed during the same analytical session. For each standard, the R_{STD} was plotted versus R_{SIMS} to construct a fractionation factor curve. A linear regression analysis produced equation 5:

$$R_{CORR} = m*R_{SMPL} + b \qquad (5)$$

where R_{CORR} is the corrected ratio for the mineral of interest, m is the slope of the curve, R_{SMPL} denotes the ratio of the mineral of interest obtained by SIMS, and b is the y-intercept.

Ratios corrected for mass bias (R_{CORR}) were used to calculate U-Pb isotopic ages using the ISOPLOT program (Ludwig, 1993).

Chapter 4: Results

4.1 Petrography and Mineral Paragenesis

The rocks that host uraninite at the Kianna deposit are heavily altered. The alteration forms extensive haloes around uranium mineralization, extending over 250 m vertically and up to 200 m laterally. Perched, unconformity, and basement-hosted mineralization each have their own mineral paragenesis and alteration mineral assemblage because of their disparate host-rock compositions. Figure 4A-C displays the mineral paragenesis for basement, unconformity, and perched mineralization, respectively.

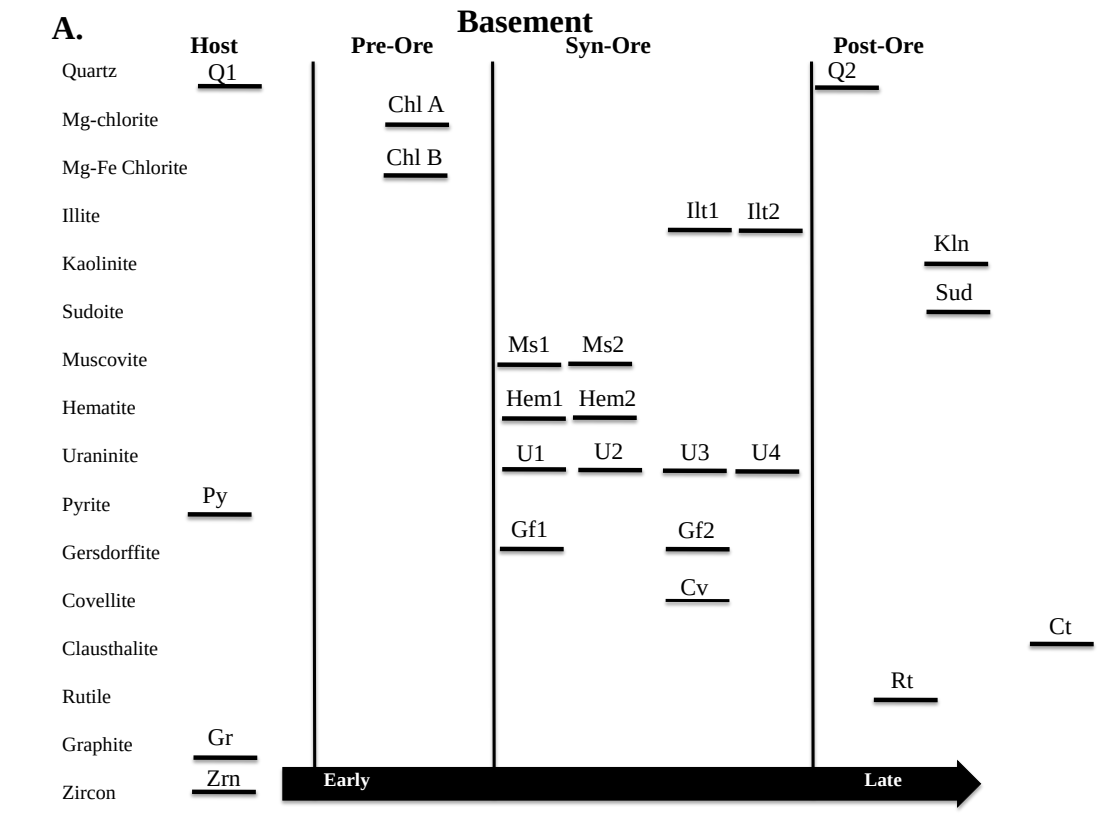
A.
Basement
Host
Pre-Ore
Syn-Ore
Post-Ore
Quartz
Mg-chlorite
Mg-Fe Chlorite
Illite
Kaolinite
Sudoite
Muscovite
Hematite
Uraninite
Pyrite
Gersdorffite
Covellite
Clausthalite
Rutile
Graphite
Zircon
Q1
Chl A
Chl B
Ilt1
Ilt2
Q2
Kln
Sud
Ms1
Ms2
Hem1
Hem2
U1
U2
U3
U4
Py
Gf1
Gf2
Cv
Ct
Rt
Gr
Zrn
Early
Late

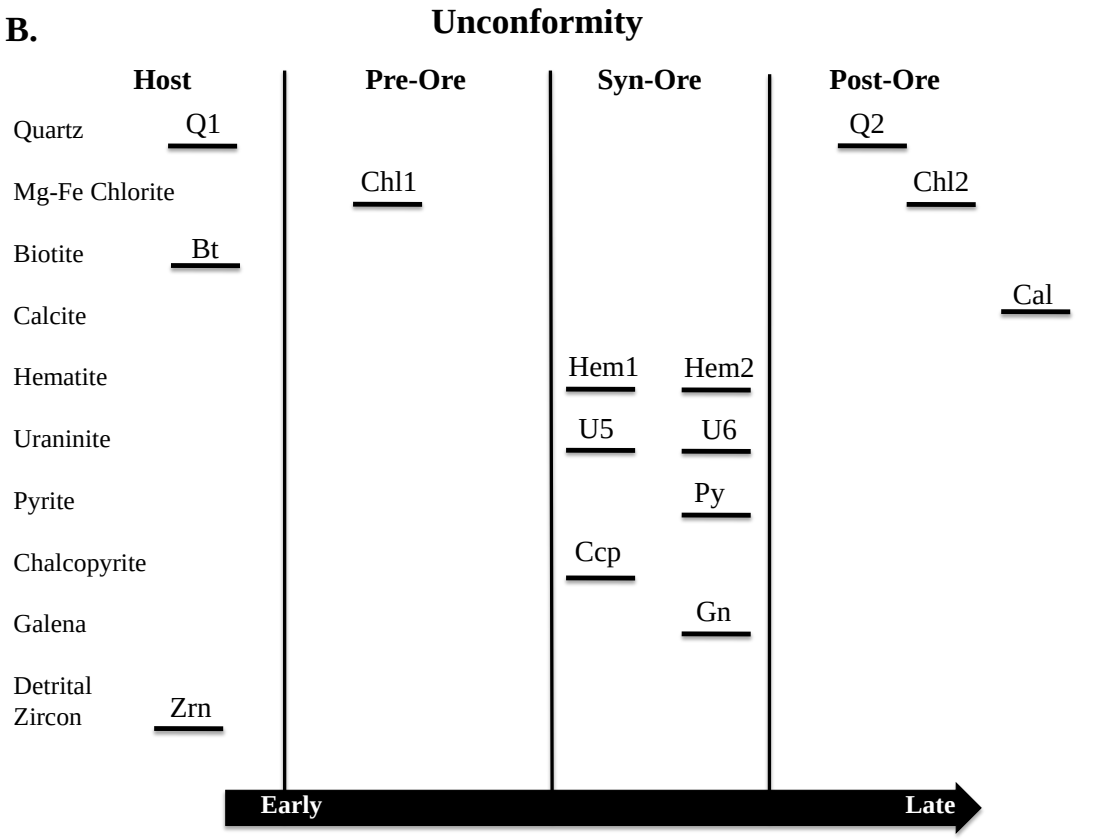
B.
Unconformity
Host
Pre-Ore
Syn-Ore
Post-Ore
Quartz
Mg-Fe Chlorite
Biotite
Calcite
Hematite
Uraninite
Pyrite
Chalcopyrite
Galena
Detrital Zircon
Q1
Chl1
Q2
Chl2
Bt
Cal
Hem1
Hem2
U5
U6
Py
Ccp
Gn
Zrn
Early
Late

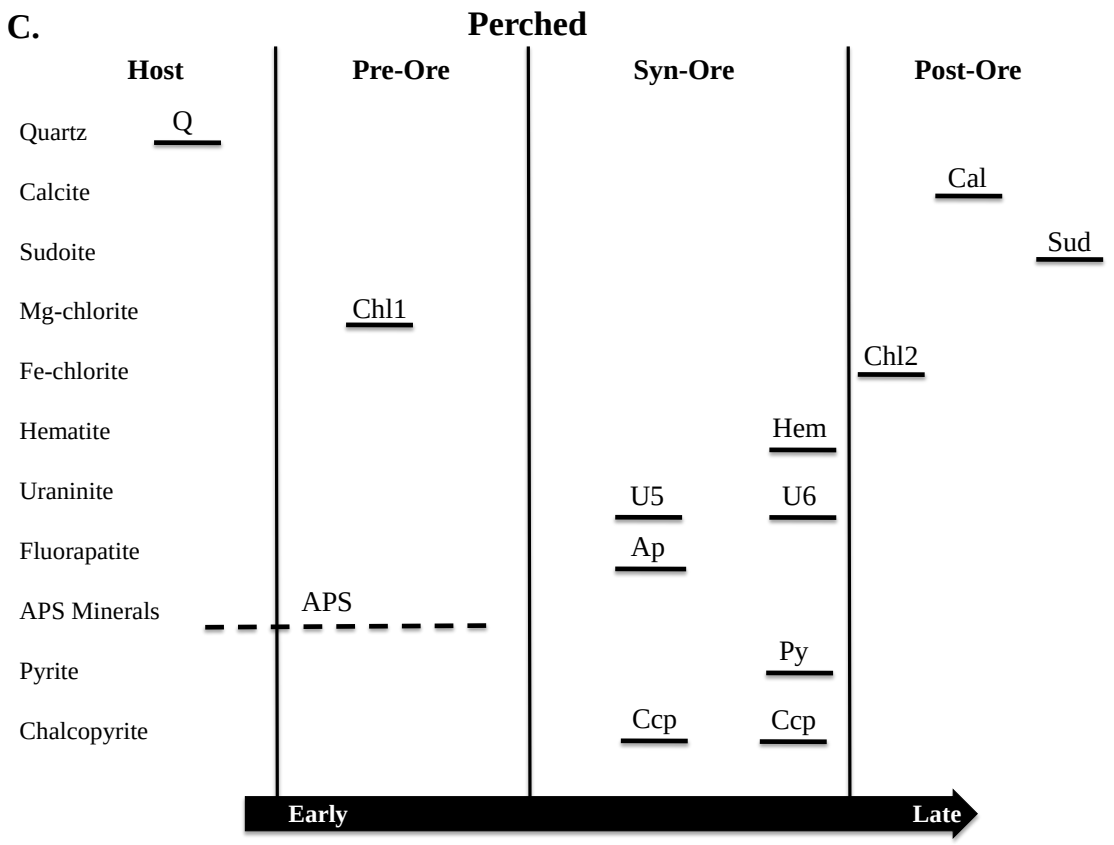

Figure 4: Mineral paragenesis for: A) basement-hosted mineralization below the unconformity, B) mineralization at the unconformity, hosted in sandstone and shallow basement meta-pelite, C) perched mineralization, above the unconformity hosted in Athabasca Group sandstone

Alteration styles observed in drill-core include argillization, hematization, bleaching, silicification, and de-silicification. Argillization results in the destruction of feldspars and ferromagnesian minerals and formation of clay minerals, and changes the rheology (reduces induration/increases friability) of the host rock. The resulting coloration is typical; pervasive light to medium green often indicates the presence of chlorite or sudoite, while off-white to white often indicates illite or kaolinite.

4.1.1 Basement

Basement uraninite is hosted in altered pelitic, mafic, and felsic gneisses. Original metamorphic host-rock minerals (e.g., feldspar, biotite, amphibole) are rarely preserved as they are commonly completely destroyed during argillization. Metamorphic host-rock

minerals observed include quartz (Q1), zircon (Zrn), and pyrite (Py). The pyrite is anhedral and corroded; grains range from <50 to 300 μm in diameter. Graphite blebs (Gr) occur in the meta-pelitic gneiss, and are associated with uraninite in both basement pods. These blebs range in size from 100 μm to up to 1 cm, with the larger blebs being associated with lower basement uraninite (Fig. 5A). Argillization of the metamorphic host rocks resulted in Mg-chlorite (Chl A) and Mg-Fe chlorite (Chl B).

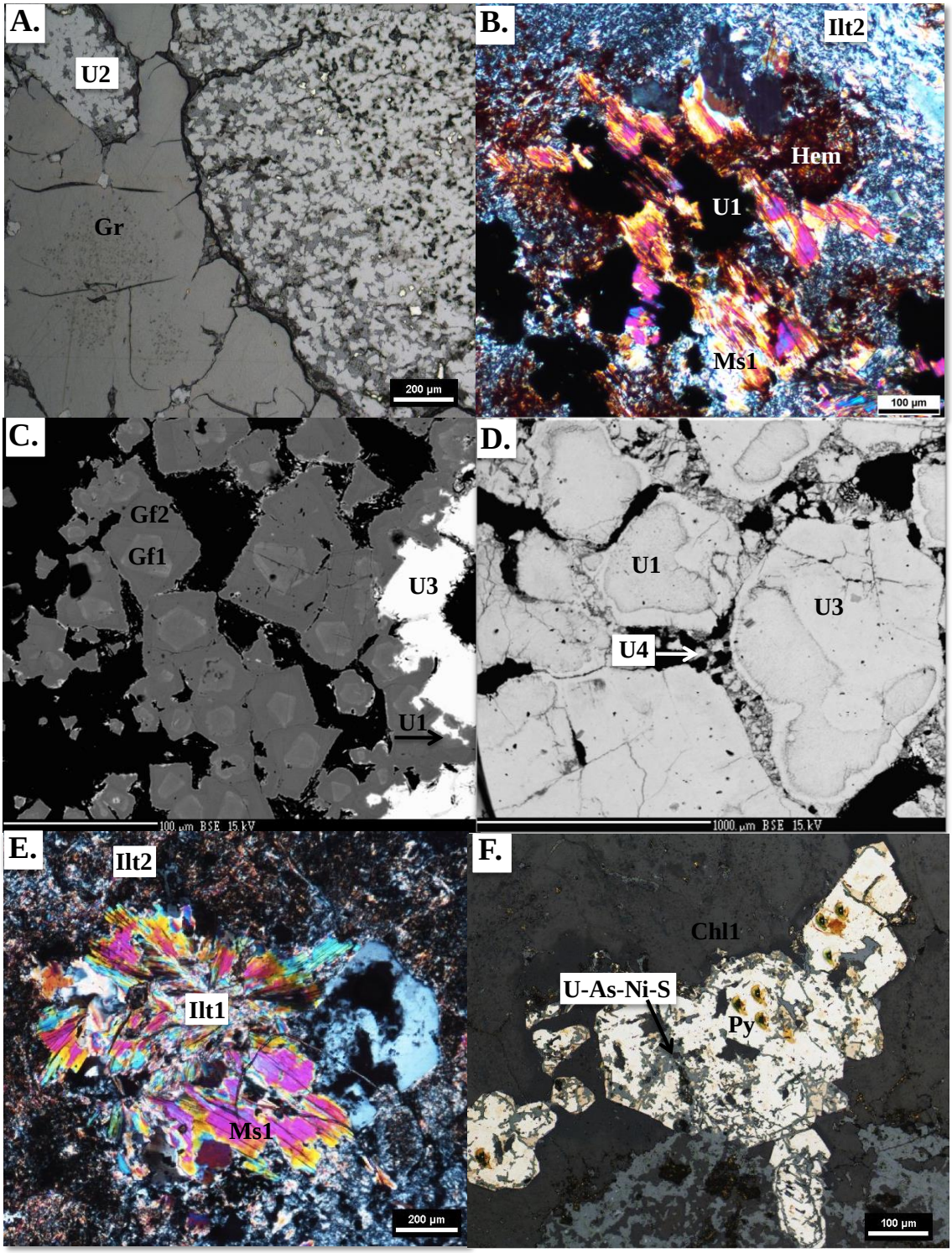

Figure 5: A) Reflected light photomicrograph of lower basement U2 and associated graphite, B) transmitted light photomicrograph of U1 with coeval muscovite and hematite, and later illite, C) BSE image of two generations of gersdorffite associated with U1 and U3, D) BSE image of basement-hosted U1, U3, and U4, E) transmitted light photomicrograph of muscovite altering to coarse-grained illite and late fine-grained illite, F) reflected light photomicrograph of altered metamorphic pyrite.

Stage 1 uraninite (U1) is intergrown with muscovite (Ms), hematite (Hem), and gersdorffite (Gf) (Figs. 5B and 5C). Muscovite grains are tabular with visible cleavage, and range in length from ~50 to 400 μm. Gersdorffite grains are subhedral and cubic. U1 is relatively unaltered, with <3 wt% SiO_2 + CaO. Stage 2 uraninite (U2) occurs in the lower basement pod in petrographic contact with muscovite and hematite, and replaces graphite blebs. It also has <3 wt% SiO_2 + CaO. Stage 1 uraninite (U1) is recrystallized to U3 (Fig. 5D). U3 has up to 5 wt% SiO_2 + CaO and is associated with coarse-grained illite (Ilt1). This illite replaces the tabular muscovite (Fig. 5E). Brecciated uraninite (U4) is anhedral, with grains up to 100 μm in diameter (Fig. 5D). U4 has up to 5 wt% SiO_2 + CaO and occurs with late, fine-grained illite (Ilt2).

Muscovite and coarse-grained illite can be indistinguishable in thin section. Similarly, fine-grained sericite and illite may have a similar appearance in thin section. Therefore, chemical compositions obtained by EPMA were used to calculate Si and K atoms per formula unit (apfu) to help distinguish between muscovite and illite (Fig. 6; Table B5 of Appendix B). Muscovite grains have ~1 K apfu whereas illite grains have ~0.75 K apfu. Figure 6 shows that many grains plot in proximity to ideal muscovite. Coarse-grained illite is more finely crystalline than muscovite but its chemical composition may plot within the muscovite field, as it approaches muscovite in mineral composition.

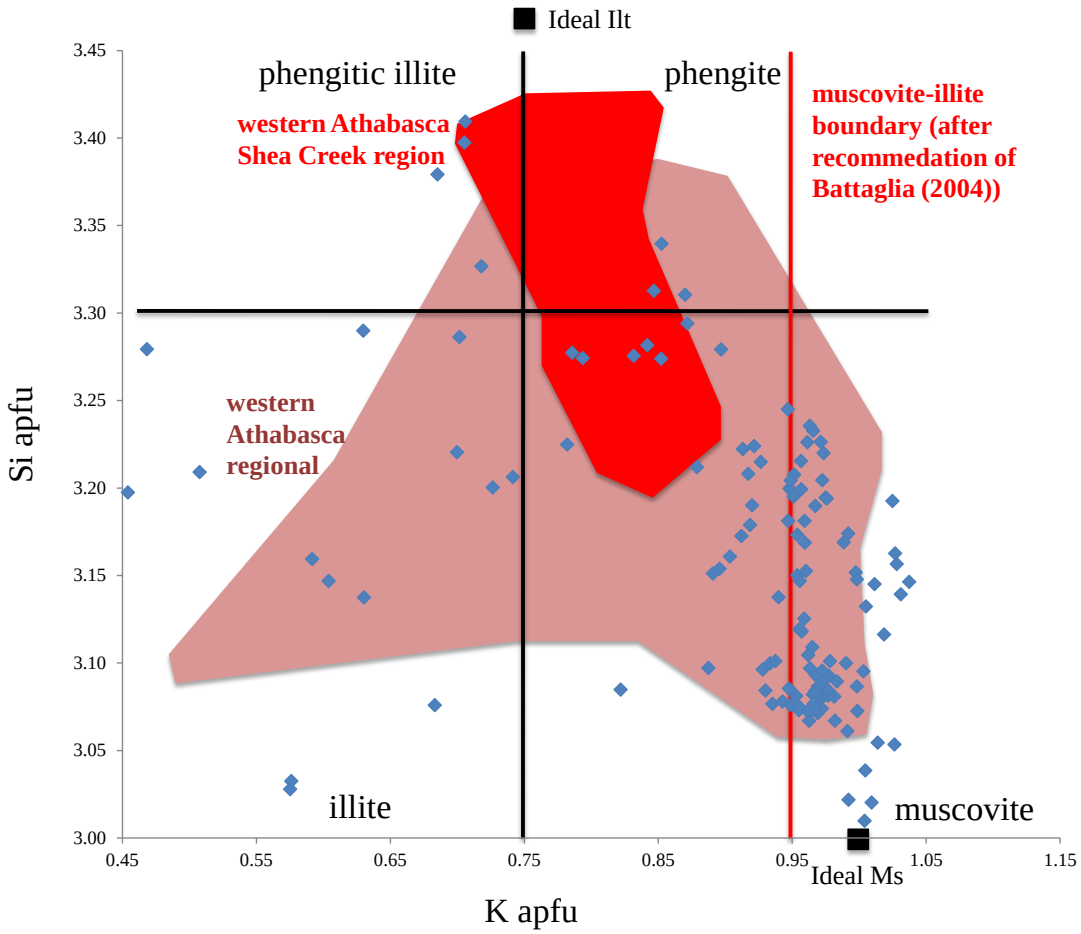

Figure 6: Calculated Si and K atoms per formula unit (apfu) for muscovite and illite from the Kianna deposit (blue diamonds; Table B5) are plotted along with the ideal muscovite and illite Si and K apfu values (black squares; Modified from Quirt, 2010). Also included are the Battaglia (2004) recommended muscovite-illite boundary and data from previous studies of Athabasca Basin muscovite and illite.

Syn-ore sulfide minerals include covellite (CuS) and gersdorffite ((Ni, Fe)AsS), and form at the expense of metamorphic pyrite. Covellite (Cv) occurs as thin veins near uraninite grains. There are two generations of gersdorffite (Gf); Gf1 is coeval with U1 and consists of NiAsS, whereas Gf2 is coeval with U3 and consists of (Ni, Fe)AsS. Figure 5C shows Gf2 rimming Gf1, with the gersdorffite precipitating along uraninite grain boundaries. The mineralizing fluid altered the metamorphic pyrite, leaching iron and sulfur (Fig. 5F).

Late hydrothermal alteration includes drusy quartz (Q2), kaolinite (Kln), sudoite (Sud), minor rutile (Rt), and very minor clausthalite (Ct). Kaolinite and sudoite formed at the expense of early chlorite. The clausthalite (PbSe) is infrequent and fine-grained (<25 μm), overprinting kaolinite and sudoite grains.

4.1.2 Unconformity

Uraninite at the unconformity is hosted by both the Athabasca Group sandstone and upper basement pelitic gneiss. Primary sandstone quartz (Q1) hosts detrital zircons (Zrn). Pelitic gneiss host rock minerals were largely destroyed during argillization, however minor biotite (Bt) remains. Argillization resulted in Mg-Fe chlorite (Chl1). Uraninite at the unconformity (U5) is intermixed with hematite (Hem1) and chalcopyrite (Ccp) (Fig. 7A) and occurs in veins (Fig. 7B). U5 has up to 7 wt% SiO_2 + CaO. Another generation of uraninite at the unconformity (U6) occurs with hematite (Hem2), pyrite (Py) and traces of galena (Gn). U6 also occurs in veins and relict botryoids (Fig. 7C) and is moderately altered, with up to 9.5 wt% SiO_2 + CaO.

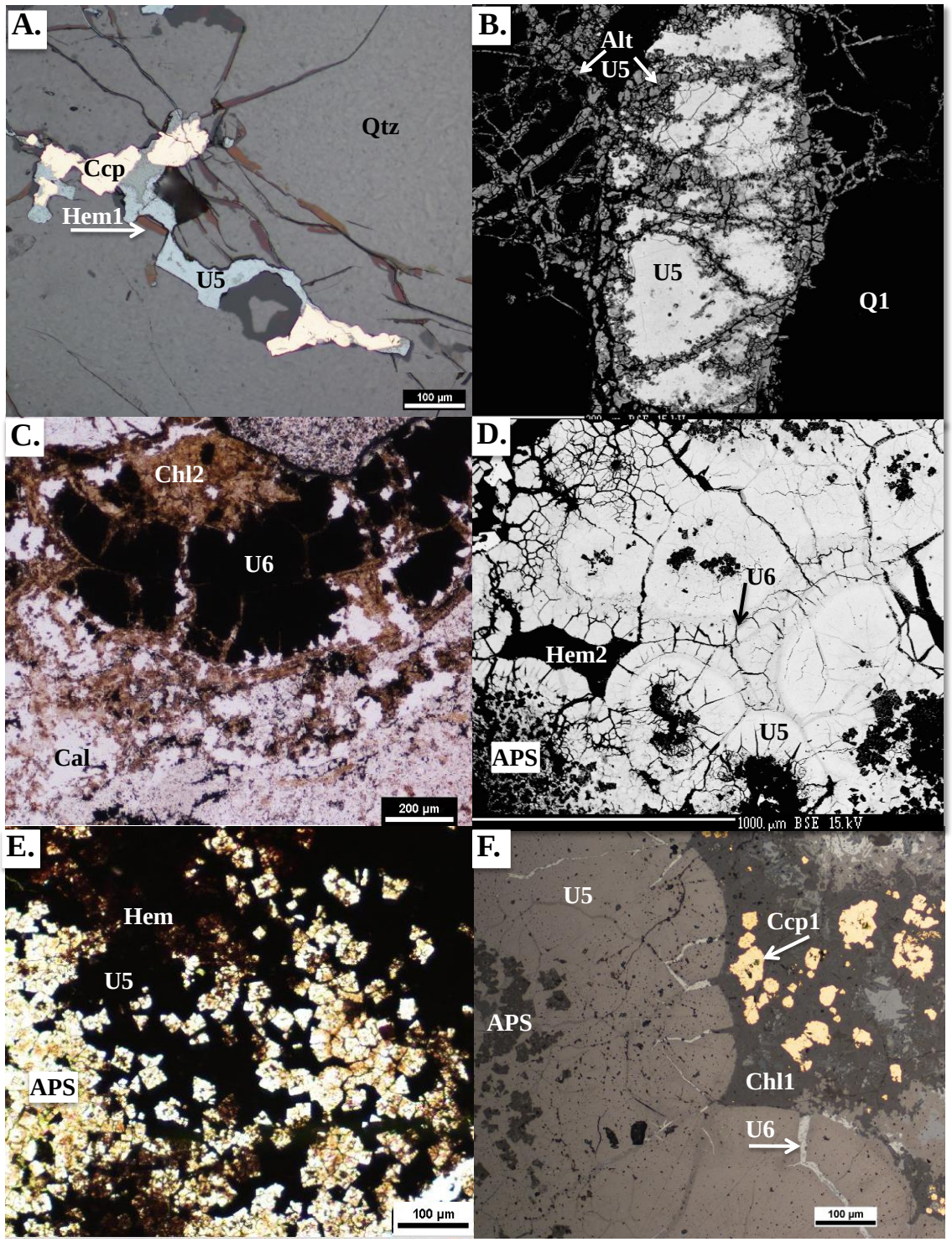

Figure 7: A) Photomicrograph of U5, Ccp, and Hem1 at the unconformity, B) BSE image of U5 at the unconformity and altered U5, C) photomicrograph of altered botryoidal U6 at the unconformity, D) BSE image of perched U5 altering APS minerals and U6 rimming U5, E) photomicrograph of APS minerals being altered by U5, F) photomicrograph of botryoidal U5 and associated Ccp.

Post-ore alteration includes quartz veins (Q2) and Mg-Fe chlorite (Chl2), which crosscuts uraninite (Fig. 7C). These late, Si-rich fluids likely contributed to the relatively high SiO_2 + CaO composition of uraninite at the unconformity. Late calcite (Cal) occurs in veins or as grains with triple junctions. The veins are observed cross cutting Q1 and Chl2.

4.1.3 Perched

The perched uraninite is hosted in Athabasca Group sandstone, which is dominantly comprised of quartz (Q) with interstitial Mg-chlorite (Chl1) and alumino-phosphate sulfate (APS) minerals. The quartz grains are well rounded and matrix-supported, with pre-ore Mg-chlorite replacing most of the matrix. APS minerals include goyazite, which is Sr-rich and rare earth element (REE) poor, generally 50 μm in diameter, and often pseudocubic. The APS mineral grains are highly fractured and corroded, and are replaced by uraninite (Figs. 7D and 7E).

Perched uraninite (U5) is syngenetic with fluorapatite (Ap) and chalcopyrite (Ccp) (Fig. 7F), with the fluorapatite forming at the expense of the APS minerals. Chalcopyrite grains are subhedral to anhedral and up to 100 μm in diameter. U5 is massive to botryoidal (Fig. 7F) in texture but can occur as disseminated grains. It has up to 5 wt% SiO_2 + CaO. Late perched uraninite (U6) is associated with hematite (Hem), chalcopyrite, and pyrite, and occurs in veins that crosscut U5 or rimming U5 botryoidal grains (Fig. 7D). It has higher SiO_2 + CaO contents (up to 7 wt%) relative to U5 uraninite.

Post-ore alteration includes veins of Fe-chlorite (Chl2) forming at the expense of hematite, as well as late sudoite (Sud) and calcite (Cal). Where sudoite occurs, it replaces original matrix minerals and pre-ore chlorite, and occurs as a very fine groundmass

among Q and disseminated sulfides. The calcite occurs as thin veins, cross cutting uraninite, hematite, and Fe-chlorite.

The SiO_2 + CaO wt% composition of uraninite can be an indication of uraninite alteration. For example, under reducing conditions, Si-rich fluids can alter uraninite to coffinite, which contains approximately 15 wt% SiO_2. Elevated concentrations of SiO_2 and CaO, suggestive of uraninite alteration, may indicate that the ages of uraninite grains have been reset during the alteration process. Uraninite incorporates very little to no Pb when it initially crystallizes; thus, Pb contained in ancient uraninite is almost exclusively radiogenic. However, incompatibility of Pb in the uraninite structure makes it susceptible to Pb loss; fluid and thermal events affecting uraninite after original formation may therefore result in complete or partial resetting of the U-Pb systematics (Fayek and Kyser, 1997). A plot of total SiO_2 + CaO weight percent versus the chemical Pb age (Fig. 8; Table B6 of Appendix B) shows that uraninites with younger chemical Pb ages (i.e. low Pb concentrations) have higher concentrations of SiO_2 and CaO.

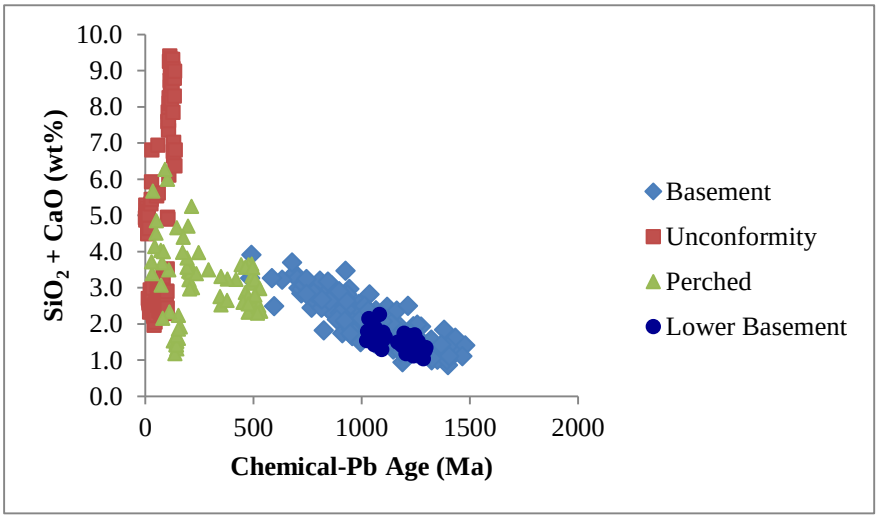

Figure 8: A plot of chemical lead (Pb) ages vs. weight percent (wt%) SiO_2 + CaO of uraninite (Data from Table B6).

4.2 Stable Isotope Geochemistry

4.2.1 Silicates, Clay Minerals, and Oxides

Muscovite, coarse-grained illite, and fine-grained illite were analyzed by SIMS to obtain $\delta^{18}O$ and δD values to characterize mineralizing fluids. Table 1 displays $\delta^{18}O$ data for muscovite, coarse-grained illite, and fine-grained illite. δD data for muscovite, coarse-grained illite, and fine-grained illite are displayed in Table 2. Appendix C includes all hydrogen (Table C1) and oxygen (Table C2) isotope data collected on muscovite, coarse-grained illite, and fine-grained illite, including standardization for each day of analyses. Muscovite and coarse-grained illite have consistent average $\delta^{18}O$ V-SMOW values of 0.7 ± 4.3‰ and 0.4 ± 4.1‰, respectively. However, muscovite δD values range from -20 ± 1.4‰ to -52 ± 1.3‰, with an average of -33 ± 12‰, whereas coarse-grained illite δD values range from -57 ± 1.0‰ to -103 ± 1.3‰, with an average of -79 ± 16‰. Late fine-grained illite from the basement rocks has an average $\delta^{18}O$ value of 6.5 ± 1.6‰ and δD values ranging from -112 ± 1.1‰ to -175 ± 1.7‰, with an average of -145 ± 21‰.

Table 1: Measured mineral $\delta^{18}O$ and calculated $\delta^{18}O$ values for fluids in equilibrium with muscovite, coarse-grained illite, and fine-grained illite

Muscovite mineral values		**Fluid values**	
$\delta^{18}O_{V\text{-}SMOW}$ (‰)	**1σ (‰)**	**$\delta^{18}O_{V\text{-}SMOW}$ (‰)**	**1σ (‰)**
-4.2	1.2	-4.2	1.2
-4.7	1.3	-4.7	1.3
-2.8	1.1	-2.8	1.1
1.3	1.1	1.3	1.1
2.5	1.2	2.5	1.2
1.2	1.3	1.2	1.3
-8.0	1.2	-8.0	1.2
2.8	1.2	2.8	1.2
3.9	1.2	3.9	1.2
3.2	1.2	3.3	1.2
5.6	1.2	5.6	1.2
3.5	1.2	3.5	1.2
2.3	1.2	2.3	1.2
0.4	1.1	0.4	1.1
8.3	1.2	8.3	1.2
-4.1	1.2	-4.1	1.2

Table 1(continued): Measured mineral $\delta^{18}O$ and calculated $\delta^{18}O$ values for fluids in equilibrium with muscovite, coarse-grained illite, and fine-grained illite

Coarse-grained illite mineral values		**Fluid values**	
$\delta^{18}O_{V\text{-}SMOW}$ (‰)	**1σ (‰)**	**$\delta^{18}O_{V\text{-}SMOW}$ (‰)**	**1σ (‰)**
0.4	1.1	-2.2	1.1
4.9	1.2	2.2	1.2
2.4	1.2	-0.3	1.2
4.6	1.2	1.9	1.2
0.7	1.2	-2.0	1.2
2.1	1.2	-0.6	1.2
-2.3	1.2	-5.0	1.2
-3.1	1.1	-5.8	1.1
-5.3	1.2	-7.9	1.2
-6.0	1.2	-8.7	1.2
5.9	1.2	3.2	1.2
Fine-grained illite mineral values		**Fluid values**	
$\delta^{18}O_{V\text{-}SMOW}$ (‰)	**1σ (‰)**	**$\delta^{18}O_{V\text{-}SMOW}$ (‰)**	**1σ (‰)**
6.2	1.2	-12.9	1.2
3.8	1.2	-15.3	1.2
8.2	1.2	-10.9	1.2
5.3	1.2	-13.8	1.2
6.4	1.1	-12.7	1.1
6.3	1.2	-12.8	1.2
5.5	1.2	-13.6	1.2
5.2	1.2	-13.8	1.2
3.5	1.1	-15.5	1.1
7.8	1.1	-11.3	1.1
4.9	1.1	-14.2	1.1
5.1	1.1	-14.0	1.1
6.5	1.2	-12.6	1.2
3.7	1.2	-15.4	1.2
9.2	1.2	-9.9	1.2
9.6	1.2	-9.5	1.2
6.7	1.2	-12.4	1.2
8.8	1.1	-10.3	1.1
9.2	1.2	-9.9	1.2
8.2	1.2	-10.9	1.2
7.0	1.2	-12.1	1.2
4.9	1.2	-14.1	1.2
5.9	1.1	-13.2	1.1
4.8	1.1	-14.3	1.1
4.9	1.1	-14.2	1.1
7.2	1.2	-11.8	1.2
6.6	1.2	-12.4	1.2
7.1	1.1	-12.0	1.1
8.3	1.2	-10.8	1.2
7.1	1.2	-11.9	1.2
7.6	1.1	-11.5	1.1
7.6	1.1	-11.4	1.1
6.5	1.2	-12.5	1.2

Table 2: Measured mineral δD and calculated δD values for fluids in equilibrium with muscovite, coarse-grained illite, and fine-grained illite

Muscovite mineral values		**Fluid values**	
$\delta D_{V\text{-}SMOW}$ (‰)	**1σ (‰)**	**$\delta D_{V\text{-}SMOW}$ (‰)**	**1σ (‰)**
-43	1.1	-14	1.1
-20	1.3	9	1.3
-20	1.4	10	1.4
-28	1.3	1	1.3
-26	1.3	3	1.3
-23	1.2	7	1.2
-22	1.3	8	1.3
-34	1.2	-4	1.2
-44	1.1	-15	1.1
-52	1.2	-22	1.2
-27	1.2	3	1.2
-52	1.3	-22	1.3
Coarse-grained illite mineral values		**Fluid values**	
$\delta D_{V\text{-}SMOW}$ (‰)	**1σ (‰)**	**$\delta D_{V\text{-}SMOW}$ (‰)**	**1σ (‰)**
-95	1.2	-107	1.2
-100	1.3	-111	1.3
-79	1.2	-90	1.2
-103	1.3	-115	1.3
-90	1.6	-101	1.6
-62	1.3	-74	1.3
-57	1.0	-68	1.0
-76	1.3	-87	1.3
-78	1.2	-90	1.2
-69	1.2	-80	1.2
-79	1.2	-91	1.2
-57	1.2	-69	1.2
Fine-grained illite mineral values		**Fluid values**	
$\delta D_{V\text{-}SMOW}$ (‰)	**1σ (‰)**	**$\delta D_{V\text{-}SMOW}$ (‰)**	**1σ (‰)**
-122	1.4	-77	1.4
-129	1.1	-83	1.1
-123	1.1	-77	1.1
-113	1.1	-67	1.1
-114	1.1	-69	1.1
-124	1.0	-78	1.0
-149	1.2	-104	1.2
-144	1.3	-98	1.3
-170	1.1	-125	1.1
-160	1.0	-115	1.0
-161	1.2	-116	1.2
-128	1.1	-82	1.1
-112	1.1	-67	1.1
-164	1.0	-118	1.0
-138	1.3	-93	1.3
-124	1.2	-79	1.2
-127	1.1	-81	1.1
-162	1.1	-116.	1.1
-168	1.1	-122	1.1
-140	1.1	-94	1.1
-142	1.1	-97	1.1
-166	1.6	-121	1.6

Table 2(continued): Measured mineral δD and calculated δD values for fluids in equilibrium with muscovite, coarse-grained illite, and fine-grained illite

Fine-grained illite mineral values		**Fluid values**	
$\delta D_{V\text{-}SMOW}$ (‰)	**1σ (‰)**	**$\delta D_{V\text{-}SMOW}$ (‰)**	**1σ (‰)**
-173	1.7	-128	1.7
-171	1.6	-126	1.6
-167	1.8	-121	1.8
-175	1.7	-130	1.7
-149	1.6	-103	1.6
-157	1.7	-111	1.7
-143	1.7	-98	1.7
-113	1.2	-67	1.2

The average $\delta^{18}O_{V\text{-}SMOW}$ values for perched, unconformity, and basement uraninite are -21.0 ± 2.3‰, -22.2 ± 1.1‰, and -21.8 ± 2.9‰, respectively (Table 3). Table C3 of Appendix C displays all uraninite oxygen isotope data, including standardization.

Table 3: Measured $\delta^{18}O$ values for uraninite hosted in the basement, at the unconformity, and perched above the unconformity

Mineralized Zone	Generation	$\delta^{18}O_{V\text{-}SMOW}$ (‰)	1σ (‰)
Basement	U1	-24.8	1.1
Basement	U1	-20.9	1.1
Basement	U1	-21.3	1.2
Basement	U1	-27.3	1.2
Basement	U1	-18.9	1.1
Basement	U1	-22.9	1.2
Basement	U1	-20.4	1.0
Basement	U1	-21.1	1.2
Basement	U1	-29.4	1.1
Basement	U1	-23.7	1.1
Basement	U1	-21.4	1.1
Basement	U1	-20.6	1.2
Basement	U3	-18.0	1.2
Basement	U3	-20.5	1.1
Basement	U3	-20.0	1.1
Basement	U3	-21.3	1.1
Basement	U3	-20.1	1.2
Basement	U3	-19.7	1.2
Unconformity	U5	-22.6	1.2
Unconformity	U5	-22.6	1.2
Unconformity	U5	-23.2	1.2
Unconformity	U5	-22.2	1.2
Unconformity	U5	-21.7	1.3
Unconformity	U5	-20.0	1.2
Unconformity	U5	-23.2	1.2
Perched	U6	-22.5	1.2
Perched	U6	-21.8	1.2
Perched	U6	-20.0	1.2
Perched	U6	-20.0	1.2
Perched	U6	-21.1	1.2
Perched	U6	-21.5	1.2
Perched	U6	-24.8	1.2
Perched	U6	-16.6	1.2

4.2.2 Sulfides

Pyrite and chalcopyrite from basement, unconformity, and perched samples were analyzed by SIMS to obtain $\delta^{34}S$ values (Table 4) and determine a source for the sulfur. Table C4 of Appendix C includes all sulfur isotope data collected, including standardization data for each day of analyses. Pyrite in the basement has $\delta^{34}S$ values ranging from 2.1 ± 0.3‰ to 4.7 ± 0.4‰. Chalcopyrite at the unconformity has $\delta^{34}S$ values that range from 2.0 ± 0.3‰ to 8.1 ± 0.3‰, whereas pyrite associated with

unconformity uraninite ranges from 15.1 ± 0.3‰ to 18.9 ± 0.3‰. Pyrite associated with perched uraninite has $\delta^{34}S$ values that range from 18.8 ± 0.9‰ to 25.4 ± 0.9‰, whereas chalcopyrite associated with perched uraninite has two distinct populations of $\delta^{34}S$ values, from -1.9 ± 0.3‰ to 6.9 ± 0.3‰ and from 16.3 ± 0.3‰ to 19.2 ± 0.3‰.

Table 4: Measured $\delta^{34}S$ values for metamorphic pyrite in the basement, pyrite and chalcopyrite associated with uraninite at the unconformity, and pyrite and chalcopyrite associated with perched uraninite

Zone	Mineral	$\delta^{34}S$ (‰)	1σ (‰)
Basement	Pyrite	2.1	0.3
Basement	Pyrite	2.7	0.3
Basement	Pyrite	4.7	0.4
Basement	Pyrite	2.6	0.3
Basement	Pyrite	2.5	0.3
Basement	Pyrite	4.3	0.4
Unconformity	Chalcopyrite	7.9	0.3
Unconformity	Chalcopyrite	7.4	0.3
Unconformity	Chalcopyrite	8.1	0.3
Unconformity	Chalcopyrite	3.2	0.3
Unconformity	Chalcopyrite	5.1	0.3
Unconformity	Chalcopyrite	2.0	0.3
Unconformity	Pyrite	17.2	0.3
Unconformity	Pyrite	17.6	0.3
Unconformity	Pyrite	16.4	0.3
Unconformity	Pyrite	18.9	0.3
Unconformity	Pyrite	17.7	0.3
Unconformity	Pyrite	15.1	0.3
Unconformity	Pyrite	18.9	0.3
Perched	Pyrite	21.0	0.8
Perched	Pyrite	21.4	0.6
Perched	Pyrite	25.4	0.9
Perched	Pyrite	18.8	0.9
Perched	Pyrite	22.4	0.6
Perched	Chalcopyrite	3.8	0.3
Perched	Chalcopyrite	1.5	0.3
Perched	Chalcopyrite	1.1	0.3
Perched	Chalcopyrite	5.9	0.3
Perched	Chalcopyrite	1.3	0.3
Perched	Chalcopyrite	3.0	0.3
Perched	Chalcopyrite	-1.9	0.3
Perched	Chalcopyrite	6.9	0.3
Perched	Chalcopyrite	18.2	0.3
Perched	Chalcopyrite	19.2	0.3
Perched	Chalcopyrite	16.8	0.3
Perched	Chalcopyrite	16.4	0.3
Perched	Chalcopyrite	16.3	0.3
Perched	Chalcopyrite	16.3	0.3
Perched	Chalcopyrite	17.1	0.3
Perched	Chalcopyrite	16.6	0.3
Perched	Chalcopyrite	16.8	0.3

4.3 Geochronology

In situ U-Pb isotopic analyses of basement, unconformity, and perched uraninite were obtained by SIMS (Table C5 of Appendix C). Data were obtained from the least-altered uraninite in the samples being studied (i.e. well-preserved grains with negligible common lead). Common lead (^{204}Pb) in the uraninite grains may generate older, inaccurate ages.

Uranium-lead isotope ratios, ^{206}Pb/^{238}U and ^{207}Pb/^{235}U, for the basement, lower basement, unconformity, and perched uraninite were plotted on Concordia diagrams. The SIMS U-Pb data used to plot the Concordia diagrams are provided in Table C6. The earliest age for the samples from U1 basement uraninite is 1495 ± 26 Ma (Fig. 9A). Samples from the lower basement pod of uraninite (U2) give an age of 1280 ± 30 Ma (Fig. 9B). Samples of recrystallized uraninite (U3) in the basement give an age of 1088 ± 22 Ma (Fig. 9C), while U4 in the samples of the basement uraninite formed at 855 ± 27 Ma (Fig. 9D). U-Pb data from samples of both the perched uraninite and the uraninite at the unconformity (U5) provide an upper intercept age of 739 ± 58 Ma (Fig. 9E). Samples of secondary uraninite (U6) from both the perched and unconformity pods give an age of 482 ± 11 Ma (Fig. 9F).

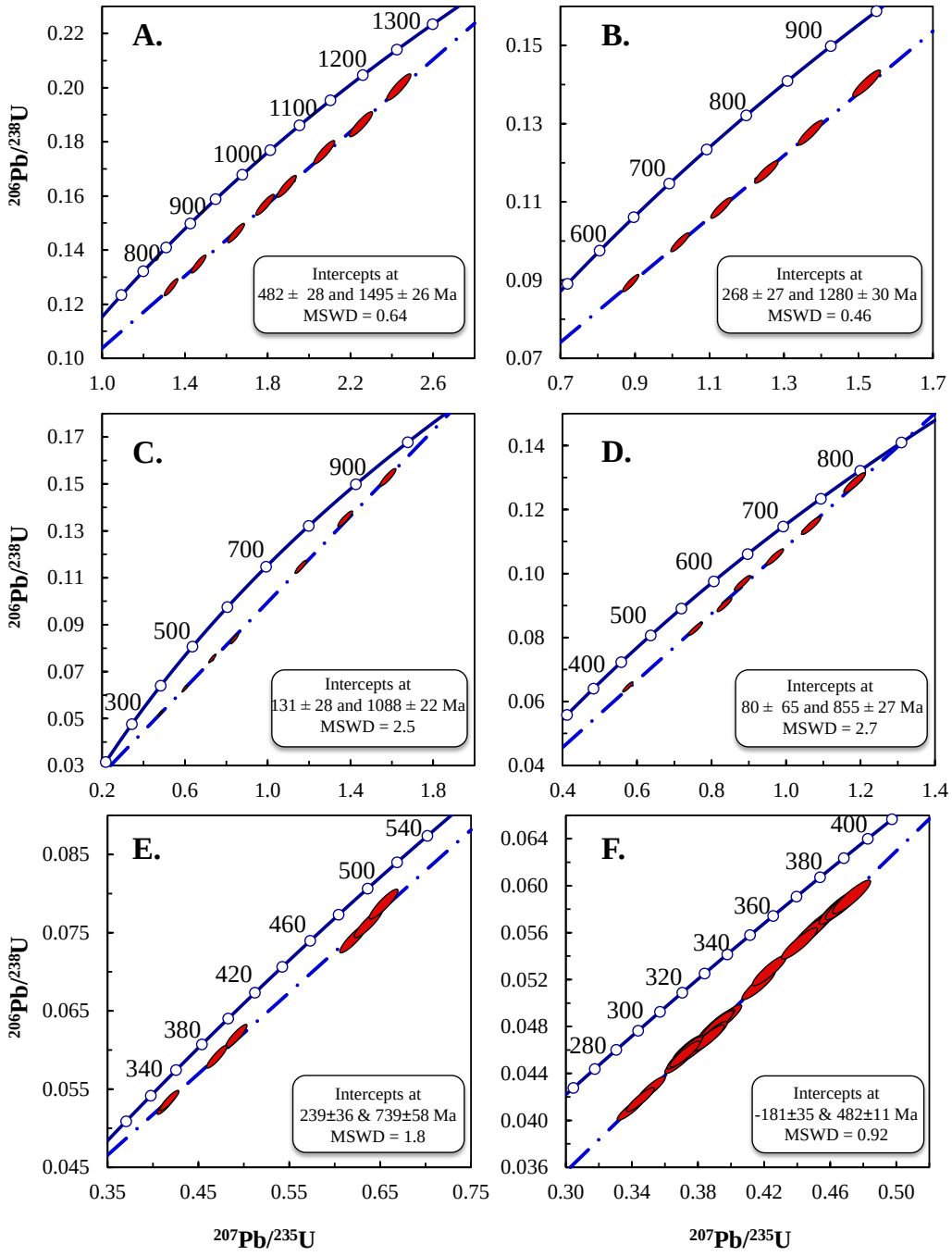

Figure 9: U-Pb Concordia diagrams where the upper intercept represents the minimum age of uraninite: A) basement-hosted primary uraninite, U1 B) U2 hosted in the lower basement, C) recrystallized basement uraninite, U3, D) U4 hosted in the basement, E) U5 hosted at and above the unconformity, and F) U6 hosted at and above the unconformity (Data from Table C6).

Chapter 5: Discussion

5.1 Characterization of the Mineralizing Fluids

The $\delta^{18}O$ values for all generations of uraninite from the Kianna deposit are similar and have an average value of -21.7 ± 2.5‰ (Table 3), which is similar to the oxygen isotopic composition of uraninites from eastern Athabasca deposits (Kotzer and Kyser, 1993; Fayek et al., 2002a; Fayek et al., 2010). At ~200°C, uraninite that precipitated from a basinal brine with an isotopic composition similar to SMOW should have a $\delta^{18}O$ value of approximately -10‰ (Fayek and Kyser, 2000). The anomalously low $\delta^{18}O$ values of uraninite from the Athabasca Basin are likely the result of meteoric water interaction with uraninite under reducing conditions (Fayek et al., 2002a). Oxygen diffusion in uraninite is orders of magnitude faster than in clay minerals and other silicates (Cole and Ohmoto, 1986; Fayek et al., 2011), which is why the oxygen isotopic composition of uraninite can be easily reset whereas clay and silicate minerals can retain their original oxygen isotopic composition. Uraninite-mineral (e.g., quartz, illite) oxygen isotope fractionation factors are often used to calculate isotope equilibrium temperatures; however, since the $\delta^{18}O$ of uraninite at the Kianna deposit has been reset, uraninite-mineral oxygen isotope fractionation factors cannot be used to calculate the equilibrium temperatures. Therefore, precipitation temperatures for muscovite and illite in the basement of the Kianna deposit were estimated using previously published temperatures for similar minerals with a similar paragenesis from eastern Athabasca uranium deposits (Kotzer and Kyser, 1995; Beshears, 2010).

Illite is a low-temperature mineral that forms at temperatures <300°C and generally between 0-150°C (Vidal et al., 2007). The oxygen isotopic composition of late-stage fine-

grained illites from the Kianna deposit plot between 25 and 50°C on Kotzer and Kyser's (1995) calculated isotherms (Fig. 10). Late, low temperature (~50°C) fluids have been reported at various deposits in the eastern Athabasca Basin. For example, the isotopic compositions of kaolinites from McArthur River and Key Lake indicate that they recrystallized in the presence of mid- to high-latitude, low temperature (<50°C) meteoric water descending along faults (Wilson and Kyser, 1987; Kotzer and Kyser, 1995). In addition, the equilibrium isotope temperature for late druzy quartz-uraninite veins from the Millennium deposit was calculated to be 50°C (Beshears, 2010). The temperature of formation for late fine-grained illite from the Kianna deposit is therefore estimated to be 50°C.

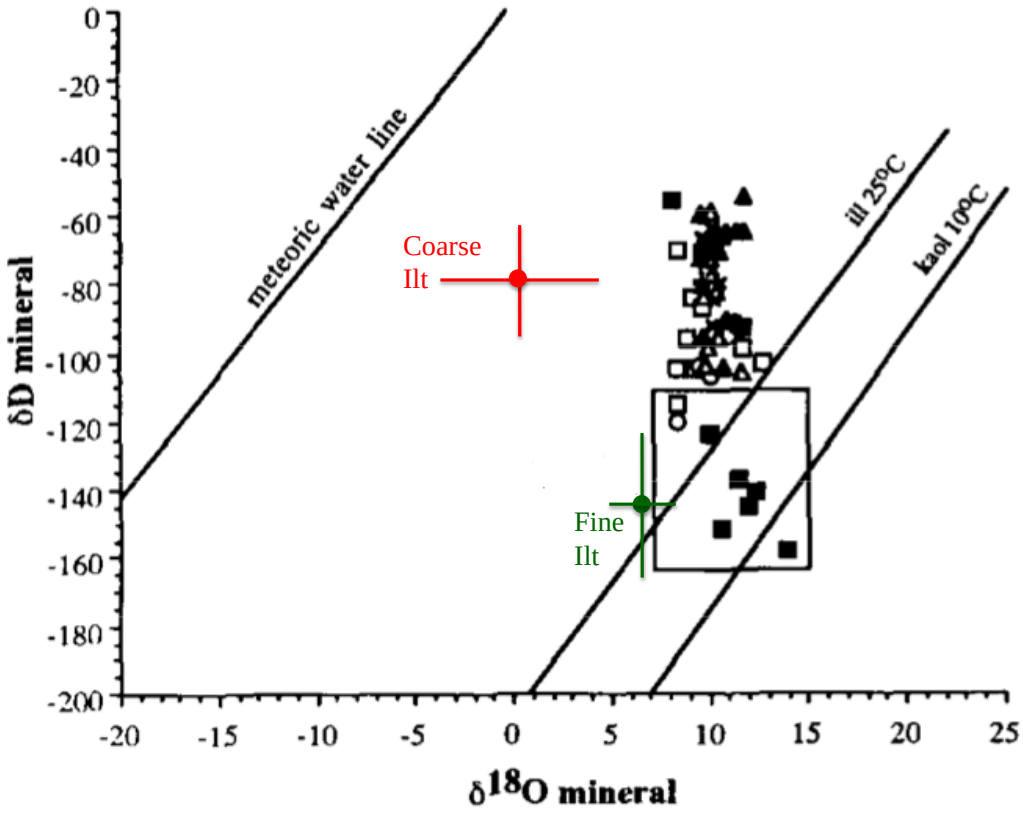

Figure 10: Measured $\delta^{18}O$ and δD mineral values (‰) for coarse-grained illite and fine-grained illite (modified after Kotzer and Kyser (1995). Also shown are Kotzer and Kyser's (1995) calculated illite and kaolinite isotherms and the meteoric water line.

The oxygen and hydrogen isotopic data for coarse-grained illites from the Kianna deposit plot well above the 25-50°C calculated isotherms (Fig. 10). The temperature of formation for coarse-grained illites was therefore calculated using the Battaglia (2004) illite geothermometer. Battaglia (2004) showed that the chemical composition of illite changes as a function of temperature, with progressive increase of K content as temperatures increase, and a correlation between Fe and Mg content. The relationship determined by Battaglia (2004) between temperature and K, Fe, and Mg apfu is presented in equation 7:

$$T\ (°C) = 267.95x + 31.50 \qquad (7)$$

where x = K + |Fe-Mg|. Chemical compositions obtained by EPMA were used to calculate the K, Fe, and Mg apfu.

Based on this geothermometer, the average calculated temperature of formation for the coarse-grained illite is ~270°C, with a range from 238°C to 323°C (Table B7 of Appendix B). The Battaglia (2004) geothermometer could not be used for the fine-grained illite, because the chemical composition of the fine-grained illite falls outside the range defined by the Battaglia geothermometer. The average K apfu of the illite in the Battaglia (2004) study is 0.78, which is consistent with the composition of the coarse-grained illite from the Kianna deposit.

Muscovite forms at temperatures >300°C and generally at temperatures above 350°C (Vidal et al., 2007). A recent model for fluid flow along structures by Weatherley and Henley (2013) based on complex quartz veins suggests that steep fluid temperature gradients can be localized along faults, where seismic activity drives large volumes of heated (200-400°C) fluid to flow along the faults and temperatures may exceed 400°C. Based on the Weatherley and Henley (2013) model, and the muscovite temperature of formation, we estimated that muscovite associated with uraninite from the Kianna deposits formed around 400°C.

Using these temperature estimates and the oxygen isotope illite-water fractionation factor by Zheng (1993) and the hydrogen isotope illite-water fractionation factor by Capuano (1992), the average $\delta^{18}O$ and δD values for water in equilibrium with late fine-grained illite from the Kianna deposit are -12.9 ± 2.1‰ and -99 ± 21‰, respectively. The average $\delta^{18}O$ and δD values for water in equilibrium with coarse-grained illite from the Kianna deposit are -2.3 ± 4.1‰ and -90 ± 16‰, respectively. The muscovite-water

oxygen (Zheng, 1993) and hydrogen (Suzuoki and Epstein, 1976) fractionation factors were used to calculate average $\delta^{18}O$ and δD values for the water in equilibrium with muscovite, which are 0.7 ± 4.3‰ and -3 ± 12‰, respectively. The calculated isotopic composition of the water in equilibrium with each mineral is distinct (Fig. 11). Based on these *in situ* data, and the difficulty involved in the separation of muscovite from illite, stable isotopic compositions of bulk illite or muscovite mineral separates (Alexandre et al., 2009a; Cloutier et al., 2009) need to be considered average values (Fig. 11).

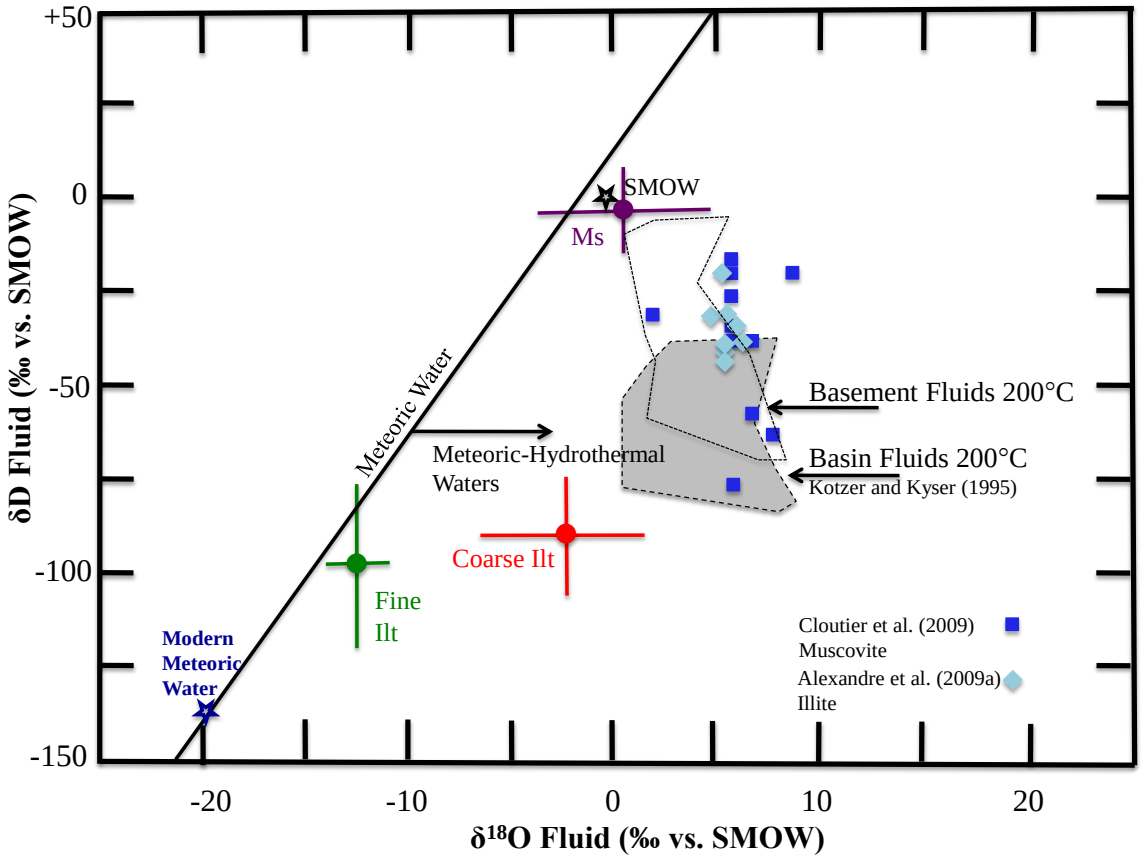

Figure 11: Calculated δD and $\delta^{18}O$ values of fluids in equilibrium with muscovite, coarse-grained illite, and fine-grained illite in the basement at the Kianna deposit (modified after Kotzer and Kyser (1995)). Also shown are the meteoric water line, the isotopic composition of standard mean ocean water (SMOW), the value of modern Athabasca Basin meteoric waters (Kotzer and Kyser, 1995), and data from previous Athabasca Basin stable isotope studies by Cloutier et al. (2009), Alexandre et al. (2009a), and Kotzer and Kyser (1995).

Figure 11 shows that the fluids in equilibrium with muscovite are isotopically distinct from the fluids in equilibrium with coarse- and fine-grained illite. Fluids associated with muscovite have an isotopic composition consistent with a marine source, fluids in equilibrium with coarse-grained illite have an isotopic composition consistent with hydrothermal fluids, and late fine-grained illite formed from fluids with an isotopic composition consistent with meteoric waters (Kotzer and Kyser, 1990, 1995).

The muscovite and basement-hosted uraninite are intimately intergrown and therefore paragenetically coeval (Fig. 5B). Although muscovite can be a metamorphic mineral, its isotopic composition suggests that it formed from or was overprinted by a fluid with an isotopic composition consistent with a marine source. This fluid penetrated deep into the basement rocks along faults. Muscovite only forms at temperatures >300ºC (Vidal et al., 2007). Based on equations from Crank (1975) and diffusion constants from Cole and Ohmoto (1986), muscovite grains would have to have been in isotopic equilibrium with the >300ºC fluid for at least one million years in order for the oxygen and hydrogen stable isotopic compositions to be overprinted. This would mean that the fault structures remained open to heated fluids for at least one million years, which is unlikely, as faults generally seal immediately after rupture (Claesson et al., 2007; Kame et al., 2014).

Whether the muscovite precipitated with U1 or was overprinted by the marine brine at the time of U1 formation, the muscovite isotopic composition has two implications: 1) a marine brine ingressed into the basement rocks and 2) early mineralizing fluids along faults could have reached temperatures >300°C. With the steep geothermal gradients associated with fault movement and hydrothermal fluid flow (Weatherley and Henley,

2013), brines were likely superheated during their ingress into the basement rocks along newly opened fault systems.

Muscovite is intergrown with U1 uraninite, which formed around 1500 Ma. Paleolatitude reconstructions of Laurentia for ca. 1500 Ma indicate that the paleolatitude of the Kianna deposit was approximately 20° (Fig. 12A, Pesonen et al., 2003). The muscovite associated with U1 formed from a fluid with the isotopic composition of seawater, which is similar to the isotopic signature of present day equatorial gulf coast brines (Kotzer and Kyser, 1995). Coarse-grained illite is coeval with U3, which crystallized ~1100 Ma. Paleolatitude reconstructions of Laurentia for ca. 1100 Ma indicate that at that time the Kianna deposit was at a mid-latitude, approximately 45° (Fig. 12B, Pesonen et al., 2003). This position corresponds with the evidence that the coarse-grained illite formed from a fluid with the isotopic composition of western Canada mid-latitude fluids (Kotzer and Kyser, 1995). The fluid compositions are therefore a reflection of the paleolatitude of the Kianna deposit at the time of mineral formation.

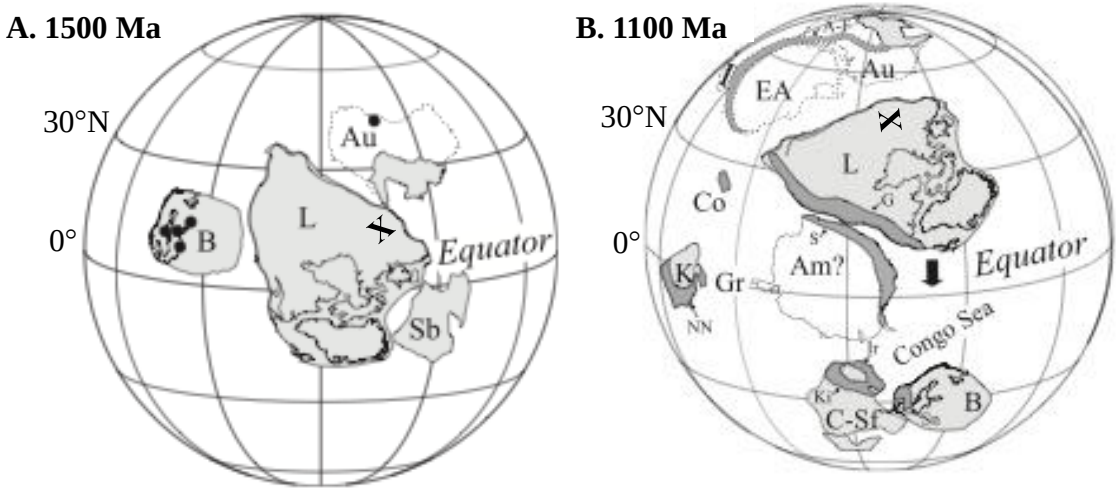

Figure 12: Paleolatitude reconstructions of Laurentia ca. 1500 Ma (A) and 1100 Ma (B), with the approximate location of the Kianna deposit at that time designated by "X" (modified from Pesonen et al., 2003).

The late-stage, low temperature fine-grained illite from the Kianna deposit is consistent with the ingress of late, low-temperature meteoric fluids that have been documented in deposits in the eastern Athabasca Basin (Wilson and Kyser, 1987; Kotzer and Kyser, 1995; Fayek et al., 2002a; Fayek et al., 2010). The meteoric fluids originate in the basin and descend along faults during fault reactivation (Kotzer and Kyser, 1995). The fluids overprint the oxygen isotopic composition of uraninite, and produce large clay mineral alteration envelopes (Wilson and Kyser, 1987; Fayek et al., 2002a).

Very few studies of the unconformity-related uranium deposits have reported sulfur isotopic compositions of sulfides associated with uranium minerals, such as Kotzer and Kyser (1990, 1992). Figure 13 is a plot of $\delta^{34}S$ values for common sources and reservoirs of sulfur, and the $\delta^{34}S$ values for basement, unconformity, and perched sulfides from the various pods of the Kianna deposit. Pre-ore pyrite in the basement has $\delta^{34}S$ values from 2.1 to 4.7‰, suggesting that sulfur was derived from a metamorphic or igneous source (Hoefs, 2004; Seal, 2006), likely part of the metamorphic basement mineral suite. Sulfides are also associated with both generations of unconformity and perched uraninite (i.e. U5, U6). The sulfur isotopic signatures of perched and unconformity sulfides are very similar. Pyrite associated with U6 has $\delta^{34}S$ values from 15.1 to 25.4‰. Chalcopyrite associated with U6 has $\delta^{34}S$ values from 16.3 to 19.2‰, whereas chalcopyrite associated with U5 has $\delta^{34}S$ values from -1.9 to 8.1‰.

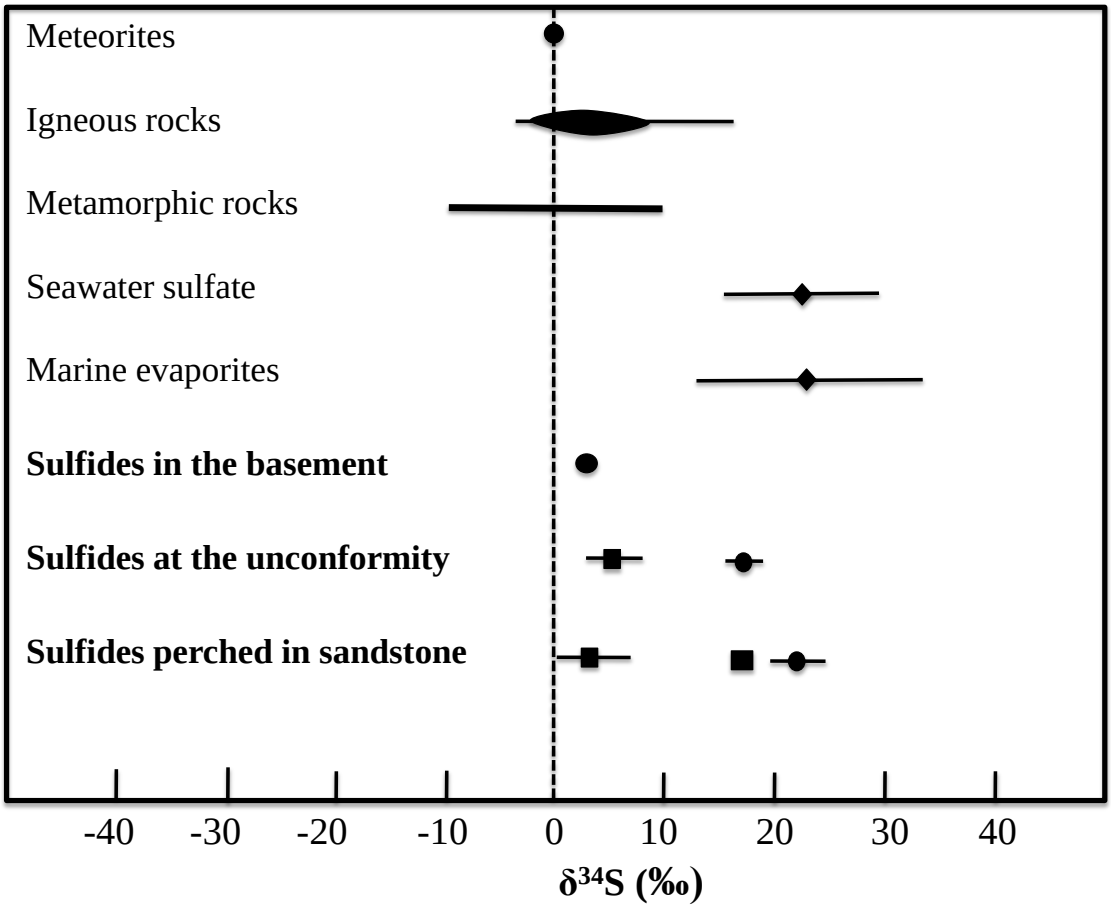

Figure 13: Measured $\delta^{34}S$ values (‰) for pyrite (circles) and chalcopyrite (squares) in each mineralized pod at the Kianna deposit. The data shown are average values with one standard deviation. Unconformity and perched sulfides are coeval with uraninite; values around 5‰ are associated with U5 whereas values around 20‰ are associated with U6. Also shown are $\delta^{34}S$ values for selected sources and reservoirs of sulfur (modified after Seal et al. (2000) with additional data from Hoefs (2004)).

These distinct populations of $\delta^{34}S$ values suggest that there were two sources of sulfur for these sulfide minerals: 1) the basement rocks and 2) the Athabasca Basin sediments. Possible sources of sulfur within the basin are the alumino-phosphate sulfate (APS) minerals, Proterozoic seawater sulfate, which had a sulfur isotopic composition of 16-32‰, (Chang et al., 2008) and/or Proterozoic evaporites that may have existed in the basin, which would have had $\delta^{34}S$ values from ~10-35‰ (Seal et al., 2000). APS minerals are commonly found in Athabasca Group sandstone (Hoeve and Quirt, 1984; Quirt et al., 1991; Gaboreau et al., 2007), and are closely associated with perched

uraninite and sulfides. There is no evidence for massive evaporites in the preserved part of the basin (Richard et al., 2011). However, the Athabasca Group sediments have been eroded from a thickness of ~5 km to ~1.5 km (Hoeve and Quirt, 1984; Ramaekers et al., 2007); thus, sediments potentially containing evaporites may have been removed by erosion and/or dissolution (Richard et al., 2011).

Kotzer and Kyser (1990) analyzed sulfide minerals that were spatially associated with uranium mineralization (e.g., gersdorffite and millerite from Key Lake and chalcopyrite from McArthur River). Their $\delta^{34}S$ data also showed that there were two isotopically distinct fluids: 1) a basement fluid with $\delta^{34}S$ around 0‰ and 2) a basinal fluid with $\delta^{34}S$ near 12‰. Their results were used to support an egress-style unconformity-related model for the formation of these uranium deposits, which included a basement fluid that equilibrated with basement sulfides mixing with the basinal brine at/around the unconformity. The $\delta^{34}S$ data from the Kianna deposit does not go as far as indicating that the sulfides formed from mixing between the basement fluid and basinal brine. Instead, the data shows that there were two sources of sulfur and therefore two distinct fluids: 1) a basement fluid that equilibrated with sulfides in the basement and egressed to the unconformity, where sulfides precipitated at and above the unconformity with $\delta^{34}S$ values around 5‰; and 2) a basinal fluid that equilibrated with APS minerals and/or possible basin sulfates and evaporites, generating sulfide minerals with $\delta^{34}S$ values around 20‰.

5.2 Geochronology and Tectonics

It is apparent from the preceding results that several tectonic events have influenced fault movement and fluid transport at the Kianna uranium deposit. The earliest age of primary basement uraninite is ~1500 Ma, which may have been related to the accretion of

juvenile crust to the south- and east-facing margins of Laurentia. This juvenile crust, the Granite-Rhyolite province, accreted over the 1.55-1.40 Ga period. Between 1.48 and 1.35 Ga, granites and associated anorthosites intruded the Granite-Rhyolite province as well as Paleoproterozoic crust farther to the west (Whitmeyer and Karlstrom, 2007). Therefore, this orogeny and related magmatism could have influenced fault movement and subsequent fluid flow in the western Athabasca Basin. The mineralization age of ca. 1500 Ma has also been previously reported in the eastern Athabasca basin, for example the "B magnetization event" that marks major uranium ore-forming events, such as at the Key Lake deposit (Kotzer et al., 1992). In addition, the Millennium and Cigar Lake deposits both have primary uraninite that generated ages of 1500-1400 Ma and 1461 Ma, respectively (Fayek et al., 2002a; Beshears, 2010).

From 1.3 to 0.9 Ga, continent-continent collisions and the assembly of supercontinent Rodinia affected Laurentia. During the Grenville orogeny, northwest-directed contraction at Laurentia's southern margin was accompanied by intracratonic extension and extensive mafic magmatism (Whitmeyer and Karlstrom, 2007). The 1.27 Ga (U-Pb) Mackenzie dyke swarm (Lecheminant and Heaman, 1989) was a significant magmatic event, which caused movement along deep structures and opened faults. The lower basement uraninite, U2, may be related to this magmatic event because it gives an age of 1280 Ma, similar to a SIMS U-Pb age for Shea Creek basement uraninite of 1281 Ma reported by Cuney et al. (2002). Previous studies have confirmed that the Mackenzie dyke swarm affected the Shea Creek area; a dyke that outcrops several kilometers north of the Shea Creek project was dated, using the Rb-Sr mineral isochron method, at 1236 Ma. The discrepancy between the 1236 Ma Rb-Sr age and the 1267 Ma U-Pb age is likely due to lower closure

temperatures for the Rb-Sr system in plagioclase and pyroxene and/or small disturbances of the Rb-Sr system (Armstrong et al., 1988).

Far-field tectonic stresses related to the Grenville orogeny and assembly of Rodinia have long been postulated to have caused fault movement and resetting of uraninite ages around 1100 Ma (e.g., Hoeve and Quirt, 1984) and they also may have caused the resetting of Kianna basement uraninite at ~1100 Ma. Secondary generations of uraninite ca. 1100 Ma have been widely reported throughout the Athabasca Basin. For example, Cloutier et al. (2009) reported a U-Pb age of 1091 Ma for the Millennium deposit. Boulanger (2012) reported a U-Pb age of 1188 for the west zone of the Roughrider deposit. Stage 2 uraninites from the McArthur River and Sue Zone deposits regressed together generated a U-Pb age of 1126 Ma (Fayek et al., 2002b). Stage 2 and 3 uraninites, coffinite, and calciouranoite from the Cigar Lake deposit when regressed together generated a U-Pb age of 1176 Ma (Fayek et al., 2002a). The Grenville orogeny appears to have affected the entire basin, causing fault movement and remobilization of fluids, as well as subsequent resetting of primary uraninite ages and/or precipitation of secondary generations of uraninite and uranium alteration minerals.

The break-up of supercontinent Rodinia began in western Laurentia between 850 and 750 Ma as east Gondwana and south China rifted away from western Laurentia (Condie, 2002). The rifting appears to have reactivated the fault systems at the Kianna deposit, resulting in precipitation of brecciated uraninite, U4, in the basement at ~850 Ma. Ages between 900-850 Ma have also been previously reported in the Athabasca basin. The “C magnetization event” occurred ca. 900 Ma (Kotzer et al., 1992) and stage 3 uraninites from the Cigar Lake deposit were dated at 876 Ma (Fayek et al., 2002a). Further rifting of

Rodinia led to the formation of the open western margin of Laurentia ca. 750-570 Ma (Nelson and Colpron, 2007). Fault movement associated with this rifting event may have led to fluid flow and the precipitation of U5 at and above the unconformity at ~750 Ma. The chemistry (Si and Ca contents) and age (~750 Ma) of U5 uraninite both perched in the sandstone and located at the unconformity are similar, suggesting that they either formed from the same fluid or were affected by fluids at ~750 Ma.

The fault systems at the Kianna deposit appear to have remained relatively inactive until they were reactivated by an event ca. 500 Ma. This event may have been related to the Carswell meteorite impact, which occurred <20 km to the northwest of the Kianna deposit. The Carswell impact structure has been variously dated using K-Ar and Ar-Ar methods and the ages reported range from less than 515 Ma to pre-Athabasca Basin (Bell, 1985; Genest et al., 2010). However, the younger ages are more common (e.g., Bell, 1985; Wanless et al., 1968). K-Ar studies by Wanless et al. (1968) on "Cluff Breccias" give an age of 485 Ma, which is considered to be the age of ultra-mylonitization produced by faulting during the late stages of the development of the Carswell structure. Ar-Ar studies by Bell (1985) give ages between 515-365 Ma, where most of the ages are between 440-500 Ma. These ages are similar to the U-Pb age for U6 unconformity and perched uraninite (~500 Ma), indicating that the there was a major fluid event that affected the western Athabasca Basin at ~400-500 Ma.

The age of primary uraninite at Cigar Lake, 1461 Ma, is within error of the age of primary uraninite at the Kianna deposit. However, primary uraninite at Cigar Lake is at the unconformity, and is much older than unconformity and perched uraninite at the Kianna deposit. The uraninite at the unconformity, U5, has an age of ~750 Ma. This may

be a reset age, as the uraninite has relatively high SiO_2 + CaO compositions and the grains are not pristine. Perched U6, however, occurs as overgrowths of new uraninite, which rim U5 grains. This indicates that the basin was not closed to oxidizing, uraniferous fluids ca. 500 Ma.

5.3 Genetic Model

5.3.1 Athabasca Basin Previous Studies

The Athabasca Basin unconformity-related uranium deposits in the eastern part of the basin have been extensively studied. Studies on deposits such as Midwest, Collins Bay, Rabbit Lake, McClean Lake, McArthur River, Cigar Lake, and Key Lake were used to develop the diagenetic-hydrothermal models for uranium mineralization (Hoeve and Sibbald, 1978a,b; Hoeve et al., 1980; Hoeve and Quirt, 1984, 1985, 1987, 1989; Wallis et al., 1985; Bruneton, 1987, 1993; Kotzer and Kyser, 1995; among others). Deposits such as Eagle Point, Rabbit Lake, Sue C, Millennium, and several of the Cluff Lake deposits are categorized as ingress-style deposits, whereas deposits such as Cigar Lake, Key Lake, Collins Bay, and Midwest are considered to be egress-style deposits (Quirt, 1989, 2003). In the ingress-style model, uraninite precipitated from fluid-rock interaction in which oxidizing basinal brine that percolated down basement structures reacted with the basement rocks, resulting in physiochemical changes to the fluid (e.g., lower fO_2). In the egress-style model, uraninite precipitated from fluid-fluid interaction between relatively reducing basement-derived fluid and oxidizing basinal brine at/around the unconformity. In both models, uraninite precipitation occurred at low temperatures (<250°C) and shallow depths (<5 km) (Hoeve and Quirt, 1984; Kotzer and Kyser, 1995; Fayek and Kyser, 1997; Hiatt and Kyser, 2006; Jefferson et al., 2007b; Cuney, 2009), and formed

the two deposit style end-members: 1) ingress-style fracture-controlled and breccia-hosted replacement ores, hosted in the sub-Athabasca metamorphic basement, such as Eagle Point and Rabbit Lake; and 2) egress-style clay-bounded, massive ore deposited along/around the unconformity and perched above the unconformity in the overlying sandstone, such as Key Lake, Cigar Lake, McClean Lake, and Midwest. The egress-style deposits may contain pods of ore at the unconformity and in the shallow basement rocks, such as at the Midwest deposit and the Deilmann deposit at Key Lake (Jefferson et al., 2007b).

The Kianna deposit has three distinct locations of uraninite pods similar to a variety of eastern Athabasca uranium deposits: (1) deep, basement-hosted ingress-style uraninite, such as at the Millennium deposit, (2) sandstone-hosted egress-style uraninite occurring at the unconformity and in pods perched above the unconformity, such as at the Midwest and Cigar Lake deposits, and (3) uraninite in the shallow basement rocks, similar to McArthur River Zone 2 ore (Fayek et al., 2010; Jefferson et al., 2007b; Alexandre et al., 2005). Therefore, to explain the formation of all three locations of uranium precipitation at the Kianna deposit, a genetic model that incorporates pulsed fluid flow along structures over several stages needs to be developed. The basic diagenetic-hydrothermal unconformity-related uranium metallogenic model containing only one of the ingress and egress styles alone cannot explain all of the characteristics of the Kianna deposit.

5.3.2 Structure Models

Sibson's (1992, 2001) fault-valve and suction pump models describe the movement of large volumes of fluid along faults. These models emphasize the dependence of fault failure on both stress and fluid pressure cycling. Fault reactivation may be induced by

rising shear stress, decreasing normal stress, or increasing fluid pressure. Two factors contribute to fault-valve behavior: 1) increased fluid pressures during crustal deformation and 2) high permeability of the newly opened faults immediately post failure. When compressional forces cause the fluid pressures in deeper rocks to be greater than the overlying rocks, the fluids move upwards along the newly opened, highly permeable faults from these overpressured areas. The fault then reseals due to hydrothermal deposition, increased frictional strength, and the cessation of stresses. The fault system goes through cycles of movement, opening, and sealing; the timing of these cycles is related to changes in stress, tectonic regime, and mineral deposition.

The flash vaporization model for hydrothermal deposition, developed by Weatherley and Henley (2013), can also be applied to the Kianna deposit. The Weatherley and Henley (2013) study was based on complex veins of gold-quartz that recorded fluid flow events caused by seismically induced successive fault failures. Before an earthquake occurs, fluids proximal to faults are under high-pressure and fill fractures (Fig. 14A). During an earthquake, extensional forces and movement of a fault jog can open a cavity in the fault, which causes a sudden drop in pressure, and the fluids flow down the newly opened cavity (Fig. 14B). Localized steep geothermal gradients are common in active fault systems, and seismic activity drives large volumes of heated (200-400°C) fluid to flow along the faults. At the Kianna deposit, locally steep geothermal gradients superheated brines during their ingress into the basement rocks along fault systems.

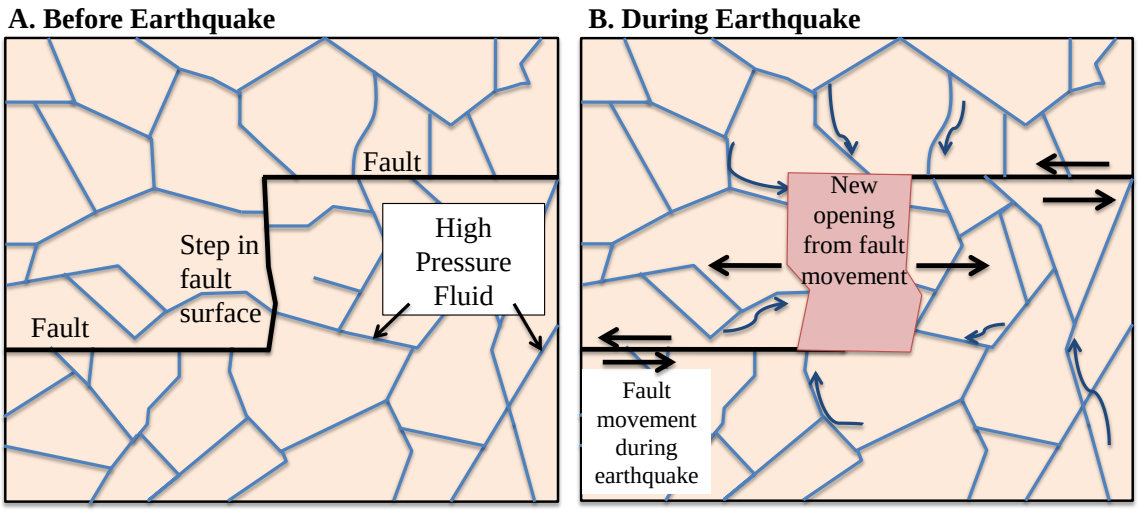

Figure 14: Plan-view schematic representation of a fault jog before an earthquake (A) and during an earthquake (B) where high-pressure fluids flow down a newly opened fault cavity (modified from Craw, 2013).

Cui et al. (2012) developed a model for fluid flow and the formation of unconformity-related uranium deposits. The study indicated that during periods of tectonic activity, reactivation of pre-existing basement structures and opening of new faults led to deformation-dominated fluid flow. Cui et al. (2012) suggest that during extensional deformation, the basement experiences a faster pressure reduction than the sedimentary cover, causing oxidizing basinal brines to flow down into the basement along faults and precipitate basement-hosted deposits. Conversely, during compressive deformation, a more rapid accumulation of pore pressure occurs in the basement, resulting in reducing fluids moving up from the basement along faults into the overlying sediments, and deposits hosted in the sandstone to precipitate.

5.3.3 Kianna Deposit Model

The model for the Kianna deposit combines aspects of the original diagenetic-hydrothermal (ingress-egress) model as well as the Sibson (1992, 2001), Weatherley and

Henley (2013), and Cui et al. (2012) fault models. The genetic model for the Kianna deposit at Shea Creek includes the following stages:

1) Tectonic activity related to the accretion of the Granite-Rhyolite province (1.55-1.40 Ga) and associated magmatism caused fault propagation to form a jog in the Kianna deposit transverse fault. Opening of the fault jog created a drop in pressure, which allowed oxidizing marine brine to move down the fault and into the basement rocks. Fault activation caused localized, high geothermal gradients that superheated the fluids moving along the faults (Fig. 15). The oxidizing, marine brine interacted with the basement rocks, which caused physiochemical changes to the fluid (e.g., lower fO_2). Ingress-style uraninite, muscovite, and hematite precipitated in basement rocks at ~1500 Ma (Fig. 15A). The presence of muscovite indicates that the fluid was >300°C. Mineral precipitation in this basement-rooted fault and increased frictional strength caused the fault to self-seal.

2) Magmatism associated with the Mackenzie dyke swarm caused faults and deep structures to be re-activated. Around ~1280 Ma, oxidizing brine ingressed into the lower basement along fault structures and either completely reset pre-existing uraninite, remobilized uraninite along the structures to more reducing regions, such as graphitic pelitic gneiss units, or brought additional uranium from the basin and precipitated uraninite similar to stage 1 (Fig. 15). This ingress-style uraninite (Fig. 15B) is also associated with muscovite and hematite. Once again, after the uraninite and associated hydrothermal minerals formed, the fault sealed.

3) Far-field stresses associated with the Grenville orogeny and assembly of Rodinia reactivated structures in the Kianna area and Athabasca basinal brine flowed down the fault. Basement-hosted uraninite was recrystallized at ~1100 Ma (Fig. 15A) and coarse-grained illite precipitated.

4) Extensional stresses related to the rifting of east Gondwana and south China from western Laurentia caused the fault to re-open and low-temperature meteoric fluids to flow down the fault around ~850 Ma. The $\delta^{18}O$ values of the earlier uraninite were overprinted, and fine-grained illite and uraninite precipitated (Figs. 15A and 15B). The precipitation of uraninite indicates that these fluids became reducing. A large amount of fluid was involved in this event, as fine-grained illite is the dominant alteration mineral in the basement of the Kianna deposit. Residual reducing fluid was trapped in the basement when the fault re-sealed.

5) The formation of the open western margin of Laurentia ~750 Ma reactivated the Kianna deposit faults. Compression and high fluid pressure in the basement rocks caused the reducing basement fluids to move upward along the fault (Fig. 15), until they interacted with uraniferous, oxidizing basinal fluids at the unconformity and egress-style uraninite precipitated at the unconformity (Fig. 15C) with hematite and chalcopyrite. Some of the reducing fluids continued up the fault above the unconformity within the sandstone where they interacted with the APS mineral-bearing intervals and precipitated uraninite (Fig. 15D), fluorapatite, and chalcopyrite. The reducing basement fluids could not transport enough uranium to precipitate large pods of uraninite at and above the unconformity; therefore the source of uranium for the unconformity and perched uraninite was the oxidizing basinal fluids. Again, the

hydrothermal deposition, increase in frictional strength, and cessation of stresses caused the fault to seal.

6) An event ~500 Ma, possibly the Carswell meteorite impact, caused the faults to re-open. Movement of basinal fluids along the structures in the sandstone caused a later generation of uraninite (Fig. 15D) to precipitate both at the unconformity and perched above the unconformity with hematite and sulfides.

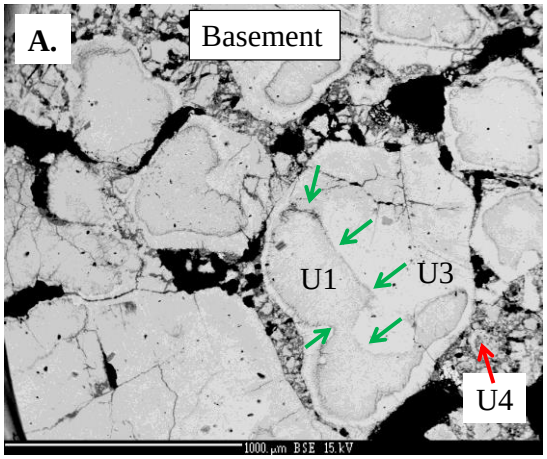

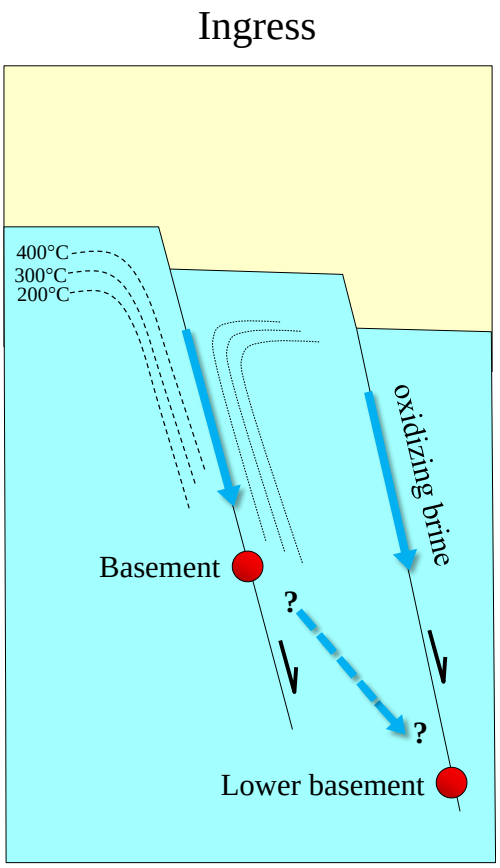

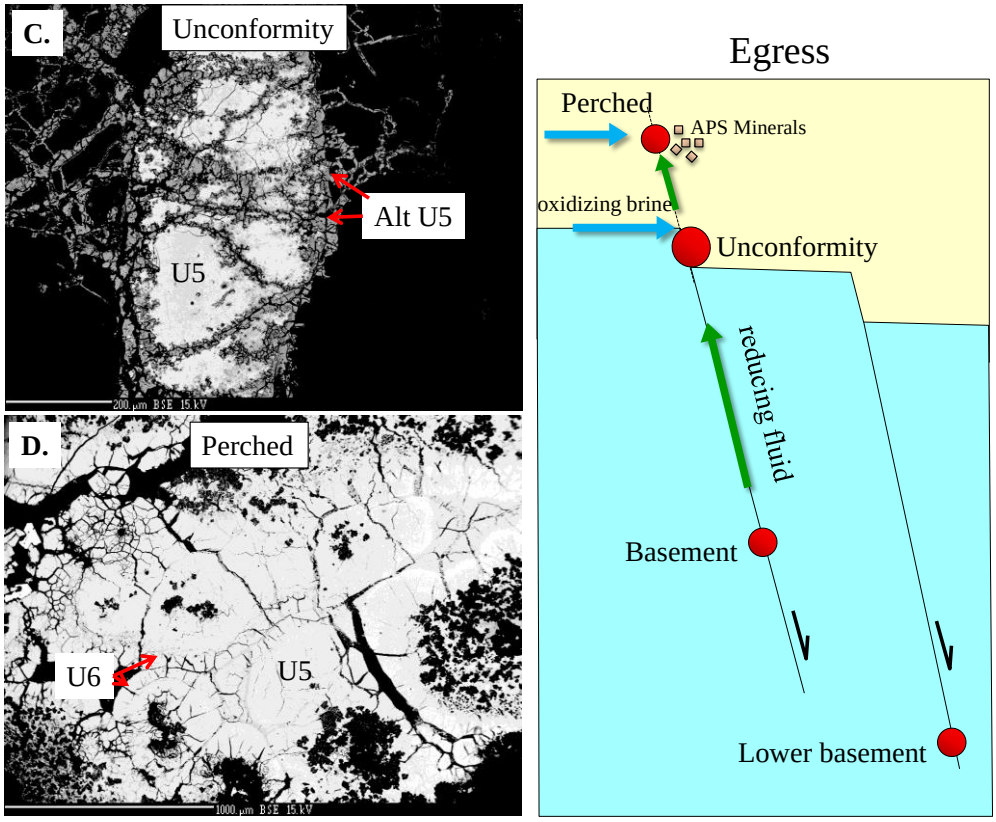

Figure 15: Schematic representation of six stages of uraninite from the Kianna deposit. Stages 1-4 formed from ingressing, uraniferous oxidizing fluids that became progressively more reducing as they migrated along faults and interacted with the basement rocks. Uraninite precipitated in the basement and lower basement. Stages 5 and 6 formed from egressing reducing fluids that interacted with uraniferous fluids and oxidizing APS minerals to form unconformity and perched uraninite. (A) shows the textural relationship between U1 (1495 Ma), U3 (1088 Ma), and U4 (855 Ma) in the basement. U3 formed as a result of an ingressing recrystallization front (green arrows) whereas U4 appears to be either brecciated U3 or a new generation of uraninite. (B) shows the textural relationship between U2 (1280 Ma) and U4 (855 Ma) in the lower basement. The source of uranium for U2 uraninite may have been remobilized U1 as a result of ingressing oxidizing basinal brines or ingressing uraniferous fluids along a fault that was activated at 1280 Ma. (C) shows highly altered U5 at the unconformity. The U-Pb isotopic system of U5 may have been reset at 739 Ma. (D) shows the relationship between U5 (739 Ma) and U6 (482 Ma) in perched uraninite. U6 occurs as a new overgrowth on U5.

Chapter 6: Conclusions and Recommendations

6.1 Conclusions

Uraninite at the Kianna deposit, Shea Creek area, formed from or was affected by six major fluid events where it and associated minerals precipitated in the crystalline basement, at the unconformity, and perched above the unconformity in the overlying Athabasca Group sandstone. The Kianna deposit is the first deposit described to host all three end-member styles of mineralization variously observed in eastern Athabasca Basin deposits. The application of *in situ* ion microprobe analyses (stable and radiogenic) has provided precise isotopic measurements on individual grains to further understand the genesis of Athabasca Basin unconformity-related uranium deposits, as well as characterize mineralizing and alteration fluids.

Concordia plots of U-Pb data obtained by SIMS of six stages of uraninite from the Kianna deposit are discordant with upper intercepts of 1495 ± 26 Ma, 1280 ± 30 Ma, 1088 ± 22 Ma, 855 ± 27 Ma, 739 ± 58 Ma and 482 ± 11 Ma. These ages correspond to significant tectonic events that are interpreted to have reactivated basement structures in the Kianna deposit area and enabled fluid flow along faults. The events include the accretion of the Granite-Rhyolite province to Laurentia, the Mackenzie dyke swarm, the Grenville orogeny, the rifting of Rodinia, and possibly the Carswell meteorite impact.

Uraninite precipitated due to both ingress of oxidizing fluids into the basement along faults and egress of reducing fluids from the basement to the unconformity. SIMS analyses of muscovite intergrown with ingress-style U1 suggest that muscovite formed from marine brine that penetrated into the basement rocks along faults. The identification

of hydrothermal muscovite coeval with uraninite indicates that mineralizing fluids for primary uraninite must have been at least 300°C. The brines were likely heated during their ingress into the basement rocks due to the steep geothermal gradients associated with fault movement and hydrothermal fluid flow. Previous studies may have generated lower temperatures due to the difficulty in separating muscovite from low-temperature illite during bulk analyses.

SIMS stable isotopic analyses of coarse-grained illite coeval with U3 and fine-grained illite coeval with U4 indicate that the coarse-grained illite formed from Athabasca basinal brine, whereas fine-grained illite formed from meteoric waters. The meteoric waters overprinted the oxygen isotopic composition of earlier-formed uraninite.

SIMS stable isotopic analyses of chalcopyrite associated with U5 unconformity and perched uraninite suggest that the source of sulfur was from the metamorphic basement, indicating that the mineralizing fluid had previously equilibrated with basement sulfides. Perched and unconformity egress-style uraninite formed from, or was affected by, fluids ~750 Ma. SIMS analyses of pyrite and chalcopyrite associated with U6 unconformity and perched uraninite indicate that the sulfides precipitated from a fluid that had equilibrated with APS minerals, sulfates, and/or evaporites in the Athabasca Basin.

6.2 Recommendations for Future Work

To fully characterize the history of the Kianna deposit, further analyses are necessary, including:

1) *In situ* Ar-Ar geochronology of the muscovite, coarse-grained illite, and fine-grained illite to complement the U-Pb geochronology on associated uraninites.

Determining the age of muscovite would help determine whether the muscovite associated with U1 was neo-formed or overprinted by a marine brine.

2) Detailed geochronology of the structures in the area.
3) Geochemistry, geochronology, and structural geology studies of the Colette, Anne, and 58B deposits at Shea Creek, to complete the metallogenic model of the Shea Creek area.

References

Alexandre, P., Kyser, K., Polito, P., and Thomas, D., 2005, Alteration mineralogy and stable isotope geochemistry of paleoproterozoic basement-hosted unconformity-type uranium deposits in the Athabasca Basin, Canada, Economic Geology, v. 100, p. 1547-1563.

Alexandre, P., Kyser, K., and Jiricka, D., 2009a, Critical geochemical and mineralogical factors for the formation of unconformity-related uranium deposits: Comparison between barren and mineralized systems in the Athabasca Basin, Canada, Economic Geology, v. 104, p. 413-435.

Alexandre, P., Kyser, K., Thomas, D., Polito, P., and Marlatt, J., 2009b, Geochronology of unconformity-related uranium deposits in the Athabasca Basin, Saskatchewan, Canada and their integration in the evolution of the basin, Mineralium Deposita, v. 44, p. 41-59.

Annesley, I.R., Madore, C., and Portella, P., 2005, Geology and thermotectonic evolution of the western margin of the Trans-Hudson Orogen: evidence from the eastern sub-Athabasca basement, Saskatchewan, Canadian Journal of Earth Sciences, v. 42, p. 573-597.

AREVA Resources Canada Inc., 2012, Internal presentation to the Shea Creek Joint Venture meeting, November 9.

Armstrong, R.L., Quirt, D., and Hoeve, J., 1988, Rb-Sr dating of diabase dikes in the Athabasca basin, northern Saskatchewan, Saskatchewan Research Council, Publication no. R-855-3-A-88.

Battaglia, S., 2004, Variations in the chemical composition of illite from five geothermal fields: a possible geothermometer, Clay Minerals, v. 39, p. 501-510.

Bell, K., 1985, Geochronology of the Carswell area, northern Saskatchewan, *in* Laine, R., Alonso, D., and Svab, M., eds., The Carswell structure uranium deposits, Saskatchewan, Geological Association of Canada Special Paper 29, p. 33-46.

Beshears, C.J., 2010, The geology and geochemistry of the Millennium uranium deposit, Athabasca Basin, Saskatchewan, Canada: Unpublished M.Sc. thesis, Winnipeg, Canada, University of Manitoba.

Boulanger, R.A., 2012, Geological, petrographic and geochemical characterization of the Roughrider West Zone unconformity-type uranium deposit, Athabasca Basin, Saskatchewan: Unpublished M.Sc. thesis, Regina, Canada, University of Regina.

Bruneton, P., 1987, Geology of the Cigar Lake uranium deposit (Saskatchewan, Canada), *in* Gilboy, C.F. and Vigras, L.W., eds., Economic Minerals of Saskatchewan, Saskatchewan Geological Society Special Publication, no. 8, p. 99-119.

Bruneton, P., 1993, Geological environment of the Cigar Lake uranium deposit, Canadian Journal of Earth Sciences, v. 30, p. 653-673.

Cameron-Schiman, M., 1978, Electron microprobe study of uranium minerals and its application to some Canadian deposits: Unpublished Ph.D. Thesis, Edmonton, Canada, University of Alberta.

Capuano, R.M., 1992, The temperature dependence of hydrogen isotope fractionation between clay minerals and water: Evidence from a geopressured system, Geochimica et Cosmochimica Acta, v. 56, p. 2547-2554.

Card, C.D., 2002, New investigations of basement to the western Athabasca Basin, *in* Summary of investigations 2002, v. 2, Saskatchewan Geological Survey, Saskatchewan Energy and Mines, Miscellaneous Report 2002-4-2, p. 17.

Card, C.D., Pană, D., Portella, P., Thomas, D.J., and Annesley, I.R., 2007, New insights into the geological history of the basement rocks to the southwestern Athabasca Basin, Saskatchewan and Alberta, Geological Survey of Canada Bulletin, v. 4, issue 18, p. 119-133.

Carroll, J., Robbins, J., and Koning, E., 2006, The Shea Creek deposits, west Athabasca Basin, Saskatchewan, *in* Uranium: Athabasca deposits & analogues, 2006 CIM Field Conference, CIM Geological Society, Saskatoon Section, Saskatoon, Saskatchewan, September 13-14, 2006, Field Trip 3 "Cluff Lake and Shea Creek deposits" guidebook, p. 33-48.

Chang, Z., Large, R.R., and Maslennikov, V., 2008, Sulfur isotopes in sediment-hosted orogenic gold deposits: evidence for an early timing and a seawater sulfur source, Geology, v. 36, no. 12, p. 971-974.

Claesson, L., Skelton, A., Graham, C., and Mörth, C.M., 2007, The timescale and mechanisms of fault sealing and water-rock interaction after an earthquake, Geofluids, v. 7, p. 427-440.

Cloutier, J., Kyser, K., Olivo, G.R., Alexandre, P., and Halaburda, J., 2009, The Millennium uranium deposit, Athabasca Basin, Saskatchewan, Canada: An atypical basement-hosted unconformity-related uranium deposit, Economic Geology, v. 104, p. 815-840.

Cole, D.R. and Ohmoto, H., 1986, Chapter 2: Kinetics of isotopic exchange at elevated temperatures and pressures, *in* Valley, J.W., Taylor, H.P., and O'Neil, J.R., eds., Stable isotopes in high temperature geological processes, Mineralogical Society of America, Reviews in Mineralogy, v. 16, p. 41-90.

Condie, K.C., 2002, Supercontinents, superplumes and continental growth: the Neoproterozoic record, *in* Yoshida, M., Windley, B.F., and Dasgupta, S., eds.,

Proterozoic East Gondwana: Supercontinent Assembly and Breakup, Geological Society of London special publication no. 206, Bath, UK.

Crank, J., 1975, The mathematics of diffusion, 2nd ed., Oxford University Press, Oxford, England.

Craw, D., 2013, Gilded by earthquakes, Nature Geoscience, v. 6, p. 248-250.

Cui, T., Yang, J., and Samson, I.M., Tectonic deformation and fluid flow: Implications for the formation of unconformity-related uranium deposits, Economic Geology, v. 107, p. 147-163.

Cuney, M.L., 2009, The extreme diversity of uranium deposits, Mineralium Deposita, v. 44, p. 3-9.

Cuney, M.L., Chabiron, A., Kister, P., Golubev, V., and Deloule, E., 2002, Chemical versus ion microprobe isotopic dating (CAMECA IMS 3F) of the Shea Creek unconformity type uranium deposit (West Athabasca, Saskatchewan, Canada), *in* Program with Abstracts - Geological Association of Canada; Mineralogical Association of Canada: Joint Annual Meeting, v. 27, p. 25.

Fayek, M. and Kyser, T.K., 1997, Characterization of multiple fluid-flow events and rare-earth-element mobility associated with formation of unconformity-type uranium deposits in the Athabasca Basin, Saskatchewan, The Canadian Mineralogist, v. 35, p. 627-658.

Fayek, M. and Kyser, T.K., 2000, Low temperature oxygen isotopic fractionation in the uraninite-UO_3-CO_2-H_2O system, Geochimica et Cosmochimica Acta, v. 64, no. 13, p. 2185-2197.

Fayek, M., Janeczek, J., and Ewing, R.C., 1997, Mineral chemistry and oxygen isotopic analysis of uraninite, pitchblende, and uranium alteration minerals from the Cigar Lake deposit, Saskatchewan, Canada, Applied Geochemistry, v. 12, p. 549-565.

Fayek, M., Harrison, M.T., Grove, M., and Coath, C.D., 2000, A rapid in situ method for determining the ages of uranium oxide minerals: Evolution of the Cigar Lake deposit, Athabasca Basin, International Geology Review, v. 42, p. 163-171.

Fayek, M., Harrison, T.M., Ewing, R.C., Grove, M., and Coath, C.D., 2002a, O and Pb isotope analyses of uranium minerals by ion microprobe and U-Pb ages from the Cigar Lake deposit, Chemical Geology, 185, p. 205-225.

Fayek, M., Kyser, T.K., and Riciputi, L.R., 2002b, U and Pb isotopic analysis of uranium minerals by ion microprobe and the geochronology of the McArthur River and Sue Zone uranium deposits, Saskatchewan, Canada, The Canadian Mineralogist, v. 40, p. 1553-1569.

Fayek, M., Camacho, A., Beshears, C., Jiricka, D., and Halaburda, J., 2010, Two sources of uranium at the Millennium uranium deposit, Athabasca Basin, Saskatchewan, Canada, GeoCanada 2010: Working with the Earth.

Fayek, M., Anovitz, L.M., Cole, D.R., and Bostick, D.A., 2011, O and H diffusion in uraninite: Implications for fluid-uraninite interactions, nuclear waste disposal, and nuclear forensics, Geochimica et Cosmochimica Acta, v. 75, p. 3677-3686.

Fission Uranium Corp., 2014, Patterson Lake South (PLS), http://www.fissionuranium.com/project/pls/ June 25, 2014.

Gaboreau, S., Cuney, M., Quirt, D., Beaufort, D., Patrier, P., and Mathieu, R., 2007, Significance of aluminum phosphate-sulfate minerals associated with U unconformity-type deposits: the Athabasca Basin, Canada, American Mineralogist, v. 92, p. 267-280.

Genest, S., Robert, F., and Duhamel, I., 2010, The Carswell impact event, Saskatchewan, Canada: Evidence for a pre-Athabasca multiring basin?, *in* The Geological Society of America Special Paper 465, p. 543-570.

Hiatt, E. and Kyser, K., 2006, Sequence stratigraphy, hydrostratigraphy, and mineralizing fluid flow in the Proterozoic Manitou Falls Formation, eastern Athabasca Basin, Saskatchewan, *in* Jefferson, C.W. and Delaney, G., eds., EXTECH IV: Geology and uranium exploration technology of the Proterozoic Athabasca Basin, Saskatchewan and Alberta, Geological Survey of Canada, Bulletin 588, p. 489-506.

Hoefs, J., 2004, Stable isotope geochemistry, 5th ed., Springer-Verlag, Berlin, Heidelberg, New York.

Hoeve, J., Sibbald, T.I.I., Ramaekers, P. and Lewry, J.F., 1980, Athabasca Basin unconformity-type uranium deposits: A special class of sandstone-type deposits? *in* Ferguson, J. and Goleby, A.B., eds., Uranium in the Pine Creek Geosyncline, International Atomic Energy Agency, Vienna, p. 575-594.

Hoeve, J., and Quirt D., 1984, Mineralization and host rock alteration in relation to clay mineral diagenesis and evolution of the Middle-Proterozoic, Athabasca Basin, northern Saskatchewan, Canada, Saskatchewan Research Council, SRC Technical Report 187.

Hoeve, J., and Quirt D., 1985, A stationary redox front as a critical factor in the formation of high-grade, unconformity-type uranium ores in the Athabasca Basin, Saskatchewan, *in* Program and Extended Abstracts, Concentration mechanisms of uranium in geological environments, Nancy, France, p. 219-224.

Hoeve, J., and Quirt D., 1987, A stationary redox front as a critical factor in the formation of high-grade, unconformity-type uranium ores in the Athabasca Basin, Saskatchewan, Canada. Bulletin de Minéralogie, v. 110, p. 157-171.

Hoeve, J. and Quirt, D.H., 1989, A common diagenetic-hydrothermal origin for unconformity-type uranium deposits and stratiform copper deposits, *in* Boyle, R.W., Brown, A.C., Jefferson, C.W., Jowett, E.C., and Kirkham, R.V., eds., Sediment-hosted stratiform copper deposits, Geological Association of Canada, Special Paper 36, p. 151-172.

Hoeve, J. and Sibbald, T.I.I., 1978a, Mineralogy and geological setting of unconformity-type uranium deposits in northern Saskatchewan, *in* Kimberly, M.M., ed., Uranium deposits, their mineralogy and origin, Mineralogical Association of Canada short course, University of Toronto, p. 457-474.

Hoeve, J. and Sibbald, T.I.I., 1978b, On the genesis of Rabbit Lake and other unconformity-type uranium deposits in northern Saskatchewan, Canada, Economic Geology, v. 73, p. 1450-1473.

Hulbert, L., Williamson, B. and Thériault, R., 1993, Geology of Middle Proterozoic Mackenzie diabase suites from Saskatchewan: an overview and their potential to host Noril'sk-type Ni-Cu-PGE mineralization, *in* Summary of Investigations 1993, Saskatchewan Geological Survey, Saskatchewan Energy and Mines, Miscellaneous Report 93-4, p. 112-125.

Jefferson, C.W., Thomas, D., Quirt, D., Mwenifumbo, C.J. and Brisbin D., 2007a, Empirical models for Canadian unconformity-associated deposits, *in* Proceedings of Exploration 07: Fifth Decennial International Conference on Mineral Exploration, Milkereit, B., ed., p. 741-769.

Jefferson, C.W., Thomas, D.J., Gandhi, S.S., Ramaekers, P., Delaney, G., Brisbin, D., Cutts, C., Quirt, D., Portella, P., and Olson, R.A., 2007b, Unconformity-associated uranium deposits of the Athabasca Basin, Saskatchewan and Alberta, *in* Goodfellow, W.D., ed., Mineral deposits of Canada: A synthesis of major deposit-types, district metallogeny, the evolution of geological provinces, and exploration methods, Geological Association of Canada Mineral Deposits Division, Special Publication no. 5, p. 273-305.

Kame, N., Nagata, K., Nakatani, M., and Kusakabe, T., 2014, Feasibility of acoustic monitoring of strength drop precursory to earthquake occurrence, Earth, Planets and Space, v. 66:41.

Kotzer, T. and Kyser, T.K., 1990, The use of stable and radiogenic isotopes in the identification of fluids and processes associated with unconformity-type uranium deposits, *in* Beck, L.S., Harper, C.T., and Richmond-Johnson, N., eds., Modern exploration techniques, Saskatchewan Geological Society, p. 115-131.

Kotzer, T.G. and Kyser, T.K., 1992, U, Pb, O, and S isotopic variations in uraninites and sulfides from a Proterozoic sandstone basin; implications for tracing late fluid movements, *in* Eos, transactions, American Geophysical Union, v. 73, issue 14, suppl. p. 140

Kotzer, T.G. and Kyser, T.K., 1993, O, U, and Pb isotopic and chemical variations in uraninite: Implications for determining the temporal and fluid history of ancient terrains, American Mineralogist, v. 78, p. 1262-1274.

Kotzer, T.G., and Kyser, T.K., 1995, Petrogenesis of the Proterozoic Athabasca Basin, northern Saskatchewan, Canada, and its relation to diagenesis, hydrothermal uranium mineralization and paleohydrogeology, Chemical Geology, v. 120, p. 45-89.

Kotzer, T.G., Kyser, T.K., and Irving, E., 1992, Paleomagnetism and the evolution of fluids in the Proterozoic Athabasca Basin, northern Saskatchewan, Canada, Canadian Journal of Earth Sciences, v. 29, p. 1474-1491.

Laverret, E., Patrier Mas, P., Beaufort, D., Kister, P., Quirt, D., Bruneton, P., and Clauer, N., 2006, Mineralogy and geochemistry of the host-rock alterations associated with the Shea Creek unconformity-type uranium deposits (Athabasca Basin, Saskatchewan, Canada). Part 1: Spatial variation of illite properties, Clays and Clay Minerals, v. 54, no. 3, p. 275-294.

Laverret, E., Clauer, N., Fallick, A., Mercadier, J., Patrier, P., Beaufort, D., and Bruneton, P., 2010, K-Ar dating and $\delta^{18}O$-δD tracing of illitization within and outside the Shea Creek uranium prospect, Athabasca Basin, Canada, Applied Geochemistry, v. 25, p. 856-871.

LeCheminant, A.N. and Heaman, L.M., 1989, MacKenzie igneous events, Canada: Middle Proterozoic hotspot magmatism associated with ocean opening, Earth and Planetary Science Letters, v. 96, p. 38-48.

Ludwig, K., 1993, ISOPLOT, Excel based program for plotting radiogenic isotopes; USGS, Open file report, no. 91-445, p. 1-42.

Mercadier, J., Cuney, M., Cathelineau, M., and Lacorde, M., 2011, U redox fronts and kaolinisation in basement-hosted unconformity-related U ores of the Athabasca Basin (Canada): late U remobilisation by meteoric fluids, Mineralium Deposita, v. 46, p. 105-135.

Nelson, J., and Colpron, M., 2007, Tectonics and metallogeny of the British Columbia, Yukon, and Alaskan Cordillera, 1.8 Ga to the present, *in* Goodfellow, W.D., ed., Mineral Deposits of Canada: A synthesis of major deposit-types, district metallogeny, the evolution of geological provinces, and exploration methods, Geological Association of Canada Mineral Deposits Division, Special Publication no. 5, p. 755-791.

Pesonen, L.J., Elming, S.A., Mertanen, S., Pisarevsky, S., D'Agrella-Filho, M.S., Meert, J.G., and Schmidt, P.W., 2003, Paleomagnetic configuration of continents during the Proterozoic, Tectonophysics, v. 375, p. 289-324.

Quirt, D.H., 1989, Host rock alteration at Eagle Point South, Saskatchewan Research Council, Publication No. R-855-1-E-89.

Quirt, D.H., 1993, Petrology and geochemistry of the Helikian Athabasca diabase dykes, Saskatchewan, *in* Summary of Investigations 1993, Saskatchewan Geological Survey, Saskatchewan Energy and Mines, Miscellaneous Report 93-4, p. 174-182.

Quirt, D.H., 2003, Athabasca unconformity-type uranium deposits: One deposit type with many variations, *in* Cuney, M., ed., Uranium Geochemistry, International Conference Proceedings, Nancy 2003, p. 309-312.

Quirt, D., 2010, Is illite still a pathfinder mineral for the geological environment of Athabasca unconformity-type uranium deposits?: GeoCanada joint conference, Calgary, Alberta, May 10-14.

Quirt, D., Kotzer, T., and Kyser, T.K., 1991, Tourmaline, phosphate minerals, zircon and pitchblende in the Athabasca Group: Maw Zone and McArthur River areas, *in* Summary of Investigations 1991: Saskatchewan Geological Survey, Saskatchewan Energy and Mines, Report 91-4, p. 181-191.

Quirt, D., Modeland, S., and Demange, C, 2012, Shea Creek uranium project: Anne deposit, Northern Mining District, Saskatchewan, NTS Map Areas 74K/4 and 5, AREVA Resources Canada Inc. 2010 Mineral Resource Technical Report # 11-CND-585-05.

Ramaekers, P., 1990, Geology of the Athabasca Group (Helikian) in northern Saskatchewan, Saskatchewan Energy and Mines, Report 195.

Ramaekers, P., Jefferson, C.W., Yeo, G.M., Collier, B., Long, D.G.F., Drever, G., McHardy, S., Jiricka, D., Cutts, C., Wheatley, K., Catuneanu, O., Bernier, S., Kupsch, B., and Post, R.T., 2007, Revised geological map and stratigraphy of the Athabasca Group, Saskatchewan and Alberta, *in* Jefferson, C.W. and Delaney, G., eds., EXTECH IV: Geology and uranium exploration technology of the Proterozoic Athabasca Basin, Saskatchewan and Alberta, Geological Survey of Canada, Bulletin 588, p. 155-191.

Richard, A., Banks, D.A., Mercadier, J., Boiron, M-C., Cuney, M., and Cathelineau, M., 2011, An evaporated seawater origin for the ore-forming brines in unconformity-related uranium deposits (Athabasca Basin, Canada): Cl/Br and δ^{37}Cl analysis of fluid inclusions, Geochimica et Cosmochimica Acta, v. 75, p. 2792-2810.

Seal, R.R., 2006, Sulfur isotope geochemistry of sulfide minerals, Reviews in Mineralogy and Geochemistry, v. 61, p. 633-677.

Seal, R.R., Alpers, C.N., and Rye, R.O., 2000, Stable isotope systematics of sulfate minerals, Reviews in Mineralogy and Geochemistry, v. 40, p. 541-602.

Sibbald, T.I.I., Quirt, D.H., and Gracie, A.J., 1990, Uranium deposits of the Athabasca Basin, Saskatchewan, Field Trip 11 Guidebook, 8th IAGOD Symposium, Ottawa, Ontario, Geological Survey of Canada, Open File 2166.

Sibson, R.H., 1992, Implications of fault-valve behavior for rupture nucleation and recurrence, Tectonophysics, 211, p. 283-293.

Sibson, R.H., 2001, Seismogenic framework for hydrothermal transport and ore deposition, *in* Reviews in economic geology, Society of Economic Geologists, Boulder, CO, v. 14, p. 25-50.

Suzuoki, T. and Epstein, S., 1976, Hydrogen isotope fractionation between OH-bearing minerals and water, Geochimica et Cosmochimica Acta, v. 40, p. 1229-1240.

Vidal, O., Baldeyrou, A., Dubac, B., DeAndrade, V., Jullien, M. and Lanson, B., 2007, Thermodynamics of phyllosilicates and low temperature thermometry, *in* Nieto, F. and Jiménez-Millán, J., eds., Diagenesis and low-temperature metamorphism. Theory, methods and regional aspects, Seminarios SEM, 3, p. 79-84.

Wallis, R.H., Saracoglu, N., Brummer, J.J. and Golightly, J.P., 1985, Geology of the McClean uranium deposits, *in* Sibbald, T.I. and Petruk, W., eds., Geology of Uranium Deposits: Canadian Institute of Mining and Metallurgy Special Volume 32, p. 101-131.

Wanless, R.K., Stevens, R.D., Lachance, G.R., and Edmonds, C.M., 1968, Age determinations and geological studies, K-Ar isotopic ages, report 8, Geological Survey of Canada Paper 67-2, part A, p. 141.

Weatherley, D.K. and Henley, R.W., 2013, Flash vaporization during earthquakes evidenced by gold deposits, Nature Geoscience, v. 6, p. 294-298.

Whitmeyer, S.J. and Karlstrom, K.E., 2007, Tectonic model for the Proterozoic growth of North America, Geosphere, v. 3, no 4, p. 220-259.

Wilson, M.R. and Kyser, T.K., 1987, Stable isotope geochemistry of alteration associated with the Key Lake uranium deposit, Canada, Economic Geology, v. 82, p. 1540-1557.

Zheng, Y.F., 1993, Calculation of oxygen isotope fractionation in hydroxyl-bearing silicates, Earth and Planetary Science Letters v. 120, p. 247-263.

Appendices

Appendix A
Thin-Section Sample Descriptions

Table A.1: Thin-section descriptions from perched mineralization samples, Kianna Deposit, Shea Creek Project

No.	Depth (m)	Mineral Assemblage	Grain Size	Color	Habit	Alteration	Structure	Comments
CS-10	674.2	90% quartz	0.2-0.5 mm, uniform sizes	yellow to blue to medium grey XPL	euhedral		hematite replaced the original sst matrix	yellowy tint to the sample under naked eye because of the yellowy-brown hematite supporting qtz clasts
		10% hematite	very fine	yellowy brown to med brown	matrix filling			
		trace uraninite	very fine	silvery grey under refl lt	bleby to matrix filling			
		trace pyrite	very fine to 0.1 mm	bright yellowy gold under refl lt	anhedral			
CS-9a/b	676.9	85% quartz	0.1-0.5 mm	clear ppl, blue - grey xpl	subhedral-euhedral, rounded		urn/hem coeval mixture comprise the matrix of the brecciated sandstone	original sst was matrix-supported. Matrix now replaced with urn/hem mixture
		8% hematite	-	yellow brown to brick red	hem and urn are intermixed, fracture filling, matrix replacing blebs/veins			
		6% uraninite	-	opaque xpl, grey refl lt				
		1% chalcopyrite	<0.1 mm	brassy yellow-gold, reflective	v. fine subhedral grains associated with quartz			
		trace calcite	-	white ppl, birefringent xpl	late, fracture filling			

Table A.1: Thin-section descriptions from perched mineralization samples, Kianna Deposit, Shea Creek Project

No.	Depth (m)	Mineral Assemblage	Grain Size	Color	Habit	Alteration	Structure	Comments
CS-13-18	679.2	80% quartz	up to 1 mm	medium blue - grey xpl, white - grey ppl	subhedral to euhedral, many well-rounded	original sst grains	matrix-supported sandstone	Pyrite possibly leached Fe from chl, hem + urn replaces chl matrix
		10% chlorite	very fine	med brown - green	matrix	chl replaced original sst matrix		
		5% uraninite	<0.5 mm	opaque in PPL, grey in refl.	fracture-filling and matrix-replacing	some grains form veins of broken grains		
		5% hematite	fine	dark reddy brown	matrix-replacing, with uraninite	intermixed with urn		
		trace pyrite	<0.1 mm	reflective yellow-gold	disseminated in chl			
CS-11	680.7	85% quartz	0.2-0.7 mm	colorless in PPL, grey-black in XPL	subhedral	some grain boundaries altered by chl	uraninite forming along grain boundaries between chl and qtz	sandstone cement and possibly some qtz has been chloritized and predates uraninite
		10% chlorite	very fine	browny-green to light green	replacing cement			
		3% uraninite	<0.05 mm	black	euhedral disseminated			
		2% hematite	<0.05 mm	med to lt reddy brown	massive, forming with uraninite			

Table A.1: Thin-section descriptions from perched mineralization samples, Kianna Deposit, Shea Creek Project

No.	Depth (m)	Mineral Assemblage	Grain Size	Color	Habit	Alteration	Structure	Comments
CS-23	680.7	80% quartz	0.5-1 mm	colorless in PPL, grey-black in XPL	anhedral	edges altered by kaolinite	kaolinite matrix creates a fabric through the sample, folding around grains and sometimes eating at grain boundaries	kaolinite has replaced chloritization of sandstone host
		15% matrix	clay	grey in PPL, birefringent	acicular very fine grains			
		5% pyrite	0.1-2 mm	yellowy-gold, very shiny metallic	subhedral	some grain edges altered by kaolinite		
		trace calcite	.2 mm long, 0.05 mm thick	colorless in PPL, highly birefringent in XPL	veins cutting quartz			
CS-19	682.8	90% quartz	0.3-1 mm	lt blue-dark grey in XPL	subhedral, mostly uniform grain size (0.3 mm) with large outliers		uraninite and hematite occur along qtz grain boundaries, fracture-filling. Acicular pyrite precipitating out of urn/hem mixture	sample has yellow colouring due to the yellowy-brown hematite. Hematite and uraninite are coeval.
		4% uraninite	very fine	black	fracture filling, massive			
		4% hematite	very fine	yellowy brown to med brown	fracture filling, assoc with uraninite			
		2% Pyrite	100 µm	silver-lt gold refl. light	acicular very fine grains			

Table A.1: Thin-section descriptions from perched mineralization samples, Kianna Deposit, Shea Creek Project

No.	Depth (m)	Mineral Assemblage	Grain Size	Color	Habit	Alteration	Structure	Comments
CS-4	684.7	30% uraninite	very fine	black, dull reflectivity	massive		great deal of veining with some holes in the sample	relationship between chl and hem is sometimes uncertain, but they are thought to be coeval and cutting earlier hematite and uraninite
		10% early hematite	very fine	dark maroon red	massive, forming with uraninite			
		20% late hematite	>0.3 mm	bright orange	veins cutting u and early hem	some anhedral grain boundaries, some botryoidal		
		15% chlorite	>0.3 mm	light green	veins forming with late hematite			
		15% APS minerals	0.02 mm	beige-light brown	subhedral grains being broken by uraninite			
		5% chalcopyrite	0.1 mm	brassy yellow to orange refl	subhedral grains disseminated			
		5% pyrite	<0.1 mm	bright yellow in reflected light	anhedral grains disseminated	occuring in chl		

Table A.1: Thin-section descriptions from perched mineralization samples, Kianna Deposit, Shea Creek Project

No.	Depth (m)	Mineral Assemblage	Grain Size	Color	Habit	Alteration	Structure	Comments
CS-13-28	687.5	60% quartz	0.5 mm	medium blue - grey xpl, white - grey ppl	subhedral to anhedral	original sst grains	matrix-supported sandstone	Hem + urn breaks apart quartz and looks like it replaces chl matrix
		20% chlorite	very fine	dark green	replaces original sst matrix			
		10% uraninite	finely replacing matrix to up to 1 cm long	opaque in PPL, grey in refl.	massive to relict botryoidal to finely replacing matrix with hem	some grains form veins of broken massive grains		
		10% hematite	very fine	dark reddy brown	fills fractures and holes with urn	intimately intermixed with urn		
		trace marcasite	0.1 mm	reflective yellow-gold	acicular needles in chl matrix			
CS-17	688	90% quartz	100-500 μm	light blue - dark black grey in XPL	euhedral-subhedral, uniform grains		uraninite and pyrite have replaced the original sandstone matrix, filling pore space. Quartz clasts are matrix supported.	Pyrite may have replaced hematite. Fracturing of pyrite grains likely caused by subsequent fluid event
		7% uraninite	very fine	med-dark black	massive, filling pore space among qtz	some grains have rough edges		
		3% pyrite	0.2 - 0.5 mm	bright yellow, very reflective	anhedral and fracture filling	rough edges, broken grains, holes in grains		
		trace hematite	very fine	med brown-dark brown	fracture filling, assoc. with urn			

Table A.2: Thin-section descriptions from unconformity mineralization samples, Kianna Deposit, Shea Creek Project

No.	Depth (m)	Mineral Assemblage	Grain Size	Color	Habit	Alteration	Structure	Comments
CS-13-27	707	50% chlorite	very fine	light green to med brown	matrix/ groundmass	likely from original meta-pelite host	Large carbon blebs are associated with massive uraninite grains	Chl is likely Fe-rich because of brown color, pyrite may be leaching Fe from chl and/or hem; py occurs within fractures in the chl matrix or hem grains
		34% hematite	<<0.1 - 1 mm	orange to lt brown ppl	anhedral, silicified, broken			
		10% uraninite	<0.5 mm	opaque in PPL, grey in refl.	fracture-filling with few relict botryoidal and massive grains	intimately associated with hematite		
		5% carbon	1-2 mm	dark black ppl, silvery grey xpl	blebs, soft edges, various shapes, grains lack texture	some blebs broken by hematite		
		1% pyrite	up to 0.2 mm	reflective yellow-gold	anhedral, disseminated			
CS-20a	714	80% quartz	0.1-1 mm	lt blue-beige brown in XPL	anhedral, range of grain sizes	broken, fractured grains	hematite is veining through broken quartz grains, chl shows some spinifex-like textures	original rock was likely chloritized sandstone prior to fluid event which caused urn/hem precipitation
		10% hematite	very fine	orange-red to dark red	matrix & fracture-filling to massive	Hem consumes chl		
		5% uraninite		opaque, black				
		5% chlorite	very fine	lt-med. green	fractured, pitted			
		trace pyrite	0.1 mm	bright gold in reflected light	anhedral			

Table A.2: Thin-section descriptions from unconformity mineralization samples, Kianna Deposit, Shea Creek Project

No.	Depth (m)	Mineral Assemblage	Grain Size	Color	Habit	Alteration	Structure	Comments
CS-14a	719.1	85% early quartz	0.5-3 mm	colorless in PPL, light blue-black in XPL	anhedral		hydrothermal veins of fluorapatite, quartz, calcite	original host was sandstone, the source of early quartz
		5% late quartz	<0.2 mm		veins cutting early qtz			
		5% chlorite	very fine	medium green to light brown	filling pore space and fractures, veining	forming at expense of pyrite		
		1% pyrite	0.05 mm	yellowy gold	anhedral	being altered by chl		
		1% fluorapatite		translucent	very fine veins			
		2% muscovite	0.05-.1 mm	highly birefringent	fracture filling grains and fine veins	forming at expense of chl		
		1% calcite		colorless PPL birefringent in XPL	0.1 mm thick veins			
		trace zircon	0.2 mm	yellow-med brown	euhedral grains			
		trace rutile	<0.03 mm	Birefring. Xpl	assoc. with py			

Table A.2: Thin-section descriptions from unconformity mineralization samples, Kianna Deposit, Shea Creek Project

No.	Depth (m)	Mineral Assemblage	Grain Size	Color	Habit	Alteration	Structure	Comments
CS-14b	719.1	60% early quartz	0.5-2.5 mm	colorless in PPL, light blue-dark grey in XPL	anhedral	grains fractured	contact between zone with quartz and chlorite and the zone of calcite: uraninite, hematite, and pyrite in the contact	calcite seen veining through earlier minerals, first qtz likely from sandstone and second generation veins through first generation. Retrograde metamorphism? Marble?
		15% late quartz	<0.2 mm		anhedral, veins cutting early qtz			
		15% calcite	up to 2 mm	highly birefringent in XPL	veining to euhedral masses	triple junctions present		
		5% chlorite	very fine	light to medium browny green	filling pore space and fractures, veining			
		3% uraninite	0.2-0.5 mm	black	subhedral to anhedral	botryoidal remnants present		
		2% pyrite	0.01 mm	yellowy gold	anhedral, fracture filling	associated with uraninite		
CS-18a	720.4	75% chlorite	very fine	med to dark forest green		chl being replaced by hem	hematite looks to be replacing chl as it fractures through, fills holes and grows through it in blebs. Some remnant bt grains associated with hem and chl	bt may have been from original host rock, it is assoc with chl, some birefring. seen within chl matrix - mica? - original chl may have formed at expense of mica
		15% quartz	0.1-0.5 mm	lt grey to reddy brown XPL	anhedral	fractured, hematite veins through broken grains		
		8% hematite	very fine	maroon to dark brown	fracture filling, blebs			
		2% uraninite	0.1-1 mm	black	vein-type	vein has been broken apart to form smaller and larger grains		
		trace pyrite	very fine	yellowy gold	anhedral			
		trace biotite	<0.1 mm	yellow-brn	tabular			

Table A.2: Thin-section descriptions from unconformity mineralization samples, Kianna Deposit, Shea Creek Project

No.	Depth (m)	Mineral Assemblage	Grain Size	Color	Habit	Alteration	Structure	Comments
CS-18b	720.4	70% early quartz	0.5-1 mm	colorless in PPL, light blue-black in XPL	subhedral			Host most likely shallow gneiss but could have been sandstone because of the presence of large, early qtz
		2% late quartz	<0.2 mm		anhedral	hydrothermal veins		
		15% chlorite	0.5 mm	light green	tabular to lathlike to massive	chloritization of host		
		10% hematite	very fine	dark brown	veining through quartz	forming at the expense of bt		
		3% biotite	<0.3 mm	medium brown	tabular	being altered to hem		
CS-13-22	737.8	60% quartz	<0.1 to up to 1 mm	medium blue – grey xpl	subhedral to anhedral, some well-rounded	some grains fractured by urn + hem	matrix-supported sandstone	
		25% uraninite	no individual grains observed, mostly vein-like and fracture-filling	opaque in PPL, grey in refl.	Fracture-filling and matrix-replacing	urn + hem replaces most of the sandstone matrix		
		10% hematite	fine, fracture-filling	med brown to brick red	matrix-replacing, with uraninite, replaces the chlorite matrix	hem + urn replace chl		
		5% chlorite	very fine	med-dk green	sandstone matrix			

Table A.3: Thin-section descriptions from basement mineralization samples, Kianna Deposit, Shea Creek Project

No.	Depth (m)	Mineral Assemblage	Grain Size	Color	Habit	Alteration	Structure	Comments
CS-7a/b/c	803.5	20% early quartz	<0.3 mm	colorless in PPL, light blue-black in XPL	subhedral to anhedral		fracture filling uraninite forms boundary between chl matrix and drusy quartz, illite forming associated with urn and hem, possibly at expense of chl	gersdorffite – AsNiCoS in core, AsNiFeCo in rim.
		20% late quartz	up to 1 mm		drusy, crystal faces seen	associated with early qtz		
		25% chlorite	very fine	med-dark green to brown	massive	product of alteration of gneiss		
		10% uraninite	0.2-0.5 mm	light black	fracture filling	phases into gersdorffite		
		10% gersdorffite	<0.1 mm	highly reflective silver	euhedral cubic, massive to disseminated	zoned, Fe-gersdorffite forming along rim		
		7% hematite	fine	med brown	thin veins			
		5% muscovite	up to 0.3 mm	yellow-pink, highly birefringent	radiating, acicular	forming out of gneiss host, possibly from chl or kspar		
		3% pyrite	<0.1 mm	reflective yellow gold	subhedral to anhedral			
		trace illite	very fine, clay		acicular	possibly forming at expense of chl		
		trace covellite	0.02 mm	sky blue	disseminated			

Table A.3: Thin-section descriptions from basement mineralization samples, Kianna Deposit, Shea Creek Project

No.	Depth (m)	Mineral Assemblage	Grain Size	Color	Habit	Alteration	Structure	Comments
CS-5	809.9	50% illitized matrix	very fine	bluey grey under XPL			Urn, hem, msc appear together and were likely coeval due to their very integrated nature. Sample in some areas looked sheared – there are urn, hem, msc grains that look untouched right next to very sheared elongated linear grains	
		20% hematite	very fine	yellow brown to dark maroon	fracture filling to well-formed almost tabular blebs			
		20% uraninite	range of sizes up to 1 mm	opaque PPL, dull grey refl.	Euhedral to subhedral disseminated blebs to elongated tabular grains			
		5% muscovite	variation in size, very fine to up to 0.25 mm	birefringent XPL – pastel pink, blue	tabular, anhedral to subhedral	Msc being altered to illite		
		5% galena	range of sizes, very fine up to 0.5 mm	bright silver refl. Lt	range of shapes, anhedral to euhedral, some cubic and others fractured	associated with urn		
		trace pyrite	0.5 mm	brassy yellow gold refl.	Subhedral, sporadic grains			
		trace covellite	0.05 mm	medium blue refl.	Subhedral, sporadically disseminated			

Table A.3: Thin-section descriptions from basement mineralization samples, Kianna Deposit, Shea Creek Project

No.	Depth (m)	Mineral Assemblage	Grain Size	Color	Habit	Alteration	Structure	Comments
CS-15a	809.9	20% early quartz	0.5-1 mm	clear to brown in PPL, lt to dark blue in XPL	anhedral grains	grains being eaten up by hem	Mg chlorite mesh texture indicates retrograde metamorphism, mg chlorite could be alteration of serpentinization	mg chlorite is being altered to very fine acicular clay, mesh texture includes bands of very fine mineral
		20% late quartz	0.5-1 mm		anhedral, rough boundaries	altering to acicular clay		
		5% rutile	0.05 mm	brown to bright pink	subhedral	being broken up by chlorite		
		3% uraninite	up to 1 mm	light black	anhedral	being broken apart by late quartz		
		20% early hematite	<0.5 mm	reddy brown	massive	phasing into early qtz and being altered by late qtz		
		2% muscovite	very fine	highly birefringent	acicular, radiating			
		30% chlorite	very fine	medium green	massive			
		trace zircon	0.1 mm	yellow-pink	euhedral			

Table A.3: Thin-section descriptions from basement mineralization samples, Kianna Deposit, Shea Creek Project

No.	Depth (m)	Mineral Assemblage	Grain Size	Color	Habit	Alteration	Structure	Comments
CS-13b	817.3	70% chlorite	very fine	light to med. Green	massive, matrix	being altered to illite or other clay	foliation and metamorphic fabric seen throughout sample, looks quite deformed	chl comes from chloritization of gneiss, illite could be product of deformation or hydrothermal alteration
		15% uraninite	<0.2 mm	light to dark black	vein and fracture filling			
		10% hematite	<0.2 mm	medium brown	disseminated-massive with uraninite			
		5% illite	very fine	white to lt blue	matrix			
CS-3	837.7	98% uraninite	<0.1 – 2 mm	black	range of grain size, massive to disseminated	range of grain sizes likely due to fracturing of massive grains	remobilization event may have caused fracturing of sulfides, some u grains more intact than others	urn: two shades of grey suggests multiple generations (core is darker, older)
		2% pyrite	<0.1 mm	tarnished gold	fractured remnants			
		trace covellite	0.001 mm	medium blue	anhedral			
		trace galena	0.005 mm	silver	anhedral			

Table A.3: Thin-section descriptions from basement mineralization samples, Kianna Deposit, Shea Creek Project

No.	Depth (m)	Mineral Assemblage	Grain Size	Color	Habit	Alteration	Structure	Comments
CS-12b	839.7	43% illite	very fine	creamy white PPL, medium blue-grey XPL	acicular groundmass	Ilt is forming at expense of Ms		Ms not as well preserved in this sample - don't see very coarse, tabular laths because they have been broken apart to form Ilt. Largest Ms grains intimately associated with Urn
		35% uraninite	0.1 to 2 mm	opaque in PPL, grey in refl.	massive to disseminated	Some vein-like textures with links of 0.1 mm grains		
		20% muscovite	0.05-0.3 mm	birefringent to pastel pink, blue XPL	mostly broken laths, some larger intact laths, cleavage visible	Ms grains broken and scattered throughout Ilt groundmass		
		2% carbon	.1 mm	silvery grey in refl. Lt	amorphous blebs, irregular shapes	associated with urn		
		trace pyrite	very fine up to 0.05 mm	yellow gold refl.	subhedral			
CS-8	842.3	90% clay matrix (illite)	very fine	medium blue XPL			interesting patchwork texture likely caused by the illitization of original host rock and muscovite grains	
		5% carbon material	2-3 mm	opaque PPL, brown-grey refl.	blebby, euhedral	some blebs have dissem. pyrite within		
		4% remnant muscovite	varied size, up to 0.2 mm	birefringent to pastel pink, blue XPL	varied shape, mostly tabular			
		1% unknown reflective min	1 mm	silvery grey in refl. Lt	subhedral	acicular grains within the 1 mm grain		
		trace pyrite	very fine up to 0.05 mm	yellow gold refl.	subhedral			

Table A.3: Thin-section descriptions from basement mineralization samples, Kianna Deposit, Shea Creek Project

No.	Depth (m)	Mineral Assemblage	Grain Size	Color	Habit	Alteration	Structure	Comments
CS-13-25	850.6-850.7	85% uraninite	0.1 to 2 mm	opaque ppl, grey reflective	disseminated to massive grains, subhedral to anhedral	grains are fractured and broken, disseminated grains with ilt vein through massive grains		possibly two generations of uraninite, first being large massive fractured grains, second being small disseminated grains assoc. with ilt
		10% carbon	up to 1 mm	dark black ppl, silvery grey refl	very large, intact blebs, soft edges, little to no texture to blebs	some smaller blebs broken by urn		
		5% illite	very fine	creamy white to grey ppl, med blue xpl	acicular groundmass and veins	ilt partly veins through urn grains		
CS-21	883.6	85% uraninite	1 mm	black	massive	some anhedral grains, likely fractured off massive grains	illite fractures through uraninite, breaks up massive ore	urn: two shades of grey under reflected suggests multiple generations, second generation could be caused by illite event
		15% illite	very fine, clay	medium grey, birefringent in XPL				
CS-22a1	883.95	100% uraninite	up to 0.5 cm	light to medium grey in reflected lt	blebs to circular to long and thin, euhedral to subhedral			two shades of grey in urn suggests multiple generations
		trace pyrite	up to 0.5 mm	brassy, dim gold in refl.	anhedral, fractured grains			

Table A.3: Thin-section descriptions from basement mineralization samples, Kianna Deposit, Shea Creek Project

No.	Depth (m)	Mineral Assemblage	Grain Size	Color	Habit	Alteration	Structure	Comments
CS-22a2	883.95	15% kaolinite	very fne	white to grey	massive to acicular			roll front white green zone (kaolinite, dravite, chlorite, clausthalite) - look for dravite in other samples
		30% mg kaolinite	very fine	med to dark grey	acicular grains radiation from kaolinite			
		trace clausthalite	<0.05 mm	lt black	subhedral			
		15% illite	very fine	white to grey	veins through uraninite			
		40% uraninite		med black	massive			
CS-13-24	893.5	40% sudoite	very fine	medium green-grey	groundmass	likely forming at expense of Chl in host	Large carbon blebs are associated with massive uraninite grains	Relict Ms grains mostly seen associated with urn
		30% uraninite	up to 1 cm	opaque in PPL, grey in refl.	massive, subehdral			
		20% illite	very fine	med white-lt grey ppl, blue-med grey xpl	acicular groundmass, some veining through urn and other clay			
		10% carbon	up to 0.5 cm	dark black ppl, silvery grey xpl	blebs, soft edges, various shapes, grains lack texture			

Table A.4: Thin-section descriptions from lower basement mineralization samples, Kianna Deposit, Shea Creek Project

No.	Depth (m)	Mineral Assemblage	Grain Size	Color	Habit	Alteration	Structure	Comments
CS-13-4	961.4	70% illite	very fine	creamy white-brn ppl, med blue xpl	acicular groundmass		Disseminated urn mostly associated with the illitized groundmass, possibly urn was reset by ilt fluid	
		25% uraninite	<0.05 mm to 1 mm	black ppl, grey refl.	massive to disseminated grains			
		5% carbon	0.5 mm long	dark black ppl, silvery grey refl	blebs, soft edges, various shapes, grains lack texture			
CS-13-7	962.1	51% uraninite	< 0.05 mm to up up to 1 mm	opaque in PPL, grey in refl.	massive, subhedral, also 0.2 mm thick veins of subhedral grain clusters		Large carbon blebs are associated with massive uraninite grains, py assoc. with edges of graphite blebs	Relict Ms grains mostly seen associated with urn
		45% illite	very fine	ppl: creamy white-grey, blue grey xpl	acicular groundmass	Relict Ms grains visible in groundmass		
		3% carbon	up to 0.5 cm	dark black ppl, silvery grey xpl	blebs, soft edges, various shapes, grains lack texture			
		1% muscovite	mostly < 0.1 mm, some up to 0.3 mm	highly birefring. xpl	fine relicts and coarse tabular laths, cleavage	Ilt forming at expense of Ms		
		trace pyrite	0.1 mm	gold refl.	subhedral grains			
		trace zircon	< 0.1 mm	zoned, highly birefringent xpl	euhedral, prismatic			

Table A.4: Thin-section descriptions from lower basement mineralization samples, Kianna Deposit, Shea Creek Project

No.	Depth (m)	Mineral Assemblage	Grain Size	Color	Habit	Alteration	Structure	Comments
CS-13-9	981.3-981.5	49% uraninite	0.1 mm	opaque ppl, grey refl	small disseminated grains, subhedral, few massive grains	Massive urn broken apart by Ilt to become small disseminated grains		Relict Ms seen within Ilt groundmass where Ilt is forming at its expense. The few remant well-preserved Ms grains are intimately associated with urn
		45% carbon	<1 mm - 0.5 cm	dark black ppl, silvery grey xpl	blebs, soft edges, various shapes, grains lack texture			
		5% illite	very fine	creamy grey ppl, low birefringence	acicular veins/groundmass			
		1% muscovite	up to 0.1 mm	highly birefringent xpl	tabular laths, cleavage visible			
CS-13-11	985.8	60% carbon	up to 5 cm thick	dark black ppl, silvery grey refl	blebs, soft edges, various shapes, grains lack texture	blebs are broken apart by uraninite		
		39% uraninite	<0.1 mm to 0.5 mm	black ppl, grey refl., more reflective than carbon	urn occurs as massive grains to clusters of fine subhedral grains			
		1% pyrite	0.5 mm	yellow gold refl.	anhedral, disseminated	fractured, broken, holes		

Table A.4: Thin-section descriptions from lower basement mineralization samples, Kianna Deposit, Shea Creek Project

No.	Depth (m)	Mineral Assemblage	Grain Size	Color	Habit	Alteration	Structure	Comments
CS-13-13a	992.2-992.4	45% uraninite	<0.05 mm to 1 mm	black ppl, grey refl.	massive to dissem. grains	forms around carbon blebs	Urn disseminated among illitized groundmass - possible that two generations of urn exist, with U1 being massive and U2 being disseminated and associated with ilt	Ms remnant laths broken apart in illitized groundmass
		40% carbon	4 mm x 1 mm	dark black ppl, silvery grey refl	blebs, soft edges, various shapes			
		10% illite	very fine	creamy white-brown ppl, med blue xpl	acicular groundmass			
		1% muscovite	up to 0.3 mm	highly birefringent xpl	fine to coarse tabular laths	Ilt forming at expense of Ms		
		1% pyrite	<<0.05 mm	yellow gold refl.	anhedral, disseminated			
CS-13-13b	992.2-992.4	92% illite	very fine	white-grey ppl, blue-dark grey xpl	acicular groundmass		Kln likely forming at expense of host-rock chl or feldspar	Highly illitized sample with blebs of carbon (graphite?) sporadically disseminated throughout, like CS-8
		4% carbon	0.1 - 0.3 mm	silvery grey refl	blebs, soft edges, various shapes	grains lack texture		
		2% kaolinite	very fine	cream-grey ppl, low birefringence	bursts of acicular needles	within ilt groundmass		
		1% muscovite	up to 0.4 mm	high birefring. xpl	fine relicts and coarse tabular laths, cleavage	Ilt forming at expense of Ms		
		1% pyrite	0.1 mm	yellow gold refl.	subhedral grains	Py associated with C blebs		
		trace uraninite	0.2 mm	grey refl lt				
		trace zircon	< 0.1 mm	zoned, highly birefringent xpl	euhedral, prismatic			

Table A.4: Thin-section descriptions from lower basement mineralization samples, Kianna Deposit, Shea Creek Project

No.	Depth (m)	Mineral Assemblage	Grain Size	Color	Habit	Alteration	Structure	Comments
CS-13-15	993	48% carbon	up to 2 mm long	dark black ppl, silvery grey refl	blebs, soft edges, various shapes, grains lack texture			Ms remnant laths broken apart in illitized groundmass
		45% uraninite	<0.05 mm to 2 mm	black ppl, grey refl.	massive to disseminated grains			
		5% illite	very fine	creamy white-brown ppl, med blue xpl	acicular groundmass			
		2% muscovite	up to 0.1 mm	highly birefringent xpl	fine relict laths	Most intact laths intimately associated with urn		

Appendix B
Electron Probe Microanalysis (EPMA)
Standards and Data

Table B.1: Elements and their respective standards for EPMA instrumental calibration. Errors associated with EPMA measurements are <±0.1 wt%

Element	Standard
Na	Albite
Si	Diopside
Ca	Diopside
U	UO2
Fe	Fayalite
Pb	PbTe
Al	Andalusite
Th	ThO2
S	Pyrite
K	Orthoclase
F	Riebeckite
Mg	Olivine
Cl	Tugtuphite
P	Apatite
Ti	Sphene
V	VP2O7
Ni	Pentlandite
Cu	Chalcopyrite
As	Cobalt
Se	CdSe
Zr	ZrO2
Sr	SrTiO3
Ba	Barite
Co	Cobalt
Zn	ZnS
Ag	SRM1 Au20Ag80
Sn	Cassiterite
Sb	Stibnite
Bi	Bi2Se3
Y	YPO4
La	LaPO4
Ce	CePO4
Pr	PrPO4
Nd	NdPO4
Sm	SmPO4
Eu	EuPO4
Gd	GdPO4
Tb	TbPO4
Dy	DyPO4
Ho	HoPO4
Er	ErPO4
Tm	TmPO4
Yb	YbPO4
Lu	LuPO4

Table B.2: Chemical compositions (wt%) and calculated Chemical-Pb ages (Ma) for uraninite at the Kianna deposit

Sample No.	SiO_2	UO_2	CaO	Fe_2O_3	PbO	Al_2O_3	ThO_2	Total	U wt%	Pb wt%	Th wt%	Chem. Pb Age (Ma)
CS-4a	0.33	88.78	2.20	0.67	3.91	0.11	0.02	97.45	78.26	3.63	0.02	350
CS-4a	0.51	88.25	3.52	0.47	1.15	0.15	0.00	96.80	77.79	1.07	0.00	104
CS-4a	1.07	84.27	4.93	2.02	0.97	0.21	0.00	96.19	74.28	0.90	0.00	91
CS-4a	0.78	82.45	5.49	2.84	1.52	0.22	0.00	95.98	72.68	1.41	0.00	146
CS-4a	0.23	87.34	3.27	0.75	3.21	0.22	0.04	97.22	76.99	2.98	0.04	292
CS-4a	0.50	86.65	4.16	0.87	0.85	0.15	0.00	96.60	76.38	0.79	0.00	78
CS-4a	0.22	88.41	3.47	0.72	2.14	0.24	0.00	97.08	77.94	1.99	0.00	193
CS-4a	0.72	87.09	3.10	0.88	0.57	0.12	0.00	95.83	76.77	0.52	0.00	51
CS-4a	0.58	85.00	4.27	0.84	0.37	0.26	0.00	96.28	74.93	0.35	0.00	35
CS-4a	3.38	79.88	2.29	4.29	0.44	0.37	0.01	94.58	70.41	0.41	0.01	44
CS-4a	0.25	87.98	3.89	0.83	1.95	0.22	0.00	96.95	77.55	1.81	0.00	176
CS-4a	0.51	87.63	2.62	0.15	5.39	0.05	0.00	98.28	77.25	5.00	0.00	489
CS-4a	0.47	84.85	3.92	0.74	0.35	0.15	0.00	94.30	74.80	0.32	0.00	32
CS-4a	2.05	86.43	1.34	0.08	0.32	0.17	0.00	95.59	76.19	0.30	0.00	30
CS-4a	0.43	87.05	2.06	0.15	5.60	0.03	0.00	96.84	76.74	5.20	0.00	512
CS-4a	0.22	87.43	3.50	0.70	1.90	0.33	0.02	95.91	77.07	1.76	0.02	172
CS-4a	0.19	86.82	4.51	0.60	2.17	0.14	0.00	96.22	76.53	2.01	0.00	198
CS-4a	0.40	86.78	2.24	0.22	5.48	0.07	0.00	96.58	76.50	5.09	0.00	502
CS-4a	0.31	88.06	3.18	0.91	2.42	0.24	0.00	96.66	77.63	2.25	0.00	219
CS-4a	0.34	88.40	3.63	0.62	2.74	0.19	0.01	97.44	77.93	2.54	0.01	246
CS-4a	0.41	86.46	2.10	0.13	5.71	0.07	0.04	96.48	76.21	5.30	0.04	525
CS-4a	0.29	88.71	3.17	0.76	2.24	0.26	0.00	97.31	78.20	2.08	0.00	201
CS-4a	0.60	86.51	3.38	1.92	0.79	0.19	0.00	96.61	76.26	0.74	0.00	73
CS-4a	0.71	88.20	2.36	0.22	0.94	0.27	0.05	96.32	77.75	0.87	0.04	84
CS-4a	0.17	87.53	2.17	0.23	5.47	0.03	0.00	96.83	77.16	5.08	0.00	497
CS-4a	0.30	86.87	1.99	0.20	5.57	0.04	0.02	96.59	76.57	5.17	0.02	510
CS-4a	0.34	86.81	2.31	0.51	4.13	0.09	0.00	95.70	76.53	3.83	0.00	378
CS-4a	0.33	88.68	3.10	0.71	2.32	0.23	0.00	96.88	78.17	2.15	0.00	208
CS-4a	0.42	87.59	2.34	0.19	5.25	0.07	0.00	97.24	77.21	4.87	0.00	476
CS-4a	0.47	86.85	2.86	0.22	5.40	0.09	0.00	97.60	76.56	5.01	0.00	494
CS-4a	0.36	86.18	3.29	0.19	5.34	0.05	0.02	97.58	75.97	4.96	0.01	493
CS-4a	1.74	83.16	3.51	1.50	0.85	0.15	0.00	94.55	73.31	0.79	0.00	81

Table B.2: Chemical compositions (wt%) and calculated Chemical-Pb ages (Ma) for uraninite at the Kianna deposit

Sample No.	SiO_2	UO_2	CaO	Fe_2O_3	PbO	Al_2O_3	ThO_2	Total	U wt%	Pb wt%	Th wt%	Chem. Pb Age (Ma)
CS-4a	0.72	87.58	1.44	0.15	0.55	0.26	0.02	95.66	77.21	0.51	0.02	50
CS-4a	1.73	83.99	2.78	0.94	0.76	0.15	0.07	94.16	74.04	0.71	0.06	72
CS-4a	0.48	87.04	2.74	0.20	5.55	0.06	0.00	97.84	76.73	5.15	0.00	507
CS-4a	0.40	87.45	2.58	0.18	5.81	0.05	0.00	98.16	77.09	5.40	0.00	529
CS-4a	0.34	88.04	2.26	0.33	5.00	0.05	0.00	97.53	77.61	4.65	0.00	452
CS-4a	0.39	86.91	2.41	0.24	5.55	0.08	0.00	97.26	76.61	5.15	0.00	508
CS-4a	0.36	85.69	2.19	0.23	5.13	0.07	0.00	95.45	75.54	4.76	0.00	476
CS-4a	0.25	88.24	3.18	0.74	2.35	0.27	0.00	97.04	77.78	2.18	0.00	212
CS-4a	0.40	86.53	3.24	0.20	5.20	0.08	0.01	97.76	76.28	4.82	0.01	477
CS-4a	0.35	87.00	3.29	0.37	4.85	0.08	0.00	97.91	76.69	4.51	0.00	444
CS-4a	0.19	88.15	3.05	0.61	4.22	0.07	0.00	98.06	77.71	3.91	0.00	380
CS-4a	0.20	88.13	3.11	0.53	3.88	0.09	0.02	97.90	77.68	3.60	0.02	350
CS-4a	0.37	85.66	3.20	0.30	4.99	0.07	0.00	96.43	75.51	4.63	0.00	463
CS-4a	0.42	86.28	3.14	0.19	5.39	0.07	0.02	97.56	76.06	5.01	0.02	497
CS-4a	0.30	88.17	3.09	0.61	2.63	0.19	0.00	97.25	77.72	2.44	0.00	237
CS-4a	0.39	86.14	3.61	2.21	1.37	0.13	0.01	95.97	75.93	1.28	0.01	127
CS-4a	0.12	87.02	2.23	0.11	5.84	0.00	0.00	96.49	76.71	5.42	0.00	533
CS-4a	0.31	89.95	2.69	0.62	2.47	0.22	0.00	98.05	79.29	2.29	0.00	218
CS-4a	0.28	87.88	2.94	0.68	2.24	0.24	0.00	96.49	77.47	2.08	0.00	203
CS-4a	0.30	87.68	2.46	0.74	3.81	0.08	0.00	96.93	77.29	3.54	0.00	346
CS-4a	0.36	86.58	2.51	0.35	5.04	0.07	0.00	96.79	76.32	4.68	0.00	463
CS-4a	0.26	86.64	2.06	0.16	5.20	0.05	0.00	95.94	76.37	4.82	0.00	477
CS-4a	0.26	87.76	2.71	0.67	2.27	0.25	0.00	96.17	77.36	2.11	0.00	206
CS-4a	0.61	85.91	2.62	0.27	4.53	0.06	0.00	96.59	75.73	4.21	0.00	420
CS-4a	0.16	86.57	2.14	0.15	5.66	0.01	0.00	95.90	76.31	5.25	0.00	519
CS-4b	0.55	86.21	3.63	1.96	0.34	0.24	0.00	97.62	76.00	0.32	0.00	31

Table B.2: Chemical compositions (wt%) and calculated Chemical-Pb ages (Ma) for uraninite at the Kianna deposit

Sample No.	SiO_2	UO_2	CaO	Fe_2O_3	PbO	Al_2O_3	ThO_2	Total	U wt%	Pb wt%	Th wt%	Chem. Pb Age (Ma)
CS-17	4.51	84.47	1.64	2.01	0.39	0.37	0.00	94.45	74.46	0.36	0.00	37
CS-17	4.31	82.84	2.14	2.18	0.60	0.41	0.00	94.20	73.02	0.56	0.00	58
CS-17	4.50	83.83	1.59	1.53	0.67	0.43	0.11	94.39	73.89	0.62	0.10	63
CS-17	3.24	86.21	2.01	1.15	0.30	0.36	0.04	94.67	75.99	0.28	0.03	28
CS-17	3.83	83.52	1.84	1.27	0.65	0.53	0.00	93.78	73.62	0.60	0.00	62
CS-17	4.14	84.43	1.61	1.44	0.47	0.43	0.01	94.24	74.42	0.44	0.01	45
CS-17	4.51	83.08	2.34	1.59	0.58	0.48	0.00	94.19	73.23	0.54	0.00	56
CS-17	4.42	84.22	1.69	1.54	0.66	0.44	0.00	94.62	74.24	0.61	0.00	62
CS-17	4.37	84.60	2.42	1.52	0.61	0.40	0.00	95.63	74.57	0.57	0.00	58
CS-17	4.43	83.57	1.74	1.80	0.47	0.45	0.00	93.98	73.67	0.44	0.00	45
CS-17	4.13	84.33	1.60	1.42	0.50	0.48	0.00	94.16	74.34	0.46	0.00	47
CS-17	4.34	84.02	1.70	1.62	0.47	0.45	0.00	94.14	74.07	0.43	0.00	44
CS-17	3.86	85.59	1.71	1.44	0.32	0.44	0.04	94.79	75.45	0.30	0.03	30
CS-17	4.03	78.77	1.51	3.09	2.73	0.44	0.00	96.82	69.43	2.54	0.00	276
CS-17	4.50	83.77	1.93	1.61	0.64	0.44	0.01	94.52	73.85	0.59	0.01	60
CS-17	4.37	83.36	1.91	1.79	0.53	0.44	0.00	94.15	73.48	0.49	0.00	50
CS-17	1.23	86.08	1.38	2.09	0.77	0.05	0.04	93.86	75.88	0.71	0.04	71
CS-17	4.26	83.99	1.90	1.54	0.67	0.38	0.00	94.53	74.04	0.62	0.00	63
CS-17	4.54	83.87	1.53	1.92	0.57	0.46	0.00	94.58	73.93	0.53	0.00	54
CS-17	4.71	82.36	1.48	2.04	0.48	0.42	0.03	93.14	72.60	0.45	0.03	47
CS-17	3.17	86.16	1.88	1.29	0.32	0.44	0.01	95.27	75.95	0.30	0.00	30
CS-17	4.13	85.49	1.79	1.37	0.30	0.35	0.00	94.78	75.36	0.27	0.00	27
CS-17	4.41	83.36	1.86	2.17	0.37	0.35	0.00	94.02	73.49	0.35	0.00	36
CS-17	3.50	85.66	1.85	1.26	0.28	0.34	0.01	94.31	75.51	0.26	0.01	26
CS-17	1.24	85.52	1.59	1.64	0.33	0.05	0.00	92.28	75.38	0.31	0.00	31
CS-17	3.58	86.14	1.83	1.17	0.34	0.37	0.07	95.06	75.93	0.32	0.06	32
CS-17	4.03	83.70	1.80	1.67	0.56	0.38	0.02	93.88	73.78	0.52	0.02	53

Table B.2: Chemical compositions (wt%) and calculated Chemical-Pb ages (Ma) for uraninite at the Kianna deposit

Sample No.	SiO_2	UO_2	CaO	Fe_2O_3	PbO	Al_2O_3	ThO_2	Total	U wt%	Pb wt%	Th wt%	Chem. Pb Age (Ma)
CS-9b	3.11	84.52	2.08	1.64	0.58	0.29	0.01	93.88	74.51	0.54	0.01	55
CS-9b	4.24	82.95	2.09	1.89	0.48	0.48	0.00	93.96	73.12	0.45	0.00	46
CS-9b	2.79	81.92	3.65	2.95	0.22	0.25	0.04	93.00	72.21	0.20	0.04	21
CS-9b	2.28	87.22	1.88	1.58	0.78	0.23	0.00	95.24	76.89	0.72	0.00	71
CS-9b	2.62	84.07	2.85	2.37	0.40	0.30	0.02	94.24	74.11	0.37	0.01	38
CS-9b	3.08	85.03	2.15	1.69	0.67	0.32	0.01	94.97	74.95	0.62	0.01	62
CS-9b	4.75	80.40	3.60	1.82	0.88	0.58	0.01	93.41	70.87	0.81	0.01	86
CS-9b	6.00	78.56	2.95	3.05	0.46	0.18	0.03	92.79	69.25	0.43	0.02	47
CS-9b	3.64	83.04	2.15	1.89	0.60	0.40	0.06	93.45	73.20	0.56	0.05	58
CS-9b	2.16	87.35	1.83	1.62	0.84	0.23	0.00	95.40	77.00	0.78	0.00	76
CS-9b	0.37	88.49	1.87	1.28	1.71	0.09	0.00	94.66	78.00	1.59	0.00	154
CS-9b	0.81	88.15	1.52	1.39	1.25	0.11	0.00	94.31	77.70	1.16	0.00	113
CS-9b	0.36	89.58	1.24	1.34	1.72	0.08	0.00	95.38	78.96	1.60	0.00	153
CS-9b	0.38	89.35	1.12	1.20	1.61	0.09	0.03	94.63	78.76	1.49	0.03	143
CS-9b	0.36	89.86	1.07	1.15	1.60	0.10	0.04	95.08	79.21	1.48	0.03	141
CS-9b	0.37	89.04	0.94	1.22	1.64	0.10	0.04	94.38	78.49	1.52	0.03	146
CS-9b	0.32	90.21	0.86	1.29	1.55	0.09	0.00	95.19	79.52	1.44	0.00	137
CS-9b	0.46	89.81	1.07	1.56	1.46	0.09	0.00	95.39	79.17	1.36	0.00	130
CS-9b	0.46	89.59	1.06	1.34	1.65	0.10	0.00	95.03	78.98	1.53	0.00	146
CS-9b	0.32	89.42	1.60	1.53	1.83	0.09	0.00	95.53	78.82	1.70	0.00	163
CS-9b	0.58	87.04	2.99	1.20	2.12	0.09	0.01	95.06	76.73	1.97	0.01	194
CS-9b	0.35	88.36	1.07	1.24	1.60	0.09	0.00	93.61	77.89	1.49	0.00	144
CS-9b	0.35	89.81	1.33	1.17	1.64	0.09	0.02	95.25	79.17	1.52	0.02	145
CS-9b	0.26	89.17	1.60	1.24	1.72	0.08	0.00	94.78	78.61	1.60	0.00	154
CS-9b	1.12	84.01	2.38	2.27	1.15	0.04	0.00	92.24	74.06	1.07	0.00	109

Table B.2: Chemical compositions (wt%) and calculated Chemical-Pb ages (Ma) for uraninite at the Kianna deposit

Sample No.	SiO_2	UO_2	CaO	Fe_2O_3	PbO	Al_2O_3	ThO_2	Total	U wt%	Pb wt%	Th wt%	Chem. Pb Age (Ma)
CS-9b	1.15	85.11	2.45	2.20	0.28	0.05	0.03	92.58	75.02	0.26	0.03	26
CS-9b	1.05	83.74	3.00	2.49	0.31	0.07	0.00	92.21	73.81	0.28	0.00	29
CS-9b	1.15	84.36	2.65	2.10	0.33	0.04	0.00	92.00	74.36	0.30	0.00	30
CS-9b	1.31	85.44	2.10	1.78	0.45	0.08	0.00	92.69	75.31	0.42	0.00	42
CS-9b	1.23	83.95	3.27	2.85	0.15	0.07	0.00	92.59	74.00	0.14	0.00	14
CS-9b	1.16	84.34	2.36	2.05	0.63	0.05	0.00	91.86	74.35	0.59	0.00	60
CS-9b	1.08	84.32	2.55	2.10	0.62	0.07	0.04	92.12	74.33	0.58	0.04	59
CS-9b	1.10	83.08	2.77	2.19	0.72	0.02	0.06	91.35	73.23	0.66	0.05	68
CS-9b	1.04	83.94	2.69	1.91	0.66	0.04	0.00	91.53	74.00	0.61	0.00	62
CS-9b	1.06	85.14	3.11	2.30	0.23	0.05	0.01	93.13	75.05	0.21	0.01	21
CS-13-18	0.65	87.12	2.42	2.07	0.70	0.05	0.00	94.41	76.80	0.65	0.00	64
CS-13-18	0.57	87.33	2.21	1.99	0.96	0.04	0.02	94.24	76.98	0.90	0.02	88
CS-13-18	0.70	88.73	2.33	2.08	0.73	0.04	0.00	96.00	78.21	0.68	0.00	66
CS-13-18	2.43	76.52	4.34	2.95	0.08	1.20	0.04	89.45	67.45	0.07	0.04	8
CS-13-18	0.95	85.33	2.89	2.28	0.40	0.10	0.00	93.40	75.22	0.37	0.00	37
CS-13-18	1.12	86.51	3.03	2.33	0.28	0.10	0.00	94.78	76.25	0.26	0.00	26
CS-13-18	1.94	77.90	4.36	2.08	0.00	1.12	0.02	89.48	68.67	0.00	0.02	0
CS-13-18	1.49	79.13	4.57	1.33	0.01	0.23	0.00	89.17	69.75	0.01	0.00	1
CS-13-18	1.95	78.10	4.43	1.79	0.02	0.70	0.00	89.23	68.85	0.02	0.00	2
CS-13-18	1.32	84.88	3.65	2.67	0.07	0.17	0.04	94.77	74.82	0.07	0.04	7
CS-13-18	1.16	85.63	3.55	2.59	0.10	0.10	0.00	94.88	75.48	0.09	0.00	9
CS-13-18	0.80	85.87	2.60	2.14	0.63	0.09	0.02	93.77	75.69	0.59	0.02	59
CS-13-18	0.85	84.13	2.46	2.16	1.47	0.09	0.00	93.08	74.16	1.37	0.00	139
CS-13-18	0.55	89.13	2.19	1.88	0.86	0.04	0.00	95.69	78.56	0.80	0.00	77
CS-13-18	1.62	86.54	2.59	2.35	0.24	0.15	0.00	95.04	76.28	0.22	0.00	22
CS-13-18	1.48	87.23	2.95	2.47	0.29	0.16	0.00	95.91	76.89	0.27	0.00	27
CS-13-18	1.78	85.83	3.01	2.54	0.18	0.25	0.00	94.73	75.66	0.17	0.00	17
CS-13-18	1.11	87.19	2.54	2.48	0.37	0.06	0.00	95.27	76.85	0.35	0.00	34
CS-13-18	1.38	86.87	3.05	2.67	0.20	0.12	0.00	95.62	76.57	0.18	0.00	18
CS-13-18	1.83	86.58	2.93	2.69	0.19	0.19	0.00	95.72	76.32	0.18	0.00	18
CS-13-18	1.45	85.04	2.75	2.42	0.43	0.14	0.01	93.61	74.97	0.40	0.01	40

Table B.2: Chemical compositions (wt%) and calculated Chemical-Pb ages (Ma) for uraninite at the Kianna deposit

Sample No.	SiO_2	UO_2	CaO	Fe_2O_3	PbO	Al_2O_3	ThO_2	Total	U wt%	Pb wt%	Th wt%	Chem. Pb Age (Ma)
CS-13-18	0.74	87.51	3.27	2.08	0.35	0.03	0.07	95.44	77.14	0.33	0.06	32
CS-13-18	1.78	79.74	4.61	1.58	0.02	0.22	0.00	90.03	70.29	0.02	0.00	2
CS-13-18	1.16	82.35	4.68	1.76	0.00	0.10	0.03	91.77	72.59	0.00	0.03	0
CS-13-18	1.24	80.91	4.44	1.23	0.07	0.06	0.03	90.07	71.32	0.07	0.03	7
CS-13-18	1.12	87.33	3.48	2.46	0.18	0.11	0.00	96.34	76.98	0.16	0.00	16
CS-13-18	1.29	86.45	2.92	2.40	0.18	0.08	0.05	94.62	76.20	0.17	0.04	17
CS-13-18	1.55	85.57	3.18	2.67	0.10	0.14	0.03	94.55	75.43	0.09	0.03	9
CS-13-18	1.22	86.23	3.62	2.73	0.12	0.14	0.02	95.74	76.01	0.11	0.02	11
CS-13-18	0.71	85.33	2.78	2.61	0.26	0.06	0.00	93.41	75.22	0.24	0.00	24
CS-13-18	1.92	68.95	3.67	1.10	0.02	0.33	0.03	78.03	60.77	0.01	0.02	1
CS-13-18	1.99	78.22	5.08	1.99	0.01	0.75	0.00	90.74	68.95	0.01	0.00	1
CS-13-18	1.64	78.41	4.94	1.69	0.02	0.28	0.00	89.10	69.12	0.02	0.00	2
CS-13-28	3.54	85.93	2.53	1.61	0.82	0.34	0.02	96.72	75.75	0.76	0.02	76
CS-13-28	4.34	85.45	1.93	1.63	0.60	0.67	0.00	96.63	75.32	0.56	0.00	56
CS-13-28	3.25	85.40	2.23	1.72	0.53	0.31	0.03	95.39	75.28	0.49	0.02	49
CS-13-28	3.14	86.84	1.95	1.57	0.60	0.32	0.00	96.39	76.55	0.56	0.00	55
CS-13-28	6.63	81.45	3.39	1.30	0.00	0.79	0.02	94.98	71.80	0.00	0.01	0
CS-13-28	6.69	80.94	3.19	1.36	0.02	0.93	0.00	94.97	71.35	0.02	0.00	2
CS-13-28	6.83	79.41	3.45	1.04	0.04	0.83	0.03	93.18	70.00	0.03	0.02	3
CS-13-28	5.26	81.55	3.37	1.25	0.01	0.50	0.00	93.24	71.88	0.01	0.00	1
CS-13-28	3.79	86.40	1.70	1.41	0.53	0.43	0.01	96.25	76.16	0.50	0.01	50
CS-13-28	3.30	86.76	2.02	1.52	0.63	0.32	0.00	96.73	76.48	0.59	0.00	58
CS-13-28	3.28	86.18	2.14	1.63	0.62	0.35	0.00	96.43	75.97	0.58	0.00	58
CS-13-28	3.43	85.94	1.78	1.64	0.68	0.47	0.00	96.26	75.76	0.63	0.00	63
CS-13-28	3.83	86.66	1.56	1.81	0.52	0.45	0.01	96.73	76.39	0.48	0.01	47
CS-13-28	4.70	82.16	2.62	1.78	0.00	0.83	0.02	93.82	72.43	0.00	0.01	0
CS-13-28	4.52	87.43	1.72	1.07	0.42	0.47	0.00	97.16	77.06	0.39	0.00	38
CS-13-28	5.90	82.30	2.40	1.47	0.00	0.51	0.00	94.05	72.54	0.00	0.00	0
CS-13-28	2.82	87.42	2.14	1.25	0.29	0.32	0.00	95.89	77.06	0.27	0.00	26
CS-13-28	2.50	82.57	3.62	1.56	0.00	0.34	0.00	92.51	72.79	0.00	0.00	0
CS-13-28	2.38	82.04	3.59	1.54	0.00	0.32	0.00	91.92	72.32	0.00	0.00	0
CS-13-28	5.42	83.98	2.20	1.36	0.10	0.43	0.00	95.08	74.03	0.09	0.00	9

Table B.2: Chemical compositions (wt%) and calculated Chemical-Pb ages (Ma) for uraninite at the Kianna deposit

Sample No.	SiO_2	UO_2	CaO	Fe_2O_3	PbO	Al_2O_3	ThO_2	Total	U wt%	Pb wt%	Th wt%	Chem. Pb Age (Ma)
CS-20b1	4.50	73.30	6.44	4.29	0.43	1.24	0.00	92.56	64.61	0.40	0.00	47
CS-20b1	3.95	74.66	6.94	3.25	0.51	1.74	0.00	93.43	65.81	0.47	0.00	54
CS-20b1	1.68	79.29	6.42	3.84	0.54	0.21	0.00	93.87	69.89	0.51	0.00	55
CS-20b1	2.49	77.19	5.76	4.36	0.60	0.37	0.00	92.97	68.04	0.55	0.00	61
CS-20b1	5.26	71.77	5.22	5.17	0.52	1.67	0.01	92.33	63.27	0.48	0.01	57
CS-20b1	3.13	76.36	6.13	3.86	0.59	0.66	0.00	93.38	67.31	0.54	0.00	61
CS-20b1	8.05	63.48	5.17	6.15	0.37	2.57	0.03	89.23	55.96	0.35	0.02	47
CS-20b1	4.10	74.04	6.68	3.97	0.43	1.16	0.00	92.58	65.26	0.40	0.00	46
CS-20b1	2.60	76.78	6.81	4.24	0.46	0.59	0.06	93.67	67.68	0.42	0.05	47
CS-20b1	1.40	78.95	6.70	3.52	0.50	0.07	0.07	93.28	69.59	0.47	0.06	51
CS-20b1	3.40	75.17	6.13	4.02	0.50	0.73	0.00	92.54	66.26	0.46	0.00	52
CS-20b1	6.07	71.54	5.96	4.44	0.57	2.84	0.00	94.64	63.06	0.53	0.00	63
CS-20b1	2.34	76.87	6.39	3.98	0.60	0.37	0.04	93.05	67.76	0.56	0.04	62
CS-20b1	1.89	79.10	6.66	3.26	0.53	0.19	0.00	94.29	69.73	0.49	0.00	53
CS-20b1	7.24	68.37	5.70	4.58	0.40	2.28	0.00	91.70	60.27	0.37	0.00	46
CS-20b1	1.73	77.26	7.77	2.81	0.46	0.12	0.00	92.24	68.11	0.43	0.00	48
CS-20b1	3.25	74.85	6.32	4.72	0.54	0.75	0.00	92.36	65.98	0.50	0.00	57
CS-20b1	6.28	67.85	5.21	7.29	0.36	2.64	0.07	92.15	59.81	0.34	0.06	43
CS-20b1	4.30	72.50	6.17	4.73	0.46	1.17	0.00	91.71	63.91	0.43	0.00	51
CS-20b1	2.17	77.98	6.90	3.07	0.57	0.40	0.05	93.47	68.74	0.53	0.05	58
CS-20b1	2.01	78.11	6.68	3.47	0.58	0.44	0.00	93.92	68.85	0.54	0.00	59
CS-20b1	1.47	78.43	6.87	3.03	0.46	0.09	0.00	92.73	69.13	0.43	0.00	47
CS-20b1	2.83	75.28	6.49	4.25	0.48	0.97	0.03	92.85	66.36	0.45	0.03	51
CS-20b1	1.89	78.27	6.24	4.01	0.55	0.20	0.02	93.29	69.00	0.51	0.01	56
CS-20b1	1.71	79.72	6.87	3.06	0.50	0.29	0.01	94.50	70.27	0.46	0.01	49
CS-20b1	2.29	76.57	6.91	3.80	0.49	0.48	0.00	93.02	67.50	0.46	0.00	51
CS-20b1	4.39	72.33	6.88	4.10	0.46	1.34	0.07	92.00	63.76	0.43	0.06	51
CS-20b1	1.82	78.21	6.78	3.16	0.50	0.36	0.04	93.60	68.94	0.47	0.03	51
CS-20b1	1.72	78.29	7.21	3.11	0.55	0.28	0.06	93.38	69.01	0.51	0.05	56
CS-20b1	2.32	76.59	6.94	3.70	0.51	0.44	0.00	92.74	67.51	0.47	0.00	53

Table B.2: Chemical compositions (wt%) and calculated Chemical-Pb ages (Ma) for uraninite at the Kianna deposit

Sample No.	SiO_2	UO_2	CaO	Fe_2O_3	PbO	Al_2O_3	ThO_2	Total	U wt%	Pb wt%	Th wt%	Chem. Pb Age (Ma)
CS-20b1	1.88	77.12	7.17	3.56	0.51	0.22	0.00	92.78	67.98	0.47	0.00	52
CS-20b1	1.07	80.16	5.69	3.38	0.64	0.12	0.00	93.42	70.66	0.60	0.00	64
CS-20b1	0.99	80.55	6.03	3.31	0.46	0.07	0.00	93.84	71.00	0.43	0.00	46
CS-20b1	1.01	80.25	5.63	3.46	0.63	0.01	0.01	93.83	70.74	0.58	0.01	62
CS-20b1	2.30	78.09	6.50	3.52	0.51	0.32	0.00	94.02	68.83	0.47	0.00	52
CS-20b1	2.29	76.31	6.50	4.21	0.59	0.44	0.00	92.94	67.26	0.55	0.00	62
CS-20b1	1.26	78.69	7.04	3.32	0.55	0.08	0.02	92.95	69.37	0.51	0.01	56
CS-20b1	1.75	78.19	7.23	2.98	0.54	0.21	0.00	93.09	68.93	0.50	0.00	55
CS-20b1	1.13	80.69	5.24	3.26	0.57	0.05	0.00	93.14	71.12	0.53	0.00	56
CS-20b1	0.90	80.24	5.91	3.59	0.53	0.07	0.00	93.43	70.73	0.49	0.00	52
CS-20b1	1.15	80.60	6.27	3.40	0.58	0.09	0.00	94.66	71.04	0.54	0.00	57
CS-20b1	1.63	77.53	6.57	3.07	0.55	0.07	0.01	92.02	68.34	0.51	0.01	56
CS-20b1	3.29	75.01	7.03	4.17	0.50	0.81	0.05	93.37	66.12	0.47	0.04	54
CS-20b1	2.31	76.18	7.45	3.89	0.49	0.48	0.05	92.93	67.15	0.45	0.05	51
CS-20b1	2.48	76.49	6.42	3.89	0.45	0.40	0.05	92.61	67.43	0.42	0.05	47
CS-20b1	2.02	77.03	6.97	3.60	0.49	0.22	0.00	92.63	67.90	0.45	0.00	50
CS-20b1	3.53	74.15	6.41	4.35	0.47	0.92	0.01	92.49	65.37	0.43	0.01	50
CS-20b2	1.08	82.86	4.57	2.59	0.79	0.37	0.00	94.65	73.04	0.73	0.00	75
CS-20b2	1.21	80.03	6.72	3.52	0.58	0.06	0.00	93.86	70.54	0.54	0.00	58
CS-20b2	1.16	80.59	6.54	3.45	0.49	0.03	0.00	93.99	71.04	0.45	0.00	48
CS-20b2	1.10	78.97	6.54	5.08	0.51	0.06	0.00	93.88	69.61	0.47	0.00	51
CS-20b2	1.09	81.97	6.00	3.42	0.61	0.03	0.00	95.09	72.26	0.57	0.00	60
CS-20b2	1.15	79.20	6.82	3.81	0.47	0.06	0.02	93.18	69.82	0.44	0.02	48
CS-14b	0.77	87.69	1.93	0.44	3.47	0.00	0.00	98.73	77.30	3.23	0.00	315
CS-14b	0.67	85.97	1.99	0.45	3.50	0.04	0.00	97.29	75.78	3.25	0.00	324
CS-14b	0.74	87.83	1.85	0.42	3.27	0.04	0.00	98.55	77.42	3.03	0.00	295
CS-14b	2.40	84.68	2.24	1.22	2.33	0.11	0.03	96.62	74.65	2.16	0.03	218

Table B.2: Chemical compositions (wt%) and calculated Chemical-Pb ages (Ma) for uraninite at the Kianna deposit

Sample No.	SiO_2	UO_2	CaO	Fe_2O_3	PbO	Al_2O_3	ThO_2	Total	U wt%	Pb wt%	Th wt%	Chem. Pb Age (Ma)
CS-14b	0.67	81.71	1.88	0.68	2.76	0.03	0.00	91.93	72.03	2.57	0.00	269
CS-14b	0.64	86.93	1.87	0.59	3.22	0.03	0.00	97.86	76.63	2.99	0.00	295
CS-14b	0.63	86.69	1.70	0.54	3.40	0.04	0.04	97.53	76.42	3.16	0.04	312
CS-14b	0.60	85.95	1.73	0.51	3.22	0.00	0.00	96.74	75.77	2.99	0.00	298
CS-14b	0.63	87.31	2.04	0.35	3.49	0.02	0.00	98.36	76.96	3.24	0.00	318
CS-14b	0.81	86.29	2.13	1.16	3.16	0.03	0.00	98.09	76.06	2.93	0.00	291
CS-14b	0.71	86.86	1.74	0.78	2.83	0.03	0.00	97.63	76.57	2.63	0.00	259
CS-14b	0.62	88.34	1.93	0.47	3.19	0.02	0.03	99.09	77.87	2.97	0.03	288
CS-14b	3.11	84.64	2.51	1.36	1.59	0.11	0.08	96.88	74.61	1.47	0.07	149
CS-14b	0.68	88.43	1.84	0.39	3.42	0.01	0.00	99.60	77.95	3.18	0.00	308
CS-14b	0.68	87.00	1.88	0.42	3.37	0.03	0.00	97.95	76.69	3.13	0.00	308
CS-14b	0.93	84.22	2.16	0.63	3.81	0.06	0.04	96.64	74.24	3.54	0.03	360
CS-14b	0.61	86.34	2.01	0.49	3.56	0.02	0.00	97.71	76.11	3.30	0.00	327
CS-14b	0.81	88.29	2.00	0.46	3.13	0.03	0.00	99.10	77.83	2.91	0.00	282
CS-14b	4.30	81.34	2.64	1.66	0.24	0.25	0.00	93.50	71.70	0.23	0.00	24
CS-14b	0.81	86.91	1.79	0.36	3.86	0.05	0.00	98.06	76.61	3.58	0.00	353
CS-14b	0.88	85.69	1.89	0.49	3.32	0.03	0.09	97.33	75.54	3.08	0.08	308
CS-14b	0.68	86.68	2.31	0.52	3.05	0.03	0.00	97.29	76.41	2.83	0.00	280
CS-14b	0.59	86.31	1.76	0.37	3.70	0.04	0.00	98.44	76.08	3.43	0.00	340
CS-14b	0.72	86.83	1.60	0.39	3.17	0.01	0.05	97.90	76.54	2.94	0.04	290
CS-14b	0.50	85.25	1.94	0.37	3.07	0.01	0.06	96.89	75.15	2.85	0.05	286
CS-14b	0.78	84.11	1.65	0.27	4.26	0.02	0.04	97.06	74.14	3.96	0.04	403
CS-14b	0.46	87.35	1.79	0.72	2.53	0.01	0.00	98.14	77.00	2.35	0.00	230
CS-14b	0.45	84.09	2.04	0.57	4.15	0.04	0.03	97.03	74.13	3.85	0.03	392
CS-14b	15.39	66.58	3.79	0.34	0.13	0.66	0.00	91.39	58.69	0.12	0.00	15
CS-14b	0.59	86.94	1.62	0.66	3.01	0.02	0.00	97.29	76.64	2.79	0.00	275
CS-14b	0.27	85.92	1.69	0.79	3.34	0.03	0.01	97.82	75.73	3.10	0.01	309
CS-14b	0.49	85.89	1.77	0.46	3.21	0.04	0.00	97.62	75.71	2.98	0.00	297
CS-14b	0.57	85.57	1.76	0.41	4.22	0.01	0.00	98.35	75.43	3.92	0.00	392
CS-14b	12.51	52.73	3.19	0.37	15.92	0.45	0.01	93.07	46.48	14.78	0.01	2401
CS-18a	0.62	84.68	4.70	0.76	3.65	0.02	0.03	95.88	74.64	3.38	0.02	342
CS-14b	0.62	83.65	1.69	0.32	4.45	0.03	0.03	96.62	73.74	4.13	0.03	423

Table B.2: Chemical compositions (wt%) and calculated Chemical-Pb ages (Ma) for uraninite at the Kianna deposi

Sample No.	SiO_2	UO_2	CaO	Fe_2O_3	PbO	Al_2O_3	ThO_2	Total	U wt%	Pb wt%	Th wt%	Chem. Pb Age (Ma)
CS-14b	0.88	85.59	1.66	0.33	3.68	0.05	0.04	96.93	75.45	3.42	0.03	342
CS-14b	0.64	86.46	1.41	0.33	3.65	0.03	0.09	97.50	76.22	3.39	0.08	336
CS-14b	0.51	85.47	1.99	0.36	3.89	0.01	0.08	97.59	75.34	3.61	0.07	362
CS-14b	0.68	86.88	1.86	0.39	2.88	0.00	0.00	97.76	76.59	2.67	0.00	263
CS-14b	0.62	85.38	1.62	0.35	3.36	0.02	0.04	96.55	75.26	3.12	0.04	313
CS-14b	0.55	85.92	1.70	0.56	3.04	0.02	0.04	97.07	75.74	2.83	0.04	282
CS-14b	0.69	87.00	1.91	0.45	3.44	0.01	0.03	98.10	76.69	3.19	0.03	314
CS-14b	0.55	84.76	1.97	0.45	3.73	0.04	0.00	97.37	74.72	3.46	0.00	350
CS-18a	0.73	85.36	4.20	0.70	3.41	0.03	0.03	96.27	75.25	3.17	0.02	318
CS-18a	0.81	84.37	4.47	0.71	3.58	0.03	0.00	95.64	74.37	3.32	0.00	337
CS-18a	0.67	84.29	4.20	0.68	3.51	0.04	0.00	95.08	74.30	3.26	0.00	331
CS-18a	0.65	85.09	4.36	0.70	3.39	0.03	0.00	95.90	75.01	3.15	0.00	317
CS-18a	0.63	84.57	4.52	0.66	3.27	0.02	0.00	95.68	74.55	3.04	0.00	308
CS-18a	0.51	85.12	4.49	0.61	4.13	0.00	0.00	96.55	75.04	3.83	0.00	385
CS-18a	0.52	84.62	4.68	0.71	4.25	0.00	0.00	96.35	74.59	3.94	0.00	399
CS-18a	0.58	84.76	4.34	0.68	3.29	0.02	0.00	95.35	74.72	3.05	0.00	308
CS-18a	0.66	84.91	4.46	0.57	2.98	0.02	0.00	95.76	74.84	2.77	0.00	279
CS-18a	0.61	84.94	4.26	1.03	3.26	0.03	0.03	95.70	74.87	3.03	0.02	306
CS-18a	0.44	85.28	4.62	0.71	4.07	0.02	0.05	96.85	75.17	3.78	0.04	380
CS-18a	0.49	85.25	4.00	0.64	3.80	0.03	0.00	95.93	75.15	3.53	0.00	355
CS-18a	0.75	84.81	4.27	0.59	3.26	0.03	0.00	95.68	74.76	3.03	0.00	306
CS-18a	0.77	84.81	4.20	0.70	3.66	0.00	0.01	96.07	74.76	3.40	0.01	343
CS-18a	2.31	74.89	5.28	1.17	0.21	0.09	0.00	86.26	66.01	0.20	0.00	23
CS-18a	2.68	75.16	5.18	1.37	0.31	0.25	0.00	87.47	66.25	0.28	0.00	32
CS-18a	2.19	75.75	5.16	1.56	0.26	0.10	0.00	87.19	66.77	0.24	0.00	27

Table B.2: Chemical compositions (wt%) and calculated Chemical-Pb ages (Ma) for uraninite at the Kianna deposit

Sample No.	SiO_2	UO_2	CaO	Fe_2O_3	PbO	Al_2O_3	ThO_2	Total	U wt%	Pb wt%	Th wt%	Chem. Pb Age (Ma)
CS-13-27	0.23	87.48	2.86	0.98	1.61	0.03	0.00	94.77	77.11	1.49	0.00	146
CS-13-27	0.15	88.40	2.38	1.06	2.15	0.05	0.02	95.70	77.92	2.00	0.02	194
CS-13-27	0.17	88.87	2.39	1.10	1.72	0.08	0.00	95.77	78.34	1.60	0.00	154
CS-13-27	0.18	89.33	2.18	1.07	1.66	0.03	0.00	95.83	78.74	1.54	0.00	148
CS-13-27	0.17	88.11	2.62	1.04	2.06	0.05	0.03	95.52	77.67	1.91	0.03	186
CS-13-27	0.36	87.66	2.81	0.98	1.51	0.31	0.00	95.01	77.28	1.40	0.00	137
CS-13-27	0.24	88.35	2.44	0.98	1.65	0.03	0.00	94.94	77.88	1.53	0.00	148
CS-13-27	0.18	89.97	2.59	0.96	1.59	0.05	0.00	96.74	79.31	1.48	0.00	141
CS-13-27	0.23	88.40	2.57	1.07	1.55	0.07	0.02	95.15	77.92	1.44	0.01	140
CS-13-27	0.18	87.88	2.73	0.95	2.27	0.06	0.00	95.60	77.47	2.11	0.00	206
CS-13-27	0.17	88.47	2.42	1.16	1.59	0.05	0.00	95.29	77.98	1.47	0.00	142
CS-13-27	0.18	88.33	2.25	1.16	1.73	0.06	0.00	95.09	77.86	1.60	0.00	155
CS-13-27	0.17	87.54	2.08	1.04	1.57	0.04	0.01	93.91	77.17	1.45	0.00	142
CS-13-27	0.16	88.96	2.15	1.09	1.77	0.03	0.00	95.47	78.42	1.64	0.00	158
CS-13-27	0.25	88.90	2.37	1.14	1.77	0.07	0.00	95.89	78.36	1.64	0.00	158
CS-13-27	0.25	87.35	2.74	0.90	1.54	0.08	0.03	94.45	77.00	1.43	0.03	140
CS-13-27	0.22	87.57	2.40	0.94	1.59	0.05	0.00	94.19	77.19	1.48	0.00	145
CS-13-27	0.20	87.47	2.59	1.07	1.57	0.04	0.00	94.40	77.11	1.46	0.00	143
CS-13-27	0.15	87.67	2.18	1.04	1.64	0.07	0.01	94.45	77.28	1.53	0.01	149
CS-13-27	0.32	87.62	2.60	0.88	1.47	0.08	0.00	94.35	77.23	1.37	0.00	134
CS-13-27	0.28	86.90	2.88	0.89	1.41	0.04	0.00	93.84	76.61	1.31	0.00	129
CS-13-27	0.32	86.42	2.98	0.97	1.51	0.09	0.02	93.81	76.18	1.40	0.02	139
CS-13-27	0.18	86.80	2.34	1.05	1.88	0.02	0.02	93.76	76.51	1.75	0.02	173
CS-13-27	0.17	86.42	2.30	1.10	1.84	0.06	0.01	93.31	76.18	1.71	0.01	169
CS-13-27	0.19	87.97	2.25	1.06	1.60	0.05	0.00	94.40	77.55	1.48	0.00	144
CS-13-27	0.21	87.43	2.34	0.97	2.12	0.04	0.00	94.33	77.07	1.97	0.00	193
CS-13-27	0.18	87.36	2.47	1.20	1.94	0.04	0.01	94.39	77.00	1.80	0.01	176
CS-13-27	0.18	88.38	2.43	0.95	1.98	0.05	0.09	95.76	77.91	1.84	0.07	178
CS-13-27	0.17	87.41	2.45	1.05	1.93	0.05	0.04	94.53	77.05	1.79	0.03	175
CS-13-27	3.83	80.75	2.77	2.65	0.51	1.06	0.01	93.02	71.18	0.47	0.01	50
CS-13-27	0.17	86.29	2.46	0.97	2.01	0.04	0.01	93.40	76.06	1.86	0.01	185
CS-13-27	0.21	87.22	2.34	0.93	1.72	0.04	0.00	93.95	76.88	1.60	0.00	157
CS-13-27	0.23	88.53	2.12	1.08	1.51	0.05	0.01	95.52	78.04	1.40	0.01	135

Table B.2: Chemical compositions (wt%) and calculated Chemical-Pb ages (Ma) for uraninite at the Kianna deposit

Sample No.	SiO_2	UO_2	CaO	Fe_2O_3	PbO	Al_2O_3	ThO_2	Total	U wt%	Pb wt%	Th wt%	Chem. Pb Age (Ma)
CS-13-27	0.24	89.30	2.14	1.04	1.62	0.03	0.03	96.51	78.71	1.50	0.02	144
CS-13-27	0.21	89.63	2.24	1.09	1.74	0.05	0.00	96.51	79.01	1.62	0.00	155
CS-13-27	0.20	88.97	2.20	1.00	1.87	0.04	0.00	96.02	78.43	1.73	0.00	167
CS-13-27	0.19	89.74	2.56	1.02	2.00	0.03	0.00	97.05	79.10	1.85	0.00	177
CS-13-27	0.22	89.87	2.07	1.13	1.85	0.04	0.00	97.08	79.22	1.72	0.00	164
CS-13-27	0.18	87.83	2.73	1.03	2.06	0.03	0.00	95.33	77.42	1.91	0.00	186
CS-13-27	0.33	88.47	2.57	1.03	1.42	0.06	0.02	95.64	77.99	1.32	0.02	128
CS-13-27	0.21	88.55	2.23	1.06	1.64	0.01	0.00	95.12	78.06	1.52	0.00	147
CS-13-22	1.51	84.87	3.23	2.72	0.45	0.01	0.00	94.39	74.81	0.41	0.00	41
CS-13-22	1.28	85.97	2.74	2.66	0.73	0.02	0.03	95.27	75.78	0.68	0.03	68
CS-13-22	1.41	85.95	3.24	2.79	0.42	0.02	0.00	95.40	75.77	0.39	0.00	39
CS-13-22	2.98	76.68	6.10	2.93	0.18	0.03	0.00	91.10	67.59	0.17	0.00	19
CS-13-22	2.99	77.73	6.84	3.05	0.15	0.02	0.00	92.68	68.52	0.14	0.00	15
CS-13-22	1.49	84.41	3.88	3.23	0.24	0.00	0.01	94.97	74.41	0.22	0.01	22
CS-13-22	1.54	82.82	4.38	3.92	0.30	0.00	0.03	94.41	73.00	0.28	0.03	29
CS-13-22	2.82	78.91	6.01	3.10	0.05	0.03	0.04	92.36	69.56	0.05	0.03	5
CS-13-22	3.04	76.70	6.78	3.53	0.21	0.00	0.00	92.00	67.61	0.19	0.00	21
CS-13-22	1.48	84.54	4.00	3.63	0.30	0.03	0.01	95.79	74.52	0.28	0.01	28
CS-13-22	2.28	79.26	4.76	4.01	0.17	0.00	0.01	92.37	69.87	0.16	0.01	17
CS-13-22	1.49	84.88	3.19	2.98	0.21	0.02	0.00	94.32	74.82	0.19	0.00	19
CS-13-22	1.66	84.42	3.50	2.81	0.26	0.02	0.00	94.11	74.42	0.24	0.00	24
CS-13-22	1.88	82.70	4.64	2.98	0.15	0.02	0.00	93.69	72.90	0.14	0.00	14
CS-13-22	3.37	77.02	5.56	3.15	0.15	0.11	0.00	91.08	67.90	0.14	0.00	16
CS-13-22	4.10	77.84	4.81	4.37	0.11	0.51	0.00	93.30	68.61	0.10	0.00	11
CS-13-22	2.77	78.50	5.44	3.40	0.13	0.01	0.00	91.79	69.19	0.12	0.00	13
CS-13-22	3.32	76.95	5.59	2.91	0.15	0.09	0.03	90.94	67.83	0.14	0.03	16
CS-13-22	4.26	74.89	4.87	5.62	0.06	0.37	0.00	92.02	66.02	0.06	0.00	7
CS-13-22	3.60	76.03	5.65	3.32	0.09	0.09	0.04	90.93	67.02	0.08	0.03	9
CS-13-22	2.81	78.58	5.23	2.57	0.16	0.03	0.00	91.29	69.27	0.14	0.00	15
CS-13-22	2.81	79.04	5.23	2.50	0.17	0.04	0.02	91.60	69.68	0.16	0.02	17
CS-13-22	2.84	78.92	5.18	2.34	0.07	0.01	0.00	91.10	69.56	0.06	0.00	7

Table B.2: Chemical compositions (wt%) and calculated Chemical-Pb ages (Ma) for uraninite at the Kianna deposit

Sample No.	SiO_2	UO_2	CaO	Fe_2O_3	PbO	Al_2O_3	ThO_2	Total	U wt%	Pb wt%	Th wt%	Chem. Pb Age (Ma)
CS-13-22	2.86	78.52	5.63	3.68	0.12	0.03	0.03	92.63	69.21	0.11	0.03	12
CS-13-22	1.84	82.28	4.49	3.73	0.16	0.03	0.00	94.18	72.53	0.15	0.00	16
CS-13-22	1.85	81.98	4.98	3.41	0.19	0.03	0.00	94.42	72.27	0.17	0.00	18
CS-13-22	6.65	72.20	4.74	7.78	0.00	0.96	0.00	93.79	63.64	0.00	0.00	0
CS-13-22	4.84	71.50	4.50	5.68	0.01	0.40	0.00	88.38	63.03	0.01	0.00	1
CS-13-22	0.54	88.45	2.98	1.69	1.22	0.06	0.00	96.62	77.97	1.13	0.00	109
CS-13-22	0.43	87.23	4.52	0.74	1.34	0.11	0.02	96.40	76.89	1.25	0.02	123
CS-13-22	8.45	77.64	2.59	4.51	0.37	0.03	0.00	94.54	68.44	0.35	0.00	39
CS-13-22	6.52	79.39	3.22	4.39	0.36	0.03	0.05	94.80	69.98	0.34	0.05	37
CS-13-22	3.63	86.14	2.37	2.15	0.32	0.31	0.02	96.95	75.93	0.30	0.02	30
CS-13-22	3.05	86.57	2.30	2.00	0.54	0.20	0.00	96.63	76.31	0.50	0.00	49
CS-13-22	3.97	85.03	2.45	2.59	0.29	0.33	0.02	96.37	74.95	0.27	0.02	27
CS-13-22	4.85	85.38	2.29	2.33	0.24	0.41	0.04	97.27	75.27	0.23	0.04	23
CS-13-22	0.61	87.79	4.29	0.67	1.32	0.39	0.00	96.61	77.39	1.23	0.00	120
CS-13-22	1.44	88.44	3.07	1.84	0.88	0.11	0.00	97.41	77.96	0.81	0.00	78
CS-13-22	1.62	87.91	2.90	2.09	0.77	0.11	0.02	97.14	77.49	0.72	0.02	70
CS-18a	2.37	75.69	5.25	1.24	0.23	0.10	0.01	87.07	66.72	0.21	0.01	24
CS-18a	1.24	81.32	4.87	1.92	1.42	0.04	0.00	92.79	71.68	1.32	0.00	139
CS-18a	0.70	85.21	4.74	1.00	3.24	0.00	0.02	96.51	75.11	3.01	0.01	303
CS-18a	1.12	81.73	4.81	1.38	2.81	0.01	0.04	93.85	72.04	2.61	0.04	273
CS-18a	1.39	77.19	5.42	3.02	2.28	0.14	0.00	91.70	68.05	2.12	0.00	235

Table B.2: Chemical compositions (wt%) and calculated Chemical-Pb ages (Ma) for uraninite at the Kianna deposit

Sample No.	SiO_2	UO_2	CaO	Fe_2O_3	PbO	Al_2O_3	ThO_2	Total	U wt%	Pb wt%	Th wt%	Chem. Pb Age (Ma)
CS-21	0.90	81.78	1.70	0.28	9.47	0.07	0.00	95.09	72.09	8.79	0.00	921
CS-21	0.70	81.40	2.11	0.50	9.16	0.06	0.02	94.88	71.75	8.51	0.02	895
CS-21	0.45	82.36	1.83	0.40	9.99	0.01	0.06	96.13	72.60	9.27	0.05	964
CS-21	1.16	82.03	1.81	0.25	9.74	0.12	0.05	97.51	72.31	9.04	0.04	944
CS-21	1.20	84.59	2.71	0.58	5.23	0.09	0.00	95.61	74.57	4.85	0.00	491
CS-21	0.59	81.67	1.96	0.58	10.15	0.02	0.06	96.01	71.99	9.42	0.05	988
CS-21	0.25	80.86	1.57	0.32	11.07	0.04	0.04	95.20	71.28	10.27	0.03	1088
CS-21	0.39	81.31	1.43	0.38	11.10	0.01	0.00	95.58	71.68	10.30	0.00	1085
CS-21	0.56	81.56	1.76	0.35	9.75	0.04	0.01	95.05	71.90	9.05	0.01	950
CS-21	0.94	82.53	2.46	0.63	7.17	0.05	0.03	95.06	72.75	6.65	0.03	690
CS-21	0.42	81.66	1.63	0.29	11.76	0.02	0.02	96.44	71.98	10.91	0.02	1144
CS-21	0.11	79.37	1.23	0.24	12.28	0.02	0.02	94.46	69.96	11.40	0.02	1230
CS-21	0.44	81.87	1.41	0.36	11.87	0.02	0.03	97.10	72.17	11.02	0.03	1153
CS-21	0.20	81.52	1.49	0.37	10.92	0.01	0.00	95.86	71.86	10.14	0.00	1065
CS-21	0.21	80.57	0.89	0.25	13.37	0.00	0.19	96.30	71.02	12.41	0.17	1318
CS-21	0.27	80.42	0.96	0.21	14.23	0.02	0.12	97.11	70.89	13.21	0.11	1406
CS-21	1.07	81.84	3.18	0.55	5.93	0.08	0.03	93.80	72.15	5.50	0.03	575
CS-21	0.36	81.50	2.11	0.25	11.46	0.05	0.00	96.60	71.84	10.64	0.00	1118
CS-21	0.67	81.67	2.15	0.33	10.65	0.07	0.00	96.58	71.99	9.88	0.00	1036
CS-21	0.29	80.62	1.06	0.23	13.73	0.03	0.00	96.59	71.06	12.74	0.00	1354
CS-21	0.23	82.73	1.63	0.36	9.89	0.02	0.00	95.91	72.93	9.18	0.00	950
CS-21	0.48	83.30	2.27	0.38	9.17	0.05	0.00	96.93	73.43	8.51	0.00	875
CS-21	0.11	81.50	0.88	0.16	13.57	0.02	0.19	97.16	71.84	12.60	0.17	1323
CS-21	0.73	80.72	0.56	0.11	13.83	0.08	0.01	96.84	71.16	12.84	0.01	1362
CS-21	0.84	83.47	2.41	0.52	7.37	0.04	0.00	95.62	73.57	6.84	0.00	702
CS-21	0.58	84.67	1.87	0.44	8.18	0.04	0.02	96.86	74.64	7.60	0.02	769
CS-21	0.08	80.64	0.55	0.05	14.91	0.00	0.04	97.08	71.08	13.84	0.03	1470
CS-21	0.16	82.04	1.31	0.28	11.03	0.00	0.02	96.02	72.32	10.24	0.02	1069
CS-21	0.01	78.06	1.45	0.06	16.45	0.00	0.00	96.90	68.81	15.28	0.00	1677

Table B.2: Chemical compositions (wt%) and calculated Chemical-Pb ages (Ma) for uraninite at the Kianna deposit

Sample No.	SiO_2	UO_2	CaO	Fe_2O_3	PbO	Al_2O_3	ThO_2	Total	U wt%	Pb wt%	Th wt%	Chem. Pb Age (Ma)
CS-21	0.13	78.69	1.35	0.28	14.54	0.00	0.00	96.17	69.37	13.50	0.00	1469
CS-21	0.04	79.47	1.27	0.23	14.47	0.01	0.00	96.61	70.05	13.43	0.00	1447
CS-21	0.45	81.47	1.92	0.66	9.88	0.02	0.00	95.81	71.81	9.18	0.00	965
CS-21	0.29	81.54	1.62	0.35	10.81	0.00	0.00	95.59	71.88	10.03	0.00	1054
CS-21	0.12	79.92	0.90	0.12	14.10	0.01	0.00	96.03	70.45	13.09	0.00	1403
CS-21	0.34	80.61	1.67	0.33	11.80	0.04	0.00	95.86	71.05	10.95	0.00	1164
CS-21	0.40	81.02	1.79	0.46	10.06	0.01	0.00	94.88	71.42	9.34	0.00	987
CS-21	0.33	80.27	1.40	0.33	11.02	0.01	0.03	94.35	70.76	10.23	0.02	1091
CS-21	0.47	83.03	1.85	0.35	9.29	0.04	0.04	96.48	73.19	8.63	0.03	890
CS-21	0.18	78.27	1.33	0.18	14.68	0.03	0.01	95.87	68.99	13.63	0.01	1492
CS-21	0.29	82.25	1.58	0.36	10.93	0.03	0.03	96.74	72.51	10.15	0.02	1057
CS-21	0.20	80.29	1.73	0.15	12.87	0.00	0.00	96.14	70.77	11.95	0.00	1275
CS-21	0.11	79.80	0.75	0.18	14.04	0.00	0.07	95.79	70.34	13.04	0.07	1399
CS-21	0.89	83.36	1.94	0.34	7.82	0.08	0.07	95.67	73.48	7.26	0.06	746
CS-21	0.06	77.26	1.29	0.09	16.07	0.01	0.00	95.70	68.11	14.92	0.00	1654
CS-21	0.05	76.79	1.32	0.10	16.23	0.00	0.02	95.80	67.69	15.07	0.02	1681
CS-21	0.19	79.06	1.43	0.17	14.25	0.03	0.02	96.14	69.69	13.23	0.02	1433
CS-21	0.09	78.93	1.08	0.21	14.79	0.04	0.03	96.31	69.58	13.73	0.03	1490
CS-21	0.07	78.02	1.17	0.12	15.25	0.01	0.06	96.01	68.77	14.16	0.05	1554
CS-21	0.02	78.97	1.00	0.06	15.59	0.00	0.06	96.74	69.61	14.47	0.05	1569
CS-21	0.10	81.46	1.03	0.21	14.00	0.00	0.02	97.62	71.81	12.99	0.02	1366
CS-21	0.58	83.05	1.66	0.48	9.62	0.03	0.00	96.56	73.21	8.93	0.00	921
CS-21	0.29	80.68	1.65	0.23	12.58	0.00	0.03	96.88	71.12	11.68	0.03	1240
CS-21	0.00	77.66	1.51	0.08	15.13	0.02	0.02	95.39	68.46	14.05	0.02	1549
CS-21	0.09	80.28	1.58	0.27	12.64	0.02	0.00	95.97	70.77	11.73	0.00	1251
CS-21	0.43	82.71	0.83	0.20	13.11	0.03	0.05	98.32	72.91	12.17	0.04	1260
CS-22a2	0.02	77.20	0.94	0.11	16.25	0.00	0.07	95.80	68.05	15.08	0.06	1673
CS-22a2	0.43	81.17	1.66	0.46	9.91	0.00	0.01	94.71	71.55	9.20	0.01	971
CS-22a2	0.41	80.22	1.79	0.43	10.12	0.04	0.01	94.06	70.71	9.39	0.01	1003
CS-22a2	0.57	82.24	2.16	0.52	8.42	0.06	0.13	95.25	72.50	7.82	0.11	814

Table B.2: Chemical compositions (wt%) and calculated Chemical-Pb ages (Ma) for uraninite at the Kianna deposit

Sample No.	SiO_2	UO_2	CaO	Fe_2O_3	PbO	Al_2O_3	ThO_2	Total	U wt%	Pb wt%	Th wt%	Chem. Pb Age (Ma)
CS-22a2	0.21	77.97	1.35	0.43	12.25	0.01	0.05	93.51	68.73	11.37	0.05	1249
CS-22a2	0.40	80.45	1.71	0.39	10.93	0.00	0.02	94.79	70.92	10.15	0.02	1080
CS-22a2	0.88	82.50	1.79	0.38	8.08	0.05	0.00	94.68	72.73	7.50	0.00	779
CS-22a2	0.37	79.99	1.81	0.50	9.78	0.01	0.08	93.81	70.51	9.08	0.07	972
CS-22a2	0.14	77.01	1.28	0.20	14.38	0.02	0.03	94.28	67.89	13.35	0.03	1484
CS-22a2	0.54	81.37	1.91	0.46	8.34	0.02	0.03	93.73	71.73	7.740	0.02	815
CS-22a2	0.59	80.23	2.32	0.59	9.05	0.00	0.01	94.05	70.72	8.40	0.01	897
CS-22a2	0.07	78.39	1.22	0.13	13.66	0.01	0.08	94.78	69.10	12.68	0.07	1385
CS-22a2	0.05	75.37	0.99	0.13	15.82	0.00	0.07	93.83	66.44	14.69	0.06	1669
CS-22a2	0.06	77.91	1.35	0.12	14.50	0.03	0.03	95.38	68.68	13.46	0.02	1480
CS-22a2	0.08	75.64	0.94	0.09	15.27	0.01	0.12	93.44	66.68	14.18	0.10	1605
CS-22a2	0.20	79.28	1.37	0.29	11.99	0.01	0.10	94.70	69.89	11.13	0.09	1202
CS-22a2	0.22	79.70	1.52	0.39	11.72	0.02	0.08	95.03	70.25	10.88	0.07	1169
CS-22a2	0.54	81.02	2.01	0.52	9.24	0.06	0.07	94.86	71.42	8.58	0.06	907
CS-22a2	0.81	81.78	2.41	0.57	6.52	0.07	0.03	93.47	72.09	6.05	0.03	634
CS-22a2	0.44	80.85	1.82	0.40	9.64	0.04	0.04	94.35	71.27	8.94	0.04	947
CS-22a2	0.63	79.76	2.18	0.53	9.38	0.04	0.04	93.87	70.31	8.71	0.04	935
CS-22a2	0.10	79.04	1.40	0.24	12.74	0.00	0.09	95.00	69.68	11.83	0.08	1281
CS-22a2	0.62	80.55	2.13	0.44	8.71	0.04	0.10	93.73	71.00	8.09	0.09	860
CS-22a2	0.88	84.10	1.61	0.43	6.31	0.04	0.00	94.22	74.13	5.85	0.00	596
CS-22a2	0.46	80.73	1.81	0.45	9.81	0.04	0.05	94.48	71.16	9.10	0.04	965
CS-22a2	0.11	80.27	0.90	0.19	13.64	0.00	0.05	96.27	70.75	12.66	0.04	1351
CS-22a2	0.58	81.67	2.16	0.47	9.19	0.04	0.07	95.62	71.99	8.54	0.06	895
CS-22a2	0.33	78.88	1.24	0.27	13.12	0.03	0.00	94.75	69.54	12.18	0.00	1322
CS-22a1	0.12	78.89	1.08	0.10	15.87	0.02	0.01	98.46	69.54	14.73	0.00	1599
CS-22a1	0.52	83.49	1.80	0.45	9.08	0.05	0.14	97.76	73.59	8.42	0.12	863
CS-22a2	0.14	79.99	1.42	0.27	12.43	0.02	0.04	95.63	70.51	11.54	0.04	1235
CS-22a1	0.74	82.59	1.56	0.33	10.78	0.04	0.16	98.37	72.80	10.01	0.14	1037

Table B.2: Chemical compositions (wt%) and calculated Chemical-Pb ages (Ma) for uraninite at the Kianna deposit

Sample No.	SiO_2	UO_2	CaO	Fe_2O_3	PbO	Al_2O_3	ThO_2	Total	U wt%	Pb wt%	Th wt%	Chem. Pb Age (Ma)
CS-22a1	4.17	84.94	1.76	0.38	1.70	0.54	0.19	95.55	74.88	1.57	0.16	158
CS-22a1	0.27	82.06	0.95	0.28	13.51	0.01	0.01	99.01	72.34	12.54	0.01	1309
CS-22a1	0.52	82.94	1.60	0.35	10.94	0.04	0.03	98.20	73.11	10.16	0.02	1049
CS-22a1	0.07	77.99	1.59	0.17	16.79	0.00	0.00	98.76	68.75	15.59	0.00	1712
CS-22a2	0.59	83.95	1.64	0.40	8.34	0.02	0.01	96.52	74.00	7.74	0.01	790
CS-22a2	0.74	84.81	1.97	0.40	7.56	0.04	0.00	97.77	74.76	7.02	0.00	709
CS-22a2	0.04	79.13	1.06	0.07	15.10	0.02	0.09	97.82	69.75	14.02	0.08	1517
CS-22a2	0.74	81.56	1.66	0.32	10.33	0.05	0.00	97.39	71.89	9.59	0.00	1007
CS-22a2	0.12	79.32	1.31	0.12	13.66	0.03	0.14	97.38	69.92	12.68	0.12	1368
CS-22a2	0.43	78.74	1.55	0.33	12.45	0.05	0.05	94.42	69.41	11.56	0.04	1257
CS-22a2	0.57	79.23	1.80	0.38	11.58	0.06	0.05	94.45	69.84	10.75	0.04	1162
CS-22a2	0.25	78.42	1.59	0.26	13.63	0.02	0.08	95.40	69.13	12.65	0.07	1381
CS-22a2	0.29	80.03	1.64	0.45	11.21	0.02	0.05	94.86	70.54	10.41	0.04	1114
CS-22a2	0.53	83.25	1.56	0.40	8.66	0.03	0.17	96.85	73.38	8.04	0.15	827
CS-15a	1.20	82.74	2.14	0.52	6.74	0.05	0.03	95.85	72.93	6.26	0.02	648
CS-3	0.98	82.93	2.72	0.59	7.08	0.07	0.00	95.03	73.10	6.57	0.00	679
CS-3	0.58	82.60	2.05	0.65	8.83	0.03	0.00	95.53	72.81	8.20	0.00	850
CS-3	0.73	83.03	2.34	0.63	8.99	0.05	0.07	96.57	73.19	8.34	0.06	860
CS-3	0.52	83.27	1.73	0.55	9.13	0.01	0.02	95.91	73.40	8.48	0.02	872
CS-3	0.35	83.70	1.39	0.46	9.59	0.00	0.00	96.23	73.78	8.90	0.00	911
CS-3	0.50	82.10	1.86	0.54	9.04	0.01	0.03	95.06	72.37	8.39	0.03	875
CS-3	0.61	83.45	1.88	0.56	9.44	0.03	0.00	96.79	73.56	8.76	0.00	899
CS-3	0.69	82.37	2.14	0.56	9.22	0.02	0.04	95.87	72.61	8.56	0.03	890
CS-3	0.77	84.72	2.19	0.55	7.69	0.06	0.00	96.81	74.68	7.14	0.00	722
CS-3	0.51	84.39	1.76	0.55	9.27	0.03	0.00	97.33	74.39	8.60	0.00	873
CS-3	0.72	82.88	2.09	0.59	9.13	0.03	0.00	96.13	73.06	8.47	0.00	875
CS-3	0.95	85.63	2.32	0.68	6.31	0.05	0.03	96.82	75.48	5.85	0.03	585
CS-3	0.81	83.30	2.39	0.65	8.46	0.02	0.02	96.52	73.43	7.85	0.02	807
CS-3	0.73	84.18	2.35	0.57	7.77	0.06	0.02	96.53	74.21	7.21	0.02	733
CS-3	0.79	83.11	2.38	0.61	8.82	0.05	0.00	96.73	73.26	8.19	0.00	844

Table B.2: Chemical compositions (wt%) and calculated Chemical-Pb ages (Ma) for uraninite at the Kianna deposit

Sample No.	SiO_2	UO_2	CaO	Fe_2O_3	PbO	Al_2O_3	ThO_2	Total	U wt%	Pb wt%	Th wt%	Chem. Pb Age (Ma)
CS-3	0.72	83.41	2.05	0.62	8.37	0.02	0.03	96.03	73.53	7.77	0.02	798
CS-3	0.49	79.03	1.33	0.57	8.20	0.02	0.00	92.72	69.66	7.61	0.00	825
CS-3	0.48	78.03	1.35	0.54	10.14	0.00	0.07	93.57	68.79	9.41	0.07	1032
CS-3	0.61	82.79	2.10	0.57	9.61	0.05	0.03	96.58	72.98	8.92	0.02	923
CS-3	0.31	81.05	1.15	0.44	10.80	0.02	0.00	95.41	71.44	10.03	0.00	1060
CS-3	0.53	81.33	1.85	0.46	10.90	0.02	0.00	96.13	71.69	10.12	0.00	1066
CS-3	0.66	82.42	2.19	0.57	8.07	0.06	0.05	94.76	72.65	7.49	0.04	778
CS-3	0.70	81.86	2.15	0.57	9.25	0.03	0.04	95.33	72.16	8.59	0.03	899
CS-3	0.33	78.62	1.41	0.41	12.16	0.04	0.00	95.07	69.30	11.28	0.00	1229
CS-3	0.53	83.95	1.78	0.45	9.15	0.04	0.01	96.79	74.00	8.50	0.01	867
CS-3	0.26	80.54	1.03	0.42	11.97	0.00	0.00	95.43	70.99	11.11	0.00	1182
CS-3	0.15	79.68	1.04	0.36	12.58	0.04	0.03	95.70	70.24	11.67	0.02	1254
CS-3	0.47	82.66	1.60	0.52	9.96	0.04	0.00	96.09	72.86	9.25	0.00	959
CS-3	0.63	81.99	2.05	0.51	8.41	0.04	0.05	94.38	72.27	7.81	0.04	816
CS-3	0.88	84.07	2.36	0.61	7.87	0.03	0.01	96.60	74.11	7.31	0.01	745
CS-3	0.86	82.11	2.61	0.67	9.56	0.06	0.00	96.74	72.38	8.88	0.00	926
CS-3	0.36	80.09	1.23	0.46	10.81	0.02	0.07	94.89	70.60	10.04	0.06	1073
CS-3	0.40	84.39	1.72	0.44	9.41	0.03	0.00	97.16	74.39	8.73	0.00	886
CS-3	0.14	81.37	1.15	0.49	11.73	0.02	0.00	96.24	71.72	10.89	0.00	1146
CS-3	0.23	80.13	0.86	0.26	13.39	0.02	0.00	95.99	70.63	12.43	0.00	1329
CS-3	0.41	79.54	1.25	0.53	9.58	0.03	0.00	94.44	70.11	8.89	0.00	957
CS-3	0.73	84.17	2.26	0.53	7.50	0.05	0.04	96.08	74.19	6.96	0.04	708
CS-3	1.06	85.70	2.21	0.61	5.23	0.05	0.00	95.63	75.54	4.85	0.00	485
CS-7c	5.21	84.01	2.58	0.46	0.59	0.50	0.00	93.85	74.06	0.55	0.00	56
CS-7c	1.74	87.10	2.61	0.81	3.41	0.15	0.01	96.70	76.77	3.16	0.01	311
CS-7c	1.88	85.57	3.25	0.92	3.37	0.14	0.00	96.16	75.43	3.13	0.00	313
CS-7c	1.89	84.84	3.30	0.91	3.34	0.14	0.01	95.28	74.79	3.10	0.01	313
CS-7c	1.76	85.91	3.43	0.95	3.87	0.14	0.01	96.86	75.73	3.59	0.01	358
CS-7c	2.61	84.88	2.48	0.48	3.57	0.21	0.00	95.34	74.82	3.31	0.00	334
CS-7c	2.59	84.95	3.08	0.75	2.57	0.21	0.00	95.00	74.88	2.38	0.00	240

Table B.2: Chemical compositions (wt%) and calculated Chemical-Pb ages (Ma) for uraninite at the Kianna deposit

Sample No.	SiO_2	UO_2	CaO	Fe_2O_3	PbO	Al_2O_3	ThO_2	Total	U wt%	Pb wt%	Th wt%	Chem. Pb Age (Ma)
CS-7c	1.79	86.88	3.13	0.86	3.20	0.13	0.01	96.99	76.59	2.97	0.01	293
CS-7c	5.29	84.10	2.56	0.37	0.97	0.44	0.00	94.46	74.13	0.90	0.00	92
CS-7c	1.72	87.12	3.21	0.87	3.66	0.11	0.02	97.65	76.79	3.40	0.02	334
CS-7c	1.25	84.88	2.87	0.65	5.47	0.05	0.00	95.80	74.82	5.08	0.00	513
CS-7c	1.09	84.91	2.70	0.58	6.17	0.07	0.06	96.25	74.85	5.72	0.05	577
CS-7c	1.93	85.81	2.95	0.85	2.70	0.16	0.00	95.45	75.64	2.51	0.00	251
CS-7c	2.54	84.32	2.88	0.66	2.86	0.21	0.00	94.73	74.33	2.66	0.00	270
CS-7c	2.19	82.59	2.46	0.55	5.98	0.15	0.00	95.20	72.80	5.55	0.00	576
CS-7c	0.56	86.04	1.59	0.45	8.80	0.01	0.05	98.07	75.84	8.17	0.04	813
CS-7c	0.69	82.92	1.82	0.45	9.30	0.04	0.00	95.71	73.09	8.63	0.00	891
CS-7c	1.55	85.20	3.25	0.77	4.47	0.11	0.00	96.20	75.10	4.15	0.00	417
CS-7c	1.23	85.57	2.57	0.62	5.54	0.09	0.00	96.12	75.43	5.15	0.00	515
CS-7c	3.28	85.76	2.85	0.65	2.21	0.28	0.00	96.08	75.60	2.05	0.00	205
CS-7c	1.32	83.82	2.89	0.80	5.50	0.09	0.00	95.11	73.89	5.10	0.00	521
CS-7c	1.46	84.32	3.07	0.83	5.03	0.09	0.00	95.40	74.32	4.67	0.00	474
CS-7c	1.41	86.91	2.53	0.69	4.99	0.10	0.08	97.38	76.61	4.63	0.07	456
CS-7c	1.85	86.21	3.31	0.84	3.65	0.11	0.00	96.78	75.99	3.39	0.00	337
CS-12a	0.73	80.21	1.70	0.38	9.57	0.05	0.06	93.74	70.70	8.88	0.05	948
CS-12a	0.57	80.39	1.35	0.38	11.25	0.05	0.03	94.90	70.86	10.44	0.03	1112
CS-12a	0.53	80.53	1.23	0.28	11.73	0.02	0.05	95.11	70.99	10.89	0.04	1158
CS-12a	0.51	79.02	1.36	0.37	11.18	0.04	0.05	93.50	69.66	10.38	0.05	1125
CS-12a	0.77	81.06	1.63	0.41	9.48	0.05	0.02	94.43	71.45	8.80	0.02	930
CS-12a	0.53	81.32	1.27	0.38	10.68	0.01	0.11	95.26	71.68	9.92	0.10	1044
CS-12a	0.44	81.34	1.12	0.28	11.72	0.04	0.01	95.93	71.71	10.88	0.01	1145
CS-12a	1.02	82.51	1.93	0.48	7.61	0.02	0.02	94.94	72.74	7.06	0.01	733
CS-12a	0.25	76.17	0.75	0.31	13.35	0.00	0.00	93.70	67.15	12.40	0.00	1394
CS-12a	0.75	82.09	1.56	0.42	9.29	0.02	0.08	95.11	72.37	8.63	0.07	900
CS-12a	1.60	74.77	1.92	0.45	16.24	0.10	0.04	98.42	65.91	15.07	0.04	1726

Table B.2: Chemical compositions (wt%) and calculated Chemical-Pb ages (Ma) for uraninite at the Kianna deposit

Sample No.	SiO_2	UO_2	CaO	Fe_2O_3	PbO	Al_2O_3	ThO_2	Total	U wt%	Pb wt%	Th wt%	Chem. Pb Age (Ma)
CS-12a	0.83	83.34	1.54	0.48	8.32	0.05	0.1	95.57	73.46	7.73	0.08	794
CS-12a	0.96	84.38	1.85	0.56	6.83	0.08	0.00	95.91	74.38	6.34	0.00	644
CS-12a	0.73	78.54	1.77	0.39	11.99	0.04	0.04	94.45	69.23	11.13	0.03	1214
CS-12a	0.75	80.21	1.48	0.40	10.13	0.03	0.00	94.19	70.70	9.40	0.00	1004
CS-12a	0.48	80.51	1.05	0.25	12.47	0.02	0.00	95.60	70.97	11.58	0.00	1232
CS-12a	0.55	80.21	1.21	0.30	12.24	0.04	0.07	95.62	70.70	11.36	0.06	1213
CS-12a	0.43	79.73	1.12	0.20	12.62	0.01	0.07	95.13	70.28	11.72	0.06	1259
CS-12a	0.51	80.45	1.22	0.30	12.38	0.02	0.07	95.81	70.91	11.49	0.06	1223
CS-12a	1.10	81.29	1.97	0.55	7.82	0.09	0.00	93.96	71.66	7.26	0.00	765
CS-12a	0.44	80.46	1.05	0.26	11.97	0.05	0.05	95.18	70.92	11.12	0.04	1184
CS-12a	0.53	79.34	1.25	0.34	11.79	0.02	0.03	94.24	69.94	10.95	0.03	1182
CS-12a	0.63	80.24	1.39	0.42	11.49	0.05	0.09	95.51	70.73	10.66	0.08	1137
CS-7b	0.59	83.54	1.48	0.39	8.75	0.02	0.00	95.28	73.64	8.13	0.00	834
CS-7b	0.76	85.44	1.87	0.53	7.72	0.02	0.04	97.03	75.32	7.17	0.04	719
CS-7b	1.40	86.84	3.02	0.74	4.60	0.15	0.02	97.51	76.55	4.27	0.02	421
CS-7b	1.14	83.59	2.66	0.64	6.87	0.06	0.00	95.64	73.69	6.37	0.00	653
CS-7b	0.88	83.84	2.04	0.56	8.89	0.05	0.00	96.85	73.90	8.25	0.00	843
CS-7b	0.90	84.60	2.13	0.54	7.54	0.08	0.00	96.38	74.58	7.00	0.00	709
CS-7b	0.98	83.47	2.46	0.56	7.36	0.08	0.02	95.53	73.58	6.84	0.02	702
CS-7b	0.98	83.25	2.43	0.62	8.76	0.09	0.00	96.80	73.38	8.13	0.00	836
CS-7b	0.98	85.08	2.02	0.58	6.80	0.10	0.04	96.15	75.00	6.32	0.03	636
CS-7b	0.89	84.75	2.14	0.54	7.25	0.06	0.00	96.20	74.70	6.73	0.00	680
CS-7b	2.74	84.52	1.77	0.44	4.59	0.17	0.00	95.09	74.50	4.26	0.00	432
CS-7b	1.10	84.42	2.73	0.68	6.37	0.08	0.00	96.00	74.42	5.92	0.00	601
CS-7b	0.97	82.95	2.40	0.64	6.93	0.07	0.00	94.45	73.12	6.43	0.00	664
CS-7b	1.01	83.96	2.73	0.67	6.28	0.06	0.02	95.44	74.01	5.83	0.02	595
CS-7b	2.30	84.95	3.18	0.69	2.79	0.15	0.00	94.78	74.88	2.59	0.00	261
CS-7b	1.08	86.00	2.87	0.60	6.33	0.09	0.07	97.75	75.81	5.87	0.07	584

Table B.2: Chemical compositions (wt%) and calculated Chemical-Pb ages (Ma) for uraninite at the Kianna deposit

Sample No.	SiO_2	UO_2	CaO	Fe_2O_3	PbO	Al_2O_3	ThO_2	Total	U wt%	Pb wt%	Th wt%	Chem. Pb Age (Ma)
CS-7b	1.61	83.82	3.11	0.92	4.62	0.10	0.04	95.31	73.88	4.29	0.04	438
CS-13-24	0.43	82.52	0.51	0.14	12.36	0.03	0.33	97.39	72.74	11.47	0.29	1189
CS-13-24	7.05	82.10	0.59	0.22	0.34	0.80	0.34	93.29	72.37	0.32	0.30	33
CS-13-24	0.20	81.20	0.91	0.20	14.38	0.02	0.50	98.60	71.58	13.35	0.44	1405
CS-13-24	4.52	87.47	0.97	0.32	0.23	0.39	0.28	95.42	77.11	0.22	0.25	22
CS-13-24	3.48	86.66	1.15	0.31	0.62	0.30	0.25	94.23	76.39	0.58	0.22	57
CS-13-24	0.67	85.60	1.21	0.34	7.54	0.05	0.35	97.65	75.46	7.00	0.30	699
CS-13-24	1.06	86.60	0.99	0.38	6.36	0.05	0.51	98.17	76.33	5.90	0.45	582
CS-13-24	0.95	85.62	0.87	0.22	9.20	0.11	0.45	99.47	75.48	8.54	0.39	853
CS-13-24	0.34	81.84	0.71	0.20	13.67	0.00	0.55	98.37	72.14	12.69	0.49	1325
CS-13-24	0.41	84.33	0.92	0.22	12.45	0.06	0.60	100.12	74.33	11.56	0.53	1171
CS-13-24	1.11	85.98	0.97	0.28	5.87	0.12	0.74	97.37	75.79	5.45	0.65	541
CS-13-24	0.35	83.06	0.87	0.22	12.35	0.07	0.56	98.84	73.22	11.47	0.50	1180
CS-13-24	5.04	86.34	0.99	0.23	0.22	0.41	0.42	95.01	76.11	0.20	0.37	20
CS-13-24	0.41	83.83	1.26	0.29	11.61	0.04	0.53	98.93	73.90	10.78	0.46	1099
CS-13-24	7.45	82.10	0.62	0.18	0.12	0.53	0.27	92.81	72.37	0.11	0.24	11
CS-13-24	4.99	83.89	1.51	0.31	0.57	0.45	0.33	92.70	73.95	0.53	0.29	54
CS-13-24	4.13	86.72	0.96	0.31	0.27	0.35	0.36	93.94	76.44	0.25	0.32	25
CS-13-25	0.56	84.47	1.96	0.42	9.87	0.03	0.04	98.06	74.46	9.16	0.04	929
CS-13-25	0.53	83.59	2.03	0.43	10.75	0.03	0.03	98.24	73.69	9.98	0.02	1022
CS-21	0.76	84.68	2.08	0.41	7.68	0.05	0.00	96.93	74.64	7.13	0.00	721
CS-21	0.43	81.92	1.31	0.28	11.94	0.05	0.02	96.71	72.21	11.09	0.02	1159
CS-21	0.12	81.58	1.38	0.26	13.06	0.00	0.01	97.46	71.91	12.12	0.01	1272
CS-13-25	0.70	83.42	1.13	0.23	11.02	0.08	0.01	97.44	73.53	10.23	0.00	1050

Table B.2: Chemical compositions (wt%) and calculated Chemical-Pb ages (Ma) for uraninite at the Kianna deposit

Sample No.	SiO_2	UO_2	CaO	Fe_2O_3	PbO	Al_2O_3	ThO_2	Total	U wt%	Pb wt%	Th wt%	Chem. Pb Age (Ma)
CS-13-25	0.70	85.22	2.23	0.47	8.68	0.06	0.01	97.90	75.12	8.06	0.01	810
CS-13-25	0.91	86.59	1.90	0.48	7.22	0.07	0.02	97.92	76.33	6.71	0.02	664
CS-13-25	0.10	82.07	0.94	0.16	14.31	0.00	0.00	98.18	72.34	13.29	0.00	1387
CS-13-25	0.46	85.32	1.59	0.41	9.95	0.04	0.00	98.50	75.21	9.23	0.00	927
CS-13-25	0.16	84.73	1.13	0.21	12.58	0.01	0.00	99.55	74.69	11.68	0.00	1181
CS-13-25	0.98	80.30	1.50	0.38	13.69	0.15	0.00	99.36	70.79	12.71	0.00	1356
CS-13-25	1.65	86.73	1.64	0.31	4.59	0.08	0.02	96.03	76.45	4.26	0.02	421
CS-13-25	1.15	86.46	1.42	0.39	6.29	0.06	0.02	96.40	76.22	5.84	0.02	578
CS-13-25	0.59	84.46	2.04	0.48	9.87	0.03	0.02	98.34	74.45	9.16	0.02	929
CS-13-25	0.37	83.08	1.48	0.39	12.92	0.00	0.02	98.98	73.23	12.00	0.02	1237
CS-13-25	0.51	86.36	1.58	0.30	10.03	0.05	0.00	99.35	76.12	9.31	0.00	923
CS-13-25	1.41	86.45	1.94	0.35	6.36	0.08	0.02	97.61	76.21	5.90	0.01	584
CS-13-25	1.02	84.62	2.55	0.42	8.64	0.07	0.00	97.93	74.59	8.02	0.00	812
CS-13-25	0.20	86.28	1.30	0.22	10.81	0.02	0.04	99.38	76.06	10.03	0.04	995
CS-13-25	1.29	84.79	1.69	0.38	8.52	0.07	0.04	97.59	74.74	7.90	0.03	798
CS-13-25	0.74	85.50	1.78	0.41	7.62	0.06	0.00	96.88	75.37	7.07	0.00	708
CS-13-25	0.46	85.26	1.27	0.21	10.16	0.02	0.01	98.05	75.15	9.43	0.01	947
CS-13-25	1.63	85.94	1.29	0.37	7.27	0.13	0.01	97.22	75.76	6.75	0.00	673
CS-13-25	1.11	86.50	2.17	0.47	5.51	0.09	0.04	97.40	76.25	5.11	0.03	506
CS-13-25	0.71	84.33	1.79	0.33	10.74	0.05	0.02	98.53	74.33	9.97	0.01	1013
CS-13-25	0.27	84.47	1.30	0.26	12.16	0.02	0.05	99.37	74.46	11.29	0.05	1144
CS-13-25	0.54	84.02	1.62	0.35	10.55	0.04	0.04	98.15	74.07	9.80	0.03	999
CS-13-25	0.56	83.20	1.51	0.33	11.48	0.03	0.01	98.06	73.34	10.66	0.01	1097
CS-13-25	0.52	83.98	1.85	0.40	10.89	0.00	0.01	98.49	74.03	10.11	0.01	1031
CS-13-25	4.56	75.36	0.89	0.03	4.18	0.21	0.03	93.07	66.43	3.88	0.03	441

Table B.2: Chemical compositions (wt%) and calculated Chemical-Pb ages (Ma) for uraninite at the Kianna deposit

Sample No.	SiO_2	UO_2	CaO	Fe_2O_3	PbO	Al_2O_3	ThO_2	Total	U wt%	Pb wt%	Th wt%	Chem. Pb Age (Ma)
CS-13-9	0.19	82.11	0.89	0.25	14.18	0.00	0.13	98.87	72.38	13.16	0.11	1372
CS-13-9	0.04	82.15	0.46	0.10	15.46	0.00	0.21	99.14	72.42	14.35	0.18	1495
CS-13-9	0.31	82.34	0.90	0.22	13.29	0.05	0.08	97.98	72.59	12.34	0.07	1283
CS-13-9	0.37	83.95	0.99	0.24	12.68	0.02	0.07	99.19	74.00	11.77	0.06	1201
CS-13-9	0.30	83.42	0.91	0.25	13.22	0.01	0.09	99.20	73.54	12.27	0.08	1259
CS-13-9	0.43	84.91	1.37	0.36	10.97	0.02	0.08	99.25	74.85	10.19	0.07	1028
CS-13-9	0.98	85.48	1.36	0.42	8.46	0.03	0.10	98.16	75.35	7.85	0.09	786
CS-13-9	5.10	84.01	1.25	0.16	0.24	0.31	0.06	92.80	74.06	0.22	0.05	22
CS-13-9	0.26	83.70	0.92	0.29	13.14	0.03	0.02	99.28	73.78	12.19	0.02	1247
CS-13-9	0.81	85.16	2.01	0.47	7.83	0.05	0.04	97.51	75.07	7.27	0.04	731
CS-13-9	0.39	83.65	1.38	0.41	11.56	0.03	0.04	98.66	73.74	10.73	0.04	1098
CS-13-9	0.53	83.32	1.21	0.31	12.54	0.16	0.11	99.14	73.45	11.64	0.09	1196
CS-13-9	0.17	83.03	0.90	0.16	13.89	0.00	0.01	98.97	73.19	12.90	0.01	1331
CS-13-9	0.31	83.36	1.13	0.30	12.82	0.00	0.03	98.72	73.48	11.90	0.03	1223
CS-13-9	0.35	82.16	1.35	0.30	12.86	0.01	0.00	97.90	72.43	11.94	0.00	1245
CS-13-9	0.40	82.68	1.03	0.28	12.97	0.04	0.01	98.14	72.89	12.04	0.00	1247
CS-13-9	0.20	83.17	0.91	0.20	14.64	0.02	0.03	99.88	73.32	13.59	0.03	1399
CS-13-9	0.25	82.67	1.02	0.20	14.45	0.04	0.00	99.60	72.87	13.42	0.00	1390
CS-13-9	0.16	82.92	0.80	0.19	14.65	0.01	0.02	99.21	73.09	13.60	0.02	1405
CS-13-9	0.30	82.72	1.21	0.22	13.13	0.01	0.05	98.59	72.92	12.18	0.04	1261
CS-13-9	0.59	84.62	1.71	0.46	10.44	0.05	0.03	98.88	74.59	9.69	0.02	981
CS-13-9	0.90	84.29	2.00	0.37	10.07	0.18	0.03	98.85	74.30	9.35	0.03	950
CS-13-9	0.33	84.88	0.95	0.30	12.90	0.02	0.01	100.11	74.82	11.98	0.01	1209
CS-13-11	2.23	86.26	1.20	0.50	4.81	0.19	0.04	96.65	76.03	4.46	0.04	443
CS-13-11	1.33	88.32	1.69	0.33	4.61	0.13	0.04	97.45	77.85	4.28	0.04	415
CS-13-11	0.64	85.44	1.30	0.36	9.85	0.07	0.02	98.49	75.32	9.15	0.02	917
CS-13-11	1.10	87.27	1.31	0.33	6.94	0.08	0.04	97.85	76.93	6.45	0.03	633

Table B.2: Chemical compositions (wt%) and calculated Chemical-Pb ages (Ma) for uraninite at the Kianna deposit

Sample No.	SiO_2	UO_2	CaO	Fe_2O_3	PbO	Al_2O_3	ThO_2	Total	U wt%	Pb wt%	Th wt%	Chem. Pb Age (Ma)
CS-13-11	0.72	85.95	1.06	0.24	10.72	0.06	0.00	99.29	75.76	9.95	0.00	992
CS-13-11	0.59	84.78	0.95	0.23	10.91	0.05	0.00	97.93	74.73	10.13	0.00	1023
CS-13-11	0.37	83.84	1.30	0.29	12.88	0.02	0.02	99.24	73.90	11.96	0.01	1222
CS-13-11	1.87	88.06	2.02	0.45	4.14	0.24	0.00	97.62	77.63	3.85	0.00	374
CS-13-11	1.17	87.63	1.78	0.39	5.74	0.10	0.00	97.79	77.25	5.33	0.00	521
CS-13-11	1.52	88.30	1.74	0.45	4.70	0.12	0.05	97.70	77.83	4.37	0.05	424
CS-13-11	1.37	87.22	1.36	0.39	5.90	0.12	0.00	97.40	76.89	5.47	0.00	537
CS-13-11	0.97	86.45	1.08	0.28	9.16	0.07	0.01	98.76	76.20	8.50	0.01	842
CS-13-11	1.67	77.95	1.03	0.32	17.21	0.13	0.04	103.10	68.72	15.97	0.03	1754
CS-13-11	1.07	87.05	2.25	0.50	6.05	0.09	0.04	97.85	76.73	5.62	0.04	553
CS-13-11	1.24	86.87	2.41	0.50	4.35	0.08	0.03	96.50	76.57	4.04	0.02	398
CS-13-11	0.77	85.79	1.83	0.37	8.32	0.05	0.03	98.12	75.62	7.72	0.03	771
CS-13-11	0.31	83.58	1.04	0.24	13.63	0.02	0.00	99.22	73.67	12.66	0.00	1297
CS-13-11	0.29	83.80	1.12	0.27	12.51	0.02	0.01	98.75	73.87	11.61	0.01	1187
CS-13-11	0.54	83.62	1.88	0.36	10.70	0.06	0.01	97.89	73.71	9.93	0.01	1017
CS-13-11	0.71	84.61	1.22	0.35	10.13	0.02	0.00	97.59	74.59	9.40	0.00	951
CS-13-11	1.03	87.30	2.57	0.49	6.58	0.08	0.00	99.01	76.95	6.11	0.00	599
CS-13-11	0.82	86.58	1.96	0.47	7.71	0.06	0.04	98.36	76.32	7.15	0.03	707
CS-13-11	0.32	84.20	1.05	0.22	12.78	0.01	0.05	99.31	74.22	11.87	0.04	1207
CS-13-11	0.60	86.17	1.41	0.35	10.93	0.08	0.03	100.43	75.96	10.15	0.03	1009
CS-13-11	0.63	85.94	1.55	0.32	10.39	0.02	0.00	99.52	75.75	9.65	0.00	962
CS-13-11	0.16	82.39	0.62	0.15	15.22	0.03	0.00	99.02	72.62	14.13	0.00	1469
CS-13-11	0.55	84.86	2.01	0.36	10.01	0.02	0.04	98.74	74.81	9.29	0.03	937
CS-13-11	0.60	86.16	1.39	0.32	9.90	0.07	0.04	99.10	75.95	9.19	0.04	913
CS-13-11	0.74	85.50	2.07	0.42	9.19	0.07	0.00	98.91	75.37	8.53	0.00	854
CS-13-11	0.16	82.59	0.74	0.14	14.96	0.00	0.00	99.22	72.80	13.89	0.00	1441
CS-13-11	0.91	86.44	1.59	0.46	8.38	0.06	0.03	98.71	76.20	7.78	0.02	771
CS-13-11	0.57	85.81	1.49	0.28	10.60	0.04	0.06	99.58	75.64	9.84	0.06	982
CS-13-11	0.50	85.15	1.78	0.36	10.80	0.03	0.00	99.32	75.06	10.02	0.00	1008

Table B.2: Chemical compositions (wt%) and calculated Chemical-Pb ages (Ma) for uraninite at the Kianna deposit

Sample No.	SiO_2	UO_2	CaO	Fe_2O_3	PbO	Al_2O_3	ThO_2	Total	U wt%	Pb wt%	Th wt%	Chem. Pb Age (Ma)
CS-13-11	1.29	87.16	2.06	0.42	5.45	0.16	0.00	97.39	76.83	5.05	0.00	496
CS-13-15	0.55	86.60	1.97	0.44	7.26	0.03	0.02	97.35	76.34	6.74	0.01	667
CS-13-15	0.82	86.71	2.09	0.41	6.53	0.03	0.00	97.28	76.44	6.06	0.00	599
CS-13-15	0.53	83.45	2.03	0.29	10.30	0.03	0.08	97.67	73.56	9.56	0.07	981
CS-13-15	0.52	84.00	1.95	0.30	10.27	0.03	0.00	97.92	74.04	9.53	0.00	972
CS-13-15	1.21	84.06	1.25	0.27	8.48	0.14	0.02	96.39	74.09	7.87	0.02	802
CS-13-15	0.27	84.16	1.21	0.34	11.96	0.03	0.00	98.54	74.19	11.10	0.00	1130
CS-13-15	0.60	86.35	2.40	0.41	8.18	0.05	0.02	99.07	76.12	7.59	0.02	753
CS-13-15	0.71	85.72	1.85	0.47	8.79	0.03	0.01	98.23	75.56	8.16	0.01	815
CS-13-15	0.47	84.10	1.64	0.27	11.14	0.02	0.00	98.18	74.14	10.34	0.00	1053
CS-13-15	0.25	83.88	0.93	0.25	12.71	0.06	0.04	98.64	73.94	11.80	0.03	1205
CS-13-15	0.60	86.16	2.31	0.40	8.38	0.04	0.07	98.57	75.95	7.78	0.06	773
CS-13-15	0.89	86.91	3.02	0.47	6.40	0.06	0.00	98.49	76.61	5.95	0.00	586
CS-13-15	0.87	83.30	2.73	0.39	7.76	0.07	0.06	95.84	73.43	7.21	0.06	741
CS-13-15	0.28	85.09	1.36	0.32	11.87	0.02	0.00	99.37	75.01	11.02	0.00	1109
CS-13-15	0.72	86.05	2.31	0.37	8.04	0.04	0.00	98.36	75.85	7.47	0.00	744
CS-13-15	0.77	85.69	2.60	0.38	8.10	0.06	0.04	98.28	75.54	7.52	0.03	751
CS-13-15	0.52	85.08	2.04	0.27	9.00	0.02	0.03	97.59	75.00	8.36	0.03	841
CS-13-15	0.34	82.00	1.50	0.52	10.02	0.02	0.00	96.83	72.28	9.30	0.00	971
CS-13-15	0.50	85.40	2.01	0.42	8.62	0.02	0.00	98.38	75.28	8.00	0.00	802
CS-13-15	0.72	82.14	1.68	0.50	8.31	0.04	0.04	97.06	72.40	7.72	0.04	805
CS-13-15	0.61	82.03	1.75	0.44	9.68	0.03	0.03	97.54	72.31	8.98	0.03	937
CS-13-15	0.62	86.32	1.64	0.35	7.85	0.06	0.01	98.29	76.09	7.29	0.00	723
CS-13-15	0.25	82.84	1.20	0.26	12.33	0.01	0.00	97.93	73.03	11.45	0.00	1184
CS-13-15	0.24	86.10	1.19	0.31	11.46	0.00	0.03	99.84	75.90	10.64	0.03	1058
CS-13-15	0.21	83.87	1.29	0.36	12.32	0.00	0.03	98.74	73.93	11.43	0.02	1167
CS-13-15	0.49	84.21	1.01	0.23	11.22	0.03	0.00	98.17	74.23	10.42	0.00	1060
CS-13-15	0.39	83.82	1.87	0.39	11.40	0.01	0.00	98.42	73.89	10.59	0.00	1082

Table B.2: Chemical compositions (wt%) and calculated Chemical-Pb ages (Ma) for uraninite at the Kianna deposit

Sample No.	SiO_2	UO_2	CaO	Fe_2O_3	PbO	Al_2O_3	ThO_2	Total	U wt%	Pb wt%	Th wt%	Chem. Pb Age (Ma)
CS-13-15	0.58	85.97	1.54	0.39	7.45	0.05	0.00	97.14	75.78	6.91	0.00	688
CS-13-15	0.35	84.26	1.75	0.49	10.11	0.03	0.07	98.12	74.28	9.39	0.06	954
CS-13-4	0.40	84.02	1.14	0.38	12.69	0.03	0.06	99.38	74.06	11.78	0.06	1201
CS-13-4	0.51	87.69	1.49	0.38	9.52	0.03	0.02	100.49	77.30	8.84	0.02	863
CS-13-4	0.26	85.96	1.06	0.36	13.03	0.01	0.01	101.44	75.77	12.09	0.01	1205
CS-13-4	0.98	87.02	1.73	0.45	7.78	0.09	0.04	99.26	76.71	7.22	0.03	711
CS-13-4	0.66	86.87	1.82	0.51	8.77	0.04	0.02	99.46	76.58	8.14	0.02	802
CS-13-4	1.30	91.25	2.26	0.52	3.00	0.07	0.00	99.41	80.44	2.79	0.00	262
CS-13-4	0.37	85.71	0.92	0.23	11.78	0.02	0.01	99.70	75.55	10.94	0.01	1093
CS-13-4	0.41	85.67	1.22	0.29	11.56	0.00	0.04	99.97	75.52	10.73	0.03	1073
CS-13-4	0.32	84.20	0.80	0.26	13.12	0.00	0.00	99.40	74.22	12.18	0.00	1239
CS-13-4	0.20	83.62	0.92	0.19	13.46	0.03	0.03	99.43	73.71	12.50	0.03	1280
CS-13-4	0.32	84.32	1.10	0.32	12.73	0.02	0.03	99.54	74.33	11.82	0.02	1200
CS-13-4	0.60	85.17	1.62	0.33	10.63	0.04	0.05	99.25	75.08	9.86	0.04	991
CS-13-4	0.68	86.03	1.30	0.38	9.29	0.03	0.03	98.38	75.84	8.62	0.03	858
CS-13-4	0.26	83.37	1.01	0.33	13.55	0.00	0.02	99.27	73.49	12.58	0.02	1292
CS-13-4	0.63	86.38	1.81	0.47	8.51	0.06	0.02	98.63	76.14	7.90	0.02	783
CS-13-4	0.74	86.17	1.15	0.34	9.72	0.08	0.02	99.04	75.96	9.03	0.02	897
CS-13-4	0.27	84.02	0.96	0.22	12.71	0.00	0.00	98.96	74.06	11.80	0.00	1203
CS-13-4	0.57	86.72	1.62	0.41	10.53	0.05	0.05	100.64	76.44	9.78	0.04	966
CS-13-4	0.36	84.42	1.22	0.31	12.59	0.05	0.00	99.89	74.42	11.69	0.00	1186
CS-13-4	0.22	84.25	0.80	0.26	13.53	0.02	0.02	99.62	74.27	12.56	0.02	1277
CS-13-4	0.77	85.64	1.71	0.41	9.37	0.05	0.03	98.53	75.49	8.70	0.03	870
CS-13-4	0.16	83.74	0.71	0.25	14.07	0.00	0.05	99.53	73.81	13.06	0.04	1336
CS-13-4	0.22	83.59	0.82	0.27	13.52	0.04	0.04	99.10	73.69	12.55	0.04	1286
CS-13-4	0.31	84.74	1.25	0.29	11.71	0.04	0.00	99.17	74.70	10.87	0.00	1099
CS-13-4	0.52	86.22	1.32	0.35	10.71	0.04	0.02	100.11	76.01	9.94	0.02	987
CS-13-4	0.43	83.70	1.06	0.33	11.21	0.03	0.02	97.51	73.78	10.40	0.02	1064
CS-13-4	0.35	84.78	0.96	0.25	12.90	0.02	0.00	99.84	74.73	11.97	0.00	1209
CS-13-4	1.68	84.51	1.20	0.36	8.54	0.13	0.00	97.83	74.49	7.93	0.00	804

Table B.2: Chemical compositions (wt%) and calculated Chemical-Pb ages (Ma) for uraninite at the Kianna deposit

Sample No.	SiO_2	UO_2	CaO	Fe_2O_3	PbO	Al_2O_3	ThO_2	Total	U wt%	Pb wt%	Th wt%	Chem. Pb Age (Ma)
CS-13-4	0.41	84.82	1.43	0.37	11.22	0.04	0.00	98.78	74.77	10.42	0.00	1052
CS-13-4	0.52	85.58	1.41	0.43	10.44	0.08	0.03	99.29	75.44	9.69	0.03	970
CS-13-4	0.48	86.71	1.40	0.44	9.85	0.01	0.01	99.62	76.43	9.14	0.01	903
CS-13-4	0.43	84.51	0.99	0.29	11.58	0.01	0.01	98.34	74.50	10.75	0.01	1089
CS-13-13a	0.92	86.99	0.99	0.28	7.96	0.04	0.05	98.65	76.68	7.39	0.04	727
CS-13-13a	0.59	86.94	1.43	0.37	8.17	0.01	0.08	98.75	76.64	7.58	0.07	746
CS-13-13a	9.34	77.95	0.69	0.03	0.02	0.32	0.09	90.50	68.71	0.02	0.07	2
CS-13-13a	0.37	84.86	1.26	0.32	11.09	0.03	0.06	99.13	74.80	10.29	0.06	1038
CS-13-13a	0.53	84.37	1.58	0.32	10.46	0.01	0.00	98.31	74.37	9.71	0.00	986
CS-13-13a	3.68	87.79	0.42	0.11	0.36	0.30	0.00	94.66	77.38	0.34	0.00	33
CS-13-13a	2.97	88.60	0.41	0.11	1.59	0.23	0.08	95.87	78.10	1.47	0.07	142
CS-13-13a	0.72	87.25	2.04	0.42	6.25	0.02	0.02	97.86	76.91	5.80	0.02	569
CS-13-13a	0.44	84.78	1.50	0.30	10.62	0.00	0.07	98.80	74.73	9.86	0.06	996
CS-13-13a	0.49	85.30	1.86	0.33	10.06	0.04	0.06	99.37	75.19	9.34	0.05	938
CS-13-13a	1.43	87.72	1.20	0.38	3.90	0.09	0.09	97.01	77.32	3.62	0.08	353
CS-13-13a	1.26	87.33	1.10	0.30	6.56	0.07	0.05	97.93	76.98	6.09	0.05	597
CS-13-13a	0.37	83.48	1.53	0.26	11.15	0.02	0.02	98.05	73.59	10.35	0.02	1062
CS-13-13a	0.56	84.32	1.41	0.32	8.52	0.03	0.07	96.06	74.33	7.91	0.07	803
CS-13-13a	0.21	82.78	1.00	0.15	14.08	0.03	0.03	98.84	72.97	13.08	0.03	1353
CS-13-13a	0.81	86.86	1.80	0.32	7.40	0.06	0.03	98.30	76.57	6.87	0.02	677
CS-13-13a	0.31	83.87	1.36	0.23	11.95	0.04	0.05	98.86	73.93	11.10	0.04	1133
CS-13-13a	0.78	86.93	1.70	0.36	8.04	0.05	0.04	99.00	76.63	7.46	0.03	735
CS-13-13a	0.39	81.23	0.81	0.22	14.34	0.01	0.07	98.13	71.60	13.31	0.06	1403
CS-13-13a	0.35	82.06	1.19	0.23	12.56	0.00	0.07	97.54	72.34	11.66	0.06	1217
CS-13-13a	4.08	86.89	0.37	0.17	0.32	0.28	0.02	94.11	76.60	0.30	0.02	30
CS-13-13a	0.44	84.53	0.92	0.23	11.07	0.05	0.02	98.18	74.52	10.28	0.02	1041
CS-13-13a	0.92	86.85	1.49	0.34	5.87	0.07	0.01	96.91	76.56	5.45	0.01	537
CS-13-13a	0.46	85.47	1.00	0.21	10.42	0.05	0.04	98.72	75.34	9.67	0.03	969
CS-13-13a	0.39	83.13	1.42	0.22	12.64	0.03	0.07	98.98	73.28	11.73	0.06	1208
CS-13-13a	2.11	85.79	0.53	0.14	6.57	0.28	0.00	96.78	75.63	6.10	0.00	609

Table B.2: Chemical compositions (wt%) and calculated Chemical-Pb ages (Ma) for uraninite at the Kianna deposit

Sample No.	SiO_2	UO_2	CaO	Fe_2O_3	PbO	Al_2O_3	ThO_2	Total	U wt%	Pb wt%	Th wt%	Chem. Pb Age (Ma)
CS-13-13a	0.58	84.81	1.45	0.25	10.11	0.04	0.00	98.20	74.76	9.38	0.00	947
CS-13-13a	0.66	87.07	1.10	0.26	8.38	0.06	0.00	98.80	76.76	7.78	0.00	765
CS-13-13a	0.62	85.15	1.44	0.39	9.73	0.08	0.07	98.56	75.06	9.03	0.06	908
CS-13-13a	1.39	88.78	1.66	0.40	4.49	0.09	0.02	98.43	78.26	4.17	0.02	402
CS-13-13a	0.50	85.34	1.22	0.31	11.54	0.01	0.00	99.93	75.23	10.71	0.00	1075
CS-13-28	3.69	85.39	1.77	1.75	0.54	0.39	0.00	95.56	75.27	0.50	0.00	50
CS-13-28	3.46	85.90	2.17	1.17	2.32	0.38	0.00	97.84	75.72	2.15	0.00	214
CS-13-28	1.78	81.75	3.61	1.46	0.63	0.11	0.00	91.21	72.06	0.59	0.00	62
CS-13-28	2.35	80.47	3.62	1.42	1.74	0.29	0.00	92.72	70.93	1.62	0.00	172
CS-13-28	3.87	87.47	1.70	1.56	0.49	0.48	0.00	97.27	77.10	0.46	0.00	45
CS-13-28	3.36	87.98	1.78	1.63	0.53	0.33	0.05	97.42	77.56	0.49	0.04	48
CS-13-28	3.07	85.42	2.27	1.83	0.73	0.28	0.00	95.30	75.29	0.68	0.00	68
CS-13-28	5.28	84.45	2.11	1.48	0.01	0.44	0.00	95.33	74.44	0.01	0.00	1
CS-20b1	2.58	76.34	6.95	3.61	0.53	0.52	0.02	93.00	67.29	0.49	0.02	55
CS-20b1	2.07	78.74	7.24	3.24	0.47	0.35	0.00	94.42	69.41	0.44	0.00	48
CS-20b1	1.21	81.02	6.64	3.38	0.58	0.11	0.03	94.99	71.42	0.54	0.02	57
CS-22a2	0.33	80.59	1.55	0.36	10.28	0.00	0.06	94.05	71.04	9.54	0.06	1014
CS-12a	0.49	80.05	1.10	0.27	11.91	0.01	0.01	94.71	70.56	11.05	0.01	1182
CS-13-27	0.25	89.92	2.28	0.99	1.70	0.02	0.03	96.79	79.26	1.58	0.02	150
CS-13-28	5.33	85.94	1.71	1.65	0.40	0.45	0.01	97.15	75.76	0.37	0.00	37
CS-13-28	3.40	86.43	1.94	1.75	0.59	0.35	0.00	96.44	76.19	0.55	0.00	55
CS-13-4	0.65	86.47	1.23	0.35	9.31	0.02	0.00	98.86	76.23	8.65	0.00	857
CS-13-4	0.60	84.73	1.55	0.33	11.01	0.10	0.02	99.04	74.69	10.22	0.02	1033
CS-13-4	0.79	86.11	1.75	0.41	8.28	0.06	0.01	98.02	75.91	7.69	0.01	765
CS-13-4	0.90	87.48	1.21	0.42	8.31	0.08	0.03	99.08	77.11	7.71	0.03	755
CS-13-15	0.20	83.33	1.06	0.23	13.45	0.06	0.01	99.00	73.45	12.48	0.01	1283
CS-13-11	0.74	86.12	1.81	0.39	9.04	0.05	0.01	98.84	75.91	8.39	0.01	834

Table B3: Chemical compositions (wt%) of silicate minerals at the Kianna deposit

Sample No.	Mineral ID	SiO_2	K_2O	Al_2O_3	CaO	Fe_2O_3	MgO	Total
CS-14a	Mg-Fe Chlorite	35.03	0.47	27.93	0.27	12.52	8.64	86.65
CS-14a	Mg-Fe Chlorite	30.74	0.12	21.22	0.16	26.79	9.09	91.53
CS-14a	Mg-Fe Chlorite	39.91	2.08	31.58	0.17	8.33	5.52	88.86
CS-14a	Mg-Fe Chlorite	32.74	0.09	26.14	0.28	18.68	9.50	89.65
CS-14a	Mg-Fe Chlorite	29.75	0.10	20.84	0.22	25.60	9.57	88.41
CS-14a	Mg-Fe Chlorite	33.82	0.20	25.58	0.33	16.85	8.97	88.64
CS-14a	Mg-Fe Chlorite	29.50	0.11	20.73	0.19	26.69	9.30	88.52
CS-14a	Mg-Fe Chlorite	28.91	0.07	20.17	0.25	26.92	9.58	88.14
CS-14a	Mg-Fe Chlorite	28.09	0.08	20.33	0.26	27.66	10.45	89.30
CS-18b	Mg-Fe Chlorite	36.18	0.39	24.16	0.29	16.52	10.14	88.47
CS-18b	Mg-Fe Chlorite	33.63	0.20	25.06	0.32	17.10	11.40	88.65
CS-18b	Mg-Fe Chlorite	34.19	0.30	21.98	0.35	20.02	10.76	88.58
CS-18b	Mg-Fe Chlorite	39.38	0.98	20.06	0.37	18.00	7.91	87.70
CS-18b	Mg-Fe Chlorite	34.15	0.20	24.65	0.30	15.57	12.00	87.47
CS-18b	Mg-Fe Chlorite	34.21	0.25	25.28	0.29	15.38	11.34	87.97
CS-18c	Mg-Fe Chlorite	31.90	0.20	23.51	0.30	21.04	10.43	88.64
CS-18c	Mg-Fe Chlorite	32.53	0.40	22.76	0.36	22.44	10.74	90.63
CS-18c	Mg-Fe Chlorite	34.36	0.17	26.19	0.31	16.42	11.10	89.81
CS-14a	Mg-Fe Chlorite	33.62	0.08	28.73	0.24	12.89	10.61	88.18
CS-4b	Fe Chlorite	25.88	0.03	8.52	0.34	47.11	7.16	90.38
CS-4b	Fe Chlorite	24.43	0.02	8.75	0.20	53.16	4.48	92.43
CS-4b	Fe Chlorite	22.23	0.02	16.68	0.16	50.51	2.21	93.22
CS-4b	Fe Chlorite	25.02	0.03	8.20	0.28	53.61	5.11	93.59
CS-4b	Fe Chlorite	25.45	0.02	10.28	0.25	48.65	5.58	91.23
CS-4b	Fe Chlorite	23.27	0.02	10.24	1.31	55.44	1.55	93.24
CS-4b	Fe Chlorite	24.83	0.15	9.13	0.80	45.92	5.04	88.51

Table B3: Chemical compositions (wt%) of silicate minerals and hematite at the Kianna deposit

Sample No.	Mineral ID	SiO_2	K_2O	Al_2O_3	CaO	Fe_2O_3	MgO	Total
CS-22b	Mg Chlorite	30.93	0.00	21.70	0.07	10.81	26.12	90.29
CS-22b	Mg Chlorite	30.71	0.02	20.99	0.15	10.39	23.97	87.07
CS-22b	Mg Chlorite	31.29	0.01	21.43	0.12	12.03	25.29	91.04
CS-22b	Mg Chlorite	32.87	0.02	23.42	0.11	10.89	24.88	93.04
CS-4a	Mg Chlorite	33.43	0.20	29.62	0.25	3.60	15.08	83.70
CS-4a	Mg Chlorite	37.15	0.72	32.17	0.14	1.30	12.21	86.08
CS-4a	Mg Chlorite	34.57	0.08	29.37	0.21	4.17	13.87	86.81
CS-4a	Mg Chlorite	35.17	0.47	26.39	0.45	3.42	13.63	88.18
CS-4a	Mg Chlorite	33.21	0.28	26.13	0.09	6.95	20.59	88.58
CS-4a	Mg Chlorite	35.09	0.04	32.37	0.10	4.80	14.75	88.32
CS-4a	Mg Chlorite	34.98	0.04	31.13	0.11	4.57	15.89	87.85
CS-4a	Mg Chlorite	32.03	0.39	25.07	0.08	9.32	21.95	89.70
CS-4a	Mg Chlorite	35.47	0.05	31.24	0.14	4.89	16.23	89.08
CS-4a	Mg Chlorite	35.11	0.04	30.60	0.10	4.42	16.84	88.25
CS-4a	Mg Chlorite	35.88	0.21	33.88	0.10	1.86	15.20	88.40
CS-4b	Hematite	2.68	0.07	0.37	1.98	76.13	1.51	87.53
CS-4b	Hematite	2.42	0.01	0.70	0.25	79.80	1.33	85.70
CS-4b	Hematite	1.81	0.02	0.38	0.08	93.35	0.03	97.06
CS-4b	Hematite	1.93	0.02	0.46	0.29	91.06	0.06	98.60
CS-4b	Hematite	1.74	0.07	0.66	0.63	89.34	0.03	99.86
CS-23	Quartz	99.72	0.01	0.00	0.01	0.00	0.00	99.92
CS-23	Quartz	99.01	0.00	0.01	0.00	0.02	0.00	99.18
CS-23	Quartz	99.70	0.01	0.01	0.00	0.09	0.00	99.90
CS-18b	Quartz	99.61	0.00	0.03	0.00	0.28	0.00	100.25
CS-18b	Quartz	102.19	0.01	0.28	0.01	0.25	0.05	103.04
CS-18b	Quartz	92.40	0.01	0.06	0.02	0.12	0.03	92.80
CS-18b	Quartz	99.50	0.01	0.02	0.01	0.23	0.00	99.90
CS-18b	Quartz	101.20	0.00	0.03	0.01	0.40	0.00	101.89
CS-18b	Quartz	99.82	0.00	0.03	0.00	0.08	0.00	99.94

Table B3: Chemical compositions (wt%) of silicate minerals at the Kianna deposit

Sample No.	Mineral ID	SiO_2	K_2O	Al_2O_3	CaO	Fe_2O_3	MgO	Total
CS-18c	Quartz	99.37	0.00	0.03	0.00	0.10	0.00	99.67
CS-18c	Quartz	99.84	0.01	0.04	0.01	1.33	0.00	101.55
CS-14a	Quartz	99.34	0.01	0.01	0.00	0.02	0.00	99.71
CS-14a	Quartz	98.91	0.00	0.00	0.25	0.04	0.00	99.32
CS-14a	Quartz	98.40	0.04	0.20	0.03	0.12	0.06	99.01
CS-15a	Quartz	96.92	0.01	0.01	0.00	0.00	0.00	97.36
CS-15a	Quartz	93.11	0.01	0.84	0.01	1.74	0.63	96.44
CS-15a	Quartz	86.51	0.19	0.69	0.12	0.28	0.39	89.30
CS-15a	Quartz	93.46	0.08	0.14	0.02	0.25	0.02	94.75
CS-15a	Quartz	91.23	0.52	3.48	0.02	0.13	0.19	95.69
CS-15a	Quartz	90.86	0.11	1.13	0.14	0.08	0.08	92.90
CS-15a	Quartz	96.16	0.08	0.71	0.01	0.13	0.13	97.30
CS-15a	Quartz	95.24	0.06	0.62	0.01	0.02	0.01	96.36
CS-15a	Quartz	99.79	0.01	0.01	0.01	0.00	0.00	100.02
CS-14a	Quartz	99.70	0.00	0.00	0.00	0.05	0.00	100.41
CS-15a	Sudoite	36.26	0.10	36.42	0.07	0.32	14.20	89.51
CS-22a2	Sudoite	36.06	0.01	40.09	0.10	0.04	7.89	85.08
CS-22a2	Sudoite	35.49	0.01	40.70	0.15	0.07	7.92	85.41
CS-22a2	Sudoite	36.11	0.01	40.77	0.14	0.07	7.94	85.93
CS-22a2	Sudoite	41.04	0.79	36.56	0.29	0.79	6.16	87.06
CS-22b	Sudoite	35.54	0.00	40.43	0.11	0.36	7.95	84.96
CS-15a	Sudoite	45.00	1.25	27.81	0.14	3.48	9.55	88.35
CS-15a	Sudoite	50.53	0.50	26.16	0.35	2.07	10.96	92.21
CS-15a	Sudoite	41.76	1.36	29.07	0.17	4.85	12.51	90.88
CS-15a	Sudoite	41.59	1.40	29.29	0.12	3.81	11.90	89.31
CS-15a	Sudoite	42.18	1.44	31.32	0.07	2.50	11.06	89.64
CS-15a	Sudoite	36.73	0.18	37.31	0.03	0.20	13.31	90.38

Table B3: Chemical compositions (wt%) of silicate minerals at the Kianna deposit

Sample No.	Mineral ID	SiO_2	K_2O	Al_2O_3	CaO	Fe_2O_3	MgO	Total
CS-15a	Sudoite	38.20	0.36	35.64	0.13	0.72	13.68	90.84
CS-15a	Sudoite	40.41	0.91	31.83	0.26	3.24	13.36	91.78
CS-15a	Sudoite	41.12	1.48	30.31	0.53	3.52	13.11	92.11
CS-15a	Sudoite	36.62	0.13	37.87	0.03	0.14	13.80	90.92
CS-15a	Sudoite	38.11	0.36	33.94	0.12	1.71	13.72	89.49
CS-15a	Sudoite	39.21	0.58	31.75	0.22	3.39	13.31	89.82
CS-15a	Sudoite	36.62	0.14	37.05	0.05	0.59	13.96	90.49
CS-15a	Sudoite	38.93	1.26	30.48	0.10	4.27	14.86	91.20
CS-8	Sudoite	36.07	2.75	26.29	0.16	6.61	15.86	88.53
CS-15a	Sudoite	41.80	2.48	28.74	0.09	3.86	10.11	87.96
CS-13-7	Sudoite	38.03	0.90	30.65	0.36	6.54	11.24	88.71
CS-13-7	Sudoite	39.84	2.08	31.15	0.30	4.94	10.01	89.18
CS-13-7	Sudoite	38.30	0.76	30.78	0.40	6.62	10.86	88.47
CS-13-7	Sudoite	38.34	0.49	32.04	0.37	2.56	11.85	86.59
CS-13-7	Sudoite	37.80	0.80	32.16	0.29	1.56	13.11	86.36
CS-13-7	Sudoite	38.91	1.97	31.02	0.29	5.91	10.42	89.10
CS-13-7	Sudoite	41.17	2.66	29.97	0.38	5.69	9.10	89.91
CS-13-13b	Kaolinite	47.17	3.10	34.07	0.14	0.73	0.92	86.63
CS-13-13b	Kaolinite	46.79	1.54	37.56	0.07	0.23	0.18	86.79
CS-13-13b	Kaolinite	46.83	1.05	36.73	0.08	0.22	0.26	85.57
CS-13-13b	Kaolinite	46.52	0.36	37.56	0.07	0.23	0.20	85.29
CS-22a2	Kaolinite	48.62	0.02	40.49	0.06	0.01	0.13	89.67
CS-22a2	Kaolinite	46.75	0.02	39.14	0.05	0.07	0.11	87.03
CS-22a2	Kaolinite	47.38	0.01	39.80	0.04	0.05	0.05	87.99
CS-22a2	Kaolinite	48.24	0.02	39.99	0.05	0.02	0.08	88.68
CS-22b	Kaolinite	47.92	0.00	41.01	0.06	0.17	0.12	89.53
CS-22b	Kaolinite	48.42	0.01	40.73	0.06	0.07	0.11	89.63

Table B3: Chemical compositions (wt%) of silicate minerals at the Kianna deposit

Sample No.	Mineral ID	SiO_2	K_2O	Al_2O_3	CaO	Fe_2O_3	MgO	Total
CS-22b	Kaolinite	48.22	0.10	39.44	0.17	0.14	0.35	88.84
CS-22b	Kaolinite	47.06	0.22	37.58	0.13	0.50	1.72	87.63
CS-22b	Kaolinite	47.54	0.01	40.08	0.03	0.12	0.10	88.10
CS-13-13b	Kaolinite	47.78	2.27	35.61	0.11	0.51	0.68	87.40
CS-18b	Biotite	47.72	1.70	21.71	0.26	12.87	3.77	88.63
CS-18c	Biotite	44.11	3.56	18.58	0.60	19.81	6.39	94.41
CS-8	Illite	49.23	5.51	32.21	0.06	3.22	2.32	92.97
CS-8	Illite	46.55	4.17	32.17	0.19	2.01	4.46	90.21
CS-8	Illite	47.19	7.10	35.04	0.01	2.43	1.38	93.39
CS-8	Illite	46.67	6.85	34.66	0.00	2.21	1.11	91.78
CS-8	Illite	46.61	7.34	35.31	0.02	2.01	0.93	92.65
CS-8	Illite	47.07	5.24	32.45	0.07	3.40	2.79	91.30
CS-8	Illite	45.78	7.97	37.00	0.02	1.09	0.49	92.88
CS-8	Illite	48.06	5.96	34.33	0.01	2.55	1.33	92.39
CS-14a	Illite	47.61	4.65	37.52	0.00	1.56	0.46	92.30
CS-14a	Illite	48.68	5.29	37.87	0.00	1.54	0.70	94.85
CS-14a	Illite	47.87	4.56	35.64	0.01	2.01	1.26	92.18
CS-14a	Illite	48.16	4.46	35.40	0.05	1.89	1.16	92.02
CS-22a2	Illite	48.22	5.63	26.44	0.29	1.13	2.40	86.61
CS-8	Illite	49.14	5.16	38.99	0.01	1.23	0.14	96.84
CS-8	Coarse Illite	46.92	7.04	26.10	0.40	3.66	5.78	90.83
CS-13-7	Coarse Illite	46.91	7.99	31.18	1.04	1.76	2.05	92.20
CS-8	Coarse Illite	48.95	7.78	26.38	0.33	3.23	4.35	91.84
CS-8	Coarse Illite	43.45	6.47	30.18	0.22	3.36	6.83	91.34
CS-8	Coarse Illite	47.51	9.03	31.73	0.21	1.34	2.37	92.88
CS-8	Coarse Illite	48.04	9.66	31.26	0.21	0.90	1.51	92.28
CS-8	Coarse Illite	46.51	8.43	30.85	0.17	1.94	3.13	91.51

Table B3: Chemical compositions (wt%) of silicate minerals at the Kianna deposit

Sample No.	Mineral ID	SiO_2	K_2O	Al_2O_3	CaO	Fe_2O_3	MgO	Total
CS-13-13b	Coarse Illite	48.23	9.84	32.01	0.07	0.83	1.22	92.52
CS-8	Coarse Illite	48.59	8.22	29.56	0.32	2.08	2.40	92.10
CS-13-9	Coarse Illite	44.40	9.21	27.57	0.23	1.36	2.10	85.81
CS-13-9	Coarse Illite	44.52	8.92	26.94	0.33	1.31	2.52	85.54
CS-13-9	Coarse Illite	44.51	9.17	27.08	0.27	1.28	2.33	85.70
CS-13-13b	Coarse Illite	47.20	8.87	31.22	0.23	1.29	1.10	90.67
CS-13-13b	Coarse Illite	47.66	8.48	34.63	0.05	0.57	0.77	92.40
CS-13-13b	Coarse Illite	51.07	8.29	30.53	0.06	0.38	1.90	92.73
CS-8	Coarse Illite	46.25	8.74	37.08	0.01	1.21	0.69	94.34
CS-13-7	Coarse Illite	45.39	9.48	35.21	0.70	0.86	0.61	92.93
CS-13-7	Coarse Illite	47.99	8.03	30.16	0.68	1.90	2.28	92.36
CS-8	Coarse Illite	45.89	8.61	38.23	0.00	0.79	0.33	94.41
CS-8	Coarse Illite	45.25	8.95	35.97	0.00	1.46	0.63	92.65
CS-8	Coarse Illite	46.26	8.10	38.75	0.00	0.91	0.36	94.87
CS-8	Coarse Illite	49.29	8.02	26.34	0.33	3.13	4.07	92.28
CS-13-7	Coarse Illite	48.84	9.72	31.53	0.11	1.48	1.88	94.20
CS-13-7	Muscovite	48.21	10.89	32.32	0.06	1.81	1.54	95.46
CS-13-7	Muscovite	47.67	10.68	34.85	0.03	0.94	0.70	95.26
CS-13-7	Muscovite	47.93	10.74	32.17	0.05	1.62	1.41	94.47
CS-13-7	Muscovite	47.39	10.55	34.78	0.06	1.04	0.60	95.07
CS-13-7	Muscovite	47.95	10.84	33.76	0.01	1.48	0.88	95.33
CS-13-7	Muscovite	48.24	10.81	33.51	0.02	1.34	0.94	95.31
CS-13-7	Muscovite	48.04	10.67	32.33	0.07	1.54	1.46	94.77
CS-8	Muscovite	45.78	10.82	35.14	0.01	1.29	0.56	94.25
CS-8	Muscovite	46.26	10.92	34.94	0.00	1.33	0.68	94.88
CS-8	Muscovite	46.61	10.95	35.71	0.00	1.15	0.54	95.51
CS-8	Muscovite	45.61	10.95	34.87	0.01	1.44	0.59	94.34
CS-13-9	Muscovite	44.59	10.98	34.57	0.04	0.25	0.49	91.17
CS-13-9	Muscovite	44.66	10.74	33.46	0.03	0.49	0.85	90.44

Table B3: Chemical compositions (wt%) of silicate minerals at the Kianna deposit

Sample No.	Mineral ID	SiO_2	K_2O	Al_2O_3	CaO	Fe_2O_3	MgO	Total
CS-13-9	Muscovite	42.14	10.92	33.52	0.04	0.76	0.67	88.54
CS-13-9	Muscovite	42.49	10.98	29.26	0.02	2.22	1.87	87.35
CS-13-9	Muscovite	42.42	10.92	29.63	0.04	1.99	1.70	87.26
CS-13-13b	Muscovite	48.35	10.37	34.13	0.04	0.65	0.77	94.65
CS-13-13b	Muscovite	47.33	10.72	33.74	0.00	2.35	0.27	94.78
CS-13-13b	Muscovite	47.16	10.45	34.40	0.01	1.00	0.97	94.88
CS-13-13b	Muscovite	47.70	10.75	33.92	0.00	1.05	1.13	95.32
CS-13-13b	Muscovite	46.21	10.95	35.35	0.01	1.83	0.17	94.81
CS-13-7	Muscovite	48.93	10.49	31.67	0.06	1.12	1.59	94.20
CS-8	Muscovite	45.94	11.28	35.73	0.00	0.99	0.31	94.71
CS-8	Muscovite	45.94	11.19	35.98	0.01	0.99	0.34	94.99
CS-8	Muscovite	45.26	11.19	35.32	0.00	1.04	0.25	93.45
CS-8	Muscovite	45.41	11.37	34.04	0.00	1.58	0.73	93.58
CS-8	Muscovite	45.25	11.19	34.71	0.00	1.31	0.36	94.07
CS-8	Muscovite	45.64	11.12	35.33	0.00	1.28	0.54	94.50
CS-8	Muscovite	45.59	11.18	34.55	0.00	1.29	0.57	93.95
CS-8	Muscovite	45.67	11.11	34.49	0.01	1.64	0.36	93.54
CS-8	Muscovite	45.35	11.22	35.39	0.00	1.11	0.23	93.60
CS-8	Muscovite	45.75	11.24	35.82	0.01	1.03	0.35	95.49
CS-8	Muscovite	45.95	11.31	35.35	0.00	1.08	0.52	94.69
CS-8	Muscovite	45.83	11.28	35.42	0.00	1.16	0.49	94.90
CS-8	Muscovite	46.14	11.43	35.25	0.00	1.24	0.51	95.06
CS-8	Muscovite	45.91	11.38	35.21	0.02	1.29	0.60	95.21

Table B3: Chemical compositions (wt%) of silicate minerals at the Kianna deposit

Sample No.	Mineral ID	SiO_2	K_2O	Al_2O_3	CaO	Fe_2O_3	MgO	Total
CS-8	Muscovite	46.11	11.40	34.83	0.00	1.57	0.57	94.92
CS-8	Muscovite	45.35	11.19	35.26	0.00	1.03	0.49	93.86
CS-8	Muscovite	45.94	11.20	34.54	0.01	1.52	0.68	94.68
CS-8	Muscovite	45.52	11.20	35.09	0.00	1.54	0.64	94.71
CS-8	Muscovite	45.94	11.29	34.63	0.00	1.50	0.79	95.13
CS-8	Muscovite	46.02	11.49	35.27	0.00	1.22	0.57	95.20
CS-8	Muscovite	46.11	11.10	35.48	0.01	1.15	0.52	94.99
CS-8	Muscovite	46.05	11.30	35.46	0.00	1.18	0.67	95.51
CS-8	Muscovite	46.09	11.50	35.01	0.01	1.00	0.67	95.21
CS-13-9	Muscovite	45.93	11.23	31.62	0.02	2.68	1.38	93.29
CS-13-9	Muscovite	45.27	11.23	31.91	0.02	1.69	1.47	92.15
CS-13-9	Muscovite	44.12	11.24	32.99	0.00	2.38	1.35	92.53
CS-13-9	Muscovite	44.14	11.19	32.54	0.01	2.40	1.43	92.37
CS-13-9	Muscovite	45.30	11.26	32.21	0.03	1.62	1.35	92.11
CS-13-9	Muscovite	43.43	11.30	32.75	0.00	2.34	1.42	91.82
CS-13-9	Muscovite	44.81	11.44	31.22	0.00	2.31	1.26	91.53
CS-13-9	Muscovite	42.93	11.31	32.21	0.00	2.52	1.48	91.01
CS-13-9	Muscovite	44.42	11.38	32.34	0.01	1.50	1.32	91.34
CS-13-9	Muscovite	44.21	11.12	31.62	0.01	1.64	1.44	90.48
CS-13-9	Muscovite	43.41	11.17	35.41	0.01	0.91	0.29	91.59
CS-13-9	Muscovite	44.91	11.32	31.54	0.00	1.69	1.73	91.72
CS-13-9	Muscovite	45.19	11.37	30.24	0.02	1.83	1.96	91.09
CS-13-9	Muscovite	44.60	11.35	30.55	0.00	2.16	1.81	90.75
CS-13-9	Muscovite	43.65	11.09	32.53	0.02	1.74	1.06	90.54
CS-13-9	Muscovite	42.99	11.24	35.56	0.02	0.34	0.28	90.92
CS-13-9	Muscovite	43.89	11.14	34.87	0.03	0.30	0.40	90.96
CS-13-9	Muscovite	44.31	11.12	34.95	0.03	0.56	0.36	91.81
CS-13-9	Muscovite	42.34	11.09	34.73	0.01	0.33	0.36	89.20

Table B3: Chemical compositions (wt%) of silicate minerals at the Kianna deposit

Sample No.	Mineral ID	SiO_2	K_2O	Al_2O_3	CaO	Fe_2O_3	MgO	Total
CS-8	Muscovite	46.07	11.17	35.04	0.00	1.57	0.74	95.53
CS-8	Muscovite	46.36	11.26	34.87	0.00	1.21	0.61	94.93
CS-8	Muscovite	45.64	11.33	34.84	0.04	1.15	0.52	94.39
CS-8	Muscovite	46.21	11.01	35.52	0.00	1.59	0.73	95.58
CS-13-9	Muscovite	40.86	11.03	34.36	0.02	0.41	0.30	87.48
CS-13-13b	Muscovite	47.60	11.25	33.57	0.02	1.28	0.98	95.08
CS-13-13b	Muscovite	48.02	11.33	32.05	0.01	1.35	1.67	94.98
CS-13-13b	Muscovite	47.91	11.14	32.28	0.01	1.75	1.71	95.42
CS-13-13b	Muscovite	48.52	11.32	32.04	0.00	1.50	1.77	95.62
CS-13-13b	Muscovite	47.54	11.30	32.06	0.00	2.42	1.84	95.59
CS-13-13b	Muscovite	47.19	11.20	33.49	0.00	2.09	0.76	95.28
CS-13-13b	Muscovite	47.11	11.27	31.82	0.01	2.12	1.67	94.51
CS-13-13b	Muscovite	47.85	11.34	31.97	0.01	1.69	1.64	95.07
CS-13-13b	Muscovite	47.06	11.27	31.65	0.02	1.80	2.08	94.49
CS-13-13b	Muscovite	48.47	11.32	32.16	0.01	1.62	1.82	96.06
CS-13-13b	Muscovite	47.63	11.33	32.15	0.03	1.58	1.77	95.03
CS-13-13b	Muscovite	47.87	11.22	32.74	0.00	1.77	1.35	95.52
CS-13-13b	Muscovite	47.54	11.04	32.30	0.02	1.63	1.76	94.73
CS-13-13b	Muscovite	47.36	11.24	34.48	0.03	1.12	0.92	95.41
CS-13-13b	Muscovite	47.60	11.25	33.57	0.02	1.28	0.98	95.08
CS-13-13b	Muscovite	48.02	11.33	32.05	0.01	1.35	1.67	94.98
CS-13-13b	Muscovite	47.91	11.14	32.28	0.01	1.75	1.71	95.42
CS-13-13b	Muscovite	48.52	11.32	32.04	0.00	1.50	1.77	95.62
CS-13-13b	Muscovite	47.54	11.30	32.06	0.00	2.42	1.84	95.59
CS-13-13b	Muscovite	47.19	11.20	33.49	0.00	2.09	0.76	95.28
CS-13-13b	Muscovite	45.84	11.08	35.86	0.01	1.58	0.07	94.86
CS-13-13b	Muscovite	46.34	11.15	34.75	0.01	1.88	0.25	94.77
CS-13-13b	Muscovite	47.53	11.09	32.36	0.05	1.57	1.76	94.68
CS-13-13b	Muscovite	47.73	11.13	32.26	0.02	1.88	1.26	94.71

Table B3: Chemical compositions (wt%) of silicate minerals at the Kianna deposit

Sample No.	Mineral ID	SiO_2	K_2O	Al_2O_3	CaO	Fe_2O_3	MgO	Total
CS-13-7	Muscovite	48.29	11.21	32.91	0.03	1.50	1.47	95.92
CS-13-7	Muscovite	48.26	11.30	31.57	0.01	1.90	1.90	95.32
CS-13-7	Muscovite	47.83	11.16	33.66	0.01	1.52	1.08	95.58
CS-13-9	Muscovite	42.76	10.04	31.57	0.08	0.63	0.78	86.42
CS-13-9	Muscovite	43.07	10.55	29.73	0.03	1.88	1.36	87.05
CS-13-7	Muscovite	46.94	11.27	35.19	0.02	1.01	0.77	95.50
CS-13-7	Muscovite	47.50	11.34	34.54	0.00	0.98	0.94	95.64
CS-13-7	Muscovite	47.15	11.11	33.41	0.09	1.10	1.04	94.44

Table B4: Chemical compositions (wt%) of sulfide minerals at the Kianna deposit

Sample No.	Mineral ID	S	Fe	Ni	As	Cu	Pb	Se	U	Total
CS-14b	Pyrite	51.82	42.69	0.99	0.33	0.03	0.00	0.01		96.19
CS-14b	Pyrite	51.72	41.41	1.77	0.18	0.02	0.00	0.03		95.36
CS-14b	Pyrite	51.85	43.20	1.10	0.44	0.00	0.00	0.01		96.86
CS-14b	Pyrite	52.43	43.93	0.97	0.11	0.06	0.00	0.01		97.74
CS-14b	Pyrite	51.71	41.07	2.13	0.60	0.04	0.00	0.01		95.88
CS-14b	Pyrite	51.91	43.96	0.23	0.22	0.00	0.00	0.02		96.52
CS-14b	Pyrite	51.84	43.12	0.77	0.50	0.00	0.00	0.04		96.55
CS-14b	Pyrite	52.29	43.13	1.40	0.20	0.00	0.00	0.00		97.24
CS-14b	Pyrite	52.00	43.66	0.77	0.36	0.00	0.00	0.00		97.01
CS-7b	Pyrite	53.39	45.21	0.07	0.24	0.00	0.00	0.02		99.18
CS-7b	Pyrite	53.32	45.39	0.04	0.13	0.00	0.00	0.00		99.15
CS-7b	Pyrite	53.44	45.40	0.02	0.09	0.00	0.00	0.01		99.17
CS-7b	Pyrite	53.14	45.42	0.01	0.18	0.00	0.00	0.00		98.89
CS-7b	Pyrite	52.81	45.25	0.01	0.15	0.00	0.00	0.00		98.43
CS-7b	Pyrite	52.75	45.15	0.00	0.14	0.00	0.00	0.05		98.38
CS-7b	Pyrite	53.30	45.45	0.00	0.15	0.00	0.00	0.00		99.18
CS-7b	Pyrite	53.16	45.59	0.10	0.11	0.13	0.00	0.00		99.21
CS-7b	Pyrite	53.55	45.29	0.45	0.04	0.06	0.00	0.06		99.61
CS-7b	Pyrite	52.96	45.17	0.11	0.24	0.03	0.00	0.01		98.72
CS-7b	Pyrite	53.19	45.65	0.07	0.11	0.04	0.00	0.04		99.38
CS-7b	Pyrite	53.34	45.58	0.02	0.14	0.02	0.00	0.00		99.34
CS-7b	Pyrite	53.46	45.17	0.02	0.06	0.02	0.00	0.01		98.92
CS-7b	Pyrite	53.51	45.32	0.00	0.13	0.04	0.00	0.00		99.28
CS-7b	Pyrite	53.19	45.61	0.01	0.17	0.00	0.00	0.01		99.22
CS-7b	Pyrite	53.14	45.66	0.00	0.06	0.00	0.00	0.00		98.97
CS-7b	Pyrite	53.39	45.58	0.00	0.42	0.00	0.00	0.00		99.59

Table B4: Chemical compositions (wt%) of sulfide minerals at the Kianna deposit

Sample No.	Mineral ID	S	Fe	Ni	As	Cu	Pb	Se	U	Total
CS-19b	Pyrite	52.65	45.47	0.18	0.01	0.05	0.00	0.00		98.59
CS-19b	Pyrite	52.47	45.68	0.10	0.14	0.05	0.00	0.03		98.67
CS-19b	Pyrite	52.39	45.46	0.05	0.08	0.03	0.00	0.01		98.17
CS-19b	Pyrite	52.51	44.96	0.15	0.06	0.05	0.00	0.00		97.96
CS-19b	Pyrite	53.31	45.65	0.19	0.07	0.00	0.00	0.00		99.38
CS-19b	Pyrite	53.22	45.81	0.11	0.06	0.00	0.00	0.03		99.39
CS-19b	Pyrite	52.48	45.88	0.10	0.04	0.01	0.00	0.00		98.68
CS-19b	Pyrite	52.87	45.53	0.08	0.19	0.01	0.00	0.03		98.87
CS-19b	Pyrite	52.82	45.18	0.24	0.10	0.00	0.00	0.00		98.43
CS-19b	Pyrite	52.99	46.00	0.14	0.07	0.02	0.00	0.00		99.37
CS-19b	Pyrite	53.01	45.83	0.05	0.02	0.02	0.00	0.00		99.13
CS-19b	Pyrite	52.12	45.23	0.12	0.22	0.01	0.00	0.02		97.89
CS-19b	Pyrite	52.14	45.27	0.05	0.04	0.03	0.00	0.00		97.74
CS-19b	Pyrite	52.32	45.94	0.11	0.05	0.00	0.00	0.02		98.57
CS-19b	Pyrite	53.63	45.66	0.11	0.06	0.00	0.00	0.00		99.62
CS-7c	Pyrite	52.75	45.95	0.11	0.27	0.13	0.00	0.00		0.00
CS-7c	Pyrite	52.80	46.23	0.06	0.29	0.10	0.00	0.00		0.00
CS-23	Pyrite	52.12	45.09	0.00	0.17	0.37	0.18	0.17		98.33
CS-23	Pyrite	51.97	43.95	0.00	0.09	1.17	0.57	0.00		98.03
CS-7b	Pyrite	53.31	45.15	0.01	0.08	0.00	0.00	0.01		98.77
CS-15a	Galena	12.20	0.08	0.00	0.00	0.00	88.18	0.00		100.54
CS-15a	Galena	12.62	0.05	0.03	0.00	0.04	87.68	0.00		100.47
CS-14b	Galena	13.57	0.05	0.01	0.00	0.03	86.41	0.16		101.36
CS-14b	Galena	13.64	0.03	0.01	0.03	0.03	86.68	0.26		101.51
CS-15a	Galena	13.66	0.04	0.05	0.00	0.02	87.76	0.00		102.28
CS-15a	Galena	14.96	0.43	1.09	0.00	0.00	83.58	0.33		102.86
CS-15a	Galena	12.74	0.00	0.01	0.01	0.00	82.72	0.00		96.11

Table B4: Chemical compositions (wt%) of sulfide minerals at the Kianna deposit

Sample No.	Mineral ID	S	Fe	Ni	As	Cu	Pb	Se	U	Total
CS-15a	Galena	13.30	0.02	0.00	0.02	0.01	87.37	0.54		102.08
CS-15a	Galena	12.93	0.03	0.00	0.01	0.00	86.82	1.35		101.80
CS-15a	Galena	13.44	0.02	0.00	0.02	0.00	87.61	0.28		102.06
CS-15a	Galena	10.61	0.00	0.02	0.01	0.00	74.86	0.06		86.29
CS-15a	Galena	13.67	0.03	0.00	0.05	0.00	87.33	0.00		101.82
CS-7b	Gersdorffite	15.50	0.16	31.80	50.06	0.02	0.00	0.27		99.79
CS-7b	Gersdorffite	14.50	0.35	29.97	51.24	0.05	0.04	0.28		99.53
CS-7b	Gersdorffite	15.44	0.23	32.60	50.67	0.00	0.05	0.27		100.84
CS-7b	Gersdorffite	17.28	0.17	32.37	47.29	0.13	0.21	0.49		99.10
CS-7b	Gersdorffite	14.53	0.54	28.27	51.28	0.15	0.08	0.27		99.42
CS-7b	Gersdorffite	14.48	0.35	29.78	49.50	0.79	0.17	0.46		100.54
CS-7b	Gersdorffite	14.11	0.22	30.16	50.63	0.13	0.12	0.40		98.67
CS-7c	Gersdorffite	15.21	0.29	32.69	49.01	0.00	0.00	0.45		98.43
CS-7c	Gersdorffite	15.44	0.27	31.86	48.45	0.00	0.08	0.30		97.72
CS-7c	Gersdorffite	16.06	0.26	32.79	47.30	0.00	0.00	0.32		97.27
CS-7c	Gersdorffite	16.72	0.28	31.06	48.82	0.02	0.09	0.41		98.16
CS-7c	Gersdorffite	15.99	0.32	31.57	47.61	0.08	0.04	0.44		98.27
CS-7c	Gersdorffite	16.15	0.40	32.72	47.66	0.00	0.00	0.48		98.12
CS-7c	Gersdorffite	10.55	0.47	20.07	30.94	0.39	1.57	0.30		68.08
CS-7b	Gersdorffite	15.60	0.26	29.73	49.40	0.51	0.00	0.41		99.78
CS-7b	Gersdorffite	14.65	0.66	25.22	50.25	0.28	0.00	0.28		96.99
CS-7b	Gersdorffite	15.24	0.32	29.74	49.86	0.20	0.00	0.35		98.79
CS-7b	Gersdorffite	17.20	0.16	32.23	48.20	0.00	0.00	0.31		98.79
CS-7b	Gersdorffite	16.17	0.41	28.88	48.63	0.09	0.00	0.34		97.25
CS-7b	Gersdorffite	17.50	1.08	25.81	48.20	0.11	0.00	0.29		99.44
CS-7b	Gersdorffite	15.53	0.34	29.65	49.32	0.24	0.00	0.41		98.63
CS-7b	Gersdorffite	16.74	0.08	33.05	48.12	0.00	0.00	0.60		99.68

Table B4: Chemical compositions (wt%) of sulfide minerals at the Kianna deposit

Sample No.	Mineral ID	S	Fe	Ni	As	Cu	Pb	Se	U	Total
CS-7b	Gersdorffite	16.71	0.12	33.24	47.92	0.00	0.00	0.34		99.38
CS-7b	Gersdorffite	14.76	0.37	31.09	51.70	0.00	0.00	0.24		100.10
CS-7b	Gersdorffite	14.32	0.44	26.85	48.17	0.61	0.00	0.41		95.19
CS-7b	Gersdorffite	16.97	0.22	29.75	47.76	0.07	0.00	0.20		96.74
CS-7b	Gersdorffite	16.79	0.22	31.89	44.84	0.14	0.00	0.42		95.51
CS-7b	Gersdorffite	17.07	0.44	31.91	48.37	0.00	0.00	0.41		99.05
CS-7b	Gersdorffite	13.30	0.20	30.53	53.52	0.00	0.04	0.27		100.04
CS-7b	Gersdorffite	15.84	0.09	32.81	49.41	0.01	0.01	0.30		99.64
CS-7c	Fe-Gersdorffite	18.87	11.55	21.19	44.32	0.01	0.11	0.14		97.97
CS-7c	Fe-Gersdorffite	18.04	8.54	22.62	45.84	0.00	0.06	0.41		99.01
CS-7c	Fe-Gersdorffite	17.22	7.71	24.58	46.87	0.00	0.01	0.27		98.77
CS-7c	Fe-Gersdorffite	17.49	7.97	24.39	46.53	0.00	0.00	0.28		98.77
CS-7c	Fe-Gersdorffite	17.48	9.13	22.82	46.54	0.00	0.04	0.26		98.80
CS-7c	Fe-Gersdorffite	19.08	7.90	23.30	45.02	0.04	0.00	0.14		96.89
CS-7c	Fe-Gersdorffite	17.03	4.54	21.96	41.31	0.29	0.38	0.15		88.08
CS-7b	Fe-Gersdorffite	51.37	36.65	5.69	1.70	0.47	0.00	0.05		97.81
CS-7b	Fe-Gersdorffite	18.16	8.69	22.73	46.55	0.09	0.01	0.31		99.66
CS-7b	Fe-Gersdorffite	18.91	10.45	22.44	45.51	0.00	0.02	0.26		99.05
CS-7b	Fe-Gersdorffite	18.33	4.41	26.86	44.67	0.02	0.00	0.31		97.46
CS-7b	Fe-Gersdorffite	17.34	4.75	25.72	44.57	0.29	0.00	0.30		96.11
CS-7b	Fe-Gersdorffite	18.73	8.38	23.99	46.01	0.08	0.00	0.16		99.48
CS-7b	Fe-Gersdorffite	14.25	5.38	20.74	35.59	0.08	0.00	0.23		79.34
CS-7b	Fe-Gersdorffite	19.08	6.70	23.87	46.75	0.00	0.00	0.26		98.81
CS-7b	Fe-Gersdorffite	18.55	8.43	23.28	46.13	0.06	0.00	0.24		99.68
CS-7b	Fe-Gersdorffite	19.35	9.51	21.87	45.47	0.00	0.00	0.15		99.25

Table B4: Chemical compositions (wt%) of sulfide minerals at the Kianna deposit

Sample No.	Mineral ID	S	Fe	Ni	As	Cu	Pb	Se	U	Total
CS-20b2	Chalcopyrite	35.03	29.29	0.00	0.05	33.63	0.00	0.10		98.18
CS-20b2	Chalcopyrite	34.83	29.59	0.00	0.05	34.13	0.00	0.07		98.84
CS-20b2	Chalcopyrite	34.88	29.78	0.00	0.05	34.17	0.00	0.02		99.05
CS-20b2	Chalcopyrite	34.64	29.74	0.01	0.05	34.43	0.00	0.06		99.00
CS-20b2	Chalcopyrite	33.46	29.85	0.00	0.03	33.39	0.00	0.01		96.88
CS-20b2	Chalcopyrite	34.14	28.56	0.00	0.12	34.87	0.00	0.01		98.07
CS-20b2	Chalcopyrite	26.50	17.76	0.02	0.00	54.07	0.00	0.03		98.91
CS-20b2	Chalcopyrite	16.06	33.77	0.00	0.00	35.70	0.00	0.04		86.02
CS-20b2	Chalcopyrite	30.22	32.84	0.01	0.06	31.54	0.00	0.02		94.86
CS-17	Chalcopyrite	34.64	30.22	0.00	0.08	34.57	0.00	0.03		99.84
CS-17	Chalcopyrite	34.96	30.15	0.00	0.03	34.39	0.00	0.00		99.70
CS-17	Chalcopyrite	35.09	30.16	0.02	0.04	34.38	0.00	0.00		99.82
CS-17	Chalcopyrite	35.28	30.11	0.00	0.02	34.41	0.00	0.03		100.01
CS-17	Chalcopyrite	35.03	29.86	0.00	0.07	34.56	0.00	0.03		99.65
CS-17	Chalcopyrite	34.91	30.11	0.01	0.05	34.41	0.00	0.05		99.75
CS-17	Chalcopyrite	34.75	29.79	0.00	0.11	33.71	0.00	0.00		98.41
CS-17	Chalcopyrite	35.19	30.07	0.01	0.06	34.09	0.00	0.01		99.45
CS-17	Chalcopyrite	34.69	29.96	0.04	0.20	33.85	0.00	0.00		98.83
CS-17	Chalcopyrite	34.48	29.77	0.00	0.06	33.88	0.00	0.00		98.33
CS-17	Chalcopyrite	34.80	29.95	0.00	0.07	34.32	0.00	0.03		99.36
CS-17	Chalcopyrite	34.74	29.59	0.02	0.06	33.94	0.00	0.02		98.48
CS-17	Chalcopyrite	34.97	30.05	0.00	0.09	34.33	0.00	0.00		99.53
CS-17	Chalcopyrite	34.92	29.79	0.00	0.05	34.19	0.00	0.00		99.10
CS-17	Chalcopyrite	53.59	44.17	0.34	0.17	1.96	0.00	0.00		100.37
CS-17	Chalcopyrite	35.08	29.98	0.00	0.03	34.70	0.00	0.02		99.96
CS-17	Chalcopyrite	35.12	29.88	0.01	0.01	34.66	0.00	0.00		99.83

Table B4: Chemical compositions (wt%) of sulfide minerals and clausthalite at the Kianna deposit

Sample No.	Mineral ID	S	Fe	Ni	As	Cu	Pb	Se	U	Total
CS-17	Chalcopyrite	35.11	29.76	0.04	0.09	34.04	0.00	0.00		99.23
CS-17	Chalcopyrite	36.39	31.01	0.00	0.02	30.32	0.00	0.00		97.83
CS-17	Chalcopyrite	34.70	29.72	0.03	0.43	34.11	0.00	0.01		99.17
CS-17	Chalcopyrite	34.73	29.61	0.02	0.14	33.94	0.00	0.01		98.56
CS-17	Chalcopyrite	34.79	29.55	0.03	0.00	33.08	0.00	0.00		97.56
CS-17	Chalcopyrite	33.41	29.22	0.03	0.32	31.31	0.00	0.02		94.36
CS-17	Chalcopyrite	34.63	29.41	0.05	0.07	33.07	0.00	0.06		97.47
CS-17	Chalcopyrite	35.04	28.77	0.00	0.01	33.75	0.00	0.00		97.73
CS-17	Chalcopyrite	34.48	29.02	0.02	0.05	33.53	0.00	0.00		97.28
CS-4b	Chalcopyrite	33.86	30.32	0.03	0.03	33.77	0.00	0.32		98.49
CS-22a2	Clausthalite	1.13	0.00	0.02	0.21	0.02	46.69	13.65		77.39
CS-22a2	Clausthalite	0.09	0.06	0.00	0.00	0.01	44.40	23.41		93.52
CS-7b	Ni alteration of Py	52.37	38.27	5.36	1.34	0.09	0.00	0.03		99.64
CS-7c	U-As-Ni alteration of Py	3.35	1.10	6.29	11.26	3.86	1.81	0.13	36.89	92.29
CS-7c	U-As-Ni alteration of Py	2.79	0.55	6.22	9.71	4.53	5.63	0.20	34.43	91.01
CS-7c	U-As-Ni alteration of Py	1.18	0.66	3.19	5.55	1.48	2.41	0.03	43.73	83.57
CS-7c	U-As-Ni alteration of Py	0.04	0.25	0.38	0.32	0.08	0.19	0.01	59.51	86.51
CS-7c	U-As-Ni alteration of Py	0.27	0.26	1.65	2.35	0.15	1.32	0.15	49.74	83.47

Table B5: Chemical compositions (wt%) and calculated Si and K atoms per formula unit (apfu) of muscovite, coarse-grained illite, and fine-grained illite

Mineral	SiO_2	K_2O	Al_2O_3	CaO	FeO	MgO	Si apfu	K apfu
Muscovite	45.94	11.28	35.73	0.00	0.99	0.31	3.08	0.97
Muscovite	45.94	11.19	35.98	0.01	0.99	0.34	3.07	0.95
Muscovite	45.26	11.19	35.32	0.00	1.04	0.25	3.08	0.97
Muscovite	45.41	11.37	34.04	0.00	1.58	0.73	3.10	0.99
Muscovite	45.25	11.19	34.71	0.00	1.31	0.36	3.07	0.97
Muscovite	45.64	11.12	35.33	0.00	1.28	0.54	3.07	0.96
Muscovite	45.59	11.18	34.55	0.00	1.29	0.57	3.09	0.97
Muscovite	45.67	11.11	34.49	0.01	1.64	0.36	3.11	0.96
Muscovite	45.35	11.22	35.39	0.00	1.11	0.23	3.08	0.97
Muscovite	45.75	11.24	35.82	0.01	1.03	0.35	3.07	0.96
Muscovite	45.95	11.31	35.35	0.00	1.08	0.52	3.09	0.97
Muscovite	45.83	11.28	35.42	0.00	1.16	0.49	3.08	0.97
Muscovite	46.14	11.43	35.25	0.00	1.24	0.51	3.09	0.98
Muscovite	45.91	11.38	35.21	0.02	1.29	0.60	3.07	0.97
Muscovite	45.63	11.26	34.60	0.00	1.56	0.77	3.09	0.97
Muscovite	46.11	11.40	34.83	0.00	1.57	0.57	3.10	0.98
Muscovite	45.35	11.19	35.26	0.00	1.03	0.49	3.07	0.97
Muscovite	45.94	11.20	34.54	0.01	1.52	0.68	3.10	0.96
Muscovite	45.52	11.20	35.09	0.00	1.54	0.64	3.07	0.96
Muscovite	45.94	11.29	34.63	0.00	1.50	0.79	3.08	0.97
Muscovite	46.02	11.49	35.27	0.00	1.22	0.57	3.08	0.98
Muscovite	46.11	11.10	35.48	0.01	1.15	0.52	3.09	0.95
Muscovite	46.05	11.30	35.46	0.00	1.18	0.67	3.07	0.96
Muscovite	46.09	11.50	35.01	0.01	1.00	0.67	3.09	0.98
Muscovite	47.15	11.11	33.41	0.09	1.10	1.04	3.17	0.95
Muscovite	48.93	10.49	31.67	0.06	1.12	1.59	3.28	0.90
Muscovite	48.04	9.66	31.26	0.21	0.90	1.51	3.28	0.84
Muscovite	47.50	11.34	34.54	0.00	0.98	0.94	3.15	0.96
Muscovite	45.78	10.82	35.14	0.01	1.29	0.56	3.08	0.93
Muscovite	46.26	10.92	34.94	0.00	1.33	0.68	3.10	0.93
Muscovite	46.61	10.95	35.71	0.00	1.15	0.54	3.10	0.93
Muscovite	45.43	11.29	34.51	0.02	1.52	0.63	3.08	0.98
Muscovite	46.07	11.17	35.04	0.00	1.57	0.74	3.08	0.95
Muscovite	46.36	11.26	34.87	0.00	1.21	0.61	3.10	0.96

Table B5: Chemical compositions (wt%) and calculated Si and K atoms per formula unit (apfu) of muscovite, coarse-grained illite, and fine-grained illite

Mineral	SiO_2	K_2O	Al_2O_3	CaO	FeO	MgO	Si apfu	K apfu
Muscovite	45.64	11.33	34.84	0.04	1.15	0.52	3.08	0.98
Muscovite	46.21	11.01	35.52	0.00	1.59	0.73	3.08	0.94
Muscovite	45.61	10.95	34.87	0.01	1.44	0.59	3.08	0.94
Muscovite	45.93	11.23	31.62	0.02	2.68	1.38	3.17	0.99
Muscovite	45.27	11.23	31.91	0.02	1.69	1.47	3.15	1.00
Muscovite	44.12	11.24	32.99	0.00	2.38	1.35	3.07	1.00
Muscovite	44.14	11.19	32.54	0.01	2.40	1.43	3.09	1.00
Muscovite	45.30	11.26	32.21	0.03	1.62	1.35	3.15	1.00
Muscovite	43.43	11.30	32.75	0.00	2.34	1.42	3.05	1.01
Muscovite	44.81	11.44	31.22	0.00	2.31	1.26	3.16	1.03
Muscovite	42.93	11.31	32.21	0.00	2.52	1.48	3.05	1.03
Muscovite	44.42	11.38	32.34	0.01	1.50	1.32	3.12	1.02
Muscovite	44.21	11.12	31.62	0.01	1.64	1.44	3.13	1.01
Muscovite	43.07	10.55	29.73	0.03	1.88	1.36	3.17	0.99
Muscovite	43.41	11.17	35.41	0.01	0.91	0.29	3.02	0.99
Muscovite	44.91	11.32	31.54	0.00	1.69	1.73	3.15	1.01
Muscovite	45.19	11.37	30.24	0.02	1.83	1.96	3.19	1.02
Muscovite	44.60	11.35	30.55	0.00	2.16	1.81	3.16	1.03
Muscovite	43.65	11.09	32.53	0.02	1.74	1.06	3.10	1.00
Muscovite	44.59	10.98	34.57	0.04	0.25	0.49	3.10	0.97
Muscovite	42.99	11.24	35.56	0.02	0.34	0.28	3.01	1.00
Muscovite	43.89	11.14	34.87	0.03	0.30	0.40	3.06	0.99
Muscovite	44.31	11.12	34.95	0.03	0.56	0.36	3.07	0.98
Muscovite	44.66	10.74	33.46	0.03	0.49	0.85	3.13	0.96
Muscovite	42.34	11.09	34.73	0.01	0.33	0.36	3.02	1.01
Muscovite	42.14	10.92	33.52	0.04	0.76	0.67	3.04	1.00
Muscovite	40.86	11.03	34.36	0.02	0.41	0.30	2.98	1.03
Muscovite	43.03	9.84	27.74	0.16	1.16	1.95	3.24	0.95
Muscovite	42.76	10.04	31.57	0.08	0.63	0.78	3.14	0.94
Muscovite	42.49	10.98	29.26	0.02	2.22	1.87	3.15	1.04
Muscovite	42.42	10.92	29.63	0.04	1.99	1.70	3.14	1.03
Muscovite	47.11	11.27	31.82	0.01	2.12	1.67	3.19	0.97
Muscovite	47.85	11.34	31.97	0.01	1.69	1.64	3.22	0.97
Muscovite	47.06	11.27	31.65	0.02	1.80	2.08	3.19	0.98

Table B5: Chemical compositions (wt%) and calculated Si and K atoms per formula unit (apfu) of muscovite, coarse-grained illite, and fine-grained illite

Mineral	SiO_2	K_2O	Al_2O_3	CaO	FeO	MgO	Si apfu	K apfu
Muscovite	47.63	11.33	32.15	0.03	1.58	1.77	3.20	0.97
Muscovite	47.87	11.22	32.74	0.00	1.77	1.35	3.20	0.96
Muscovite	48.47	11.32	32.16	0.01	1.62	1.82	3.23	0.96
Muscovite	47.54	11.04	32.30	0.02	1.63	1.76	3.20	0.95
Muscovite	46.57	10.46	36.58	0.01	0.44	0.19	3.10	0.89
Muscovite	47.36	11.24	34.48	0.03	1.12	0.92	3.15	0.95
Muscovite	48.35	10.37	34.13	0.04	0.65	0.77	3.21	0.88
Muscovite	47.60	11.25	33.57	0.02	1.28	0.98	3.18	0.96
Muscovite	48.02	11.33	32.05	0.01	1.35	1.67	3.23	0.97
Muscovite	47.91	11.14	32.28	0.01	1.75	1.71	3.21	0.95
Muscovite	48.52	11.32	32.04	0.00	1.50	1.77	3.24	0.96
Muscovite	47.54	11.30	32.06	0.00	2.42	1.84	3.19	0.97
Muscovite	47.19	11.20	33.49	0.00	2.09	0.76	3.17	0.96
Muscovite	47.33	10.72	33.74	0.00	2.35	0.27	3.18	0.92
Muscovite	47.16	10.45	34.40	0.01	1.00	0.97	3.15	0.89
Muscovite	47.70	10.75	33.92	0.00	1.05	1.13	3.17	0.91
Muscovite	46.21	10.95	35.35	0.01	1.83	0.17	3.10	0.94
Muscovite	45.84	11.08	35.86	0.01	1.58	0.07	3.08	0.95
Muscovite	46.34	11.15	34.75	0.01	1.88	0.25	3.12	0.96
Muscovite	47.53	11.09	32.36	0.05	1.57	1.76	3.20	0.95
Muscovite	47.73	11.13	32.26	0.02	1.88	1.26	3.22	0.96
Muscovite	46.88	11.16	33.63	0.04	1.62	1.14	3.15	0.96
Muscovite	48.29	11.21	32.91	0.03	1.50	1.47	3.20	0.95
Muscovite	48.21	10.89	32.32	0.06	1.81	1.54	3.21	0.93
Muscovite	47.67	10.68	34.85	0.03	0.94	0.70	3.16	0.90
Muscovite	47.93	10.74	32.17	0.05	1.62	1.41	3.22	0.92
Muscovite	47.39	10.55	34.78	0.06	1.04	0.60	3.15	0.90
Muscovite	48.26	11.30	31.57	0.01	1.90	1.90	3.23	0.97
Muscovite	48.04	10.67	32.33	0.07	1.54	1.46	3.22	0.91
Muscovite	47.95	10.84	33.76	0.01	1.48	0.88	3.19	0.92
Muscovite	48.24	10.81	33.51	0.02	1.34	0.94	3.21	0.92
Muscovite	47.83	11.16	33.66	0.01	1.52	1.08	3.18	0.95
Muscovite	46.94	11.27	35.19	0.02	1.01	0.77	3.12	0.96

Table B5: Chemical compositions (wt%) and calculated Si and K atoms per formula unit (apfu) of muscovite, coarse-grained illite, and fine-grained illite

Mineral	SiO_2	K_2O	Al_2O_3	CaO	FeO	MgO	Si apfu	K apfu
Coarse Illite	45.39	9.48	35.21	0.70	0.86	0.61	3.08	0.82
Coarse Illite	47.99	8.03	30.16	0.68	1.90	2.28	3.29	0.70
Coarse Illite	44.40	9.21	27.57	0.23	1.36	2.10	3.29	0.87
Coarse Illite	48.84	9.72	31.53	0.11	1.48	1.88	3.28	0.83
Coarse Illite	49.29	8.02	26.34	0.33	3.13	4.07	3.40	0.71
Coarse Illite	43.45	6.47	30.18	0.22	3.36	6.83	3.03	0.58
Coarse Illite	47.51	9.03	31.73	0.21	1.34	2.37	3.22	0.78
Coarse Illite	46.51	8.43	30.85	0.17	1.94	3.13	3.21	0.74
Coarse Illite	48.16	9.15	30.93	0.21	1.39	2.21	3.27	0.79
Coarse Illite	48.59	8.22	29.56	0.32	2.08	2.40	3.33	0.72
Coarse Illite	44.52	8.92	26.94	0.33	1.31	2.52	3.31	0.85
Coarse Illite	43.43	8.69	25.35	0.41	1.36	2.66	3.34	0.85
Coarse Illite	44.51	9.17	27.08	0.27	1.28	2.33	3.31	0.87
Coarse Illite	48.23	9.84	32.01	0.07	0.83	1.22	3.27	0.85
Coarse Illite	47.20	8.87	31.22	0.23	1.29	1.10	3.28	0.79
Coarse Illite	47.66	8.48	34.63	0.05	0.57	0.77	3.20	0.73
Coarse Illite	51.07	8.29	30.53	0.06	0.38	1.90	3.41	0.71
Coarse Illite	46.91	7.99	31.18	1.04	1.76	2.05	3.22	0.70
Coarse Illite	46.92	7.04	26.10	0.40	3.66	5.78	3.29	0.63
Coarse Illite	48.95	7.78	26.38	0.33	3.23	4.35	3.38	0.69
Coarse Illite	43.45	6.47	30.18	0.22	3.36	6.83	3.03	0.58
Fine Illite	49.23	5.51	32.21	0.06	3.22	2.32	3.28	0.47
Fine Illite	48.68	5.29	37.87	0.00	1.54	0.70	3.15	0.44
Fine Illite	48.06	5.96	34.33	0.01	2.55	1.33	3.21	0.51
Fine Illite	47.07	5.24	32.45	0.07	3.40	2.79	3.20	0.45
Fine Illite	46.67	6.85	34.66	0.00	2.21	1.11	3.16	0.59
Fine Illite	46.61	7.34	35.31	0.02	2.01	0.93	3.14	0.63
Fine Illite	45.78	7.97	37.00	0.02	1.09	0.49	3.08	0.68
Fine Illite	47.19	7.10	35.04	0.01	2.43	1.38	3.15	0.60

Table B6: Chemical compositions (wt%) and calculated chemical-Pb ages (Ma) for six generations of uraninite

Stage	SiO_2	CaO	U	Pb	Th	Chemical Pb Age (Ma)	SiO_2 + CaO
U1	0.25	1.57	71.28	10.27	0.03	1088	1.8
U1	0.39	1.43	71.68	10.30	0.00	1085	1.8
U1	0.42	1.63	71.98	10.91	0.02	1144	2.1
U1	0.11	1.23	69.96	11.40	0.02	1230	1.3
U1	0.44	1.41	72.17	11.02	0.03	1153	1.9
U1	0.20	1.49	71.86	10.14	0.00	1065	1.7
U1	0.21	0.89	71.02	12.41	0.17	1318	1.1
U1	0.27	0.96	70.89	13.21	0.11	1406	1.2
U1	0.36	2.11	71.84	10.64	0.00	1118	2.5
U1	0.29	1.06	71.06	12.74	0.00	1354	1.4
U1	0.11	0.88	71.84	12.60	0.17	1323	1.0
U1	0.73	0.56	71.16	12.84	0.01	1362	1.3
U1	0.16	1.31	72.32	10.24	0.02	1069	1.5
U1	0.43	1.31	72.21	11.09	0.02	1159	1.7
U1	0.12	1.38	71.91	12.12	0.01	1272	1.5
U1	0.09	1.58	70.77	11.73	0.00	1251	1.7
U1	0.43	0.83	72.91	12.17	0.04	1260	1.3
U1	0.04	1.27	70.05	13.43	0.00	1447	1.3
U1	0.29	1.62	71.88	10.03	0.00	1054	1.9
U1	0.12	0.90	70.45	13.09	0.00	1403	1.0
U1	0.34	1.67	71.05	10.95	0.00	1164	2.0
U1	0.33	1.40	70.76	10.23	0.02	1091	1.7
U1	0.29	1.58	72.51	10.15	0.02	1057	1.9
U1	0.20	1.73	70.77	11.95	0.00	1275	1.9
U1	0.11	0.75	70.34	13.04	0.07	1399	0.9
U1	0.19	1.43	69.69	13.23	0.02	1433	1.6
U1	0.10	1.03	71.81	12.99	0.02	1366	1.1
U1	0.29	1.65	71.12	11.68	0.03	1240	1.9
U1	0.14	1.42	70.51	11.54	0.04	1235	1.6
U1	0.21	1.35	68.73	11.37	0.05	1249	1.6
U1	0.40	1.71	70.92	10.15	0.02	1080	2.1
U1	0.07	1.22	69.10	12.68	0.07	1385	1.3
U1	0.06	1.35	68.68	13.46	0.02	1480	1.4

Table B6: Chemical compositions (wt%) and calculated chemical-Pb ages (Ma) for six generations of uraninite

Stage	SiO_2	CaO	U	Pb	Th	Chemical Pb Age (Ma)	SiO_2 + CaO
U1	0.20	1.37	69.89	11.13	0.09	1202	1.6
U1	0.22	1.52	70.25	10.88	0.07	1169	1.7
U1	0.10	1.40	69.68	11.83	0.08	1281	1.5
U1	0.11	0.90	70.75	12.66	0.04	1351	1.0
U1	0.33	1.24	69.54	12.18	0.00	1322	1.6
U1	0.43	1.55	69.41	11.56	0.04	1257	2.0
U1	0.57	1.80	69.84	10.75	0.04	1162	2.4
U1	0.25	1.59	69.13	12.65	0.07	1381	1.8
U1	0.29	1.64	70.54	10.41	0.04	1114	1.9
U1	0.31	1.15	71.44	10.03	0.00	1060	1.5
U1	0.53	1.85	71.69	10.12	0.00	1066	2.4
U1	0.33	1.41	69.30	11.28	0.00	1229	1.7
U1	0.26	1.03	70.99	11.11	0.00	1182	1.3
U1	0.15	1.04	70.24	11.67	0.02	1254	1.2
U1	0.57	1.35	70.86	10.44	0.03	1112	1.9
U1	0.53	1.23	70.99	10.89	0.04	1158	1.8
U1	0.51	1.36	69.66	10.38	0.05	1125	1.9
U1	0.36	1.23	70.60	10.04	0.06	1073	1.6
U1	0.14	1.15	71.72	10.89	0.00	1146	1.3
U1	0.23	0.86	70.63	12.43	0.00	1329	1.1
U1	0.37	1.00	70.10	12.98	0.00	1398	1.4
U1	0.44	1.12	71.71	10.88	0.01	1145	1.6
U1	0.25	0.75	67.15	12.40	0.00	1394	1.0
U1	0.34	0.77	68.58	13.31	0.04	1465	1.1
U1	0.49	1.10	70.56	11.05	0.01	1182	1.6
U1	0.55	1.21	70.70	11.36	0.06	1213	1.8
U1	0.43	1.12	70.28	11.72	0.06	1259	1.6
U1	0.73	1.77	69.23	11.13	0.03	1214	2.5
U1	0.48	1.05	70.97	11.58	0.00	1232	1.5
U1	0.51	1.22	70.91	11.49	0.06	1223	1.7
U1	0.44	1.05	70.92	11.12	0.04	1184	1.5
U1	0.53	1.25	69.94	10.95	0.03	1182	1.8
U1	0.63	1.39	70.73	10.66	0.08	1137	2.0

Table B6: Chemical compositions (wt%) and calculated chemical-Pb ages (Ma) for six generations of uraninite

Stage	SiO_2	CaO	U	Pb	Th	Chemical Pb Age (Ma)	SiO_2 + CaO
U1	0.74	1.56	72.80	10.01	0.14	1037	2.3
U1	0.27	0.95	72.34	12.54	0.01	1309	1.2
U1	0.52	1.60	73.11	10.16	0.02	1049	2.1
U1	0.74	1.66	71.89	9.59	0.00	1007	2.4
U1	0.43	0.51	72.74	11.47	0.29	1189	0.9
U1	0.20	0.91	71.58	13.35	0.44	1405	1.1
U1	0.34	0.71	72.14	12.69	0.49	1325	1.1
U1	0.41	0.92	74.33	11.56	0.53	1171	1.3
U1	0.35	0.87	73.22	11.47	0.50	1180	1.2
U1	0.41	1.26	73.90	10.78	0.46	1099	1.7
U1	0.12	1.31	69.92	12.68	0.12	1368	1.4
U2	0.37	0.99	74.00	11.77	0.06	1201	1.4
U2	0.30	0.91	73.54	12.27	0.08	1259	1.2
U2	0.43	1.37	74.85	10.19	0.07	1028	1.8
U2	0.26	0.92	73.78	12.19	0.02	1247	1.2
U2	0.39	1.38	73.74	10.73	0.04	1098	1.8
U2	0.53	1.21	73.45	11.64	0.09	1196	1.7
U2	0.31	1.13	73.48	11.90	0.03	1223	1.4
U2	0.35	1.35	72.43	11.94	0.00	1245	1.7
U2	0.40	1.03	72.89	12.04	0.00	1247	1.4
U2	0.30	1.21	72.92	12.18	0.04	1261	1.5
U2	0.33	0.95	74.82	11.98	0.01	1209	1.3
U2	0.59	0.95	74.73	10.13	0.00	1023	1.5
U2	0.37	1.30	73.90	11.96	0.01	1222	1.7
U2	0.31	1.04	73.67	12.66	0.00	1297	1.4
U2	0.29	1.12	73.87	11.61	0.01	1187	1.4
U2	0.47	1.64	74.14	10.34	0.00	1053	2.1
U2	0.25	0.93	73.94	11.80	0.03	1205	1.2
U2	0.28	1.36	75.01	11.02	0.00	1109	1.6
U2	0.25	1.20	73.03	11.45	0.00	1184	1.5
U2	0.24	1.19	75.90	10.64	0.03	1058	1.4
U2	0.21	1.29	73.93	11.43	0.02	1167	1.5
U2	0.49	1.01	74.23	10.42	0.00	1060	1.5
U2	0.39	1.87	73.89	10.59	0.00	1082	2.3

Table B6: Chemical compositions (wt%) and calculated chemical-Pb ages (Ma) for six generations of uraninite

Stage	SiO_2	CaO	U	Pb	Th	Chemical Pb Age (Ma)	SiO_2 + CaO
U2	0.41	1.22	75.52	10.73	0.03	1073	1.6
U2	0.20	1.06	73.45	12.48	0.01	1283	1.3
U2	0.32	0.80	74.22	12.18	0.00	1239	1.1
U2	0.20	0.92	73.71	12.50	0.03	1280	1.1
U2	0.32	1.10	74.33	11.82	0.02	1200	1.4
U2	0.26	1.01	73.49	12.58	0.02	1292	1.3
U2	0.22	0.82	73.69	12.55	0.04	1286	1.0
U2	0.31	1.25	74.70	10.87	0.00	1099	1.6
U2	0.43	1.06	73.78	10.40	0.02	1064	1.5
U2	0.35	0.96	74.73	11.97	0.00	1209	1.3
U2	0.60	1.55	74.69	10.22	0.02	1033	2.2
U2	0.37	1.53	73.59	10.35	0.02	1062	1.9
U2	0.35	1.19	72.34	11.66	0.06	1217	1.5
U2	0.37	0.92	75.55	10.94	0.01	1093	1.3
U3	0.90	1.70	72.09	8.79	0.00	921	2.6
U3	0.70	2.11	71.75	8.51	0.02	895	2.8
U3	0.45	1.83	72.60	9.27	0.05	964	2.3
U3	0.56	1.76	71.90	9.05	0.01	950	2.3
U3	1.16	1.81	72.31	9.04	0.04	944	3.0
U3	0.58	1.66	73.21	8.93	0.00	921	2.2
U3	0.59	1.96	71.99	9.42	0.05	988	2.6
U3	0.45	1.92	71.81	9.18	0.00	965	2.4
U3	0.40	1.79	71.42	9.34	0.00	987	2.2
U3	0.47	1.85	73.19	8.63	0.03	890	2.3
U3	0.73	1.70	70.70	8.88	0.05	948	2.4
U3	0.43	1.66	71.55	9.20	0.01	971	2.1
U3	0.41	1.79	70.71	9.39	0.01	1003	2.2
U3	0.33	1.55	71.04	9.54	0.06	1014	1.9
U3	0.75	1.48	70.70	9.40	0.00	1004	2.2
U3	0.37	1.81	70.51	9.08	0.07	972	2.2
U3	0.54	2.01	71.42	8.58	0.06	907	2.6
U3	0.44	1.82	71.27	8.94	0.04	947	2.3
U3	0.63	2.18	70.31	8.71	0.04	935	2.8
U3	0.62	2.13	71.00	8.09	0.09	860	2.8

Table B6: Chemical compositions (wt%) and calculated chemical-Pb ages (Ma) for six generations of uraninite

Stage	SiO_2	CaO	U	Pb	Th	Chemical Pb Age (Ma)	SiO_2 + CaO
U3	0.73	2.34	73.19	8.34	0.06	860	3.1
U3	0.52	1.73	73.40	8.48	0.02	872	2.3
U3	0.35	1.39	73.78	8.90	0.00	911	1.7
U3	0.50	1.86	72.37	8.39	0.03	875	2.4
U3	0.61	1.88	73.56	8.76	0.00	899	2.5
U3	0.69	2.14	72.61	8.56	0.03	890	2.8
U3	0.51	1.76	74.39	8.60	0.00	873	2.3
U3	0.72	2.09	73.06	8.47	0.00	875	2.8
U3	0.48	1.35	68.79	9.41	0.07	1032	1.8
U3	0.61	2.10	72.98	8.92	0.02	923	2.7
U3	0.70	2.15	72.16	8.59	0.03	899	2.9
U3	0.53	1.78	74.00	8.50	0.01	867	2.3
U3	0.47	1.60	72.86	9.25	0.00	959	2.1
U3	0.86	2.61	72.38	8.88	0.00	926	3.5
U3	0.77	1.63	71.45	8.80	0.02	930	2.4
U3	0.53	1.27	71.68	9.92	0.10	1044	1.8
U3	1.02	1.93	72.74	7.06	0.01	733	3.0
U3	0.75	1.56	72.37	8.63	0.07	900	2.3
U3	0.67	2.15	71.99	9.88	0.00	1036	2.8
U3	0.23	1.63	72.93	9.18	0.00	950	1.9
U3	0.48	2.27	73.43	8.51	0.00	875	2.8
U3	0.40	1.72	74.39	8.73	0.00	886	2.1
U3	0.41	1.25	70.11	8.89	0.00	957	1.7
U3	0.70	2.23	75.12	8.06	0.01	810	2.9
U3	0.46	1.59	75.21	9.23	0.00	927	2.1
U3	0.59	2.04	74.45	9.16	0.02	929	2.6
U3	0.51	1.58	76.12	9.31	0.00	923	2.1
U3	0.20	1.30	76.06	10.03	0.04	995	1.5
U3	0.46	1.27	75.15	9.43	0.01	947	1.7
U3	0.71	1.79	74.33	9.97	0.01	1013	2.5
U3	0.54	1.62	74.07	9.80	0.03	999	2.2
U3	0.56	1.51	73.34	10.66	0.01	1097	2.1

Table B6: Chemical compositions (wt%) and calculated chemical-Pb ages (Ma) for six generations of uraninite

Stage	SiO_2	CaO	U	Pb	Th	Chemical Pb Age (Ma)	SiO_2 + CaO
U3	0.52	1.85	74.03	10.11	0.01	1031	2.4
U3	0.46	1.81	71.16	9.10	0.04	965	2.3
U3	0.58	2.16	71.99	8.54	0.06	895	2.7
U3	0.70	1.13	73.53	10.23	0.00	1050	1.8
U4	0.94	2.46	72.75	6.65	0.03	690	3.4
U4	0.84	2.41	73.57	6.84	0.00	702	3.3
U4	0.58	1.87	74.64	7.60	0.02	769	2.5
U4	1.20	2.71	74.57	4.85	0.00	491	3.9
U4	0.76	2.08	74.64	7.13	0.00	721	2.8
U4	0.81	2.41	72.09	6.05	0.03	634	3.2
U4	0.88	1.79	72.73	7.50	0.00	779	2.7
U4	0.54	1.91	71.73	7.74	0.02	815	2.5
U4	0.59	2.32	70.72	8.40	0.01	897	2.9
U4	0.88	1.61	74.13	5.85	0.00	596	2.5
U4	0.98	2.72	73.10	6.57	0.00	679	3.7
U4	0.58	2.05	72.81	8.20	0.00	850	2.6
U4	0.73	2.26	74.19	6.96	0.04	708	3.0
U4	1.06	2.21	75.54	4.85	0.00	485	3.3
U4	0.77	2.19	74.68	7.14	0.00	722	3.0
U4	0.95	2.32	75.48	5.85	0.03	585	3.3
U4	0.81	2.39	73.43	7.85	0.02	807	3.2
U4	0.73	2.35	74.21	7.21	0.02	733	3.1
U4	0.79	2.38	73.26	8.19	0.00	844	3.2
U4	0.72	2.05	73.53	7.77	0.02	798	2.8
U4	0.49	1.33	69.66	7.61	0.00	825	1.8
U4	0.66	2.19	72.65	7.49	0.04	778	2.9
U4	0.63	2.05	72.27	7.81	0.04	816	2.7
U4	0.88	2.36	74.11	7.31	0.01	745	3.2
U4	0.89	1.94	73.48	7.26	0.06	746	2.8
U5	0.43	2.06	76.74	5.20	0.00	512	2.5
U5	0.23	3.27	76.99	2.98	0.04	292	3.5
U5	0.51	2.62	77.25	5.00	0.00	489	3.1
U5	0.19	4.51	76.53	2.01	0.00	198	4.7
U5	0.40	2.24	76.50	5.09	0.00	502	2.6

Table B6: Chemical compositions (wt%) and calculated chemical-Pb ages (Ma) for six generations of uraninite

Stage	SiO_2	CaO	U	Pb	Th	Chemical Pb Age (Ma)	SiO_2 + CaO
U5	0.31	3.18	77.63	2.25	0.00	219	3.5
U5	0.34	3.63	77.93	2.54	0.01	246	4.0
U5	0.41	2.10	76.21	5.30	0.04	525	2.5
U5	0.29	3.17	78.20	2.08	0.00	201	3.5
U5	0.33	2.20	78.26	3.63	0.02	350	2.5
U5	0.12	2.23	76.71	5.42	0.00	533	2.4
U5	0.36	2.51	76.32	4.68	0.00	463	2.9
U5	0.26	2.06	76.37	4.82	0.00	477	2.3
U5	0.26	2.71	77.36	2.11	0.00	206	3.0
U5	0.61	2.62	75.73	4.21	0.00	420	3.2
U5	0.16	2.14	76.31	5.25	0.00	519	2.3
U5	0.73	4.20	75.25	3.17	0.02	318	4.9
U5	0.81	4.47	74.37	3.32	0.00	337	5.3
U5	0.67	4.20	74.30	3.26	0.00	331	4.9
U5	0.65	4.36	75.01	3.15	0.00	317	5.0
U5	0.63	4.52	74.55	3.04	0.00	308	5.2
U5	0.51	4.49	75.04	3.83	0.00	385	5.0
U5	0.52	4.68	74.59	3.94	0.00	399	5.2
U5	0.58	4.34	74.72	3.05	0.00	308	4.9
U5	0.66	4.46	74.84	2.77	0.00	279	5.1
U5	0.61	4.26	74.87	3.03	0.02	306	4.9
U5	0.44	4.62	75.17	3.78	0.04	380	5.1
U5	0.49	4.00	75.15	3.53	0.00	355	4.5
U5	0.75	4.27	74.76	3.03	0.00	306	5.0
U5	0.77	4.20	74.76	3.40	0.01	343	5.0
U5	0.34	2.31	76.53	3.83	0.00	378	2.7
U5	0.33	3.10	78.17	2.15	0.00	208	3.4
U5	0.42	2.34	77.21	4.87	0.00	476	2.8
U5	0.47	2.86	76.56	5.01	0.00	494	3.3
U5	0.36	3.29	75.97	4.96	0.01	493	3.7
U5	0.48	2.74	76.73	5.15	0.00	507	3.2
U5	0.40	2.58	77.09	5.40	0.00	529	3.0
U5	0.34	2.26	77.61	4.65	0.00	452	2.6

Table B6: Chemical compositions (wt%) and calculated chemical-Pb ages (Ma) for six generations of uraninite

Stage	SiO_2	CaO	U	Pb	Th	Chemical Pb Age (Ma)	SiO_2 + CaO
U5	0.20	3.11	77.68	3.60	0.02	350	3.3
U5	0.37	3.20	75.51	4.63	0.00	463	3.6
U5	0.39	2.41	76.61	5.15	0.00	508	2.8
U5	0.36	2.19	75.54	4.76	0.00	476	2.6
U5	0.25	3.18	77.78	2.18	0.00	212	3.4
U5	0.40	3.24	76.28	4.82	0.01	477	3.6
U5	0.35	3.29	76.69	4.51	0.00	444	3.6
U5	0.19	3.05	77.71	3.91	0.00	380	3.2
U5	0.42	3.14	76.06	5.01	0.02	497	3.6
U5	0.30	3.09	77.72	2.44	0.00	237	3.4
U5	0.77	1.93	77.30	3.23	0.00	315	2.7
U5	0.67	1.99	75.78	3.25	0.00	324	2.7
U5	0.74	1.85	77.42	3.03	0.00	295	2.6
U5	2.40	2.24	74.65	2.16	0.03	218	4.6
U5	0.67	1.88	72.03	2.57	0.00	269	2.6
U5	0.64	1.87	76.63	2.99	0.00	295	2.5
U5	0.63	1.70	76.42	3.16	0.04	312	2.3
U5	0.60	1.73	75.77	2.99	0.00	298	2.3
U5	0.63	2.04	76.96	3.24	0.00	318	2.7
U5	0.81	2.13	76.06	2.93	0.00	291	2.9
U5	0.71	1.74	76.57	2.63	0.00	259	2.5
U5	0.62	1.93	77.87	2.97	0.03	288	2.6
U5	0.62	4.70	74.64	3.38	0.02	342	5.3
U5	0.70	4.74	75.11	3.01	0.01	303	5.4
U5	1.12	4.81	72.04	2.61	0.04	273	5.9
U5	1.39	5.42	68.05	2.12	0.00	235	6.8
U5	0.81	1.79	76.61	3.58	0.00	353	2.6
U5	0.88	1.89	75.54	3.08	0.08	308	2.8
U5	0.68	2.31	76.41	2.83	0.00	280	3.0
U5	0.59	1.76	76.08	3.43	0.00	340	2.4
U5	0.72	1.60	76.54	2.94	0.04	290	2.3
U5	0.50	1.94	75.15	2.85	0.05	286	2.4
U5	0.78	1.65	74.14	3.96	0.04	403	2.4
U5	0.46	1.79	77.00	2.35	0.00	230	2.3

Table B6: Chemical compositions (wt%) and calculated chemical-Pb ages (Ma) for six generations of uraninite

Stage	SiO_2	CaO	U	Pb	Th	Chemical Pb Age (Ma)	SiO_2 + CaO
U5	0.51	1.99	75.34	3.61	0.07	362	2.5
U5	0.45	2.04	74.13	3.85	0.03	392	2.5
U5	0.59	1.62	76.64	2.79	0.00	275	2.2
U5	0.27	1.69	75.73	3.10	0.01	309	2.0
U5	0.49	1.77	75.71	2.98	0.00	297	2.3
U5	0.57	1.76	75.43	3.92	0.00	392	2.3
U5	0.62	1.69	73.74	4.13	0.03	423	2.3
U5	0.88	1.66	75.45	3.42	0.03	342	2.5
U5	0.64	1.41	76.22	3.39	0.08	336	2.1
U5	0.68	1.86	76.59	2.67	0.00	263	2.5
U5	0.62	1.62	75.26	3.12	0.04	313	2.2
U5	0.55	1.70	75.74	2.83	0.04	282	2.3
U5	0.69	1.91	76.69	3.19	0.03	314	2.6
U5	0.55	1.97	74.72	3.46	0.00	350	2.5
U5	4.03	1.51	69.43	2.54	0.00	276	5.5
U5	0.68	1.84	77.95	3.18	0.00	308	2.5
U5	0.68	1.88	76.69	3.13	0.00	308	2.6
U5	0.93	2.16	74.24	3.54	0.03	360	3.1
U5	0.61	2.01	76.11	3.30	0.00	327	2.6
U5	0.81	2.00	77.83	2.91	0.00	282	2.8
U6	4.30	2.64	71.70	0.23	0.00	24	6.9
U6	3.11	2.51	74.61	1.47	0.07	149	5.6
U6	0.37	1.87	78.00	1.59	0.00	154	2.2
U6	0.81	1.52	77.70	1.16	0.00	113	2.3
U6	0.36	1.24	78.96	1.60	0.00	153	1.6
U6	0.38	1.12	78.76	1.49	0.03	143	1.5
U6	0.36	1.07	79.21	1.48	0.03	141	1.4
U6	0.37	0.94	78.49	1.52	0.03	146	1.3
U6	0.32	0.86	79.52	1.44	0.00	137	1.2
U6	0.46	1.07	79.17	1.36	0.00	130	1.5
U6	0.46	1.06	78.98	1.53	0.00	146	1.5
U6	0.32	1.60	78.82	1.70	0.00	163	1.9
U6	0.58	2.99	76.73	1.97	0.01	194	3.6
U6	0.35	1.07	77.89	1.49	0.00	144	1.4

Table B6: Chemical compositions (wt%) and calculated chemical-Pb ages (Ma) for six generations of uraninite

Stage	SiO_2	CaO	U	Pb	Th	Chemical Pb Age (Ma)	SiO_2 + CaO
U6	0.36	2.81	77.28	1.40	0.00	137	3.2
U6	0.26	1.60	78.61	1.60	0.00	154	1.9
U6	1.12	2.38	74.06	1.07	0.00	109	3.5
U6	3.46	2.17	75.72	2.15	0.00	214	5.6
U6	0.23	2.86	77.11	1.49	0.00	146	3.1
U6	0.15	2.38	77.92	2.00	0.02	194	2.5
U6	0.17	2.39	78.34	1.60	0.00	154	2.6
U6	0.18	2.18	78.74	1.54	0.00	148	2.4
U6	0.17	2.62	77.67	1.91	0.03	186	2.8
U6	0.24	2.44	77.88	1.53	0.00	148	2.7
U6	0.18	2.59	79.31	1.48	0.00	141	2.8
U6	0.23	2.57	77.92	1.44	0.01	140	2.8
U6	0.18	2.73	77.47	2.11	0.00	206	2.9
U6	0.17	2.42	77.98	1.47	0.00	142	2.6
U6	0.18	2.25	77.86	1.60	0.00	155	2.4
U6	0.17	2.08	77.17	1.45	0.00	142	2.3
U6	0.16	2.15	78.42	1.64	0.00	158	2.3
U6	0.25	2.37	78.36	1.64	0.00	158	2.6
U6	0.25	2.74	77.00	1.43	0.03	140	3.0
U6	0.22	2.40	77.19	1.48	0.00	145	2.6
U6	0.20	2.59	77.11	1.46	0.00	143	2.8
U6	0.15	2.18	77.28	1.53	0.01	149	2.3
U6	0.32	2.60	77.23	1.37	0.00	134	2.9
U6	0.28	2.88	76.61	1.31	0.00	129	3.2
U6	0.32	2.98	76.18	1.40	0.02	139	3.3
U6	0.18	2.34	76.51	1.75	0.02	173	2.5
U6	0.17	2.30	76.18	1.71	0.01	169	2.5
U6	0.19	2.25	77.55	1.48	0.00	144	2.4
U6	0.21	2.34	77.07	1.97	0.00	193	2.6
U6	0.18	2.47	77.00	1.80	0.01	176	2.7
U6	0.18	2.43	77.91	1.84	0.07	178	2.6
U6	0.17	2.45	77.05	1.79	0.03	175	2.6
U6	0.17	2.46	76.06	1.86	0.01	185	2.6

Table B6: Chemical compositions (wt%) and calculated chemical-Pb ages (Ma) for six generations of uraninite

Stage	SiO_2	CaO	U	Pb	Th	Chemical Pb Age (Ma)	SiO_2 + CaO
U6	0.54	2.98	77.97	1.13	0.00	109	3.5
U6	0.21	2.34	76.88	1.60	0.00	157	2.6
U6	0.23	2.12	78.04	1.40	0.01	135	2.4
U6	0.25	2.28	79.26	1.58	0.02	150	2.5
U6	0.24	2.14	78.71	1.50	0.02	144	2.4
U6	0.21	2.24	79.01	1.62	0.00	155	2.5
U6	0.20	2.20	78.43	1.73	0.00	167	2.4
U6	0.19	2.56	79.10	1.85	0.00	177	2.8
U6	0.22	2.07	79.22	1.72	0.00	164	2.3
U6	0.18	2.73	77.42	1.91	0.00	186	2.9
U6	0.33	2.57	77.99	1.32	0.02	128	2.9
U6	0.21	2.23	78.06	1.52	0.00	147	2.4
U6	0.43	4.52	76.89	1.25	0.02	123	5.0
U6	0.61	4.29	77.39	1.23	0.00	120	4.9
U6	2.31	5.28	66.01	0.20	0.00	23	7.6
U6	2.68	5.18	66.25	0.28	0.00	32	7.9
U6	2.19	5.16	66.77	0.24	0.00	27	7.4
U6	2.37	5.25	66.72	0.21	0.01	24	7.6
U6	1.24	4.87	71.68	1.32	0.00	139	6.1
U6	1.68	6.42	69.89	0.51	0.00	55	8.1
U6	2.49	5.76	68.04	0.55	0.00	61	8.3
U6	3.13	6.13	67.31	0.54	0.00	61	9.3
U6	2.60	6.81	67.68	0.42	0.05	47	9.4
U6	1.40	6.70	69.59	0.47	0.06	51	8.1
U6	2.34	6.39	67.76	0.56	0.04	62	8.7
U6	1.89	6.66	69.73	0.49	0.00	53	8.6
U6	2.17	6.90	68.74	0.53	0.05	58	9.1
U6	2.01	6.68	68.85	0.54	0.00	59	8.7
U6	1.47	6.87	69.13	0.43	0.00	47	8.3
U6	2.83	6.49	66.36	0.45	0.03	51	9.3
U6	1.89	6.24	69.00	0.51	0.01	56	8.1
U6	1.74	3.51	73.31	0.79	0.00	81	5.3
U6	0.72	1.44	77.21	0.51	0.02	50	2.2
U6	1.73	2.78	74.04	0.71	0.06	72	4.5

Table B6: Chemical compositions (wt%) and calculated chemical-Pb ages (Ma) for six generations of uraninite

Stage	SiO_2	CaO	U	Pb	Th	Chemical Pb Age (Ma)	SiO_2 + CaO
U6	0.22	3.50	77.07	1.76	0.02	172	3.7
U6	1.07	4.93	74.28	0.90	0.00	91	6.0
U6	0.78	5.49	72.68	1.41	0.00	146	6.3
U6	0.50	4.16	76.38	0.79	0.00	78	4.7
U6	0.22	3.47	77.94	1.99	0.00	193	3.7
U6	0.72	3.10	76.77	0.52	0.00	51	3.8
U6	0.58	4.27	74.93	0.35	0.00	35	4.9
U6	3.38	2.29	70.41	0.41	0.01	44	5.7
U6	0.25	3.89	77.55	1.81	0.00	176	4.1
U6	0.47	3.92	74.80	0.32	0.00	32	4.4
U6	2.05	1.34	76.19	0.30	0.00	30	3.4
U6	0.60	3.38	76.26	0.74	0.00	73	4.0
U6	0.71	2.36	77.75	0.87	0.04	84	3.1
U6	0.39	3.61	75.93	1.28	0.01	127	4.0
U6	1.71	6.87	70.27	0.46	0.01	49	8.6
U6	2.29	6.91	67.50	0.46	0.00	51	9.2
U6	1.82	6.78	68.94	0.47	0.03	51	8.6
U6	1.72	7.21	69.01	0.51	0.05	56	8.9
U6	2.32	6.94	67.51	0.47	0.00	53	9.3
U6	2.07	7.24	69.41	0.44	0.00	48	9.3
U6	1.21	6.64	71.42	0.54	0.02	57	7.9
U6	1.88	7.17	67.98	0.47	0.00	52	9.1
U6	1.07	5.69	70.66	0.60	0.00	64	6.8
U6	0.99	6.03	71.00	0.43	0.00	46	7.0
U6	1.01	5.63	70.74	0.58	0.01	62	6.6
U6	2.30	6.50	68.83	0.47	0.00	52	8.8

Table B6: Chemical compositions (wt%) and calculated chemical-Pb ages (Ma) for six generations of uraninite

Stage	SiO_2	CaO	U	Pb	Th	Chemical Pb Age (Ma)	SiO_2 + CaO
U6	0.51	3.52	77.79	1.07	0.00	104	4.0
U6	0.35	1.33	79.17	1.52	0.02	145	1.7
U6	2.29	6.50	67.26	0.55	0.00	62	8.8
U6	1.26	7.04	69.37	0.51	0.01	56	8.3
U6	1.75	7.23	68.93	0.50	0.00	55	9.0
U6	1.13	5.24	71.12	0.53	0.00	56	6.4
U6	0.90	5.91	70.73	0.49	0.00	52	6.8
U6	1.15	6.27	71.04	0.54	0.00	57	7.4
U6	1.63	6.57	68.34	0.51	0.01	56	8.2
U6	2.48	6.42	67.43	0.42	0.05	47	8.9
U6	2.02	6.97	67.90	0.45	0.00	50	9.0

Table B7: Chemical compositions (wt%) of coarse-grained illites and calculated K, Fe, and Mg atoms per formula unit (apfu) for use in the Battaglia (2004) equation for illite as a geothermometer

	EPMA Chemical Composition										Calculated apfu				K +	Temp
Mineral	SiO_2	Al_2O_3	FeO	MnO	MgO	CaO	Na_2O	K_2O	F	Cl	Si	K	Fe^{2+}	Mg	|Fe-Mg|	(°C)
Coarse Illite	49.29	26.34	3.13	0.04	4.07	0.33	0.26	8.02	0.42	0.33	3.40	0.71	0.18	0.42	0.94	284
Coarse Illite	48.95	26.38	3.23	0.08	4.35	0.33	0.24	7.78	0.18	0.31	3.38	0.69	0.19	0.45	0.95	285
Coarse Illite	43.45	30.18	3.36	0.03	6.83	0.22	0.22	6.47	0.19	0.36	3.03	0.58	0.20	0.71	1.09	323
Coarse Illite	47.51	31.73	1.34	0.02	2.37	0.21	0.22	9.03	0.19	0.18	3.23	0.78	0.08	0.24	0.95	285
Coarse Illite	46.51	30.85	1.94	0.00	3.13	0.17	0.13	8.43	0.11	0.20	3.21	0.74	0.11	0.32	0.95	286
Coarse Illite	46.92	26.10	3.66	0.07	5.78	0.40	0.25	7.04	0.13	0.43	3.29	0.63	0.22	0.60	1.02	305
Coarse Illite	48.59	29.56	2.08	0.06	2.40	0.32	0.28	8.22	0.27	0.31	3.33	0.72	0.12	0.25	0.84	258
Coarse Illite	47.66	34.63	0.57	0.00	0.77	0.05	0.19	8.48	0.00	0.05	3.20	0.73	0.03	0.08	0.77	238
Coarse Illite	51.07	30.53	0.38	0.00	1.90	0.06	0.16	8.29	0.26	0.08	3.41	0.71	0.02	0.19	0.87	266
Coarse Illite	46.91	31.18	1.76	0.03	2.05	1.04	0.54	7.99	0.27	0.41	3.22	0.70	0.10	0.21	0.81	248
Coarse Illite	47.99	30.16	1.90	0.00	2.28	0.68	0.51	8.03	0.31	0.43	3.29	0.70	0.11	0.23	0.83	253
Coarse Illite	45.89	38.23	0.00	0.00	0.33	0.00	0.18	8.61	0.00	0.00	3.03	0.73	0.00	0.03	0.76	235
Coarse Illite	45.25	35.97	0.00	0.00	0.63	0.00	0.14	8.95	0.00	0.00	3.08	0.78	0.00	0.06	0.84	257

Appendix C

Secondary Ion Mass Spectrometry (SIMS)

Standards and Data

Table C1: SIMS analyses of mica standard and hydrogen isotope ratios in muscovite, coarse-grained illite, and fine-grained illite from the Kianna deposit

July 15 2013 Standard	D/H	1σ (‰)	FF	Mass Bias
MP-Mica	5.3921E-05	1.3	0.3702	-629.8
MP-Mica	5.4092E-05	1.3	0.3714	-628.6
MP-Mica	5.3895E-05	1.3	0.3701	-629.9
Average	5.3969E-05		0.3706	-629.4
Std. Deviation	1.1E-07		0.0007	0.7
True V-SMOW D/H	1.5576E-04			
True Std D/H	1.4564E-04			

July 15 2013 Sample	Mineral	D/H	1σ (‰)	δD (‰)	FF
CS-22a2	Muscovite	5.5510E-05	1.2	-39	0.3709
CS-22a2	Muscovite	5.4513E-05	1.2	-57	0.3709
CS-22a2	Muscovite	5.4795E-05	1.3	-52	0.3709
CS-22a2	Coarse Illite	5.3389E-05	1.3	-76	0.3709
CS-22a2	Coarse Illite	5.3246E-05	1.2	-78	0.3709
CS-22a2	Coarse Illite	5.3802E-05	1.2	-69	0.3709
CS-22a2	Coarse Illite	5.3203E-05	1.2	-79	0.3709
CS-22a2	Coarse Illite	5.4457E-05	1.2	-57	0.3709
CS-22a2	Fine Illite	5.1271E-05	1.2	-113	0.3709
CS-22a2	Fine Illite	5.0708E-05	1.4	-122	0.3709
CS-21	Fine Illite	4.8187E-05	1.6	-166	0.3709
CS-21	Fine Illite	4.7660E-05	1.7	-175	0.3709
CS-21	Fine Illite	4.9179E-05	1.6	-149	0.3709
CS-21	Fine Illite	4.7775E-05	1.7	-173	0.3709
CS-21	Fine Illite	4.7881E-05	1.6	-171	0.3709
CS-21	Fine Illite	4.8153E-05	1.8	-167	0.3709
CS-21	Fine Illite	4.8710E-05	1.7	-157	0.3709
CS-21	Fine Illite	4.9488E-05	1.7	-143	0.3709

Table C1: SIMS analyses of mica standard and hydrogen isotope ratios in muscovite, coarse-grained illite, and fine-grained illite from the Kianna deposit

July 16 2013 Standard	D/H	1σ (‰)	FF	Mass Bias
MP-Mica	5.5009E-05	1.2	0.3777	-622.3
MP-Mica	5.4968E-05	1.2	0.3774	-622.6
MP-Mica	5.5086E-05	1.2	0.3782	-621.8
MP-Mica	5.5037E-05	1.2	0.3779	-622.1
Average	5.5025E-05		0.3778	-622.2
Std. Deviation	4.9E-08		0.0003	0.3

True V-SMOW D/H	1.5576E-04
True Std D/H	1.4564E-04

July 16 2013 Sample	Mineral	D/H	1σ (‰)	δD (‰)	FF
CS-8	Coarse Illite	5.3050E-05	1.2	-95	0.3765
CS-8	Coarse Illite	5.2806E-05	1.3	-100	0.3765
CS-8	Coarse Illite	5.4025E-05	1.2	-79	0.3765
CS-8	Coarse Illite	5.5309E-05	1.0	-57	0.3765
CS-8	Coarse Illite	5.3364E-05	1.6	-90	0.3765
CS-8	Coarse Illite	5.4999E-05	1.3	-62	0.3765
CS-8	Fine Illite	5.1089E-05	1.1	-129	0.3765
CS-8	Fine Illite	5.2586E-05	1.3	-103	0.3765
CS-8	Fine Illite	5.1436E-05	1.1	-123	0.3765
CS-8	Fine Illite	5.2040E-05	1.1	-113	0.3765
CS-8	Fine Illite	5.1955E-05	1.1	-114	0.3765
CS-8	Fine Illite	5.1383E-05	1.0	-124	0.3765
CS-8	Fine Illite	4.9886E-05	1.2	-149	0.3765
CS-8	Muscovite	5.6105E-05	1.1	-43	0.3765
CS-7a	Muscovite	5.7444E-05	1.3	-20	0.3765
CS-7a	Muscovite	5.7500E-05	1.4	-20	0.3765
CS-7a	Muscovite	5.6976E-05	1.3	-28	0.3765
CS-7a	Muscovite	5.7903E-05	1.3	-13	0.3765
CS-7a	Muscovite	5.8401E-05	1.3	-4	0.3765
CS-7a	Muscovite	5.7104E-05	1.3	-26	0.3765

Table C1: SIMS analyses of mica standard and hydrogen isotope ratios in muscovite, coarse-grained illite, and fine-grained illite from the Kianna deposit

July 17 2013 Standard	D/H	1σ (‰)	FF	Mass Bias
MP-Mica	5.5439E-05	1.2	0.3807	-619.3
MP-Mica	5.5613E-05	1.2	0.3819	-618.1
MP-Mica	5.5330E-05	1.2	0.3799	-620.1
Average	5.5461E-05		0.3808	-619.2
Std. Deviation	1.4E-07		0.0001	1.0

True V-SMOW D/H	1.5576E-04
True Std D/H	1.4564E-04

July 17 2013 Sample	Mineral	D/H	1σ (‰)	δD (‰)	FF
CS-5	Muscovite	5.8119E-05	1.2	-23	0.3818
CS-5	Muscovite	5.8163E-05	1.3	-22	0.3818
CS-5	Muscovite	5.8527E-05	1.2	-16	0.3818
CS-5	Muscovite	5.7454E-05	1.2	-34	0.3818
CS-5	Muscovite	5.6843E-05	1.1	-44	0.3818
CS-5	Muscovite	5.6399E-05	1.2	-52	0.3818
CS-12b	Muscovite	5.8919E-05	1.3	-9	0.3818
CS-12b	Muscovite	5.7890E-05	1.2	-27	0.3818
CS-5	Coarse Illite	5.4970E-05	1.2	-76	0.3818
CS-5	Fine Illite	5.0930E-05	1.3	-144	0.3818
CS-5	Fine Illite	4.9332E-05	1.1	-170	0.3818
CS-5	Fine Illite	4.9936E-05	1.0	-160	0.3818
CS-12b	Fine Illite	4.9888E-05	1.2	-161	0.3818
CS-12b	Fine Illite	5.1871E-05	1.1	-128	0.3818
CS-12b	Fine Illite	5.2809E-05	1.1	-112	0.3818
CS-12b	Fine Illite	4.9741E-05	1.0	-164	0.3818
CS-12b	Fine Illite	5.1261E-05	1.3	-138	0.3818
CS-12b	Fine Illite	5.2087E-05	1.2	-124	0.3818
CS-12b	Fine Illite	5.1947E-05	1.1	-127	0.3818
CS-12b	Fine Illite	4.9855E-05	1.1	-162	0.3818
CS-12b	Fine Illite	4.9493E-05	1.1	-168	0.3818
CS-12b	Fine Illite	5.1153E-05	1.1	-140	0.3818
CS-12b	Fine Illite	5.1012E-05	1.1	-142	0.3818

Table C2: SIMS analyses of mica standard and oxygen isotope ratios in muscovite, coarse-grained illite, and fine-grained illite from the Kianna deposit

Oct 21 2013 Standard	$^{18}O/^{16}O$ Measured	FF	1σ (‰)	Mass Bias
MP-Mica	1.8894E-3	0.9357	1.2	-64.3
MP-Mica	1.8864E-3	0.9342	1.2	-65.8
MP-Mica	1.8852E-3	0.9336	1.2	-66.4
MP-Mica	1.8864E-3	0.9342	1.2	-65.8
Average	1.8869E-3	0.9345		-65.5
Std. Deviation	1.8E-6			0.9
IMF				1.8738
True V-SMOW $^{18}O/^{16}O$	2.0052E-3			
True Std $^{18}O/^{16}O$	2.0192 E-3			

Oct 21 2013 Sample	Mineral	$^{18}O/^{16}O$ Measured	1σ (‰)	$\delta^{18}O$ V-SMOW (‰)
CS-8	Coarse Illite	1.8829E-3	1.2	4.9
CS-8	Coarse Illite	1.8782E-3	1.2	2.4
CS-8	Coarse Illite	1.8824E-3	1.2	4.6
CS-8	Coarse Illite	1.8751E-3	1.2	0.7
CS-8	Coarse Illite	1.8776E-3	1.2	2.1
CS-8	Coarse Illite	1.8695E-3	1.2	-2.3
CS-8	Coarse Illite	1.8680E-3	1.1	-3.1
CS-8	Coarse Illite	1.8639E-3	1.2	-5.3
CS-8	Coarse Illite	1.8625E-3	1.2	-6.0
CS-8	Coarse Illite	1.8849E-3	1.2	5.9
CS-8	Coarse Illite	1.8746E-3	1.1	0.4
CS-8	Fine Illite	1.8854E-3	1.2	6.2
CS-8	Fine Illite	1.8809E-3	1.2	3.8
CS-8	Fine Illite	1.8891E-3	1.2	8.2
CS-8	Fine Illite	1.8836E-3	1.2	5.3
CS-8	Fine Illite	1.8857E-3	1.1	6.4
CS-8	Fine Illite	1.8856E-3	1.2	6.3
CS-8	Fine Illite	1.8841E-3	1.2	5.5
CS-22a2	Fine Illite	1.8836E-3	1.2	5.2
CS-22a2	Fine Illite	1.8804E-3	1.1	3.5
CS-22a2	Fine Illite	1.8883E-3	1.1	7.8
CS-22a2	Fine Illite	1.8829E-3	1.1	4.9
CS-22a2	Fine Illite	1.8834E-3	1.1	5.1
CS-22a2	Fine Illite	1.8860E-3	1.2	6.5
CS-22a2	Fine Illite	1.8806E-3	1.2	3.7
CS-21	Fine Illite	1.8910E-3	1.2	9.2
CS-21	Fine Illite	1.8917E-3	1.2	9.6
CS-21	Fine Illite	1.8863E-3	1.2	6.7
CS-21	Fine Illite	1.8903E-3	1.1	8.8
CS-21	Fine Illite	1.8910E-3	1.2	9.2
CS-21	Fine Illite	1.8891E-3	1.2	8.2
CS-12b	Fine Illite	1.8868E-3	1.2	7.0
CS-12b	Fine Illite	1.8830E-3	1.2	4.9
CS-12b	Fine Illite	1.8847E-3	1.1	5.9
CS-12b	Fine Illite	1.8828E-3	1.1	4.8
CS-12b	Fine Illite	1.8830E-3	1.1	4.9

Table C2: SIMS analyses of mica standard and oxygen isotope ratios in muscovite, coarse-grained illite, and fine-grained illite from the Kianna deposit

Oct 22 2013 Standard	$^{18}O/^{16}O$ Measured	FF	1σ (‰)	Mass Bias
MP-Mica	1.8884E-3	0.9352	1.2	-64.8
MP-Mica	1.8892E-3	0.9356	1.2	-64.4
MP-Mica	1.8852E-3	0.9336	1.2	-66.4
MP-Mica	1.8861E-3	0.9341	1.2	-65.9
Average	1.8872E-3	0.9346		-65.4
Std. Deviation	1.6E-6			0.9
IMF				1.8741
True V-SMOW $^{18}O/^{16}O$	2.0052E-3			
True Std $^{18}O/^{16}O$	2.0192E-3			

Oct 22 2013 Sample	Mineral	$^{18}O/^{16}O$ Measured	1σ (‰)	$\delta^{18}O$ V-SMOW (‰)
CS-7a	Muscovite	1.8662E-3	1.2	-4.2
CS-7a	Muscovite	1.8653E-3	1.3	-4.7
CS-7a	Muscovite	1.8688E-3	1.1	-2.8
CS-7a	Muscovite	1.8765E-3	1.1	1.3
CS-7a	Muscovite	1.8542E-3	1.2	-10.6
CS-7a	Muscovite	1.8788E-3	1.2	2.5
CS-7a	Muscovite	1.8763E-3	1.3	1.2
CS-7a	Muscovite	1.8591E-3	1.2	-8.0
CS-7a	Muscovite	1.8794E-3	1.2	2.8
CS-7a	Muscovite	1.8814E-3	1.2	3.9
CS-7a	Muscovite	1.8802E-3	1.2	3.2
CS-7a	Muscovite	1.8846E-3	1.2	5.6
CS-7a	Muscovite	1.8806E-3	1.2	3.5
CS-7a	Muscovite	1.8785E-3	1.2	2.3
CS-5	Muscovite	1.8749E-3	1.1	0.4
CS-5	Muscovite	1.8897E-3	1.2	8.3
CS-5	Muscovite	1.8664E-3	1.2	-4.1
CS-5	Fine Illite	1.8877E-3	1.2	7.2
CS-5	Fine Illite	1.8874E-3	1.1	7.1
CS-5	Fine Illite	1.8896E-3	1.2	8.3
CS-5	Fine Illite	1.8875E-3	1.2	7.1
CS-5	Fine Illite	1.8884E-3	1.1	7.6
CS-5	Fine Illite	1.8884E-3	1.1	7.6
CS-5	Fine Illite	1.8864E-3	1.2	6.5
CS-5	Fine Illite	1.8866E-3	1.2	6.6

Table C3: SIMS analyses of UO_2 standard and oxygen isotope ratios in uraninite at the Kianna deposit

Oct 23 2013 Standard	$^{18}O/^{16}O$ Measured	FF	1σ (‰)	Mass Bias
UO_2	1.9577E-3	0.9685	1.2	-31.5
UO_2	1.9576E-3	0.9684	1.2	-31.6
UO_2	1.9571E-3	0.9682	1.2	-31.8
UO_2	1.9561E-3	0.9677	1.2	-32.3
Average	1.9571E-3	0.9682		-31.8
Std. Deviation	7.0E-7			0.4
IMF				1.9414
True $^{18}O/^{16}O$ V-SMOW	2.0052E-3			
UO_2 Std True $^{18}O/^{16}O$	2.0214E-3			

Oct 23 2013 Sample	Mineral	$^{18}O/^{16}O$ Measured	1σ (‰)	$\delta^{18}O$ V-SMOW (‰)
CS-3	U1	1.8938E-3	1.1	-24.8
CS-3	U1	1.9013E-3	1.1	-20.9
CS-3	U1	1.9006E-3	1.2	-21.3
CS-3	U1	1.8888E-3	1.2	-27.3
CS-3	U1	1.9052E-3	1.1	-18.9
CS-3	U1	1.8974E-3	1.2	-22.9
CS-3	U2	1.9070E-3	1.2	-18.0
CS-3	U3	1.9021E-3	1.1	-20.5
CS-3	U3	1.9031E-3	1.1	-20.0
CS-3	U3	1.9006E-3	1.1	-21.3
CS-3	U3	1.9030E-3	1.2	-20.1
CS-3	U3	1.9036E-3	1.2	-19.7
CS-22a2	U1	1.9023E-3	1.0	-20.4
CS-22a2	U1	1.9010E-3	1.2	-21.1
CS-22a2	U1	1.8848E-3	1.1	-29.4
CS-22a2	U1	1.8959E-3	1.1	-23.7
CS-22a2	U1	1.9003E-3	1.1	-21.4
CS-22a2	U1	1.9019E-3	1.2	-20.6

Table C3: SIMS analyses of UO_2 standard and oxygen isotope ratios in uraninite at the Kianna deposit

Oct 25 2013 Standard	$^{18}O/^{16}O$ Measured	FF	1σ (‰)	Mass Bias
UO_2	1.9543E-3	0.9668	1.2	-33.2
UO_2	1.9535E-3	0.9664	1.2	-33.6
UO_2	1.9559E-3	0.9676	1.1	-32.4
UO_2	1.9531E-3	0.9662	1.2	-33.8
Average	1.9542E-3	0.9668		-33.2
Std. Deviation	1.2E-6			0.6
IMF				1.9385
True $^{18}O/^{16}O$ V-SMOW	2.0052E-3			
UO_2 Std True $^{18}O/^{16}O$	2.0214E-3			

Oct 25 2013 Sample	Mineral	$^{18}O/^{16}O$ Measured	1σ (‰)	$\delta^{18}O$ V-SMOW (‰)
CS-9b	U6	1.8950E-3	1.2	-22.5
CS-9b	U6	1.8963E-3	1.2	-21.8
CS-9b	U6	1.8997E-3	1.2	-20.0
CS-9b	U6	1.8998E-3	1.2	-20.0
CS-9b	U6	1.8976E-3	1.2	-21.1
CS-9b	U6	1.8968E-3	1.2	-21.5
CS-9b	U6	1.8905E-3	1.2	-24.8
CS-9b	U6	1.9064E-3	1.2	-16.6
CS-18a	U5	1.8947E-3	1.2	-22.6
CS-18a	U5	1.8948E-3	1.2	-22.6
CS-18a	U5	1.8935E-3	1.2	-23.2
CS-18a	U5	1.8954E-3	1.2	-22.2
CS-18a	U5	1.8964E-3	1.3	-21.7
CS-18a	U5	1.8998E-3	1.2	-20.0
CS-18a	U5	1.8935E-3	1.2	-23.2

Table C4: SIMS analyses of pyrite/chalcopyrite standard and sulfur isotope ratios in pyrite and chalcopyrite at the Kianna deposit

July 23 2013 Standard	$^{34}S/^{32}S$ Measured	1σ (‰)	Mass Bias
Balmat Pyrite	4.2608E-2	0.3	-67.3
Balmat Pyrite	4.2607E-2	0.3	-67.4
Balmat Pyrite	4.2626E-2	0.3	-66.9
Balmat Pyrite	4.2599E-2	0.3	-67.5
Balmat Pyrite	4.2626E-2	0.3	-66.9
Average	4.2613E-2		-67.2
Std. Deviation	1.2E-5		0.3
IMF			4.1979
RSD (%)	0.0284		
True 34/32 Py CDT	4.5005E-2		
True $^{34}S/^{32}S$ Balmat Py:	4.5684E-2		

July 23 2013 Sample	Ore Zone	Mineral	$^{34}S/^{32}S$ Measured	1σ (‰)	$\delta^{34}S$ (‰)	2σ (total)
CS-14b	Unconformity	Pyrite	4.2701E-2	0.3	17.2	0.4
CS-14b	Unconformity	Pyrite	4.2717E-2	0.3	17.6	0.4
CS-14b	Unconformity	Pyrite	4.2668E-2	0.3	16.4	0.4
CS-14b	Unconformity	Pyrite	4.2774E-2	0.3	18.9	0.4
CS-14b	Unconformity	Pyrite	4.2722E-2	0.3	17.7	0.4
CS-14b	Unconformity	Pyrite	4.2611E-2	0.3	15.1	0.4
CS-14b	Unconformity	Pyrite	4.2772E-2	0.3	18.9	0.4
CS-7b	Basement	Pyrite	4.2069E-2	0.3	2.1	0.4
CS-7b	Basement	Pyrite	4.2091E-2	0.3	2.7	0.4
CS-7b	Basement	Pyrite	4.2176E-2	0.4	4.7	0.5
CS-7b	Basement	Pyrite	4.2087E-2	0.3	2.6	0.4
CS-7b	Basement	Pyrite	4.2085E-2	0.3	2.5	0.4
CS-7b	Basement	Pyrite	4.2159E-2	0.4	4.3	0.5
CS-19b	Perched	Pyrite	4.2861E-2	0.8	21.0	0.8
CS-19b	Perched	Pyrite	4.2877E-2	0.6	21.4	0.7
CS-19b	Perched	Pyrite	4.3046E-2	0.9	25.4	0.9
CS-19b	Perched	Pyrite	4.2767E-2	0.9	18.8	0.9
CS-19b	Perched	Pyrite	4.2918E-2	0.6	22.4	0.7

Table C4: SIMS analyses of pyrite/chalcopyrite standard and sulfur isotope ratios in pyrite and chalcopyrite at the Kianna deposit

July 24 2013 Standard	$^{34}S/^{32}S$ Measured	1σ (‰)	Mass Bias
Balmat Pyrite	4.2604E-2	0.3	-67.4
Balmat Pyrite	4.2606E-2	0.3	-67.4
Balmat Pyrite	4.2557E-2	0.3	-68.5
Balmat Pyrite	4.2574E-2	0.3	-68.1
Balmat Pyrite	4.2556E-2	0.3	-68.5
Average	4.2579E-2		-68.0
Std. Deviation	2.4E-5		0.5
IMF			4.1946
RSD (%)	0.0573		
True $^{34}S/^{32}S$ Py CDT	4.5005E-2		
True $^{34}S/^{32}S$ Balmat Py:	4.5684E-2		
Standard	**$^{34}S/^{32}S$ Measured**	**1σ (‰)**	**Mass Bias**
Trout Lake Cpy	4.2011E-2	0.3	-66.8
Trout Lake Cpy	4.1998E-2	0.3	-67.1
Trout Lake Cpy	4.1970E-2	0.3	-67.7
Trout Lake Cpy	4.1987E-2	0.3	-67.3
Trout Lake Cpy	4.1960E-2	0.3	-67.9
Average	4.1985E-2		-67.4
Std. Deviation	2.1E-5		0.5
IMF			4.1973
RSD (%)	0.0491		
True $^{34}S/^{32}S$ Cpy CDT	4.5005E-2		
True $^{34}S/^{32}S$ Trout Lake Cpy	4.5018E-2		

July 24 2013 Sample	Ore Zone	Mineral	$^{34}S/^{32}S$ Measured	1σ (‰)	$\delta^{34}S$ (‰)	2σ (total)
4b-2	Perched	Chalcopyrite	4.2125E-2	0.3	3.8	0.5
4b-3	Perched	Chalcopyrite	4.2029E-2	0.3	1.5	0.5
4b-4	Perched	Chalcopyrite	4.2012E-2	0.3	1.1	0.5
4b-6	Perched	Chalcopyrite	4.2213E-2	0.3	5.9	0.5
4b-7	Perched	Chalcopyrite	4.2021E-2	0.3	1.3	0.5
4b-8	Perched	Chalcopyrite	4.2093E-2	0.3	3.0	0.5
4b-9	Perched	Chalcopyrite	4.1884E-2	0.3	-1.9	0.5
4b-10	Perched	Chalcopyrite	4.2254E-2	0.3	6.9	0.5
20b2-1	Unconformity	Chalcopyrite	4.2182E-2	0.3	5.1	0.5
20b2-3	Unconformity	Chalcopyrite	4.2052E-2	0.3	2.0	0.5

Table C4: SIMS analyses of pyrite/chalcopyrite standard and sulfur isotope ratios in pyrite and chalcopyrite at the Kianna deposit

July 25 2013 Standard	$^{34}S/^{32}S$ Measured	1σ (‰)	Mass Bias
Trout Lake Cpy	4.2032E-2	0.3	-66.3
Trout Lake Cpy	4.2040E-2	0.3	-66.2
Trout Lake Cpy	4.1990E-2	0.3	-67.3
Trout Lake Cpy	4.2035E-2	0.3	-66.3
Average	4.2024E-2		-66.5
Std. Deviation	2.3E-5		0.5
IMF			4.2012
RSD (%)	0.0547		
True $^{34}S/^{32}S$ Cpy CDT	4.5005E-2		
True $^{34}S/^{32}S$ Trout Lake Cpy	4.5018E-2		

July 25 2013 Sample	Ore Zone	Mineral	$^{34}S/^{32}S$ Measured	1σ (‰)	$\delta^{34}S$ (‰)	2σ (total)
20b2-1	Unconformity	Chalcopyrite	4.2341E-2	0.3	7.9	0.5
20b2-2	Unconformity	Chalcopyrite	4.2318E-2	0.3	7.4	0.5
20b2-4	Unconformity	Chalcopyrite	4.2349E-2	0.3	8.1	0.5
20b2-8	Unconformity	Chalcopyrite	4.2143E-2	0.3	3.2	0.5
17-1	Perched	Chalcopyrite	4.2773E-2	0.3	18.2	0.6
17-2	Perched	Chalcopyrite	4.2816E-2	0.3	19.2	0.6
17-3	Perched	Chalcopyrite	4.2712E-2	0.3	16.8	0.6
17-4	Perched	Chalcopyrite	4.2698E-2	0.3	16.4	0.6
17-5	Perched	Chalcopyrite	4.2695E-2	0.3	16.3	0.6
17-6	Perched	Chalcopyrite	4.2694E-2	0.3	16.3	0.6
17-7	Perched	Chalcopyrite	4.2725E-2	0.3	17.1	0.6
17-8	Perched	Chalcopyrite	4.2704E-2	0.3	16.6	0.6
17-10	Perched	Chalcopyrite	4.2713E-2	0.3	16.8	0.6

Table C5: SIMS analyses of UO_2 standards and U-Pb measured and corrected (CORR) isotope ratios in uraninite from the Kianna deposit

June 17 2013 Standard	$^{207}Pb/^{206}Pb$	$^{206}Pb/^{238}U$	$^{207}Pb/^{235}U$
LAMNH	0.0548	0.1132	0.8216
LAMNH	0.0547	0.1102	0.7997
LAMNH	0.0549	0.1046	0.7609
AVERAGE	0.0548	0.1094	0.7941
TRUE	0.0538	0.0554	0.4105
TKK	0.0735	0.2525	2.4827
TKK	0.0735	0.2645	2.5892
TKK	0.0736	0.2467	2.4044
AVERAGE	0.0735	0.2546	2.4921
TRUE	0.0734	0.1701	1.7213
PC-06	0.1668	0.7530	16.6629
PC-06	0.1661	0.7755	17.0358
PC-06	0.1677	0.7046	15.7058
AVERAGE	0.1669	0.7444	16.4681
TRUE	0.1678	0.3613	8.3590

Table C5: SIMS analyses of UO_2 standards and U-Pb measured and corrected (CORR) isotope ratios in uraninite from the Kianna deposit

June 17 2013 Sample No.	Ore Zone	Measured $^{207}Pb/^{206}Pb$	Measured $^{206}Pb/^{238}U$	CORR $^{206}Pb/^{238}U$	Measured $^{207}Pb/^{235}U$	CORR $^{207}Pb/^{235}U$
CS-22a2	Basement	0.0822	0.2606	0.1457	2.8415	1.6453
CS-22a2	Basement	0.0845	0.3295	0.1773	3.6936	2.0668
CS-22a2	Basement	0.0778	0.2371	0.1349	2.4533	1.4533
CS-22a2	Basement	0.0811	0.2601	0.1454	2.8401	1.6446
CS-22a2	Basement	0.0818	0.2560	0.1436	2.8114	1.6304
CS-21	Basement	0.0876	0.3804	0.2006	4.4429	2.4375
CS-21	Basement	0.0794	0.2421	0.1372	2.5835	1.5177
CS-21	Basement	0.0828	0.2716	0.1507	3.0145	1.7309
CS-21	Basement	0.0843	0.2933	0.1607	3.3092	1.8766
CS-21	Basement	0.0873	0.3393	0.1818	3.9770	2.2070
CS-21	Basement	0.0792	0.2316	0.1324	2.4468	1.4500
CS-21	Basement	0.0790	0.2454	0.1387	2.6102	1.5309
CS-21	Basement	0.0840	0.3017	0.1646	3.3843	1.9138
CS-21	Basement	0.0875	0.3399	0.1820	3.9580	2.1976
CS-21	Basement	0.0871	0.3465	0.1851	4.0381	2.2372
CS-21	Basement	0.0874	0.3321	0.1785	3.8921	2.1650
CS-21	Basement	0.0878	0.3610	0.1917	4.2307	2.3325
CS-21	Basement	0.0877	0.3569	0.1899	4.2047	2.3197

Table C5: SIMS analyses of UO_2 standards and U-Pb measured and corrected (CORR) isotope ratios in uraninite from the Kianna deposit

June 18 2013 Standard	$^{207}Pb/^{206}Pb$	$^{206}Pb/^{238}U$	$^{207}Pb/^{235}U$
LAMNH	0.0539	0.0844	0.6042
LAMNH	0.0540	0.0802	0.5755
LAMNH	0.0536	0.0824	0.5889
AVERAGE	0.0538	0.0823	0.5895
TRUE	0.0538	0.0554	0.4105
TKK	0.0732	0.2754	2.6666
TKK	0.0739	0.2715	2.6703
TKK	0.0734	0.2725	2.6639
AVERAGE	0.0735	0.2732	2.6670
TRUE	0.0734	0.1701	1.7213
PC-06	0.1659	0.6820	15.0714
PC-06	0.1645	0.6861	14.9848
PC-06	0.1668	0.7220	15.9702
AVERAGE	0.1657	0.6967	15.3421
TRUE	0.1678	0.3613	8.3590

Table C5: SIMS analyses of UO_2 standards and U-Pb measured and corrected (CORR) isotope ratios in uraninite from the Kianna deposit

June 18 2013 Sample No.	Ore Zone	$^{207}Pb/^{206}Pb$	Measured $^{206}Pb/^{238}U$	CORR $^{206}Pb/^{238}U$	Measured $^{207}Pb/^{235}U$	CORR $^{207}Pb/^{235}U$
06-18U-5-1	Basement	0.0776	0.1756	0.1098	1.8009	1.1504
06-18U-5-2	Basement	0.0787	0.2717	0.1569	2.8678	1.7195
06-18U-5-3	Basement	0.0772	0.0995	0.0725	1.0192	0.7334
06-18U-5-4	Basement	0.0752	0.1157	0.0804	1.1649	0.8111
06-18U-5-5	Basement	0.0757	0.1139	0.0795	1.1577	0.8072
06-18U-5-6	Basement	0.0780	0.1907	0.1172	1.9939	1.2533
06-18U-5-7	Basement	0.0775	0.2047	0.1240	2.1276	1.3247
06-18U-3-1	Basement	0.0787	0.2208	0.1320	2.3348	1.4352
06-18U-3-2	Basement	0.0762	0.2095	0.1264	2.1469	1.3350
06-18U-3-3	Basement	0.0767	0.2164	0.1298	2.2157	1.3717
06-18U-3-4	Basement	0.0816	0.2705	0.1563	2.9494	1.7631
06-18U-3-5	Basement	0.0803	0.2327	0.1378	2.4772	1.5112
06-18U-3-6	Basement	0.0784	0.2343	0.1385	2.4364	1.4894
06-18U-3-7	Basement	0.0810	0.2616	0.1520	2.8290	1.6989
06-18U-3-8	Basement	0.0789	0.2128	0.1280	2.2422	1.3858
06-18U-3-9	Basement	0.0802	0.2377	0.1402	2.5423	1.5459
06-18U-3-10	Basement	0.0775	0.2255	0.1342	2.3252	1.4301
06-18U-3-11	Basement	0.0772	0.1942	0.1189	1.9889	1.2507
06-18U-3-12	Basement	0.0724	0.2606	0.1515	2.5166	1.5322
06-18U-3-13	Basement	0.0695	0.2305	0.1367	2.1482	1.3356
06-18U-3-14	Basement	0.0702	0.2491	0.1458	2.3208	1.4277
06-18U-3-15	Basement	0.0663	0.0796	0.0627	0.7046	0.5655
06-18U-3-16	Basement	0.0719	0.2582	0.1503	2.4800	1.5127
06-18U-18a-1	Unconformity	0.0531	0.0612	0.0537	0.4350	0.4217
06-18U-18a-2	Unconformity	0.0530	0.0610	0.0536	0.4284	0.4181
06-18U-18a-3	Unconformity	0.0525	0.0588	0.0525	0.4097	0.4082
06-18U-18a-4	Unconformity	0.0553	0.0706	0.0583	0.5198	0.4669
06-18U-18a-5	Unconformity	0.0547	0.0763	0.0611	0.5582	0.4874
06-18U-18a-6	Unconformity	0.0547	0.0791	0.0625	0.5737	0.4957
06-18U-18a-7	Unconformity	0.0539	0.0741	0.0600	0.5328	0.4739

Table C5: SIMS analyses of UO_2 standards and U-Pb measured and corrected (CORR) isotope ratios in uraninite from the Kianna deposit

June 19 2013 Standard	$^{207}Pb/^{206}Pb$	$^{206}Pb/^{238}U$	$^{207}Pb/^{235}U$
LAMNH	0.0540	0.0823	0.5931
LAMNH	0.0541	0.0848	0.6157
LAMNH	0.0543	0.0821	0.5962
AVERAGE	0.0541	0.0831	0.6017
TRUE	0.0538	0.0554	0.4105
TKK	0.0737	0.3105	3.0757
TKK	0.0739	0.2920	2.9004
TKK	0.0738	0.2902	2.8699
AVERAGE	0.0738	0.2976	2.9487
TRUE	0.0734	0.1701	1.7213
PC-06	0.1664	0.9439	21.0346
PC-06	0.1660	0.8889	19.6213
PC-06	0.1657	0.8841	19.4656
AVERAGE	0.1661	0.9056	20.0405
TRUE	0.1678	0.3613	8.3590

Table C5: SIMS analyses of UO_2 standards and U-Pb measured and corrected (CORR) isotope ratios in uraninite from the Kianna deposit

June 19 2013 Sample No.	Ore Zone	$^{207}Pb/^{206}Pb$	Measured $^{206}Pb/^{238}U$	CORR $^{206}Pb/^{238}U$	Measured $^{207}Pb/^{235}U$	CORR $^{207}Pb/^{235}U$
CS-14b	Unconformity	0.0535	0.0535	0.0608	0.3879	0.4974
CS-14b	Unconformity	0.0530	0.0549	0.0613	0.3947	0.5001
CS-14b	Unconformity	0.0542	0.0474	0.0586	0.3499	0.4822
CS-14b	Unconformity	0.0533	0.0498	0.0595	0.3621	0.4871
CS-14b	Unconformity	0.0551	0.0426	0.0569	0.3186	0.4696
CS-20b1	Unconformity	0.0530	0.0123	0.0460	0.0877	0.3770
CS-20b1	Unconformity	0.0533	0.0131	0.0463	0.0930	0.3791
CS-20b1	Unconformity	0.0527	0.0121	0.0460	0.0848	0.3758
CS-20b1	Unconformity	0.0540	0.0120	0.0459	0.0858	0.3762
CS-20b1	Unconformity	0.0523	0.0132	0.0463	0.0924	0.3789
CS-20b1	Unconformity	0.0528	0.0116	0.0458	0.0820	0.3747
CS-9b	Perched	0.0501	0.0276	0.0515	0.1871	0.4168
CS-9b	Perched	0.0509	0.0098	0.0451	0.0678	0.3690
CS-9b	Perched	0.0501	0.0187	0.0483	0.1266	0.3926
CS-9b	Perched	0.0498	0.0178	0.0480	0.1196	0.3898
CS-9b	Perched	0.0503	0.0184	0.0482	0.1248	0.3919
CS-4a	Perched	0.0516	0.0196	0.0487	0.1372	0.3968
CS-4a	Perched	0.0512	0.0319	0.0531	0.2167	0.4287
CS-4a	Perched	0.0530	0.0155	0.0472	0.1096	0.3858
CS-4a	Perched	0.0566	0.1027	0.0785	0.7822	0.6556
CS-4a	Perched	0.0567	0.0964	0.0762	0.7371	0.6375
CS-4a	Perched	0.0569	0.0459	0.0581	0.3526	0.4832
CS-4a	Perched	0.0571	0.0908	0.0742	0.6960	0.6211

Table C5: SIMS analyses of UO_2 standards and U-Pb measured and corrected (CORR) isotope ratios in uraninite from the Kianna deposit

June 27 2013 Standard	$^{207}Pb/^{206}Pb$	$^{206}Pb/^{238}U$	$^{207}Pb/^{235}U$
LAMNH	0.0539	0.0882	0.6391
LAMNH	0.0541	0.0882	0.6437
LAMNH	0.0541	0.0865	0.6314
AVERAGE	0.0540	0.0876	0.6381
TRUE	0.0538	0.0554	0.4105
TKK	0.0736	0.2845	2.8364
TKK	0.0737	0.2901	2.8658
TKK	0.0730	0.2852	2.7925
AVERAGE	0.0734	0.2866	2.8315
TRUE	0.0734	0.1701	1.7213
PC-06	0.1660	0.7223	16.0633
PC-06	0.1654	0.7801	17.2423
PC-06	0.1660	0.7453	16.6159
AVERAGE	0.1658	0.7492	16.6405
TRUE	0.1678	0.3613	8.3590

Table C5: SIMS analyses of UO_2 standards and U-Pb measured and corrected (CORR) isotope ratios in uraninite from the Kianna deposit

June 27 2013 Sample No.	Ore Zone	$^{207}Pb/^{206}Pb$	Measured $^{206}Pb/^{238}U$	CORR $^{206}Pb/^{238}U$	Measured $^{207}Pb/^{235}U$	CORR $^{207}Pb/^{235}U$
CS-21	Basement	0.0838	0.2880	0.1564	3.2388	1.7958
CS-21	Basement	0.0804	0.3070	0.1650	3.3282	1.8397
CS-21	Basement	0.0866	0.3433	0.1814	4.0133	2.1760
CS-21	Basement	0.0855	0.3475	0.1833	4.0117	2.1753
CS-21	Basement	0.0868	0.3691	0.1931	4.3235	2.3283
CS-21	Basement	0.0875	0.3878	0.2016	4.5804	2.4545
CS-21	Basement	0.0875	0.3863	0.2010	4.5692	2.4490
CS-21	Basement	0.0839	0.3242	0.1728	3.6951	2.0198
CS-21	Basement	0.0874	0.3648	0.1912	4.3009	2.3172
CS-21	Basement	0.0778	0.2431	0.1360	2.5718	1.4682
CS-21	Basement	0.0870	0.3674	0.1924	4.3145	2.3239
CS-21	Basement	0.0878	0.3847	0.2002	4.5574	2.4432
CS-22a2	Basement	0.0877	0.3935	0.2042	4.6635	2.4953
CS-22a2	Basement	0.0827	0.2954	0.1597	3.3028	1.8272
CS-22a2	Basement	0.0835	0.3050	0.1641	3.4203	1.8849
CS-22a2	Basement	0.0871	0.3734	0.1951	4.4224	2.3769
CS-22a2	Basement	0.0865	0.3566	0.1875	4.1645	2.2503
CS-22a2	Basement	0.0833	0.2859	0.1554	3.2382	1.7955
CS-22a2	Basement	0.0836	0.3075	0.1652	3.4616	1.9052
CS-22a2	Basement	0.0792	0.2500	0.1391	2.6833	1.5230
CS-22a2	Basement	0.0831	0.3049	0.1640	3.4179	1.8837
CS-22a2	Basement	0.0844	0.3324	0.1765	3.7829	2.0629

Table C5: SIMS analyses of UO_2 standards and U-Pb measured and corrected (CORR) isotope ratios in uraninite from the Kianna deposit

November 15 2012 Standard	$^{207}Pb/^{206}Pb$	$^{206}Pb/^{238}U$	$^{207}Pb/^{235}U$
LAMNH	0.0541	0.1038	0.7459
LAMNH	0.0537	0.0997	0.7129
LAMNH	0.0541	0.0986	0.7111
AVERAGE	0.0539	0.1007	0.7233
TRUE	0.0538	0.0554	0.4105
TKK	0.0735	0.3564	3.4941
TKK	0.0735	0.3588	3.5109
TKK	0.0741	0.3545	3.4805
AVERAGE	0.0737	0.3566	3.4952
TRUE	0.0734	0.1701	1.7213
PC-06	0.1678	1.0975	24.2471
PC-06	0.1680	1.0207	22.6756
PC-06	0.1690	1.0677	23.7816
AVERAGE	0.1682	1.0620	23.5681
TRUE	0.1678	0.3613	8.3590

Table C5: SIMS analyses of UO_2 standards and U-Pb measured and corrected (CORR) isotope ratios in uraninite from the Kianna deposit

November 15 2013 Sample No.	Ore Zone	$^{207}Pb/^{206}Pb$	Measured $^{206}Pb/^{238}U$	CORR $^{206}Pb/^{238}U$	Measured $^{207}Pb/^{235}U$	CORR $^{207}Pb/^{235}U$
CS-13-13a	Low basement	0.0786	0.1762	0.0938	1.8456	0.9641
CS-13-13a	Low basement	0.0760	0.1736	0.0930	1.7493	0.9312
CS-13-13a	Low basement	0.0834	0.3563	0.1493	3.9534	1.6839
CS-13-13a	Low basement	0.0821	0.2878	0.1282	3.1341	1.4041
CS-13-13a	Low basement	0.0752	0.1553	0.0874	1.5468	0.8620
CS-13-13a	Low basement	0.0766	0.2116	0.1047	2.1641	1.0729
CS-13-13a	Low basement	0.0815	0.2603	0.1197	2.8331	1.3013
CS-13-13a	Low basement	0.0841	0.2888	0.1285	3.2541	1.4451
CS-13-13a	Low basement	0.0815	0.2499	0.1165	2.7091	1.2590
CS-13-13a	Low basement	0.0772	0.1179	0.0758	1.2112	0.7474
CS-13-15	Low basement	0.0730	0.2250	0.1088	2.1844	1.0798
CS-13-15	Low basement	0.0768	0.2072	0.1034	2.1194	1.0576
CS-13-15	Low basement	0.0701	0.1858	0.0968	1.7469	0.9304
CS-13-15	Low basement	0.0818	0.2284	0.1099	2.4713	1.1778
CS-13-15	Low basement	0.0813	0.3145	0.1364	3.3824	1.4889
CS-13-15	Low basement	0.0750	0.1936	0.0992	1.9332	0.9940
CS-13-15	Low basement	0.0840	0.2905	0.1290	3.2472	1.4427
CS-13-15	Low basement	0.0771	0.1612	0.0892	1.6593	0.9004
CS-13-25	Basement	0.0769	0.1446	0.0841	1.4843	0.8407
CS-13-25	Basement	0.0675	0.2202	0.1074	1.9656	1.0051
CS-13-25	Basement	0.0681	0.2025	0.1019	1.8380	0.9615
CS-13-25	Basement	0.0699	0.1273	0.0787	1.1785	0.7362
CS-13-25	Basement	0.0749	0.2595	0.1195	2.5998	1.2216
CS-13-25	Basement	0.0722	0.2137	0.1054	2.0540	1.0352
CS-13-24	Basement	0.0802	0.0804	0.0643	0.8616	0.6280
CS-13-24	Basement	0.0817	0.0679	0.0604	0.7423	0.5873
CS-13-24	Basement	0.0779	0.0418	0.0524	0.4333	0.4818
CS-13-24	Basement	0.0762	0.0863	0.0661	0.8810	0.6347
CS-13-24	Basement	0.0817	0.0683	0.0606	0.7486	0.5894

Table C5: SIMS analyses of UO_2 standards and U-Pb measured and corrected (CORR) isotope ratios in uraninite from the Kianna deposit

November 16 2013 Standard	$^{207}Pb/^{206}Pb$	$^{206}Pb/^{238}U$	$^{207}Pb/^{235}U$
LAMNH	0.0546	0.0762	0.5537
LAMNH	0.0542	0.0761	0.5496
LAMNH	0.0551	0.0741	0.5447
AVERAGE	0.0546	0.0755	0.5494
TRUE	0.0538	0.0554	0.4105
TKK	0.0739	0.3511	3.4264
TKK	0.0739	0.3470	3.4065
TKK	0.0737	0.3482	3.4039
AVERAGE	0.0738	0.3488	3.4123
TRUE	0.0734	0.1701	1.7213
PC-06	0.1677	1.0174	22.5372
PC-06	0.1687	0.9907	22.1204
PC-06	0.1682	1.0024	22.3680
AVERAGE	0.1682	1.0035	22.3418
TRUE	0.1678	0.3613	8.3590

Table C5: SIMS analyses of UO_2 standards and U-Pb measured and corrected (CORR) isotope ratios in uraninite from the Kianna deposit

November 16 2013 Sample No.	Ore Zone	$^{207}Pb/^{206}Pb$	Measured $^{206}Pb/^{238}U$	CORR $^{206}Pb/^{238}U$	Measured $^{207}Pb/^{235}U$	CORR $^{207}Pb/^{235}U$
CS-13-11	Low basement	0.0794	0.1709	0.0971	1.8190	0.9977
CS-13-11	Low basement	0.0824	0.1741	0.0982	1.9089	1.0300
CS-13-11	Low basement	0.0794	0.1844	0.1015	1.9480	1.0441
CS-13-11	Low basement	0.0797	0.2166	0.1119	2.2933	1.1683
CS-13-11	Low basement	0.0789	0.1852	0.1018	1.9377	1.0404
CS-13-11	Low basement	0.0798	0.2132	0.1108	2.2638	1.1577
CS-13-11	Low basement	0.0789	0.1971	0.1056	2.0696	1.0878
CS-13-11	Low basement	0.0793	0.2051	0.1082	2.1640	1.1218
CS-13-11	Low basement	0.0808	0.2463	0.1215	2.6447	1.2946
CS-13-22	Unconformity	0.0576	0.0156	0.0470	0.1191	0.3864
CS-13-22	Unconformity	0.0492	0.0129	0.0462	0.0844	0.3740
CS-13-22	Unconformity	0.0516	0.0108	0.0455	0.0744	0.3703
CS-13-22	Unconformity	0.0510	0.0123	0.0460	0.0832	0.3735
CS-13-22	Unconformity	0.0521	0.0114	0.0457	0.0792	0.3721
CS-13-27	Unconformity	0.0506	0.0452	0.0566	0.3021	0.4522
CS-13-27	Unconformity	0.0508	0.0499	0.0581	0.3351	0.4641
CS-13-27	Unconformity	0.0504	0.0434	0.0560	0.2902	0.4479
CS-13-27	Unconformity	0.0500	0.0334	0.0528	0.2218	0.4234
CS-13-27	Unconformity	0.0509	0.0500	0.0581	0.3373	0.4649
CS-13-27	Unconformity	0.0512	0.0513	0.0585	0.3482	0.4688
CS-13-27	Unconformity	0.0510	0.0529	0.0591	0.3603	0.4732
CS-13-27	Unconformity	0.0506	0.0406	0.0551	0.2722	0.4415
CS-13-4	Low basement	0.0783	0.1811	0.1005	1.8892	1.0230
CS-13-4	Low basement	0.0790	0.3013	0.1392	3.1631	1.4810
CS-13-4	Low basement	0.0783	0.2753	0.1308	2.8701	1.3757
CS-13-4	Low basement	0.0793	0.1949	0.1049	2.0583	1.0838
CS-13-4	Low basement	0.0790	0.2920	0.1362	3.0702	1.4477
CS-13-4	Low basement	0.0789	0.2287	0.1158	2.4072	1.2092
CS-13-4	Low basement	0.0775	0.2714	0.1296	2.7977	1.3496

Table C5: SIMS analyses of UO_2 standards and U-Pb measured and corrected (CORR) isotope ratios in uraninite from the Kianna deposit

November 18 2013 Standard	$^{207}Pb/^{206}Pb$	$^{206}Pb/^{238}U$	$^{207}Pb/^{235}U$
LAMNH	0.0537	0.0715	0.5071
LAMNH	0.0537	0.0681	0.4907
LAMNH	0.0537	0.0837	0.5983
AVERAGE	0.0537	0.0744	0.5320
TRUE	0.0538	0.0554	0.4105
TKK	0.0729	0.3414	3.3176
TKK	0.0737	0.3353	3.2755
TKK	0.0733	0.3341	3.2219
AVERAGE	0.0733	0.3369	3.2717
TRUE	0.0734	0.1701	1.7213
PC-06	0.1689	0.9882	21.9990
PC-06	0.1690	0.9911	22.2754
PC-06	0.1664	0.8624	18.9261
AVERAGE	0.1681	0.9472	21.0669
TRUE	0.1678	0.3613	8.3590

Table C5: SIMS analyses of UO_2 standards and U-Pb measured and corrected (CORR) isotope ratios in uraninite from the Kianna deposit

November 18 2013 Sample No.	Ore Zone	$^{207}Pb/^{206}Pb$	Measured $^{206}Pb/^{238}U$	CORR $^{206}Pb/^{238}U$	Measured $^{207}Pb/^{235}U$	CORR $^{207}Pb/^{235}U$
CS-4a	Perched	0.0563	0.1132	0.0788	0.8450	0.6527
CS-4a	Perched	0.0569	0.1455	0.0899	1.0971	0.7490
CS-4a	Perched	0.0570	0.1339	0.0859	1.0109	0.7161
CS-4a	Perched	0.0572	0.1366	0.0869	1.0407	0.7274
CS-4a	Perched	0.0524	0.0474	0.0562	0.3297	0.4558
CS-4a	Perched	0.0541	0.0524	0.0579	0.3766	0.4738
CS-4a	Perched	0.0566	0.1485	0.0910	1.1107	0.7542
CS-4a	Perched	0.0533	0.0513	0.0576	0.3630	0.4686
CS-4a	Perched	0.0534	0.0563	0.0593	0.3985	0.4821
CS-4a	Perched	0.0570	0.1407	0.0883	1.0660	0.7371
CS-13-28	Perched	0.0530	0.0200	0.0468	0.1413	0.3839
CS-13-28	Perched	0.0532	0.0215	0.0473	0.1531	0.3884
CS-13-28	Perched	0.0523	0.0182	0.0462	0.1264	0.3782
CS-13-18	Perched	0.0589	0.0032	0.0410	0.0250	0.3394
CS-13-18	Perched	0.0528	0.0081	0.0427	0.0571	0.3517
CS-13-18	Perched	0.0553	0.0054	0.0418	0.0398	0.3451

Table C5: SIMS analyses of UO_2 standards and U-Pb measured and corrected (CORR) isotope ratios in uraninite from the Kianna deposit

April 28 2013 Standard	$^{207}Pb/^{206}Pb$	$^{206}Pb/^{238}U$	$^{207}Pb/^{235}U$
LAMNH	0.0538	0.0807	0.5764
LAMNH	0.0536	0.0759	0.5411
LAMNH	0.0546	0.0818	0.5867
AVERAGE	0.0540	0.0795	0.5680
TRUE	0.0538	0.0554	0.4105
TKK	0.0739	0.3234	3.1675
TKK	0.0736	0.3178	3.0893
TKK	0.0736	0.3168	3.0826
AVERAGE	0.0737	0.3193	3.1132
TRUE	0.0734	0.1701	1.7213
PC-06	0.1695	0.8124	18.2855
PC-06	0.1683	0.7685	17.0806
PC-06	0.1700	0.7707	17.3764
AVERAGE	0.1693	0.7839	17.5808
TRUE	0.1678	0.3613	8.3590

Table C5: SIMS analyses of UO_2 standards and U-Pb measured and corrected (CORR) isotope ratios in uraninite from the Kianna deposit

April 28 2013 Sample No.	Ore Zone	$^{207}Pb/^{206}Pb$	Measured $^{206}Pb/^{238}U$	CORR $^{206}Pb/^{238}U$	Measured $^{207}Pb/^{235}U$	CORR $^{207}Pb/^{235}U$
CS-3	Basement	0.0692	0.0816	0.0608	0.7501	0.5543
CS-3	Basement	0.0682	0.1324	0.0827	1.2051	0.7655
CS-3	Basement	0.0677	0.2071	0.1149	1.8527	1.0662
CS-3	Basement	0.0682	0.1847	0.1052	1.6485	0.9714
CS-3	Basement	0.0670	0.2385	0.1284	2.1141	1.1876
CS-3	Basement	0.0668	0.1657	0.0970	1.4611	0.8844
CS-3	Basement	0.0679	0.1502	0.0904	1.3572	0.8361
CS-3	Basement	0.0646	0.0988	0.0682	0.8422	0.5970
CS-3	Basement	0.0670	0.1322	0.0826	1.1711	0.7497
CS-3	Basement	0.0675	0.2078	0.1152	1.8681	1.0734

Table C6: Measured and corrected U-Pb isotopic ratios used to construct Concordia diagrams for U-Pb ages

Generation	Measured $^{207}Pb/^{206}Pb$	1σ (%)	Measured $^{207}Pb/^{235}U$	Corrected $^{207}Pb/^{235}U$	1σ (%)	Measured $^{206}Pb/^{238}U$	Corrected $^{206}Pb/^{238}U$	1σ (%)
U1	0.0838	0.1	3.2388	1.7958	0.7	0.2880	0.1564	0.6
U1	0.0866	0.3	4.0133	2.1760	0.6	0.3433	0.1814	1.1
U1	0.0855	0.1	4.0117	2.1753	0.3	0.3475	0.1833	0.4
U1	0.0868	0.2	4.3235	2.3283	0.7	0.3691	0.1931	0.5
U1	0.0875	0.2	4.5804	2.4545	0.1	0.3878	0.2016	0.4
U1	0.0875	0.1	4.5692	2.4490	0.2	0.3863	0.2010	0.2
U1	0.0839	0.2	3.6951	2.0198	0.3	0.3242	0.1728	0.2
U1	0.0874	0.1	4.3009	2.3172	0.8	0.3648	0.1912	0.7
U1	0.0778	0.2	2.5718	1.4682	0.5	0.2431	0.1360	0.6
U1	0.0870	0.5	4.3145	2.3239	0.6	0.3674	0.1924	0.6
U1	0.0878	0.3	4.5574	2.4432	0.5	0.3847	0.2002	0.4
U1	0.0877	0.1	4.6635	2.4953	0.9	0.3935	0.2042	0.7
U1	0.0827	0.2	3.3028	1.8272	1.0	0.2954	0.1597	0.9
U1	0.0835	0.1	3.4203	1.8849	0.1	0.3050	0.1641	0.3
U1	0.0871	0.2	4.4224	2.3769	0.9	0.3734	0.1951	0.7
U1	0.0865	0.1	4.1645	2.2503	0.7	0.3566	0.1875	0.3
U1	0.0833	0.2	3.2382	1.7955	1.3	0.2859	0.1554	1.6
U1	0.0836	0.1	3.4616	1.9052	0.8	0.3075	0.1652	0.6
U1	0.0792	0.2	2.6833	1.5230	1.0	0.2500	0.1391	0.1
U1	0.0831	0.2	3.4179	1.8837	1.3	0.3049	0.1640	1.3
U1	0.0844	0.1	3.7829	2.0629	0.7	0.3324	0.1765	0.6
U1	0.0787	0.3	2.3348	1.4352	0.3	0.2208	0.1320	0.5
U1	0.0762	0.1	2.1469	1.3350	0.1	0.2095	0.1264	0.3
U1	0.0767	0.3	2.2157	1.3717	0.6	0.2164	0.1298	0.5
U1	0.0816	0.2	2.9494	1.7631	0.4	0.2705	0.1563	0.5
U1	0.0803	0.3	2.4772	1.5112	0.7	0.2327	0.1378	0.5
U1	0.0784	0.1	2.4364	1.4894	0.7	0.2343	0.1385	0.8
U1	0.0810	0.4	2.8290	1.6989	0.9	0.2616	0.1520	0.6
U1	0.0789	0.2	2.2422	1.3858	0.3	0.2128	0.1280	0.4
U1	0.0802	0.5	2.5423	1.5459	1.2	0.2377	0.1402	0.6

Table C6: Measured and corrected U-Pb isotopic ratios used to construct Concordia diagrams for U-Pb ages

Generation	Measured $^{207}Pb/^{206}Pb$	1σ (%)	Measured $^{207}Pb/^{235}U$	Corrected $^{207}Pb/^{235}U$	1σ (%)	Measured $^{206}Pb/^{238}U$	Corrected $^{206}Pb/^{238}U$	1σ (%)
U1	0.0822	0.3	2.8415	1.6453	2.2	0.2606	0.1457	2.7
U1	0.0845	0.1	3.6936	2.0668	1.8	0.3295	0.1773	1.7
U1	0.0778	0.1	2.4533	1.4533	1.4	0.2371	0.1349	1.1
U1	0.0811	0.1	2.8401	1.6446	2.5	0.2601	0.1454	2.6
U1	0.0818	0.3	2.8114	1.6304	3.5	0.2560	0.1436	3.4
U1	0.0876	0.2	4.4429	2.4375	0.6	0.3804	0.2006	0.6
U1	0.0794	0.3	2.5835	1.5177	1.1	0.2421	0.1372	1.5
U1	0.0828	0.3	3.0145	1.7309	2.5	0.2716	0.1507	2.9
U1	0.0843	0.2	3.3092	1.8766	1.2	0.2933	0.1607	1.7
U1	0.0873	0.2	3.9770	2.2070	2.1	0.3393	0.1818	2.0
U1	0.0792	0.1	2.4468	1.4500	2.5	0.2316	0.1324	2.9
U1	0.0790	0.5	2.6102	1.5309	3.1	0.2454	0.1387	2.7
U1	0.0840	0.1	3.3843	1.9138	0.9	0.3017	0.1646	1.1
U1	0.0875	0.1	3.9580	2.1976	2.4	0.3399	0.1820	2.4
U1	0.0871	0.1	4.0381	2.2372	0.4	0.3465	0.1851	0.3
U1	0.0874	0.2	3.8921	2.1650	2.0	0.3321	0.1785	2.1
U1	0.0878	0.1	4.2307	2.3325	1.5	0.3610	0.1917	1.3
U1	0.0877	0.5	4.2047	2.3197	1.1	0.3569	0.1899	1.2
U2	0.0786	0.2	1.8456	0.9641	0.4	0.1762	0.0938	0.1
U2	0.0760	0.2	1.7493	0.9312	0.4	0.1736	0.0930	0.1
U2	0.0834	0.2	3.9534	1.6839	0.4	0.3563	0.1493	0.1
U2	0.0821	0.2	3.1341	1.4041	0.4	0.2878	0.1282	0.1
U2	0.0752	0.3	1.5468	0.8620	0.4	0.1553	0.0874	0.1
U2	0.0815	0.2	2.8331	1.3013	0.4	0.2603	0.1197	0.1
U2	0.0841	0.2	3.2541	1.4451	0.4	0.2888	0.1285	0.1
U2	0.0772	0.3	1.2112	0.7474	0.4	0.1179	0.0758	0.1
U2	0.0701	0.2	1.7469	0.9304	0.4	0.1858	0.0968	0.1
U2	0.0818	0.2	2.4713	1.1778	0.4	0.2284	0.1099	0.1
U2	0.0813	0.2	3.3824	1.4889	0.3	0.3145	0.1364	0.1

Table C6: Measured and corrected U-Pb isotopic ratios used to construct Concordia diagrams for U-Pb ages

Generation	Measured $^{207}Pb/^{206}Pb$	1σ (%)	Measured $^{207}Pb/^{235}U$	Corrected $^{207}Pb/^{235}U$	1σ (%)	Measured $^{206}Pb/^{238}U$	Corrected $^{206}Pb/^{238}U$	1σ (%)
U2	0.0750	0.2	1.9332	0.9940	0.4	0.1936	0.0992	0.1
U2	0.0771	0.2	1.6593	0.9004	0.4	0.1612	0.0892	0.1
U2	0.0794	0.2	1.8190	0.9977	0.4	0.1709	0.0971	0.1
U2	0.0824	0.2	1.9089	1.0300	0.4	0.1741	0.0982	0.1
U2	0.0794	0.2	1.9480	1.0441	0.4	0.1844	0.1015	0.1
U2	0.0797	0.2	2.2933	1.1683	0.4	0.2166	0.1119	0.1
U2	0.0789	0.2	1.9377	1.0404	0.4	0.1852	0.1018	0.1
U2	0.0798	0.2	2.2638	1.1577	0.4	0.2132	0.1108	0.1
U2	0.0789	0.2	2.0696	1.0878	0.4	0.1971	0.1056	0.1
U2	0.0793	0.2	2.1640	1.1218	0.4	0.2051	0.1082	0.1
U2	0.0808	0.2	2.6447	1.2946	0.4	0.2463	0.1215	0.1
U2	0.0783	0.2	1.8892	1.0230	0.4	0.1811	0.1005	0.1
U2	0.0790	0.2	3.1631	1.4810	0.3	0.3013	0.1392	0.1
U2	0.0783	0.2	2.8701	1.3757	0.4	0.2753	0.1308	0.1
U2	0.0793	0.2	2.0583	1.0838	0.4	0.1949	0.1049	0.1
U2	0.0790	0.2	3.0702	1.4477	0.3	0.2920	0.1362	0.1
U2	0.0789	0.2	2.4072	1.2092	0.3	0.2287	0.1158	0.1
U2	0.0775	0.2	2.7977	1.3496	0.4	0.2714	0.1296	0.1
U3	0.0787	0.1	2.8678	1.7195	0.8	0.2717	0.1569	1.0
U3	0.0772	0.6	1.0192	0.7334	1.8	0.0995	0.0725	2.2
U3	0.0775	0.6	2.1276	1.3247	4.1	0.2047	0.1240	3.5
U3	0.0775	0.2	2.3252	1.4301	0.1	0.2255	0.1342	0.6
U3	0.0772	0.2	1.9889	1.2507	1.0	0.1942	0.1189	0.8
U3	0.0724	0.3	2.5166	1.5322	1.3	0.2606	0.1515	1.7
U3	0.0695	0.1	2.1482	1.3356	1.7	0.2305	0.1367	1.9
U3	0.0702	0.0	2.3208	1.4277	2.2	0.2491	0.1458	1.3
U3	0.0663	0.5	0.7046	0.5655	2.2	0.0796	0.0627	2.6
U3	0.0719	0.2	2.4800	1.5127	1.5	0.2582	0.1503	1.2
U3	0.0769	0.3	1.4843	0.8407	0.4	0.1446	0.0841	0.1
U3	0.0699	0.3	1.1785	0.7362	0.4	0.1273	0.0787	0.1

Table C6: Measured and corrected U-Pb isotopic ratios used to construct Concordia diagrams for U-Pb ages

Generation	Measured $^{207}Pb/^{206}Pb$	1σ (%)	Measured $^{207}Pb/^{235}U$	Corrected $^{207}Pb/^{235}U$	1σ (%)	Measured $^{206}Pb/^{238}U$	Corrected $^{206}Pb/^{238}U$	1σ (%)
U3	0.0749	0.2	2.5998	1.2216	0.4	0.2595	0.1195	0.1
U3	0.0802	0.3	0.8616	0.6280	0.4	0.0804	0.0643	0.1
U3	0.0817	0.4	0.7423	0.5873	0.5	0.0679	0.0604	0.1
U3	0.0779	0.5	0.4333	0.4818	0.5	0.0418	0.0524	0.1
U3	0.0762	0.3	0.8810	0.6347	0.4	0.0863	0.0661	0.1
U3	0.0817	0.4	0.7486	0.5894	0.5	0.0683	0.0606	0.1
U4	0.0692	0.4	0.7501	0.5543	0.6	0.0816	0.0608	0.1
U4	0.0682	0.4	1.2051	0.7655	0.5	0.1324	0.0827	0.1
U4	0.0677	0.3	1.8527	1.0662	0.5	0.2071	0.1149	0.1
U4	0.0682	0.4	1.6485	0.9714	0.7	0.1847	0.1052	0.1
U4	0.0670	0.3	2.1141	1.1876	0.5	0.2385	0.1284	0.1
U4	0.0668	0.3	1.4611	0.8844	0.5	0.1657	0.0970	0.1
U4	0.0679	0.3	1.3572	0.8361	0.5	0.1502	0.0904	0.1
U4	0.0646	0.4	0.8422	0.5970	0.5	0.0988	0.0682	0.1
U4	0.0670	0.4	1.1711	0.7497	0.5	0.1322	0.0826	0.1
U4	0.0675	0.3	1.8681	1.0734	0.5	0.2078	0.1152	0.1
U5	0.0566	0.1	0.7822	0.6556	1.2	0.1027	0.0785	1.0
U5	0.0567	0.2	0.7371	0.6375	1	0.0964	0.0762	0.8
U5	0.0571	0.2	0.6960	0.6211	1.4	0.0908	0.0742	1.4
U5	0.0531	0.1	0.4350	0.4217	0.8	0.0612	0.0537	0.6
U5	0.0530	0.6	0.4284	0.4181	0.9	0.0610	0.0536	0.2
U5	0.0525	0.4	0.4097	0.4082	0.8	0.0588	0.0525	0.4
U5	0.0553	0.3	0.5198	0.4669	0.7	0.0706	0.0583	1.0
U5	0.0547	0.6	0.5582	0.4874	0.4	0.0763	0.0611	0.6
U5	0.0547	0.2	0.5737	0.4957	0.8	0.0791	0.0625	0.9
U5	0.0539	0.3	0.5328	0.4739	1.3	0.0741	0.0600	0.8
U5	0.0563	0.4	0.8450	0.6527	0.5	0.1132	0.0788	0.1

Table C6: Measured and corrected U-Pb isotopic ratios used to construct Concordia diagrams for U-Pb ages

Generation	Measured $^{207}Pb/^{206}Pb$	1σ (%)	Measured $^{207}Pb/^{235}U$	Corrected $^{207}Pb/^{235}U$	1σ (%)	Measured $^{206}Pb/^{238}U$	Corrected $^{206}Pb/^{238}U$	1σ (%)
U6	0.0516	0.8	0.1372	0.3968	1.6	0.0196	0.0487	0.6
U6	0.0530	1.6	0.1096	0.3858	1.5	0.0155	0.0472	1.0
U6	0.0501	0.5	0.1871	0.4168	0.3	0.0276	0.0515	0.4
U6	0.0509	2.3	0.0678	0.3690	2.2	0.0098	0.0451	1.6
U6	0.0501	1.0	0.1266	0.3926	1.3	0.0187	0.0483	0.4
U6	0.0498	0.6	0.1196	0.3898	0.6	0.0178	0.0480	0.4
U6	0.0503	0.9	0.1248	0.3919	2.5	0.0184	0.0482	1.3
U6	0.0530	0.8	0.1413	0.3839	0.9	0.0200	0.0468	0.2
U6	0.0532	0.8	0.1531	0.3884	0.8	0.0215	0.0473	0.2
U6	0.0523	0.9	0.1264	0.3782	0.9	0.0182	0.0462	0.2
U6	0.0589	2.4	0.0250	0.3394	2.3	0.0032	0.0410	0.6
U6	0.0528	1.4	0.0571	0.3517	1.4	0.0081	0.0427	0.3
U6	0.0553	1.6	0.0398	0.3451	1.6	0.0054	0.0418	0.4
U6	0.0576	1.2	0.1191	0.3864	1.3	0.0156	0.0470	0.3
U6	0.0492	1.2	0.0844	0.3740	1.2	0.0129	0.0462	0.3
U6	0.0516	1.3	0.0744	0.3703	1.3	0.0108	0.0455	0.3
U6	0.0510	1.3	0.0832	0.3735	1.3	0.0123	0.0460	0.3
U6	0.0521	1.2	0.0792	0.3721	1.2	0.0114	0.0457	0.3
U6	0.0506	0.7	0.3021	0.4522	0.7	0.0452	0.0566	0.1
U6	0.0508	0.6	0.3351	0.4641	0.7	0.0499	0.0581	0.1
U6	0.0504	0.7	0.2902	0.4479	0.7	0.0434	0.0560	0.1
U6	0.0500	0.8	0.2218	0.4234	0.8	0.0334	0.0528	0.2
U6	0.0509	0.6	0.3373	0.4649	0.7	0.0500	0.0581	0.1
U6	0.0512	0.6	0.3482	0.4688	0.7	0.0513	0.0585	0.1